Romanian Journal of
PETROLOGY

continuation of

DĂRI DE SEAMĂ ALE ŞEDINŢELOR INSTITUTULUI DE GEOLOGIE ŞI GEOFIZICĂ
COMPTES RENDUS DES SÉANCES DE L'INSTITUT DE GÉOLOGIE ET GÉOPHYSIQUE

Founded 1906 by the Geological Institute of Romania

ISSN 1220-563X

Vol. 77

CONTENTS

(Contents continued on outside back cover)

IGR 1906

Institutul Geologic al României
Bucureşti – 1996

GEOLOGICAL INSTITUTE OF ROMANIA

Director General Dr. **G. Udubaşa** Member of the Romanian Academy

The **Geological Institute of Romania** is now publishing the following periodicals:

- Romanian Journal of Mineralogy
- Romanian Journal of Petrology
- Romanian Journal of Mineral Deposits
- Romanian Journal of Paleontology
- Romanian Journal of Stratigraphy
- Romanian Journal of Tectonics and Regional Geology
- Romanian Journal of Geophysics
- Anuarul Institutului Geologic al României
- Memoriile Institutului Geologic al României

Romanian Journals supersede "Dări de Seamă ale Şedinţelor" and "Studii Tehnice şi Economice", whose apparition goes back to 1910. Besides regular volumes, each series may occasionally contain Supplements (for abstracts and excursion guides to congresses and symposia held in Romania) and Special Issues (for larger papers of special interest). "Anuarul Institutului Geologic al României" will appear in a new form, containing both the annual activity report and review papers.

Editorial Office:
Geological Institute of Romania
Str. Caransebeş Nr. 1
RO - 79 678 Bucureşti - 32
Tel. (+40) 1 665 66 25, 665 75 30
Fax (+40) 1 312 84 44
e-mail GEOL@IGR.RO

The editor has changed the name as follows: Institutul Geologic al României (1906–1952), Comitetul Geologic (1953–1966), Comitetul de Stat al Geologiei (1967–1969), Institutul Geologic (1970–1974), Institutul de Geologie şi Geofizică (1975–1993), Institutul Geologic al României (since 1994).

ROMANIAN JOURNAL OF PETROLOGY supersedes "Dări de Seamă ale Şedinţelor", Series 1/Mineralogie-Petrologie – the last volume with this title being No. 74.

The manuscripts should be sent to the scientific editor and/or executive secretary. Correspondence concerning advertisments, announcements and subscriptions should be sent to the Managing Editor.

ISSN 1220–563x
Classification index for libraries 55(058)

Printed by the Geological Institute of Romania
Bucharest

CONTENTS

Rom. J. Petrology, 77, p. 3–10, Bucureşti, 1996

CONTRIBUTIONS TO THE PETROCHEMISTRY OF THE OGRADENA GRANITOIDS AND SOME SPATIALLY ASSOCIATED INTRUSIVE ROCKS (SOUTH BANAT)

Nicolae STAN

Institutul Geologic al României. Str. Caransebeş 1, 79 678 Bucureşti 32

Key words: Granitoids. Vein Rocks. Anatexis. Oceanic Crust. Mantle.

Abstract: Several types of rocks have been analysed from the petrochemical point of view: metagabbrodiorites, granitoids (Ogradena and Sesemin), and dyke rocks (granodiorite-porphyries ± quartz, aplites). The chemical and spectral analyses (Tabs. 1,2) show calc-alkaline characters with alkaline trends to the granitoids (Figs. 2,4). In places granitoids are leucocrate-trondhjemite with a quite narrow SiO_2 variation range (72.50–75.68). The specific discriminatory S–I parameters indicate that granitoids are the result of continental-crustal anatexis processes (mainly) in relation to melts coming from the oceanic crust and/or the mantle.

1. Introduction

The intrusive rocks and the related dykes are represented on the Orşova-Topleţ-Băile Herculane geological map (Stan, 1995).

The intrusions consist of metagabbros, metadiorites±quartz, Ogradena granitoids and tectonized Sesemin granitoids, related to granodiorite-porphyry dykes that locally grade into diorite porphyries±quartz, small-sized aplites, that cannot be mapped, and lamprophyres. Lamprophyres are altered and for this reason their chemistry cannot be taken into consideration; this is also the case of the small occurrences of serpentinized intrusive metabasites north of Topleţ.

The petrochemistry of the Ogradena granitoids was studied by Anastasiu (1976).

2. Microscopic Observations

Metagabbros and metadiorites ± quartz are closely related and regionally metamorphosed to the crystalline schists of the Neamţu Group.

Mineralogic composition: plagioclase (40–70%, An 35–40), substituted in variable percentages by sericite and zoisite; green hornblende (10–30%), locally altered into epidote, chlorite or more rarely actinote; quartz (5–15%), biotite (1–5%), partially or totally chloritized; sphene, apatite and magnetite. The femic minerals are often impregnated with magnetite powders on the cleavage trends, with pyrite or chalcopyrite. The rock structure is granonematoblastic.

Ogradena and Sesemin granitoids are intuded both in the Neamţu Group and in the

Corbu-Vodna-Neamţu tectogenetic zones (Stan, 1995). Locally, characteristic minerals – andalusite, staurolite, garnet, biotite – occur at the contact.

Ogradena granitoid displays generally a massive, more rarely oriented structure; the marginal zones and the granitoid septa, that penetrate the Neamţu Group, show poorly oriented microgranular structures; they mostly correspond to the Lucidol granitoids (Anastasiu, 1976). The boundaries between the microgranular oriented facies and the massive ones are trenchant.

The crystalline schists occur as numerous septa inside the Ogradena granitoid.

The mineralogical composition of the granitoid: plagioclase (35–45%, An 15–25), potash feldspar (15–20%), quartz (24–40%), biotite (1–10%), muscovite (1–5%), accessory minerals (0.2–0.8%), garnet (0–2%). Ogradena granitoids are leucogranites.

Sesemin granitoid is, in most cases, tectonized, the degree of tectonization varying within relatively wide ranges.

From the petrographic point of view, Sesemin granitoids are represented by leucogranites, locally with trondhjemitic aspects. Granodiorites or diorites were very rarely identified in thin sections. These petrographic aspects cannot be separated cartographically.

The mineralogic composition of the leucocrates is, as follows: quartz (25–35%), albite–oligoclase (30–45%), potash feldspar (10–20%), biotite (2–7%), muscovite (1–5%). Garnet occurs accidentally.

Trondhjemites are mostly constituted of quartz and oligoclase locally related to potash feldspar (3–5%). The femic minerals are found in small amounts (1–3%).

The quartz diorites differ from granites by the absence of the potash feldspar, a reduced participation of the quartz (5–7%), and the sporadic presence of hornblende.

In the cataclased granitoids, quartz is frequently crushed, forming the matrix of the plagioclase feldspar or potash feldspar porphyroclasts. The intensely sericitized plagioclase with sinusoidal repeated twinings is locally fissured or broken. Calcite occurrs on fissures. Potash feldspar (microcline, microperthite or microcline–perthite), more resistant to the tectonic influences, occurs with hipidiomorphic outlines and poikilitic structure. Its degree of alteration is low: sericitizations or kaolinizations occur rarely on the crystal surface. Biotite is partly chloritized, bent, aligned on the foliation planes, like sericitized muscovite. Hornblende is altered into a zoisite-epïdote aggregate, or chloritized in different stages. The textures of these granitoids are vaguely oriented and the structures are holocrystalline, hipidiomorphic.

In the massive rocks, plagioclase is partially sericitized, but the cataclastic fissures are absent; likewise, quartz with equigranular allotriomorphic outlines is no longer crushed or deformed.

Granodiorite-porphyries and diorite porphyries ± quartz. They are grey, displaying a porphyritic structure; macroscopically quartz and feldspar phenocrysts are obvious, cemented in a slightly greenish aphanitic matrix. Under the microscope, beside the mentioned minerals, biotite and more rarely potash feldspar are observed, as well. The microcrystalline or granular matrix, locally granophyric, consists of the same minerals that form the phenocrysts. The alteration phenomena (sericitization, kaolinization, epidotization, calcitization) occur frequently especially in the groundmass. Plagioclase (An_{20-30}) is often completely altered. The quartz phenocrysts represent 8–10% of the quartz diorite-porphyries or 10–25% of the granodiorite-porphyries. The gradings between these two rock types depend on the quartz amount that can vary even within the same dyke. Even the structure of the matrix varies alleatorily from microlitic to granular or granophyric.

Aplites are rare; they crop out as nests of short dykes of the meters order and consequently they have not been mapped.

Aplites consist of plagioclase feldspar (40–60%), quartz (30–50%), and muscovite (10–15%). Potash feldspar (microcline) participates in relatively small amounts (5–7%). The rock structure is microgranular-allotriomorphic, the texture is massive or slightly oriented.

Lamprophyres display a massive texture and an aphanitic, more rarely porphyritic structure. Mineralogical composition: biotite, augite, plagioclase in diverse amounts. Potash feldspar can be found in the matrix. Calcite pseudomorphs after pyroxenes are often found. Calcite and chlorite as secondary minerals are deposited also on fissures or in the voids of the groundmass. The mesostasis consists of the already mentioned minerals and is spotted with iron oxides.

3. Geochemical Characters

The chemical and spectral analyses are presented in Tables 1 and 2.

3.1. Major elements

The metamorphosed intrusions of the Neamţu Group correspond, from the chemical point of view, to gabbroic rocks (sample 704) or to dioritic rocks (sample 1011): high values of Fe_2O_3 (3.43–8.03%), FeO (4.95–7.07%), MgO (6.34–6.41%), and CaO (6.90–9.25%). The alkali values are generally low. The SiO_2 ratio is lower in the gabbroic rocks than in the dioritic ones: 48.30% and 55.70%, repectively; likewise, the values of CaO, Fe_2O_3 and FeO are visibly higher in the gabbroic rocks in comparison with the dioritic ones (Tab. 1).

Ogradena and Sesemin granitoids are characterized by high SiO_2 values, ranging within a very narrow range (72.50–75.68%). The values of the Al_2O_3 are normal (12.54–14.70%). It is of note the very low values, in most cases subunitary, of FeO (0.0–1.15%), Fe_2O_3 (0.02–1.34%) and MgO (0.05–0.77%). This points out the leucocrate character of the granitoids, particularly the Sesemin granitoids (Tab. 1). CaO values, low in the Ogradena granitoids (0.55–1.74%), are even lower in the Sesemin granitoids (0.52–1.16%). This is explained by the presence of the anorthitic constituent in greater amounts in the Ogradena granitoid. The alkali values vary, in most cases, within a narrow range: $Na_2O \sim 3$–$4.50\% \geq K_2O \sim 3$–3.50% for the Ogradena granitoids and $Na_2O \sim 3.00$–$4.00\% \leq K_2O \sim 3.50$–$4.00\%$ for the Sesemin granitoids.

Granodiorite–porphyry dykes are quite similar in chemical respect with the Ogradena and Sesemin granitoids. However, they differ by a larger SiO_2 range (68.23–72.00% as well as by higher values of FeO (1.17–1.35%), Fe_2O_3 (1.23–1.72%), MgO (0.55–1.26%), CaO (2.02–2.44%). These observations are in agreement with the more important participation of the femic minerals to granodiorite-porphyries as compared to the granitoid rocks. In the granodiorite-porphyry dyke rocks the K_2O content is lower as compared to the granitoids ones (Tab. 1).

Aplites contain a great amount of alkalies. Na_2O (3.14–4.23%) < K_2O (4.02–5.32%); FeO, Fe_2O_3, MgO and CaO display unsignificant values, and SiO_2 show high values and small variation ranges: 73.90–75.15%.

On the Q–A–P diagram (Rittmann norm) gabbro-diorites plot in the quartz monzodiorites field, and most of the granitoid rocks in the granite (monzo-syenogranites) field, very few in the granodiorites field (Fig. 1). The leucocrate character of the granitoids is shown on the TAS diagram (Andreeva et al., 1985) as well as on O'Connor diagram (1965) on which some granitoids show trondhjemitic features (Figs. 2, 3). The TAS and SiO_2-IA diagrams (Fig. 4) stress out the calc-alkaline to alkaline character of the granitoid rocks. On the TAS diagram the gabbrodiorites are plotting in the gabbros and diorites fields.

For the granitoid rocks Ab>Or>An; for gabbrodiorites An>Ab>Or (Fig. 5).

Table 1
Chemical composition

Sample No.	Location	Symbol	SiO_2	TiO_2	Al_2O_3	Fe_2O_3	FeO	MnO	MgO	CaO	K_2O	Na_2O	P_2O_5	H_2O	CO_2	S	Total
METAINTRUSIONS																	
704	Mala Valley	GB	48.30	0.07	14.70	8.03	7.07	0.22	6.71	9.25	1.37	2.84	0.02	0.87	0.00	0.24	99.70
1011	Iardaşiţa Valley	DI	55.70	0.92	14.30	3.43	4.95	0.23	6.34	6.90	1.95	3.13	0.38	1.47	0.00	0.15	99.80
OGRADENA GRANITOIDS																	
743	Lucidol Valley	SYG	75.68	0.10	12.54	0.02	1.02	0.04	0.77	1.13	3.15	3.03	0.04	0.82	0.98	0.18	99.50
715	Mala Valley	MZG	75.58	0.00	13.54	0.85	0.00	0.04	0.17	1.50	3.51	4.30	0.00	0.37	0.00	0.12	99.98
714	Mala Valley	MZG	75.45	0.00	13.90	1.10	0.00	0.03	0.22	1.15	3.70	3.94	0.00	0.38	0.00	0.11	99.98
712	Mala Valley	MZG	74.86	0.00	13.85	0.84	0.16	0.03	0.29	1.41	3.00	4.46	0.00	0.32	0.64	0.12	99.98
713	Mala Valley	MZG	74.61	0.00	13.95	0.88	0.00	0.03	0.18	1.69	3.36	4.37	0.00	0.53	0.00	0.12	99.72
725	Criviţa Valley	MZG	74.60	0.00	13.80	1.17	0.23	0.04	0.31	1.52	3.15	4.26	0.00	0.52	0.00	0.15	99.75
723	Seregova Valley	SYG	74.45	0.05	14.01	0.12	0.47	0.02	0.18	0.86	4.85	4.07	0.06	0.48	0.00	0.09	99.71
740	Criviţa Valley	MZG	74.42	0.00	14.70	0.80	0.00	0.03	0.16	1.60	2.85	4.64	0.00	0.24	0.00	0.24	99.68
722	Seregova Valley	MZG	74.32	0.00	13.94	0.93	0.48	0.05	0.37	1.58	3.25	3.89	0.00	0.65	0.00	0.12	99.58
753	Işelniţa Valley	MZG	74.30	0.12	14.20	0.11	1.15	0.04	0.43	1.67	3.21	3.93	0.05	0.52	0.85	0.10	100.70
738	Criviţa Valley	MZG	74.23	0.00	13.95	1.27	0.26	0.03	0.35	1.43	3.08	4.22	0.00	0.58	0.30	0.15	99.85
741	Criviţa Valley	MZG	73.98	0.00	14.44	1.17	0.29	0.05	0.35	1.74	3.17	4.13	0.00	0.32	0.00	0.20	99.84
739	Criviţa Valley	MZG	73.89	0.00	14.50	1.34	0.00	0.04	0.26	1.43	3.36	4.15	0.00	0.34	0.00	0.21	99.52
724	Criviţa Valley	GRD	73.73	0.00	14.70	1.01	0.36	0.03	0.30	1.75	2.08	4.95	0.00	0.49	0.00	0.20	99.60
742	Lucidol Valley	SYG	73.62	0.12	14.29	0.30	0.90	0.04	0.58	0.55	3.66	4.18	0.04	0.99	0.00	0.20	99.47
SESEMIN GRANITOIDS																	
1046	Stogier Hill	SYG	75.50	0.12	13.79	0.86	0.00	0.03	0.05	0.52	4.03	3.79	0.06	0.75	0.00	0.00	99.50
908	Lazuri Brook	MZG	75.30	0.12	12.99	0.76	0.22	0.04	0.25	0.98	3.64	4.04	0.06	1.00	0.00	0.00	99.40
1033	Sesemin Hill	MZG	75.00	0.11	13.69	0.60	0.36	0.04	0.14	0.82	3.87	4.00	0.08	0.67	0.00	0.00	99.32
1032	Sesemin Hill	SYG	74.50	0.12	13.65	0.83	0.13	0.08	0.03	0.86	5.80	3.27	0.06	0.58	0.00	0.00	99.91
1047	Stogier Hill	MZG	74.40	0.08	13.89	0.94	0.14	0.03	0.23	0.75	3.72	4.66	0.00	0.72	0.00	0.00	99.56
1034	Cerna Valley	MZG	72.50	0.28	14.40	1.33	0.45	0.06	0.41	1.16	3.24	4.76	0.04	1.09	0.00	0.00	99.72
VEIN ROCKS																	
820	Porumbilor Valley	GDP	72.00	0.14	14.66	1.31	1.21	0.04	0.55	2.02	2.82	4.10	0.08	0.79	0.00	0.08	99.80
681	Mala Valley	GDP	69.64	0.00	13.70	1.23	1.17	0.06	1.03	2.44	3.40	3.90	0.00	1.87	0.85	0.19	99.48
683	Mala Valley	GDP	68.23	0.01	14.89	1.72	1.35	0.06	1.26	2.32	3.05	4.13	0.01	1.12	1.30	0.09	99.54
710	Mala Valley	AP	75.15	0.00	14.05	0.66	0.13	0.13	0.15	0.76	4.44	3.82	0.00	0.51	0.00	0.07	99.87
711	Mala Valley	AP	74.99	0.00	14.00	0.86	0.00	0.03	0.21	1.12	4.02	4.23	0.00	0.37	0.00	0.11	99.94
708	Mala Valley	AP	73.90	0.00	13.54	1.43	0.39	0.03	0.37	0.90	5.32	3.14	0.00	0.61	0.00	0.09	99.72

Symbols: GB, gabbrodiorites; DI, diorites; SYG, syenogranites; MZG, monzogranites; GRD, granodiorites; GRP, granodiorite-porphyries; AP, aplites. Analyst: Elena Colios.

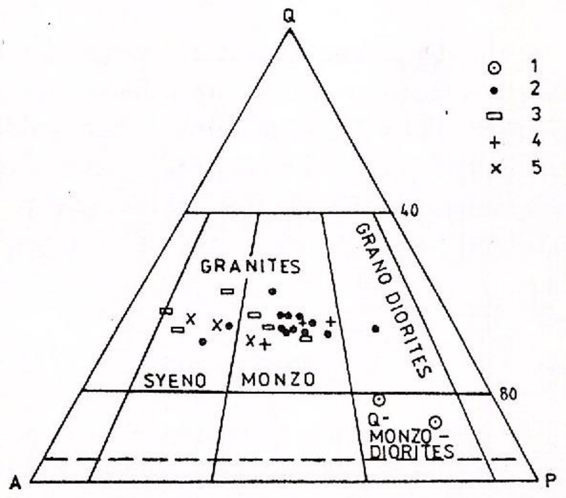

Fig. 1 – Q–A–P diagram (Rittmann norm). Symbols: 1, metagabbrodiorites ± quartziferous; 2, Ogradena granitoids; 3, Sesemin granitoids; 4, granitoid-porphyry dykes; 5, aplites.

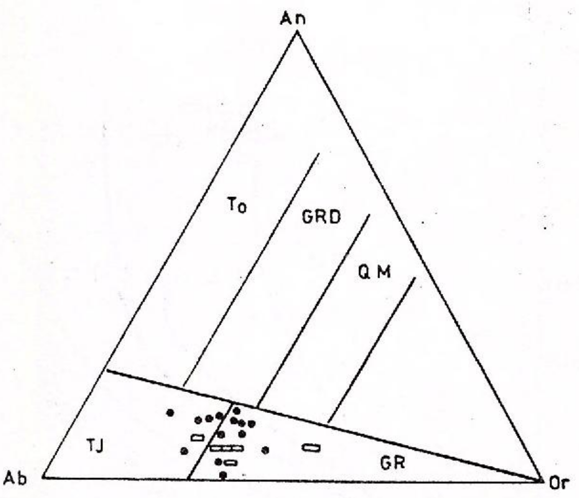

Fig. 3 – Or–Ab–An (O'Connor, 1965) diagram. TJ, trondhjemites; GR, granites. Symbols for the rock types as in Figure 1.

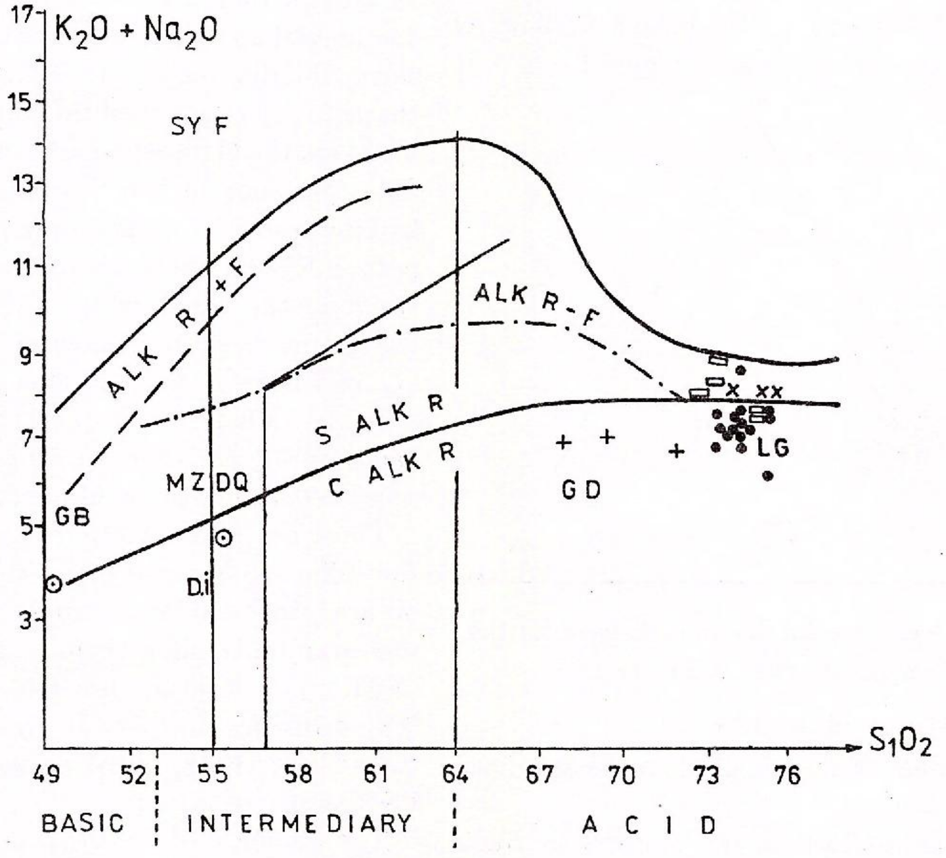

Fig. 2 – Andreeva et al. (1981) diagram. GB, gabbros; DI, diorites; MZDQ, quartziferous monzodiorites; LG, leucogranites; GD, granodiorites; ALKR+F, field of alkaline rocks with feldspatoids; ALK R-F, field of alkaline rocks without feldspatoids; S ALK R, field of alkaline rocks; C ALK R, field of calc-alkaline rocks. Symbols for the rock types as in Figure 1.

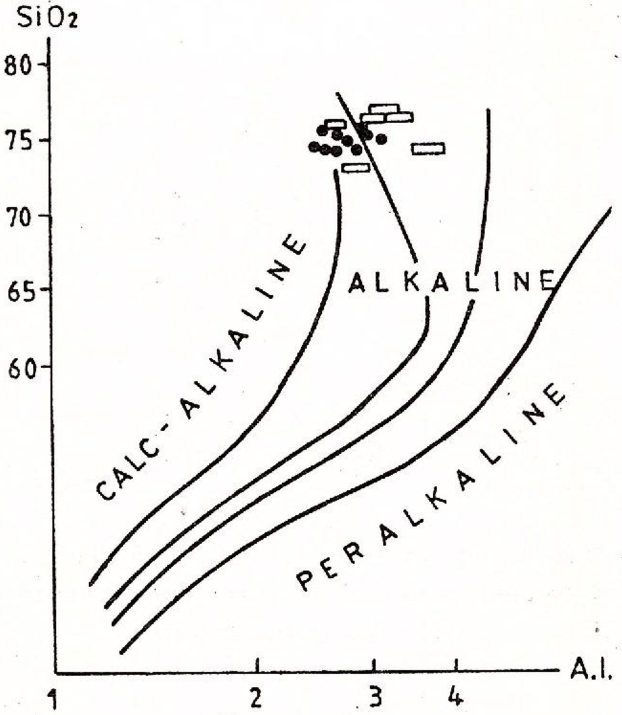

Fig. 4 – SiO_2–A.I. (Alkali index). Symbols for the rock types as in Figure 1.

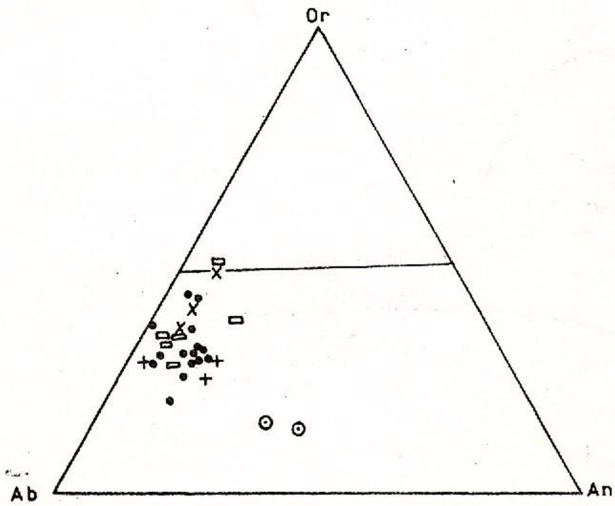

Fig. 5 – Or–Ab–An diagram. Legend for the rocks types as in Figure 1.

3.2. Minor elements

The values of the minor elements are shown on Table 2.

Metagabbrodiorites are more basic rocks and they display higher values of Ni (x=45), Co(x=29), Cr(x=220), V(x=225), Sc(x=25.5) in comparison with the other rocks.

In the granitoid and dyke rocks the minor elements show values compatible with the clarks of the respective elements.

In the Ogradena granitoid rocks the radioactive elements show low values: U=1.6–4.7 ppm, Th=2.4–13.6 ppm. For aplites: U=1.8–3.6 ppm, Th=3.4–16.5 ppm, and for granodiorite-porphyries: U=4.4–5.0 ppm, Th=7.8–12.8 ppm (analysts: E. Vâjdea, I. Tiepac).

4. Conclusions

The petrochemical parameters discriminatory for the genesis of the granitoid rocks, mentioned by Chappell and White (1974), White and Chappell (1983), Didier et al. (1982), Hine et al. (1978), Hussein et al. (1982), Pearce and Gale (1977), show that the Ogradena and Sesemin rocks mainly belong to type S; they are the result of the crustal-continental anatexis under compression conditions. In this respect the biotitic-muscovitic character of monzosyenites, the lack of hornblende in the Ogradena granitoids and its sporadic presence in the Sesemin granitoid are to be stressed out. The omnipresence of the potash feldspar both as phenocrysts and invasively, the high value of SiO_2>65% and the narrow variation range of this parameter (72.50–75.68%), the very low values of FeO (0.01–1.15%) and Fe_2O_3 (0.02–1.34%), and the values for Y and Nb (40–50 ppm and 10–26 ppm) are also to be mentioned.

These crustal-anatectic magmas underwent the influence of some melts coming from the oceanic crust and/or the upper mantle because the granitoids show values of Na_2O>3.0% (3.03–4.95% for the Ogradena granitoid and 3.27–4.76% for the Sesemin granitoid); in most cases Na_2O>K_2O. These values are specific to the granites of type I.

The influence of the melts coming from the mantle is argued by Robu and Robu (1992) based on the study on the morphology of the zircon crystals belonging to the Ogradena granitoid. The lamprophyric dykes are also the result of the differentiation of a fluid phasis from the mantle.

Table 2

Minor elements contents (ppm)

(m, minimum values; M, maximum values; $\bar{X}$, arithmetic mean; n, samples number; NT, undetermined)

Symbol		Pb	Cu	Sn	Mo	Ga	Ni	Co	Cr	V	Sc	Zr	Be	Nb	Yb	Y	La	Sr	Ba
GB-DI	m	<2	9.5	<2	NT	14	30	21	110	140	23	180	NT	NT	2.6	30	<30	520	470
n=2	M	6	16	5	NT	18	60	36	330	310	28	180	NT	NT	2.8	34	57	600	1500
	$\bar{X}$	~ 3	12.5	~ 3	-	16	45	29	220	225	25.5	180	-	-	2.7	32	~ 40	560	985
GO	m	12	1	<2	<2	13	2	<2	3	2.5	2	20	1.6	<10	0.7	10	<30	120	400
n=15	M	41	5.5	4	2	19	5.5	<2	8	8	4	110	4.0	14	3.3	26	<30	480	1200
	$\bar{X}$	26	2.8	2	~ 2	16	4	<2	4.9	5.8	2.4	64.5	2.7	~ 10	1.8	17	<30	315	957
GS	m	8.5	3.5	<2	NT	8.5	<2	<2	<2	<2	<2	14	NT	NT	<1	<10	<30	95	280
n=6	M	20	6.0	<2	NT	13	<2	<2	4	6	4	65	NT	NT	4.4	26	<30	180	800
	$\bar{X}$	11.7	5.1	<2	–	11.2	<2	<2	~ 3	~ 2	~ 2	34	–	–	~ 2	~ 18	<30	141	513
GDP	m	10	3	3	<2	17	8.5	5.5	16	34	5.5	135	1.7	10	1.8	14	32	530	920
n=3	M	12	5	3.5	4	19	12	8	17	44	7	165	2.1	15	2	17	32	720	1000
	$\bar{X}$	10.5	3.6	3	~ 2	18	11	7.3	16.5	40.6	6.6	155	1.6	13.3	1.9	16	32	656	973
AP	m	24	3	<2	<2	16	4	<2	4	2.5	3.5	27	2	10	1.5	19	<30	83	270
n=3	M	46	4.5	4.5	2.5	21	6	<2	6	9	4	240	3.5	17	3.4	31	65	300	1050
	$\bar{X}$	34	4	~ 3	~ 2	18	4.7	<2	4.6	5.3	3.6	103	2.6	13	2.7	26	~ 35	250	717

Symbols: GB-DI, metagabbrodiorites; GO, Ogradena Granitoids; GS, Sesemin Granitoids; GDP, porphyry granodiorite; AP, aplites.

Analyst: Irina Bratosin

References

Andreeva, E.D., Bogatikov, O.A., Borodaevskaia, M.B. (1981) Klassificaţia i nomenklatura magmaticeskih gornîh porod. Ed. Nedra, 159 p., Moskva.

Anastasiu, N. (1976) Masivul granitoid Ogradena. Studiu petrografic şi geochimic. *An. Inst. Geol.*, XLIX, p. 5–151, Bucureşti.

Chappell, B.W., White, A.J.R. (1974) Two contrasting granite types. *Pac. Geol.*, 8, p. 173–174.

Didier, J., Duthou, J.L., Lameyre, J. (1982) Mantle and crustal granites: genetic classification of orogenic granites and the nature of their enclaves. *Jour. Volcan. Res.*, 14, p. 125–132, Elsevier Sci. Pub. Comp. Amsterdam.

Hine, R., Williams, J.S., Chappell, B.W., White, A.J.R. (1978) Contrasts between I and S type granitoids of the Kosciusko batholith. *J. Geol. Soc. Aust.*, 25, p. 219–234.

Hussein, A.A.A., Ali, M.M., El Ramly, M.F. (1982) A proposed new classification on the granites of Egypt. *Jour. Volc. Geoth. Res.*, 14, p. 187–198, Elsevier Sci. Publ. Comp. Amsterdam.

O'Connor, J.T. (1965) A classification for quartz-rich igneous rocks based on feldspar ratios. U.S. Geol. Surv. Prof. Paper, 525-B, p. 79–84.

Pearce, J.A., Gale, G.H. (1977) Identification of ore-deposition environment from trace-element geochemistry. In Volc. Processes in Ore Genesis. Inst. Min. Metall. and Geol. Soc., London, p. 14–24.

Robu, N., Robu, L. (1992) Étude des cristaux de zircon de quelques granitoïdes de Banat (Ogradena, Cherbelezu, Sfîrdin, Cerna). *Rom. J. Mineralogy*, 75, p. 91–99, Bucureşti.

Stan, N. (1995) Tectogenetic transformations in the Pre–Alpine geologic basement of the Orşova–Topleţ–Băile Herculane Region (Banat-South Carpathians). *Rom. J. Tect. Reg. Geol.*, 76, p. 83–86, Bucureşti.

Streckeisen, A. (1973) Classification and Nomenclature of Plutonic Rocks, Recommendations. *N.Jb. Miner.*, 2–3, p. 144–240, Stuttgart.

White, A.J.R., Chappell, B.W. (1983) Granitoid types and their distribution in the Lachlan Fold Belt, southeastern Australia. *Mem. Geol. Soc. Am.*, 159, p. 21–34.

Received: January 18, 1993.
Accepted: February 1, 1993.

Rom. J. Petrology, 77, p. 11–22, Bucureşti, 1996

PETROGENETIC AND TECTONIC SIGNIFICANCE OF REE AND SOME TRACE ELEMENTS IN THE GRANITOID ROCKS OF BANAT

Nicolae STAN, Ion TIEPAC

Institutul Geologic al României. Str. Caransebeş 1, 79 678 Bucureşti 32

Key words: Granitoid rocks. REE. Minor elements. Partial melting of the crust. Eclogitic sources. Collision. Late-post-kinematic. Metagreywacke.

Abstract: The REE contents and the LREE/HREE ratios of the granitoid rocks in Banat are low (Tabs. 1,2). The Eu anomaly is absent, excepting the samples 723 and 13 (Figs. 1, 2). These data are in agreement with the hypothesis of partial melting of the continental crust as a magmatic source. The Ogradena, Cherbelezu and Sfârdin granitoids (Danubian basement) occurred probably as a result of the anatexis of some biotite plagioclase gneisses (metagreywacke). The Sicheviţa granitoid (Getic basement) formed probably by the partial fusion of some eclogitic sources in connection with sources originating in metagreywacke. The two negative anomalies indicate that feldspar was involved in a certain stage of the granitoid genesis. The analysis of the elements illustrates also the part played by the mantle and/or oceanic crust in the granitoids formation. However, the main part was played by the continental crust. Granitoids formed by collision under late- or post-kinematic conditions (Figs. 7,9).

Introduction

The granitoids of the South Banat belong to the orogenic belt of the South Carpathians.

The Sicheviţa intrusions situated in the tectonic unit of the Getic Nappe are represented by monzogranites, syenogranites, granodiorites, tonalites and trondhjemites (Stan et al., 1992). The Ogradena, Cherbelezu and Sfârdin intrusive bodies are situated in the Danubian tectonic unit. In petrographic respect, these massifs consist of monzogranites, syenogranites and, to a less extent, of granodiorites (Stan and Tiepac, 1994). The granitoids of Banat are intruded into Precambrian and/or Cambrian formations (Savu, 1979), of Barrovian type, metamorphosed in the almandine amphibolite facies (Bercia, Bercia, 1975; Savu, 1979).

The chemical parameters resulting from the processing of the major elements led to the conclusion that the granitoid rocks are mainly of crustal-anatectic origin but the origin sources underwent also the influence of magmas originating in the mantle, or/and the oceanic-basaltic crust. The granitoids are peraluminous (Mol. $Al_2O_3/Na_2O + K_2O + CaO > 1$) and belong to S-type; only a few parameters are characterisitc of I-type (Stan and Tiepac, 1994).

The study of REE and trace elements can offer some indications on the petrogenesis and tectogenesis of the granitoids in Banat. The use of the REE and trace elements for the deciphering of the petrogenesis of the granitic rocks is quite difficult because, unlike the basic rocks, granitoids can come from quite varied sources: amphibolites or gabbros at low pressures, or eclogites at high pressures; meta-greywacke, meta-arkoses, meta-clays, granitic gneisses or other intermediary eruptive rocks or, quite probably, wet peridotites. Moreover, there are also other difficulties when modelling a petrogenetic setting, e.g.: the lack of accurate data on the conditions of melting of the sources, the way in which the REE distribution between the two phases crystal-melt changes progressively according to the variation of the pressure and temperature, etc. It is worth mentioning that many patterns using REE in order to explain the petrogenesis of the granitic rocks take mostly into account only the processes of patial melting and of fractional crystallization, thus simplifying the more complex cases. The evolution and influence of the volatiles, magma mixtures, the liquid immiscibility are less mentioned in order to explain the REE distribution. Nevertheless, REE and trace elements offer significant information both as regards petrogenesis and tectogenesis of the granitoid rocks. All these data have to be corroborated with the field evidence concerning the relationships between the granitoid rocks and the adjacent rocks, the metamorphic facies of the crystalline schists in which they are intruded, petrography, mineralogy and geochemistry of the major elements beloging to the intrusions.

REE and trace elements contents. Petrogenetic implications

The REE and some minor elements distribution in the granitoid rocks is illustrated in Table 1; some ratios of these elements are rendered in Table 2.

The REE contents in the analysed rocks are low and they vary within a relatively narrow range: ΣREE=31.5–118.9, the mean value on rock types ranging between 46.1 and 100.5. The LREE/HREE ratios are also low, with a small or moderate variation range (6.2–104.1); the mean of the values of granitoids type varies between 18.0 and 77.5 (Tab. 2). In this respect it is of note the ratios La/Lu (cn)=2.9–68.0 (excepting sample 47 = 131.6) or La/Yb (cn) = 2.5–42.3 (excepting sample 244 = 55.4).

There is no relationship between the petrochemical composition of the rocks and the REE behaviour; the trend of the lines on diagrams is similar for most of the samples (Fig.1, Fig. 2).

The Eu anomaly is absent for most of the cases or it is poorly expressed (e.g. samples 723 and 13; Figs. 1,2). The lack of the Eu anomaly is illustrated also by the Eu/Sm ratio which, for the granitoids of Banat, ranges between 0.23 and 0.41 (Tab. 2).

The Cherbelezu, Sfârdin and Sicheviţa granitoids display high contents of LREE (La=50–100) and low contents of HREE (Lu=2–8). In case of the Ogradena granitoids the REE fractioning is quite obvious but less pronounced: LREE (La=12–16), HREE (Lu=5–12).

Similar situations with those presented above were also mentioned by Gromet and Silvers (1987) for the Rangers batholith in California, Dodge et al. (1982) for the Sierra Nevada granitoid batholith, and Toth (1987) for the Idaho batholith in Oregon.

The low values of ΣREE and of the LREE/HREE ratios – La/Lu (cn) and La/Yb (cn) – for the granitoids of Banat are compatible with the statistic values reported by Cullers and Graf (1984) for monzonites, syenogranites, granodiorites and tonalites without Eu anomaly.

The petrochemical uniformity of the Danubian granitoids from Banat (syenogranites-monzogranites, granodiorites) with small variation ranges of the major chemical elements,

Table 1

REE, trace elements contents (ppm) and SiO_2 values (%) in granitoid rocks (Banat)

Sample	Rb	Sr	Ba	Zr	Y	Nb	Ta	Hf	La	Ce	Sm	Eu	Ga	Tb	Yb	Lu	Cs	Sc	SiO_2
OGRADENA																			
712 (G)	61	410	995	42	20	10	0.61	1.20	8.90	19.70	1.90	0.73	17	0.62	2.20	0.24	1.40	3.70	74.86
723 (G)	88	570	378	20	10	10	0.94	0.90	4.20	5.60	1.10	0.25	17	0.48	1.10	0.15	2.40	1.80	74.45
724 (Gd)	85	480	694	63	18	12	2.40	1.80	13.30	21.10	2.30	0.70	19	0.29	1.60	0.23	2.10	2.40	73.73
743 (G)	74	125	586	83	10	10	0.45	2.80	23.40	35.20	2.80	0.66	13	0.33	1.10	0.16	2.90	1.90	75.68
CHERBELEZU																			
24 (Gd)	124	550	836	110	10	16	2.50	4.00	14.30	45.00	2.20	0.91	22	0.51	0.45	0.10	7.40	3.30	72.47
25 (G)	151	470	854	130	10.50	14	2.30	4.60	25.40	53.90	3.10	0.75	22	0.40	1.40	0.13	6.00	3.70	72.00
27 (Gd)	63	800	489	92	11	12	1.20	2.90	18.50	30.40	2.20	0.63	20	0.14	1.20	0.07	5.90	3.00	71.21
30 (G)	103	650	1241	110	12	18	1.70	4.00	30.20	54.60	3.60	0.86	21	0.33	1.60	0.05	4.10	3.90	69.81
38 (G)	103	470	892	90	9	10	1.80	4.10	25.30	41.00	2.40	0.77	23	0.13	1.10	0.07	7.30	3.40	71.19
45 (Gd)	102	800	859	95	10	12	1.30	3.30	20.50	34.00	2.40	0.70	22	0.23	1.00	0.06	7.30	3.50	71.51
47 (G)	84	620	1074	80	13	10	1.60	2.70	24.70	40.10	3.10	0.77	22	0.31	1.00	0.02	6.10	4.30	70.65
SFÂRDIN																			
210 (G)	114	550	1098	170	9	13	1.20	4.80	32.20	61.30	5.20	1.12	22	0.50	1.20	0.07	10.50	8.20	68.22
215 (G)	110	420	722	185	17	< 10	0.21	3.80	39.30	61.70	5.10	1.22	24	0.62	0.91	0.10	8.00	9.00	67.06
217 (Gd)	87	320	788	180	15.50	11	0.46	4.90	36.60	69.60	5.30	1.14	23	0.31	1.00	0.17	5.90	9.20	66.22
244 (G)	192	210	813	110	9	13	2.60	3.50	22.50	51.80	3.80	0.90	17	0.41	0.29	0.05	14.00	5.70	70.22
254 (G)	136	230	916	110	10	10	1.50	4.30	31.70	59.40	5.10	1.00	21	0.22	0.81	0.07	13.60	5.80	69.43
SICHEVIȚA																			
7 (G)	n.a.	170	950	80	15	< 10	0.20	2.70	21.30	31.40	2.50	0.77	13	0.48	0.65	0.18	1.90	2.80	75.67
13 (G)	n.a.	200	1500	75	11	< 10	0.20	2.10	10.90	16.50	2.60	0.55	12	0.43	0.46	0.11	2.60	1.80	75.46
40 (Gd)	n.a.	430	850	210	15	< 10	0.50	4.00	31.70	34.40	4.00	0.96	21	0.37	0.88	0.05	3.00	6.40	66.34
41 (To)	n.a.	500	750	220	16	10	0.40	3.50	24.90	32.00	3.90	1.00	19	0.47	0.77	0.13	3.40	6.30	65.85
74 (To)	n.a.	450	650	270	19	10	0.60	4.30	46.30	48.50	4.30	1.10	20	0.49	1.01	0.11	3.40	6.60	65.15
79 (Gd)	n.a.	400	1000	160	13	13	0.70	3.50	50.00	62.10	4.50	1.02	19	0.41	0.81	0.16	4.40	6.60	67.04
113 (Gd)	n.a.	420	900	200	13	10	0.30	3.60	21.60	26.00	4.00	0.90	17	0.29	0.65	0.08	3.70	5.00	66.87
122 (G)	n.a.	140	750	125	21	13	1.10	2.60	26.30	30.40	3.20	0.75	18	0.51	0.79	0.05	4.20	3.80	72.97

G = granite; Gd = granodiorite; To = tonalite; n.a. = not analysed   Analyst: I. Tiepac

Table 2
Some ratios of REE and trace elements (ppm) in granitoid rocks (Banat)

Sample	La/Lu cn	La/Yb cn	Ce/Yb cn	Eu/Sm	ΣREE	LREE/HREE	Zr/Hf	Nb/Ta	Y/Nb
					Ogradena				
712	3.90	2.70	3.20	0.38	34.40	10.00	35.00	16.00	2.00
723	2.90	2.50	1.50	0.23	47.00	6.20	22.00	11.00	1.00
724	5.80	5.60	3.70	0.30	39.40	17.30	35.00	5.00	1.50
743	15.00	14.50	8.70	0.24	63.60	38.60	29.00	22.00	1.00
mean values ($\bar{X}$)					46.10	18.00	30.20	11.00	1.40
					Cherbelezu				
24	17.00	21.90	26.00	0.41	63.50	58.60	28.00	6.40	0.60
25	20.20	12.30	10.00	0.24	85.00	42.60	28.00	6.00	0.75
27	28.10	10.30	6.50	0.28	53.20	36.20	31.00	10.00	0.90
30	64.60	12.70	8.80	0.24	92.10	44.60	28.00	11.00	0.67
38	11.40	4.60	9.80	0.32	70.80	52.90	23.00	6.00	0.90
45	36.60	14.00	9.80	0.29	59.00	45.10	29.00	9.00	0.83
47	131.60	17.20	8.90	0.23	70.00	52.20	30.00	6.00	1.30
mean values ($\bar{X}$)					70.50	47.50	28.10	7.80	0.80
					Sfârdin				
210	49.00	18.00	13.10	0.21	101.60	55.70	35.00	11.00	0.70
215	40.60	29.30	17.60	0.24	109.00	65.10	49.00	<50	1.70
217	22.70	25.10	18.30	0.21	114.00	75.30	36.00	24.00	1.40
244	48.00	55.40	49.20	0.24	79.70	104.10	31.00	5.00	0.70
254	48.60	26.80	19.20	0.20	98.30	87.40	26.00	6.60	1.00
mean values ($\bar{X}$)					100.50	77.50	35.00	11.60	1.10
					Sicheviţa				
7	12.30	22.20	12.40	0.31	57.20	42.10	30.00	<50	1.50
13	10.30	15.90	9.30	0.21	31.50	30.00	36.00	<50	1.10
40	68.00	24.30	10.00	0.24	72.30	55.20	52.00	<50	1.50
41	20.00	22.30	11.10	0.26	63.00	45.20	63.00	25.00	1.60
74	43.90	31.20	12.50	0.26	101.80	61.20	63.00	20.00	1.90
79	32.20	42.30	20.30	0.23	118.90	84.10	46.00	19.00	1.00
113	27.80	22.40	10.30	0.22	53.50	51.60	56.00	33.00	1.30
122	56.50	22.90	10.10	0.23	62.00	44.30	48.00	11.00	1.60
mean values ($\bar{X}$)					70.00	51.60	49.00		1.40

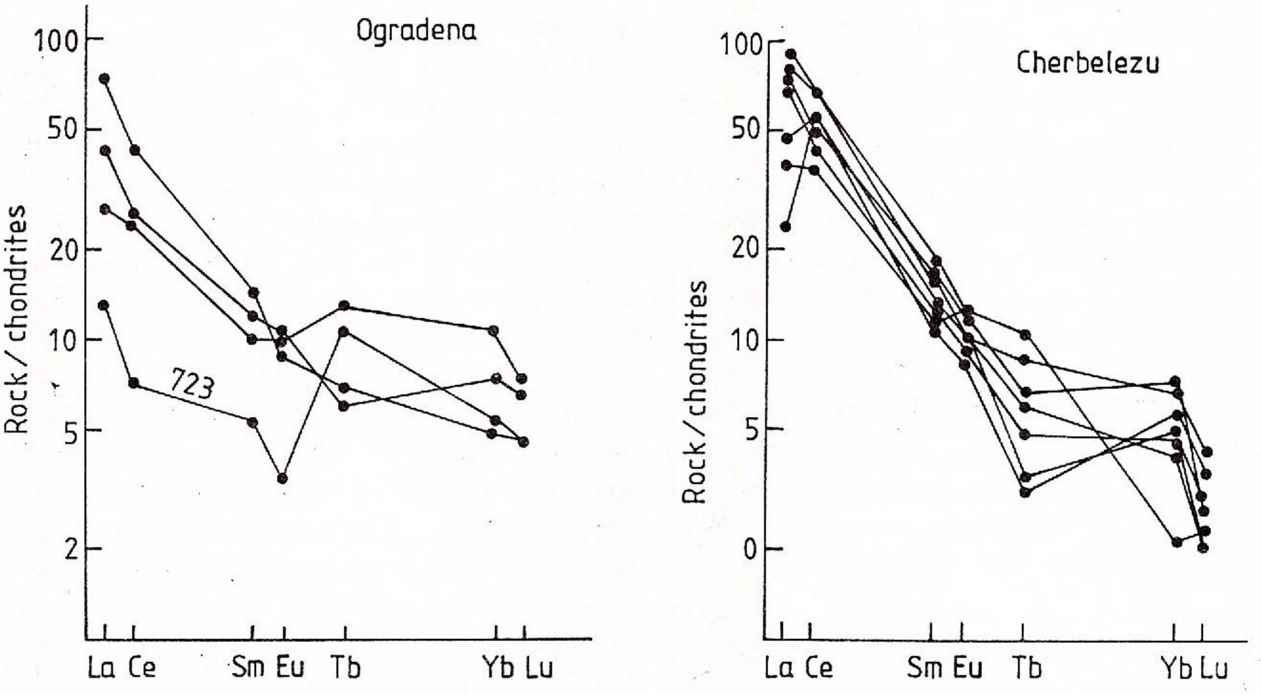

Fig. 1 – Chondrite normalized REE patterns of the Ogradena and Cherbelezu granitoids.

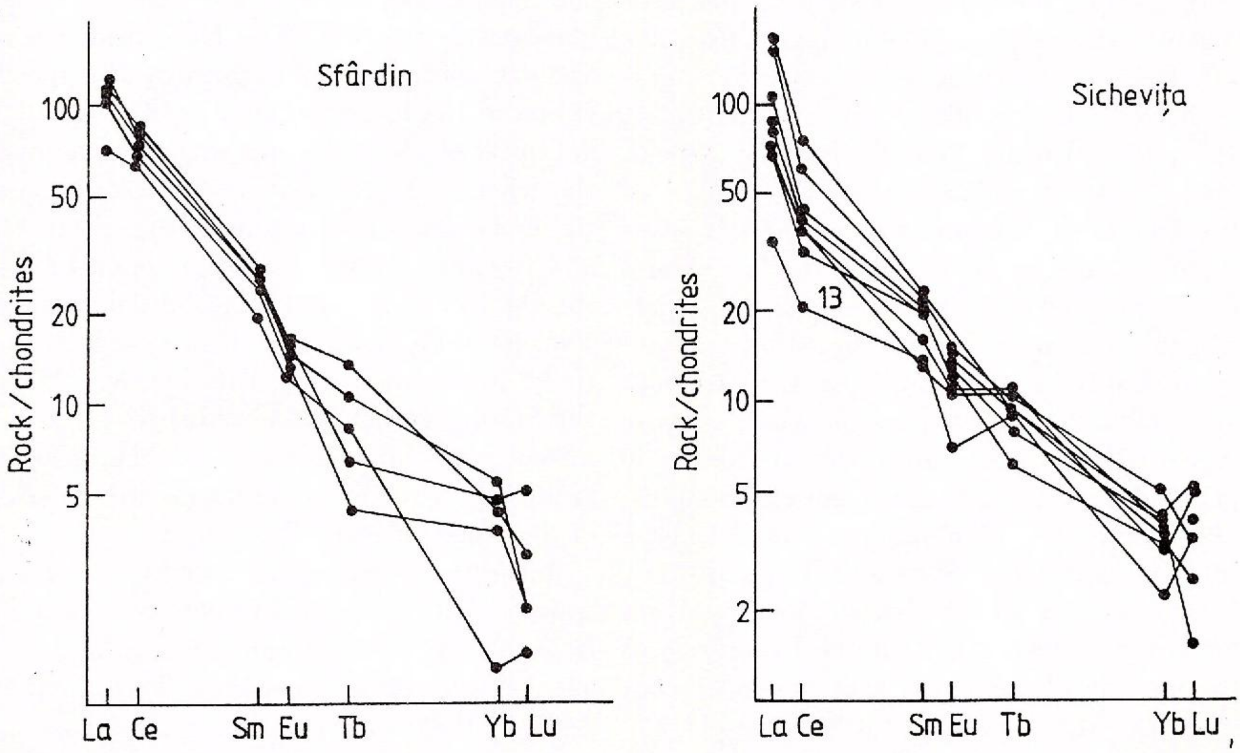

Fig. 2 – Chondrite normalized REE patterns of the Sfârdin and Sicheviţa granitoids.

corroborated with the peraluminous character of S-type of these rocks (Stan et al., 1985; Stan and Tiepac, 1994), with the absence of Eu anomaly, with the low ΣREE values and the LREE/HREE ratios suggest that these acid intrusions originate mostly in the partial melting of the crust. The granitoid rocks with such characteristics can originate, according to the researches carried out by Winkler (1979), in the melting (50%) of a biotite, quartz, plagioclase gneiss (metagreywacke), in a complex succession of reactions at a temperature of 670–690°C. The residuum consists, in such cases, of hornblende, sphene, garnet and quartz. The REE concentration is compatible with the ratios obtained in the analysed intrusive rocks (Cullers and Arnold, 1981).

In other cases, the lack of the Eu anomaly or the existence of an unsignificant Eu anomaly for monzogranites and syenogranites is justified as a result of sources devoid of residual feldspar, that cannot concentrate REE. In such situations most of the crustal sources with feldspar are out of question and, according to test data, eclogites or quartz-eclogites are frequently mentioned as source of granodiorites (Buma et al., 1971; Jahn et al., 1974, 1980; Ewing, 1979; Cullers and Arnold, 1981). It is unlikely that the source of the Ogradena, Cherbelezu and Sfârdin granitoids should be of eclogitic origin because these granitoids are little differentiated in petrographic respect. This hypothesis would be probably more suitable for the Sicheviţa granitoids, that belong to the Getic Nappe, more differentiated from the petrographic point of view (granite-granodiorites-tonalites-trondhjemites), peraluminous, of S+I-type (Stan et al., 1992; Stan and Tiepac, 1994), that also show an Eu absent anomaly. Even for the Sicheviţa granitoid the hypothesis of the melting of metagreywacke has to be considered. Moreover, the two samples (713 – Ogradena granitoid and 724 – Sicheviţa granitoid; Figs. 1,2) that display a negative Eu anomaly indicate that, at least at a certain moment, plagioclase feldspar was involved in the partial melting or fractional crystallization processes.

On the other hand, the lack of the Eu anomaly in case of the granitoid rocks might be due to the grading of Eu^{2+} to Eu^{3+}. It presumes, concomitantly with the oxidation of the magmatic chamber in course of cooling, a low pressure and a major water extraction by means of hydrothermal solutions and, therefore, REE concentration in the accessory minerals from pegmatites (Buma et al., 1971). In fact, the pegmatites from the Sicheviţa granitoids are very rare, of small sizes and constituted of: quartz, plagioclase, feldspar potash. The accessory minerals are almost lacking. Pegmatites occur only exceptionally in the Cherbelezu granitoid, whereas in the Ogradena and Sfârdin granitoids they have not been identified.

While the REE contents indicate the continental crust as origin for the granitic rocks, some ratios of the trace elements suggest that the mantle was more or less involved in the petrogenetic process. The trace elements ratios are contradictory as regards the specification of the source. Thus, Zr/Hf ratio = 30 is typical of the rocks originating in the mantle, whereas Zr/Hf ratio = 40 is characteristic of the rocks originating in the crust (Eby and Kochhar, 1990). From this point of view the Ogradena ($\bar{X} = 30$) and Cherbelezu granitoids ($\bar{X} = 28.1$) would originate, at least partially, in the melting of the mantle, whereas the Sfârdin granitoid ($\bar{X} = 35$) would have a mixed origin (mantle + crust). The Sicheviţa granitoid ($\bar{X} = 49$) would be mostly the result of the crust melting (Tab. 2).

According to Eby et al. (1992), the Nb/Ta ratio = 15–18 is typical of the magmas coming from the mantle (Hofmann, 1988), whereas the average value of the crust is 11 (Taylor and Mc Lennan, 1985). If we consider these standard values then the Ogradena ($\bar{X} = 11$), Cherbelezu ($\bar{X} = 7.8$) and Sfârdin ($\bar{X} = 11.6$) granitoids mostly come from magmas originating in the continental crust, whereas the Sicheviţa granitoid, with values ranging between 11 and 25, would originate in both, mantle and crust (Tab. 2).

Another ratio that can be taken into consideration when establishing the magmatic sources of the granitoid rocks is Y/Nb ratio (Eby et al., 1992). Thus, the magmas coming from oceanic-island basalts or from the mantle show 0.3–1.2 values, whereas the average value of the continental crust is, according to Taylor and Mc Lennan (1985), 1.8. In this respect, the Ogradena and Sicheviţa granitoids (both of them with $\bar{X}$ = 1.4) might originate in a mixed source – mantle and crust, and the Cherbelezu granitoid ($\bar{X}$=0.8) in basalt-oceanic or mantle sources, as the Sfârdin granitoid ($\bar{X}$=1.1; Tab. 2).

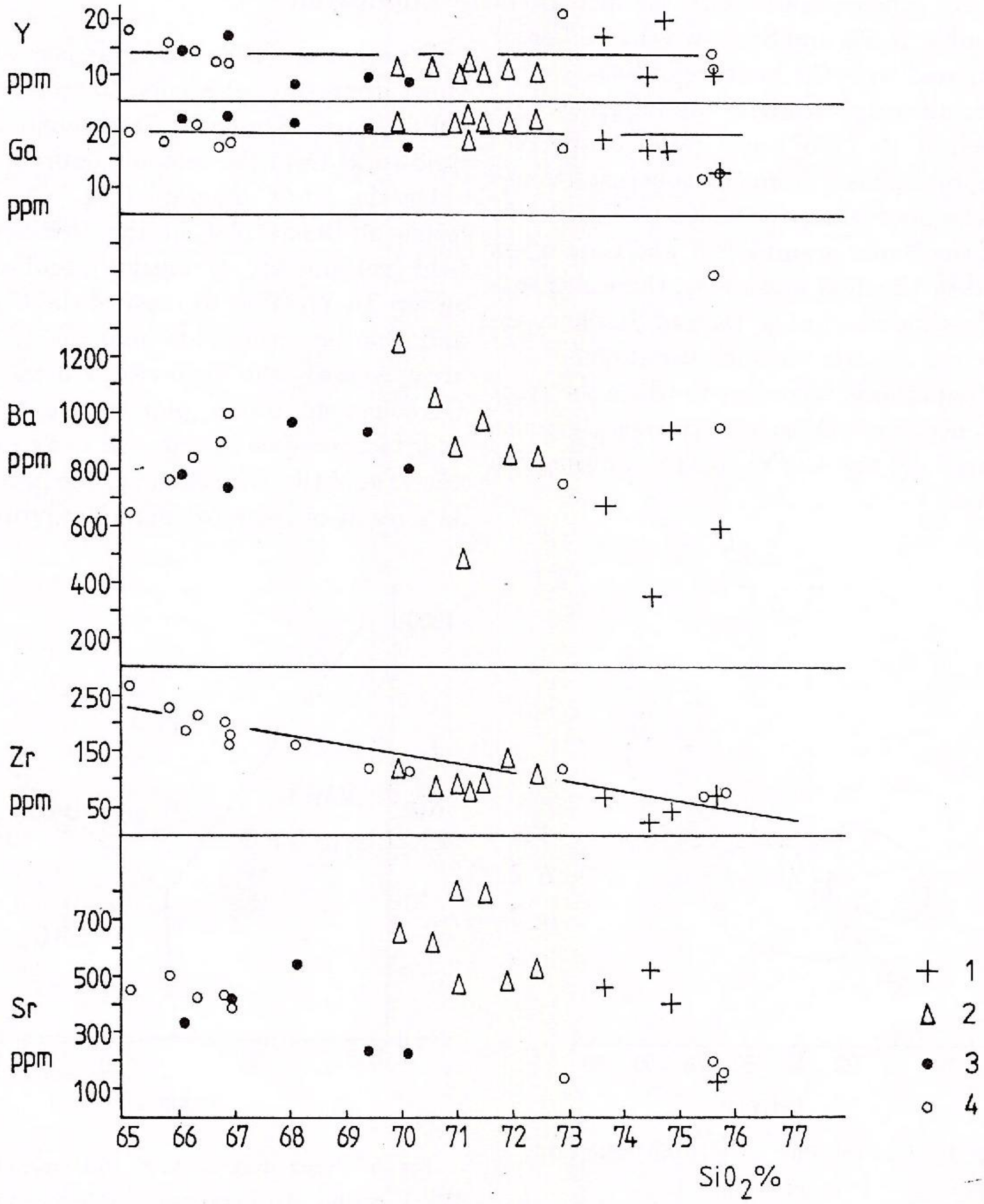

Fig. 3 – Harker diagram: SiO_2 – (Sr,Zr,Ba,Ga,Y).
1, Ogradena; 2, Cherbelezu; 3, Sfârdin; 4, Sicheviţa.

These contradictory data can be the result of the redistribution of trace elements in the crust, according to their mobility, as a result of the circulation of metasomatizing fluids coming from the mantle. In this sense one can also interpret the behaviour of the trace elements on Harker's diagram (Fig. 3): Y and Ga show quite constant values proportionally with the increase of SiO_2 value; Zr is decreasing slowly concomitantly with the increase of SiO_2; unlike it, Ba and Sr show values different as compared with the increase of SiO_2.

These aleatory variations are interpreted by Chappell et al. (1987) as a result of the successive fluid phases from the subcrustal zones in the chamber where the fusion took place. In case of the Banat granitoids Y and Ga are less affected by the fluid pulsations, these elements being less mobile, unlike Ba and Sr which are much more sensitive to such variations.

The hypothesis according to which the crust is influenced by sources from the mantle is also supported by the Ce/Yb (cn) - Ce diagram (Fig. 4).

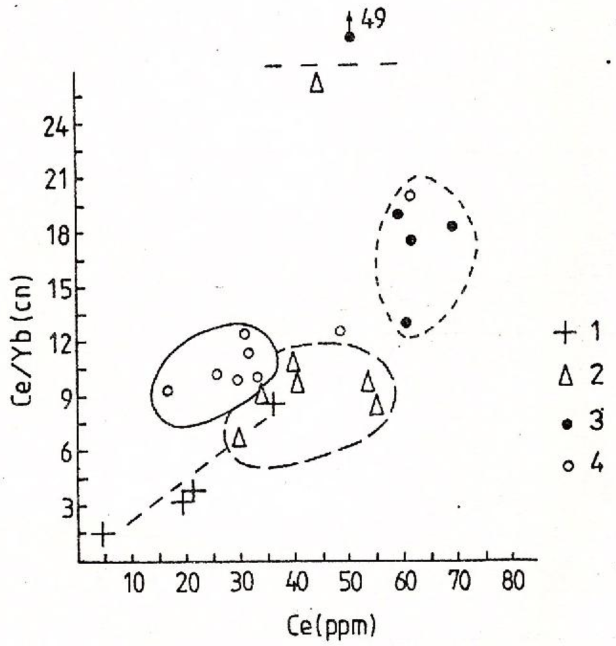

Fig. 4 – Ce/Yb (cn) – Ce (ppm) diagram. 1–4, see Figure 3.

Scott and Vogel (1980), showed that the granitoid rocks in which the Ce/Yb ratio varies proportionally to the Ce value – as in case of the Ogradena granitoids – formed by the partial melting of the sialic crust. If the rocks plotted on the respective diagram are disposed aleatory, e.g. in case of the Sicheviţa, Cherbelezu and Sfârdin granitoids, then they formed from the mantle-crust mixture.

Trace elements contents. Tectogenetic implications

Pearce et al. (1984) and Harris et al. (1986) tried, using trace elements, to make up different diagrams in order to discriminate the granitoid rocks from the tectonic point of view.

On the Nb/Y diagram (Fig. 5) the granitoids of Banat plot in the VAG + COLG field (volcanic arc + collision), and on the diagram Ta-Yb (Fig. 6) most of the Cherbelezu and Sfârdin granitoids plot in the COLG area, whereas the Sicheviţa and most of the Ogradena granitoids plot in the VAG area. This fact could be interpreted as a result of the decrease of the Ta content in the crust and/or as a result of the crust-mantle mixture.

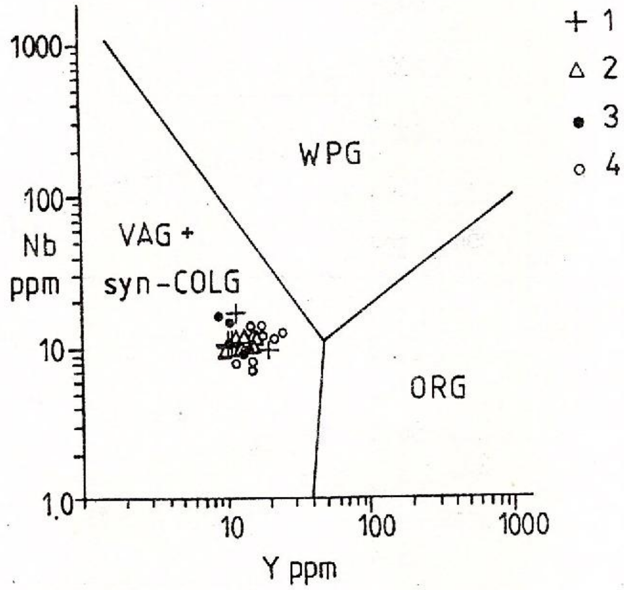

Fig. 5 – Nb–Y diagram (acc. to Pearce et al., 1984) WPG: within plate granites; VAG+Syn–COLG: volcanic arc + collisional granites; ORG: ocean ridge granites. 1–4, see Figure 3.

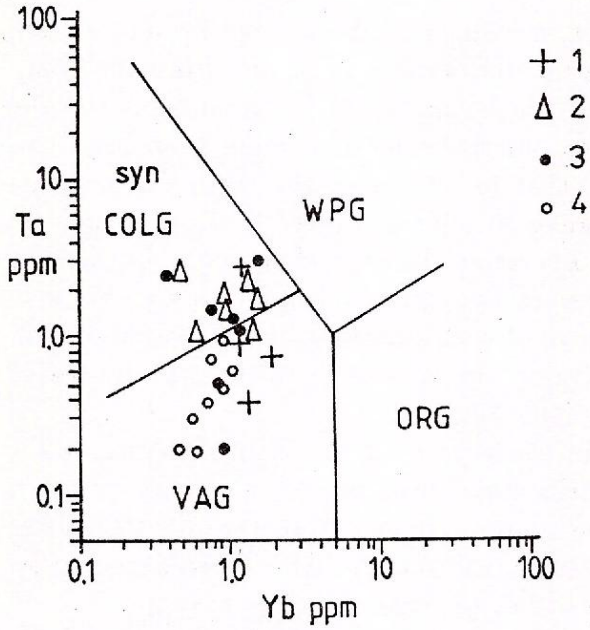

Fig. 6 – Ta–Yb diagram (Pearce et al., 1984). Legend as in Figures 3, 5.

On the Rb-(Y+Nb) diagram all granitoids (except the Sicheviţa ones, for which Rb has not been analysed) plot in the VAG area (Fig. 7).

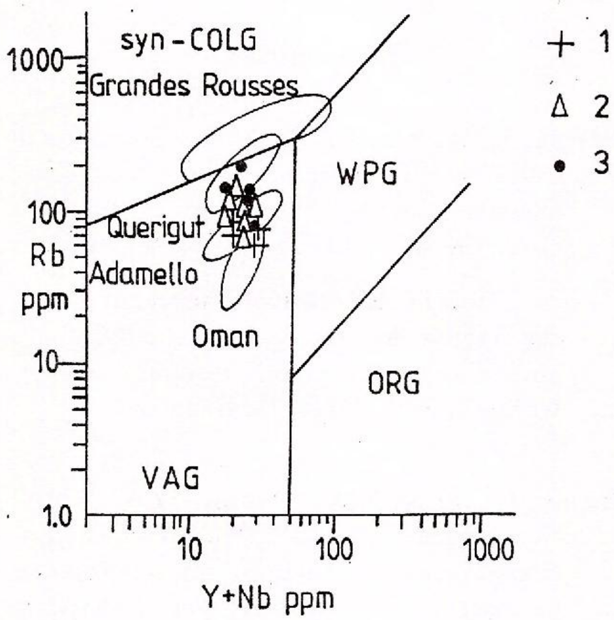

Fig. 7 – Outline of areas for some post-collisional granites in Grandes Rousses, Querigut, Adamello and Oman, on the Rb–(Y+Nb) diagram acc. to Pearce et al., 1984, as compared to the plotting of the Banat granitoids. Legend as in Figures 3, 5.

However, the field data and the geochemical data based on major elements indicate that the granitoids of Banat are of collision type (Stan and Tiepac, 1994). This fact is also confirmed by the (Rb/10) – Hf – (Ta x 3) diagram on which the granitoids surpass the COLG line, plotting in the VAG field and in the WPG field (Fig. 8); this situation was

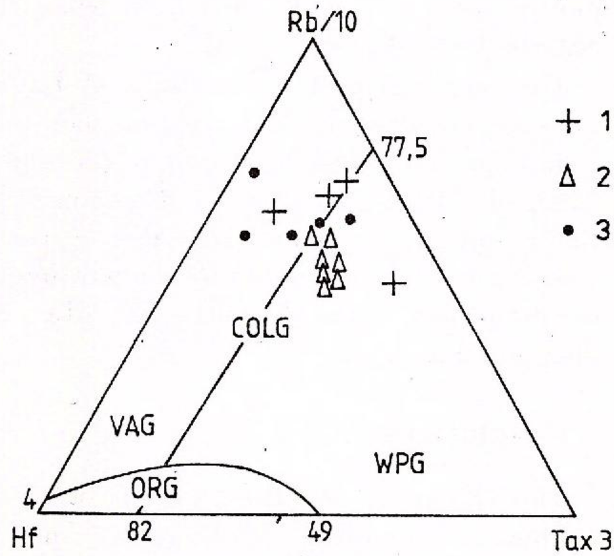

Fig. 8 – Rb/10–Hf–Tax3 diagram (acc. to Harris et al., 1986). Legend as in Figures 3, 5.

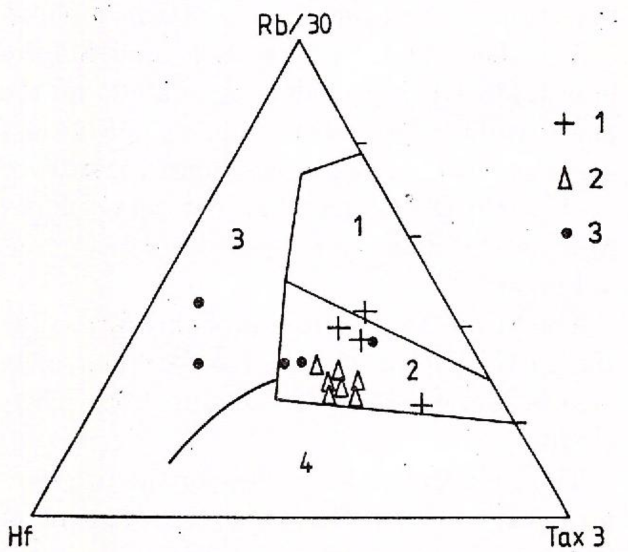

Fig. 9 – Rb/30–Hf–Tax3 diagram (acc. to Harris et al., 1986). 1, syn-collisional granites; 2, late- and post-collisional granites; 3, volcanic arc granites; 4, within plate granites.

interpreted by Harris et al. (1986) as quite characterisitc for the collision granitoids.

As regards the interpretation of the Rb – (Y + Nb) diagram (Fig. 7), Pearce et al. (1984) mentioned that sometimes the location of some collisional granitoids in the VAG field is due to the crust initially poor in Rb and Ta. Moreover, on this diagram Pearce et al. (1984) plotted some granitoids proved, on geological criteria, to be post-collisional.

The plottings of the granitoids of Banat are superposed in the VAG field on the post-collisional granitoids fields from Querigut, Adamello and Oman (Fig. 7). Consequently, the granitoids of Banat are late- or post-collisional, a fact reiterated by the plotting of the granitoids on the (Rb/30) – Hf – (Ta x 3) diagram (Fig. 9).

Conclusions

The REE contents of the granitoids of Banat are low, like the LREE/HREE ratios. The Eu anomaly is absent, excepting the samples 723 and 13 (Tabs. 1 and 2; Figs. 1,2). These data are in agreement with the hypothesis of the partial melting of the crust as magmas source.

The Ogradena, Cherbelezu and Sfârdin granitoids were probably generated by the anatexis of some biotite quartz plagioclase gneisses, that yielded a residuum constituted of hornblende, sphene, garnet and quartz. Most of the REE concentrated in these residual minerals.

The Sicheviţa granitoid probably formed by the partial fusion of some eclogitic sources in association with sources coming from metagreywacke.

The Eu negative anomalies for the two samples (723 and 13) show the involvement of feldspar, during a certain stage, in the genesis of the granitoids (Figs. 1,2).

The analysis of the trace elements suggests also the involvement of the mantle and/or oceanic crust in the formation of the granitoids. The trace elements indicate, for the acid intrusions of Banat, both sources from the mantle/oceanic crust and from the crust. This can be explained by the influence of the metasomatizing fluids coming from the mantle, that redistributed the trace elements according to their mobility. Here, one can take into account the ever changing conditions of pressure and temperature from the melts in course of consolidation, the isomorphous substitution affinities of the elements, the size of the ionic ray, etc.

In the genesis of the Banat granitoids the continental crust played a dominant part. The sources coming from the mantle and/or oceanic crust were probably more abundant for the Sicheviţa granitoids (Getic Nappe) as compared to the Ogradena, Cherbelezu or Sfârdin granitoids (Danubian unit).

The granitoids of Banat formed, as illustrated on some diagrams based on trace elements (Figs. 5,8), by continent-continent collision. The granitoids were emplaced under late or post-kinematic orogenic conditions (Figs. 7,9).

References

Bercia, I., Bercia, E. (1975) Formaţiunile cristaline din sectorul românesc al Dunării (Banat – Carpaţii Meridionali). *An. Inst. Geol., Geofiz.*, XLIII, p. 5–13, Bucureşti.

– , **Bercia, E. (1980)** The crystalline of the Danube domain from the Banat (Romania). *Rév. Roum. Géol., Géophys., Géogr., Géologie*, 24/1, p. 13–33, Bucureşti.

Buma, G., Frey, F.A., Wones, D.R. (1971) New England Granites: Trace Element Evidence Regarding Their Origin and Differentiation. *Contr. Mineral. Petrol.*, 31/4, p. 300–320.

Chappell, B.W., White, A.J.R., Wyborn, D. (1987) The importance of Residual Source Material (Restite) in granite petrogenesis. *J. Petrol.*, 28 b, p. 1111–1138.

Cullers, R.L., Graf, J.L (1984) Rare Earth Elements in Igneous Rocks of the Continental Crust: Intermediate and silicic rocks-ore petrogenesis. In: Henderson (Edition) Rare Earth Geochemistry. Developement in Geochemistry, 2, p. 275–308.

Dodge, F.C.W., Millard, H.T., Elsheimer, H.N. (1982) Compositional variations and abundances of selected elements in granitoid rocks and constituent minerals, Central Sierra Nevada batholith, California. *Geol. Surv. Prof. Paper*, 1248, 24 p., Washington.

Eby, G.N., Kochhar, N. (1990) Geochemistry and Petrogenesis of the Malani Igneous Suite, North Peninsular India. *Jour. Geol. Soc. India*, 36, p. 109–130.

– , Krueger, H. W., Creasy, J.W. (1992) Geology, geochronology and geochemistry of the White Mountain batholith, New-Hampshire. In: Puffer, J.H. and Ragland, P.C. (Editors). Eastern-North American Mesozoic Magmatism: Geological Society of America. Special Paper, 268, p. 379–397.

Ewing, T.E. (1979) Two calc-alkaline volcanic trends on the Archean: trace element evidence. *Contrib. Mineral., Petrol.*, 71, p. 1–7.

Hanson, G.N. (1978) The application of trace elements to the petrogenesis of igneous rocks of granite composition. *Earth Planet. Sci. Lett.*, 38, p. 26–43.

Harris, N.B.W., Pearce, J.A., Tindle, A.G. (1986) Geochemical characteristics of collision – zone magmatism. In Coward MP and Reis A.C., (Editors). Collision tectonics. *Spec. Publ., Geol. Soc.*, 19, p. 67–81.

Jahn, B., Sun, S.S., Nesbitt, R.W. (1974) REE distribution and petrogenesis of the Spanish Peaks igneous complex, Colorado. *Contrib. Mineral. Petrol.*, 70, p. 281–298.

– , Auvray, B., Blais, S., Capdevila, R., Cornichet, J., Vidal, R., Hameurt, J. (1980) Trace element geochemistry and petrogenesis of Finnish greenstone belts. *J. Petrol.*, 21, p. 201–244.

Pearce, J.A., Harris, N.B.W., Tindle, A.G. (1984) Trace Element Discrimination Diagrams for the Tectonic Interpretation of Granitic Rocks. *Jour. Petrol.*, 25/4, p. 956–983.

Rollinson, H. (1993) Using Geochemical data: Evaluation, Presentation, Interpretation. Logmar Sci. Teh., 351 p., New York.

Savu, H. (1979) Crystalline schists, Precambrian granitoid rocks and associated metallogenesis from the Getic nappe unit (Banat). *Rev. Roum. Géol., Géophys., Géogr., Géologie*, 23/2, p. 123–136, Bucureşti.

Scott, G.B., Vogel, T.A. (1980) The Origin of the Acidic and Basic Rocks of the Tichka Massif, Marocco, Based on Rare Earth Elements. *Contrib. Mineral., Petrol.*, 75, p. 89–95.

Stan, N. (1985) Cherbelezu and Sfârdin granitoids. Their relationships with the adjacent rocks. *D.S. Inst. Geol. Geofiz.*, LXIX/1, p. 167–180, Bucureşti.

– , Udrescu, C., Colios, E. (1985) Petrochemical study of the Cherbelezu and Sfârdin granitoids and the associated vein rocks. *D.S. Inst. Geol. Geofiz.*, LXIX/1, p. 181–193, Bucureşti.

– , Tiepac, I. (1994) Characterization S–I type granitoid rocks from Banat Region (South Carpathians). *Rom. J. Petrol*, 76, p. 33–39, Bucureşti.

Taylor, S.R., Mc Lennan, S.M. (1985) The continental crust: its composition and evolution. Blackweld, Oxford.

157939

Toth, M.T. (1987) Petrology and origin of the Bitterrost lobe of the Idaho batholith. In: L.T. Vallier and C.H. Brooks (Editors), Geology of the Blue Mountains Region of Oregon, Idaho and Washington; The Idaho Batholith and Its Border zone. *U.S. Geol. Surv. Prof. Paper*, 1436, p. 9–35.

Winkler, H.G.F. (1979) Petrogenesis of Metamorphic Rocks. 237 p., Springer-Verlag, New York.

Received: March 7, 1995.
Accepted: April 3, 1995

Rom. J. Petrology, 77, p. 23–30, Bucureşti, 1996

PETROCHEMICAL CHARACTERIZATION OF THE SYENITES IN BANAT (ROMANIA). REE AND TRACE ELEMENTS CONTENTS: PETROGENETIC AND TECTOGENETIC CONSEQUENCES

Nicolae STAN, Ion TIEPAC

Institutul Geologic al României. Str. Caransebeş 1, 79 678 Bucureşti 32

Key words: Syenites. REE. Trace Elements. Major Elements. Eu anomaly. Mantle. Continental Crust.

Abstract: The syenitic bodies (Jurassic – pre-Oligocene) are penetrating the granitic-crystalline basement of Precambrian-Cambrian age (Fig. 1). Syenites display a concentric structure: the central part is made up of nepheline syenites, and the peripheral part of alkali syenites. The rocks show peralkaline-peraluminous (Fig. 3), sub-agpaitic characteristics (Figs. 4,5). The ΣREE contents are relatively low: for nepheline syenites they are ranging between 94.5 and 151.7, and for alkali syenites the values increase up to 290.5 (Tab. 3). Eu anomaly is positive for most of the nepheline syenites and it is absent for the alkali syenites (Fig. 6). It indicates that the nepheline syenites are "cumulates" and that the alkali syenites at the periphery have been influenced by the continental crust. The ratios Nb/Ta=9.5–21.7 and Y/Nb=0.1–0.3 (Tab.3) point out that the rocks originate in the mantle. Nb–Y and Ta–Yb diagrams (Figs. 8,9) and 10,000 x Ga/Al–(Nb,Zr, partially Ce,Zn) diagrams (Fig. 7) prove the A-type anorogenic character of the syenites in Banat. The syenitic rocks are the result of the partial melting of peridotites in the mantle under conditions of distension caused by the reactivation of old faults and shear zones of the continental crust.

Introduction

The syenitic rocks in the South Banat (Fig. 1) are cropping out sporadically on reduced areas on a NNE–SSW trending alignment of 7–8 km coinciding with an old tectonic dislocation, probably of Cambrian age (Stan, 1985). Syenites were described by Streckeisen and Giuşcă (1932), Codarcea (1937) and Anastasiu (1973, 1976).

The syenitic bodies penetrate both the Precambrian-Cambrian crystalline basement of the Neamţu group and the Ogradena calc-alkaline granitoid, probably of Old Caledonian age (Codarcea, Pavelescu, 1963). According to Anastasiu (1976), these small alkaline bodies display a concentric structure: the central part consists of nepheline syenites, and the marginal zone of alkali syenites. The rock texture is massive.

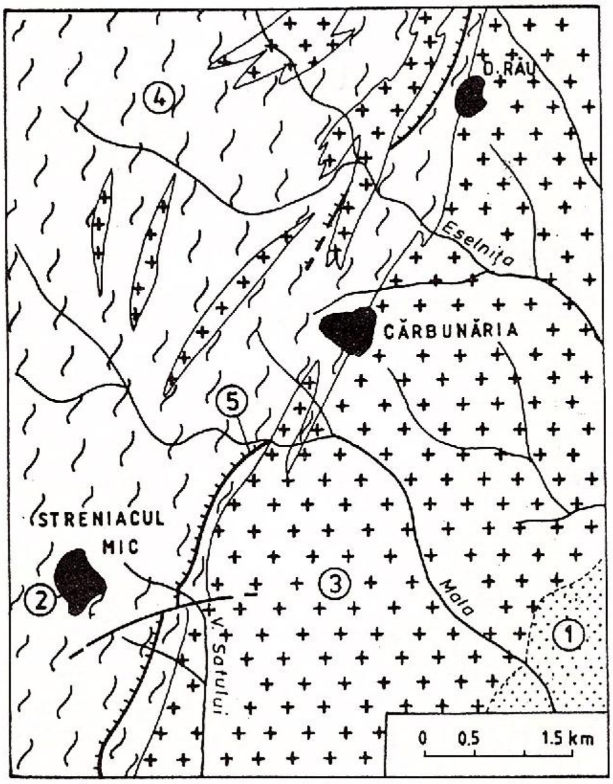

Fig. 1 – Location of syenite rocks and geologic setting. 1, Neogene deposits; 2, nepheline and alkali syenites; 3, calc-alkali granitoids (Ogradena); 4, crystalline schists (Neamţu); 5, reverse faults.

Mineralogic and petrographic data

The nepheline syenites (foyaite) show fanerocrystalline, hipidiomorphic, more rarely microcrystalline, structures. Mineralogic composition: micropertites and microcline-pertites, with frequent Karlsbad twins. The poikilitic structures are determined by nepheline augite–egyrine and apatite inclusions. Plagioclase feldspar is locally substituted by albite. Nepheline is frequently corroded by cancrinite. Sodalite occurs as masses at the expense of nepheline.

Alkali syenites are mostly feldspathic with a few femic minerals. Mineralogic composition: perthite, microcline-perthite, albite, micas and iron oxides. They show an allotriomorphic, microgranular, in places fanerocrystalline structure.

The accessory minerals of syenites are represented by zircon, apatite, sphene, rarely epidote and garnet.

Analysis of major elements of REE and trace elements: petrogenetic consequences

The primary analytical data for the characterization of syenites are presented in tables 1 and 2.

On the R_1–R_2 diagram (Fig. 2) four analyses plot in the nepheline syenites field and one analysis in the alkali syenites field.

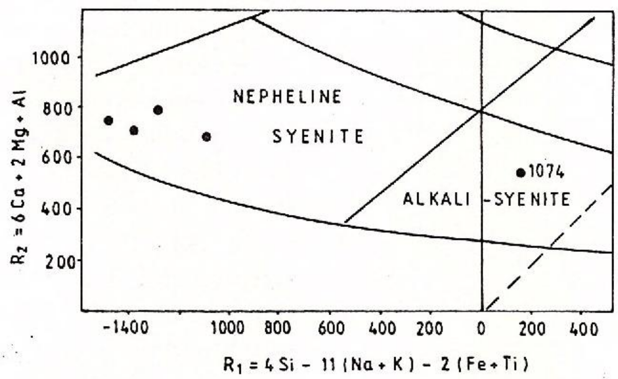

Fig. 2 – R_1–R_2 diagram (De la Roche et al., 1980).

The rocks are subsaturated in silica: SiO_2=51.90–55.35 %, but suprasaturated in alumina: Al_2O_3=20.20–21.44 %. Alkalies are found in great amounts: Na_2O=7.97–9.03 % (excepting sample 1074 where Na_2O represents 2.43 %); K_2O=6.94–10.77 %; Na_2O+K_2O=13.20–16.13 % (Tab.1).

Among the trace elements, Zr (310–580 ppm), Nb (120–230 ppm), Sr (frequently more than 1000 ppm), and Ba (1100–2100 ppm) occur in great amounts. Yb, Lu, Cs, Sc, Pb, Cu, Zn, Ni, Co, Cr are found in small or very small amounts (Tab. 2).

The rocks are peralkaline or peraluminous (Fig. 3) and they could be classified, accord-

Table 1

Major elements contents (%)

Sample no.	Locality	Rock type	SiO_2	TiO_2	Al_2O_3	Fe_2O_3	FeO	MnO	MgO	CaO	K_2O	Na_2O	P_2O_5	H_2O	CO_2	S	Total
1074	Carbunaria	Sy–alk	55.35	0.94	21.44	5.43	0.02	0.27	0.63	0.22	10.77	2.43	0.08	1.04	0.80	0.23	99.65
04	Streniacul Mic	Sy–nef	53.21	0.59	20.80	2.93	0.36	0.18	0.49	2.40	7.27	8.09	0.08	1.69	1.50	0.19	99.78
01		Sy–nef	52.69	0.51	21.14	3.10	0.44	0.19	0.43	2.39	8.16	7.97	0.16	1.50	1.00	0.20	99.50
03		Sy–nef	52.17	0.68	20.60	2.74	1.43	0.21	0.58	3.14	6.94	8.41	0.21	1.50	1.00	0.21	99.82
02		Sy–nef	51.90	0.58	20.20	3.53	0.69	0.23	0.48	3.18	7.07	9.03	0.23	1.68	1.00	0.17	99.97

Sy–alk = alkali syenites; Sy–nef = nepheline syenites

Analyst: Erna Călinescu

Table 2

REE and trace elements contents (ppm)

Sample no.	La	Ce	Sm	Eu	Tb	Y	Yb	Lu	Zr	Hf	Ta	Nb	Cs	Sc	Sr	Ba	Pb	Cu	Zn	Ga	Ni	Co	V
1074	110.7	168.1	7.5	2.6	1.0	35	0.2	0.2	540	5.6	12.6	180	2.4	0.5	280	2100	20	12	110	17	3.5	1.9	63
04	17.9	68.9	5.1	1.0	0.3	22	2.1	0.2	310	3.7	12.6	120	1.3	0.6	>1000	2000	3	4	62	16	2.0	1.9	50
01	16.8	79.0	3.4	1.7	0.4	13.1	1.2	0.2	450	4.9	9.4	170	2.0	0.5	>1000	1100	10	5	72	18	4.0	1.5	83
03	27.8	112.0	6.0	3.3	0.6	49	1.7	0.3	320	5.2	14.3	170	1.0	0.8	1000	1250	2	4	62	15	5.0	1.9	95
02	26.6	101.8	4.2	2.1	0.3	17	1.8	0.2	580	6.0	10.6	230	2.8	0.6	>1000	1300	6	8	65	18	5.0	1.8	86

Analysts: I. Tiepac, Irina Bratosin

ing to Edgar's criteria (1974) and Currie's diagrams (1976), as sub-agpaitic syenites (Figs. 4, 5).

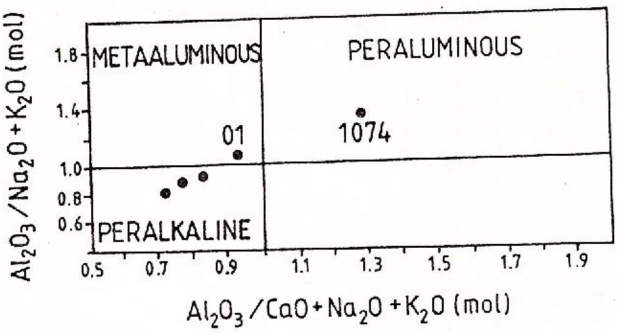

Fig. 3 – Al/Alk–Al/Alk+C (Mol.) diagram.

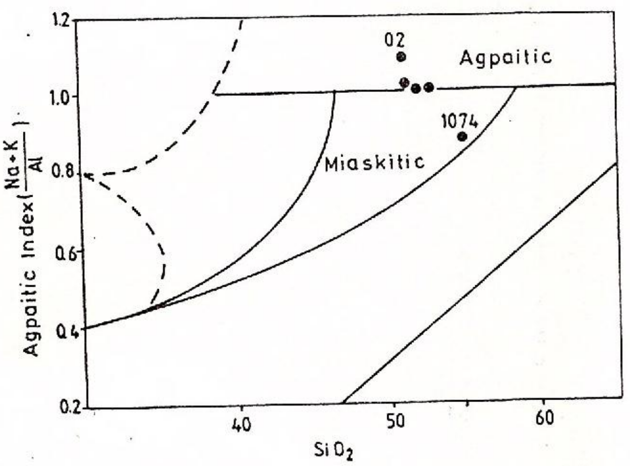

Fig. 4 – SiO_2–AI diagram.

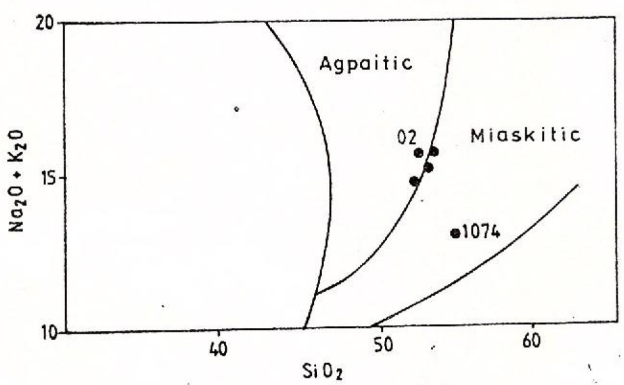

Fig. 5 – SiO_2–Na_2O+K_2O diagram.

The REE contents (ppm) of the syenitic rocks are relatively low, varying within a small interval: ΣREE=95.4–151.7, excepting sample 1074, where the ΣREE contents represent 290.5 (Tab. 3).

Table 3

REE and trace elements ratios (cn and ppm)

Sample	1074	04	01	03	02
La/Lu (cn)	119	9.6	10.8	8.7	13.2
La/Yb (cn)	502	5.8	9.5	11.0	9.9
Ce/Yb (cn)	293	8.5	17.1	17.0	14.6
Eu/Sm	0.3	0.2	0.5	0.5	0.5
ΣREE	290.2	95.4	102.6	151.7	137.0
LREE/HREE	204.5	35.6	56.3	55.8	57.1
Zr/Hf	96.4	83.8	91.8	61.5	96.6
Nb/Ta	14.3	9.5	18.1	11.9	21.7
Y/Nb	0.2	0.2	0.1	0.3	0.1

The LREE/HREE ratios range within the interval 35.6–57.1, excepting sample 1074 whose ratio is higher: 204.5. The La/Lu(cn), La/Yb(cn) and Ce/Yb(cn) ratios are illustrated in Table 3.

Eu anomaly for three out of five samples is positive, whereas for samples 04 and 1074 this anomaly is absent (Fig. 6).

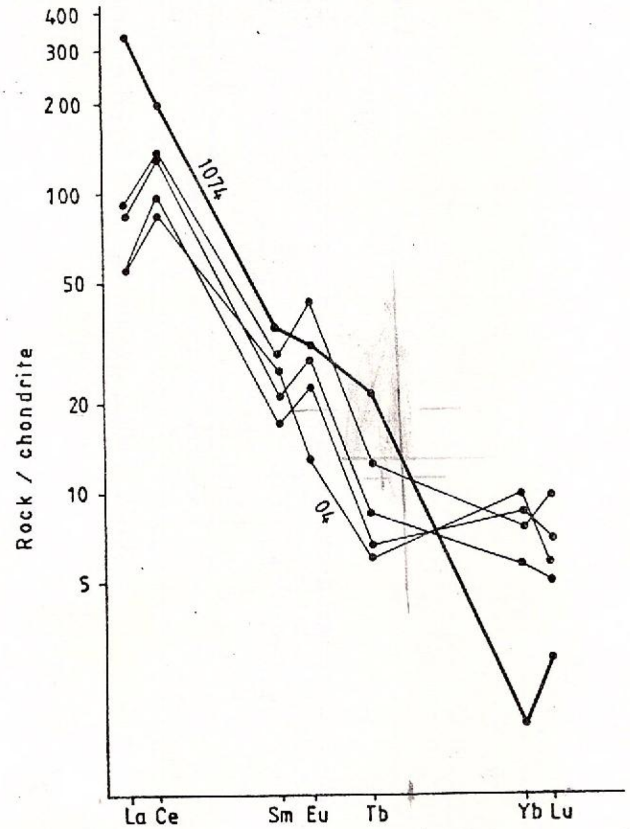

Fig. 6 – Chondrite-normalized REE patterns of the syenite rocks.

The positive Eu anomaly in such alkali rocks is interpreted as a result of the cumulus of feldspars resulting from the fractioning of melts coming from the mantle (Jones, Larsen, 1985; Garcia, 1988; Eby, Kochhar, 1990; Coneico et al., 1991). The lack of Eu anomaly signifies the absence of feldspar from the crystallization system (Buma et al., 1971; Jahn et al., 1979) or the oxydation of Eu^{2+} to Eu^{3+} in the system (Cullers, Graf, 1984).

Zr/Hf ratio is very high, ranging between 61.5 and 96.6; exceeding the average value is 30, typical of the rocks originating in the mantle, or 40, typical of the rocks originating in the continental crust; marker values estimated by Eby and Kochhar (1990). Unlike it, Nb/Ta ratio of 15–18, typical of the magmas coming from the mantle (Hofmann, 1988, mentioned by Eby et al., 1992), superposes to a large extent over the Nb/Ta values of the syenitic rocks in Banat (9.5–21.7) (Tab. 3). Likewise, Y/Nb ratio ranging between 0.1 and 0.3 (Tab. 3) is very close to the values 0.3–1.2 mentioned by Eby et al. (1992) as characteristic of the magmas originating in ocean sources – basalt island or in the mantle. Y/Nb ratio specific to the continental crust is, according to Taylor and Mc Lennan (1985), much higher (1.8).

Tectogenetic considerations

The crystalline-granitic basement penetrated by the syenitic rocks is of Precambrian–Cambrian age (Codarcea, Pavelescu, 1963). The age of the syenitic rocks in Banat is not specified yet. By comparison with rocks of the same origin from close areas whose age is well documented, e.g. the Ditrău syenites (Streckeisen, Hunziker, 1974) or the alkali rocks south of the Danube (Terzici, 1983), one can presume that they might be Jurassic or more probably post-Cretaceous – ante-Oligocene in age.

Syenites in Banat are situated in a zone that belongs to a stabilized mobile belt (Anastasiu, 1973). The location of many alkali magmas in a late post-orogenic regime is mentioned by Pitcher (1982, 1987). From the tectonic point of view, the syenites in Banat are of A-type (alkali, anorogenic, sensu Loiselle and Wones, 1979), in places modified, in chemical respect, by the crystalline-granitic basement penetrated by them (Fig. 7).

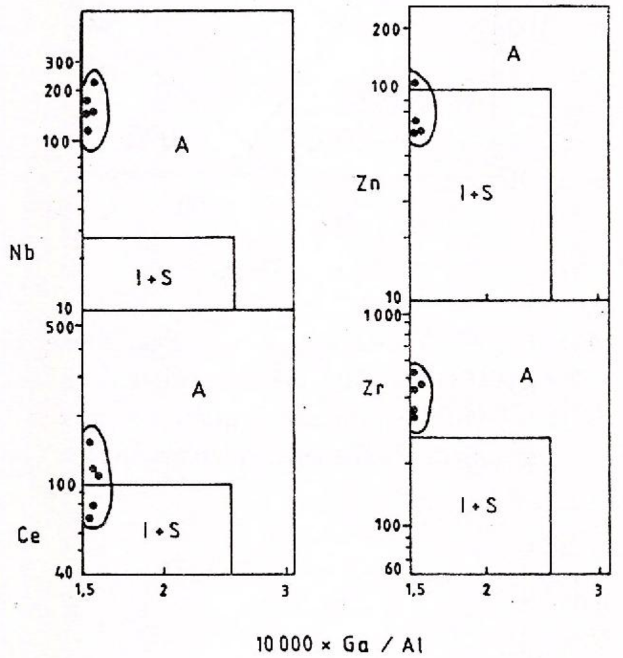

Fig.7 – 10.000 Ga/Al–(Ce,Nb,Zr,Zn) diagram acc. to Whalen et al., 1987: I–type; S–type; A–type.

The anorogenic character is illustrated also on the diagrams by Pearce et al. (1982) (Figs. 8,9).

The alkali intrusions in Banat occurred along some faults and shear zones of Cambrian age, later on reactivated during the Jurassic – ante-Oligocene time span.

The deep crustal faults, according to Currie (1976) who tried to explain the tectogenesis of the syenitic batholiths in Canada, can collect the primary alkali magmas originating in the mantle.

The syenite bodies in Banat originate in the upper mantle of the astenosphere, constituted of peridotites. According to Currie (1976) the partial melting of a peridotitic layer under conditions of a very reduced water amount (0.1 %)

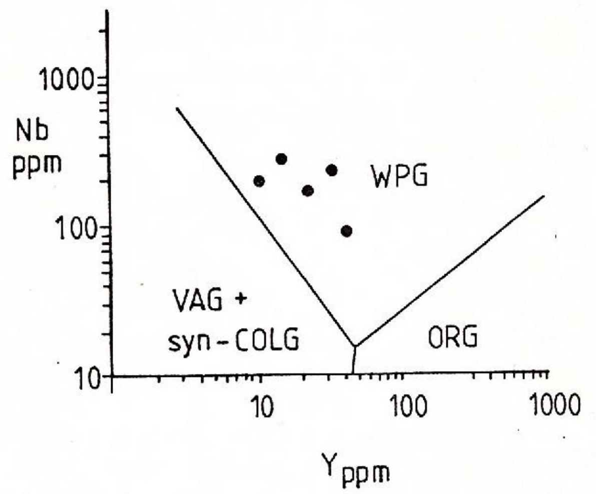

Fig. 8 – Nb–Y diagram (acc. to Pearce et al., 1984). WPG: within plate granites; VAG + Syn – COLG: volcanic arc granites+collision granites; ORG–ocean ridge granites.

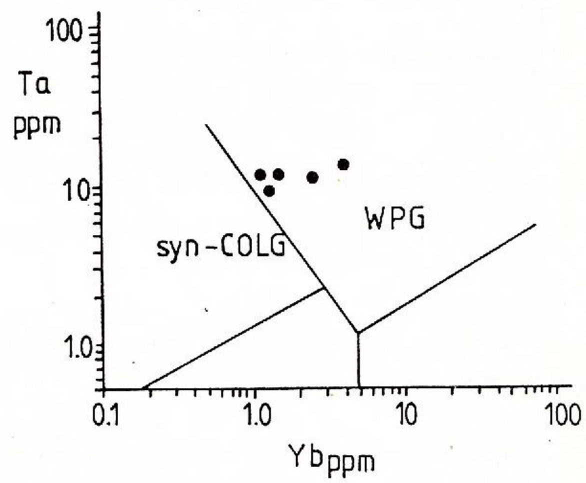

Fig. 9 – Ta–Yb diagram (acc. to Pearce et al., 1984). Symbols as in Figure 8.

at high pressures determined the formation of a alkali-basalt liquid. The magma alkalinity, that increases with depth, is due to the orthopyroxene stability at high pressures within a quite large temperature interval. Orthopyroxene, a mineral relatively rich in silica, determines the desilication of the yielded liquid, that is alkaline.

On the other hand, the part played by water and local distension in the reactivated shear zones, as well as the connection in time and space between the calc-alkali and alkali rocks were analysed by Bonin and Lameyre (1978) and by Bonin (1983, 1987, 1988, 1990). In this respect it is of note that from the anhydrous primary magmas, settled in a hydrated lithosphere, rocks suprasaturated in silica, that is calc-alkali rocks, will crystallize, and from an anhydrous primary magma that cannot be hydrated by the continental crust, rocks subsaturated in silica, that is alkali rocks, will result. An orogenic belt becomes entirely anhydrous very late, after about 500 Ma from the ceasing of the orogenic movements (Bonin, 1990). The syenitic bodies in Banat formed in an orogenic craton zone from alkali–basalt magmas through the fractional crystallization of the melting injected in the anhydrous continental crust, concomitantly with the filtering of the leucocrate liquid. These alkali magmas, a result of the feldspathic cumulates, influenced and were influenced in their turn by the continental crust in the adjacent zones. Thus, the concentric structure of the syenites in Banat is explained: the central zones constituted of nepheline syenites, subsaturated in silicas (51.90–53.21 SiO_2) in comparison with the marginal ones formed of alkali syenites less subsaturated in silicas (55.35 SiO_2) (Tab. 1).

Conclusions

The syenite rocks in Banat originate in the peridotitic mantle which, detensioned, melted partially, being transformed into an alkali–basaltic liquid. This melt, migrated in the anhydrous continental crust, yielded the feldspathic cumulates by fractional crystallization, concomitantly with an alkali leucocrate liquid subsaturated in silicas.

References

Anastasiu, N. (1973) Corpurile de roci sienitice din cristalinul Seriei de Neamţu. *Anal. Univ. Buc.*, XXII, p. 53–72, Bucureşti.

– **(1976)** Masivul granitoid Ogradena. Studiu petrografic şi geochimic. *An. Inst. Geol.*, XLIX, p. 5–151, Bucureşti.

Bonin, B., Lameyre, J. (1978) Réflexion sur la position et l'origine des complexes magmatiques anorogéniques. *Bull. Soc. France*, (7), XX/1, p. 45–59.

– **(1983)** Les complexes plutoniques alcalins. Perspective et hypothèses sur un trait géologique fondamental de zones intraplaques. *Géochronique*, 4, p. 12–14.

– **(1988)** From orogenic to anorogenic environments: evidence from associated magmatic episodes. *Schweiz. Mineral. Petrogr. Mitt.*, 68, p. 301-311.

– **(1990)** From orogenic to anorogenic setting: evolution of granitoid suites after a major orogenesis. *Geol. Jour.*, 25, p. 261–270.

Buma, G., Frey, F.A., Wones, D.R. (1971) Trace Elements Evidence Regarding Their Origin and Differentiation. *Contr. Mineral. Petrol.*, 31/4, p. 300–320.

Codarcea, Al. (1937) Note préliminaire sur certaines roches éruptives alcalines et sur quelques lamprophyres de la région d'Ogradena. *Bul. sec. géol.*, XVIII, Bucureşti.

– **, Pavelescu, L. (1963)** Considération sur la genèse des roches granitoïdes de l'autohton danubien des Carpathes Méridionales. *Congr. V, Asoc. Geol. Carpato-Balc.*, II, p. 9–15, Bucureşti.

Conceico, H., Sabaté, P., Bonin, B. (1991) The Itiuba alkaline syenite massif, Bahia State (Brazil): mineralogical, geochemical and petrological constraints – relation to the genesis of rapakivi magmatism Precambrian Research. 51, p. 283–314, Elsevier Sci. Publ. B.V., Amsterdam.

Cullers, R.L., Graf, J.L. (1984) Rare Earth Elements in Ignous Rocks of the Continental Crust: Intermediate and silicic Rocks – ore petrogenesis. In: Henderson (Editor) Rare Earth Geochemistry. Development in Geochemistry, 2, p. 275–308.

Currie, K.L. (1976) The alkaline rocks of Canada. *Geol. Survey. Canada Bull.*, 239, 225 p.

De la Roche, H., Leterriere, J., Grandelaude, P., Marchal, J. (1980) A classification of volcanic and plutonic rocks using R_1–R_2 diagram and major element analyses – Its relationships with current nomenclature. *Chem. Geol.*, 29, p. 183–210, Amsterdam.

Eby, G.N., Kochhar, N. (1990) Geochemistry and Petrogenesis of the Malani Igneous Suite, North Peninsular India. *Jour. Geol. Soc. India*, 36, p. 109–130.

– **, Krueger, H.W., Creasy, J.W. (1992)** Geology, geocronology and geochemistry of the White Mountain batholith, New-Hampshire. In: Puffer J.H. and Ragland P.C. (Editors) Eastern – North American Mesozoic Magmatism: Geological Society of America. *Special Paper*, 268, p. 379–397.

Edgar, A.D. (1974) On the use of the term "Agpaitic". *Min. Mag.*, 39, p. 729–730.

Garcia, D. (1988) Importance de la fraction cumulative dans les granitoïdes produits par cristallisation fractionnée: exemple des granites de la région de Vila Real (Nord Portugal). *C.R. Acad. Sci. Paris*, 307, Serie II, p. 1879–1885.

Jahn, B., Sun, S.S., Nesbitt, R.W. (1979) REE distribution and petrogenesis of the Spanish Peaks igneous complex, Colorado. *Cotrib. Mineral. Petrol*, 70, p. 281–298.

Jones, A.P., Larsen, L.M. (1985) Geochemistry and REE minerals of nepheline syenites from the Motzfeldt Centre, South Greenland. *Am. Min.*, 70, p. 1087–1100.

Loiselle, M.C., Wones, D.R. (1979) Characteristics and origin of anorogenic granites. *Geol. Soc. Am. Abst. With. Progr.*, 11, p. 468.

Pearce, J.A., Harris, N.B.W., Tindle, A.G. (1984) Trace Element Discrimination Diagrams for the Tectonic Interpretation of Granitic Rocks. *Jour. Petrol.*, 25/4, p. 956–983.

Pitcher, W.S. (1987) Granites and yet more granites forty years on Geol. Rund., 76/1, p. 51–79.

– **(1982)** Granite Type and Tectonic Environment. In Hsu. K (Ed) Mountain Buiding Processes Academic Press, London, p. 19–40, London.

Stan, N. (1985) Cherbelezu and Sfârdin granitoids. Their relationships with the adjacent rocks. *D.S. Inst. Geol. Geofiz.*, LXIX/1, p. 167–180, Bucureşti.

Streckeisen, A., Giuşcă, D. (1932) Der Nepheline – Cancrinit Syenit von Orşova. *Bul. Soc. Rom. Geol.*, I, p. 176–192, Bucureşti.

– **, Hunziker, J.C. (1974)** On the Origin and Age of the Nepheline Syenite Massif of Ditrău (Transylvania, Romania). SMPM 54, 1, p. 59–77, Berne.

Taylor, S.R., Mc. Lennan, S.M. (1985) The continental crust: its composition and evolution. Blackwell, Oxford.

Terzić, M. (1983) Leucite–bearing rocks of Serbia and Macedonia (Jugoslavia). *An. Inst. Geol. Geofiz.*, LXI, p. 273–283, Bucureşti.

Whalen, J.B., Currie, K.L., Chappell, B.W. (1987) A – type granites: geochemical characteristics discrimination and petrogenesis. *Contrib. Mineral. Petrol.*, 95, p. 407–419.

Received: June 19, 1995.
Accepted: October 10, 1995.

Rom. J. Petrology, 77, p. 31–40, Bucureşti, 1996

LOWER TRIASSIC BASIC DYKE SWARMS IN NORTH DOBROGEA

Ionel NICOLAE, Antoneta SEGHEDI

Institutul Geologic al României. Str. Caransebeş 1, 79 678 Bucureşti 32

Key words: Basic Dykes. Ophiolite. Tectonic Setting. North Dobrogea.

Abstract: In the Alpine chain of North Dobrogea, Triassic basic magmatic rocks occur within the main tectonic units. A suite of basic dykes (dolerites, basalts) is emplaced in the Variscan folded basement of the Măcin unit. In the Niculiţel and Tulcea units, a thick pile of basaltic rocks (mainly pillow-lavas, accompanied by dolerites, microgabbros) occur, interbedded in places with Triassic limestones (Spathian to Ladinian). The basic dyke swarm shows a consistent NW-SE direction, parallel to the main structural trend of the Alpine belt. Basic dykes are accompanied by a suite of similar trending rhyolitic dykes, suggesting a bimodal volcanism. Basic dykes and Niculiţel ophiolites show a great resemblance in geochemical features. Ti - Cr, Ti/Cr - Ni, V - Ti/1000 plots and Ba/Y ratios suggest ocean floor settings (MORB) both for the dyke swarm and the Niculiţel ophiolites. Based on geochemical features and tectonic setting, the following model for the geotectonic evolution of the basic rocks of North Dobrogea is proposed: a period of crustal extension at the beginning of the Triassic favoured the initiation of longitudinal, deep fractures, accompanied by basic dyke emplacement; meanwhile, acid magma was produced in the sialic crust and injected as rhyolitic dykes; one of the deep fractures evolved into a rift, being the site for generation of the Niculiţel ophiolites; in adjacent areas, acid and basic dykes continued to be emplaced, along secondary fractures; Jurassic or Lower Cretaceous compressional movements created the thrust-fold belt of North Dobrogea.

Introduction

Basic magmatic rocks of Triassic age are known in all the main tectonic units of North Dobrogea: basic dyke swarms are emplaced in the pre-Alpine basement of the Măcin unit, while ophiolitic rocks are part of the Mesozoic sequences in the Niculiţel and Tulcea units.

Although basic dykes are known since Murgoci (1914) and Rotman (1917), usually they were not mapped because of their small thicknesses, or because they were considered basic tuffs interbedded in Paleozoic sequences of the Măcin unit (Mirăuţă, Mirăuţă, 1962; Mirăuţă, 1966). A few basic dykes have been previously separated only within the Pricopan Massif (Giuşcă, 1934). Mapping for the Geological

Map of Romania, scale 1:50,000, enabled Seghedi to trace the development and distribution of basic dykes throughout the Măcin unit of North Dobrogea (in Seghedi et al., 1980, 1988, in Savu et al., 1988 and in Mihăilescu et al., 1988). Studies of the borehole cores (Seghedi in Baltreş et al., 1989, 1990) produced additional proofs concerning the widespread occurrence of basic dykes cutting various pre-Triassic basement rocks of the Măcin unit.

This paper intends to be a geochemical study of the basic dyke rocks from the Măcin unit compared to the Triassic ophiolites of the Niculiţel Formation, in order to establish their genetic relationships.

Basic dyke swarms

A suite of consistently NW-SE trending dyke swarms (Fig. 1) is emplaced in various pre-Alpine basement rocks of the Măcin unit: pre-Variscan metamorphic sequences, Paleozoic deposits and Variscan granitoid intrusives (Seghedi in Seghedi et al., 1980, 1988, in Savu et al., 1988 and in Mihăilescu et al., 1988). Dyke swarms extend over an area 50 km long and 12 km wide; they are accompanied by a suite of similar trending acidic dykes (with rhyolitic composition), interpreted as a bimodal volcanism related to Triassic rifting in North Dobrogea (Vlad, 1978, Cioflica et al., 1980).

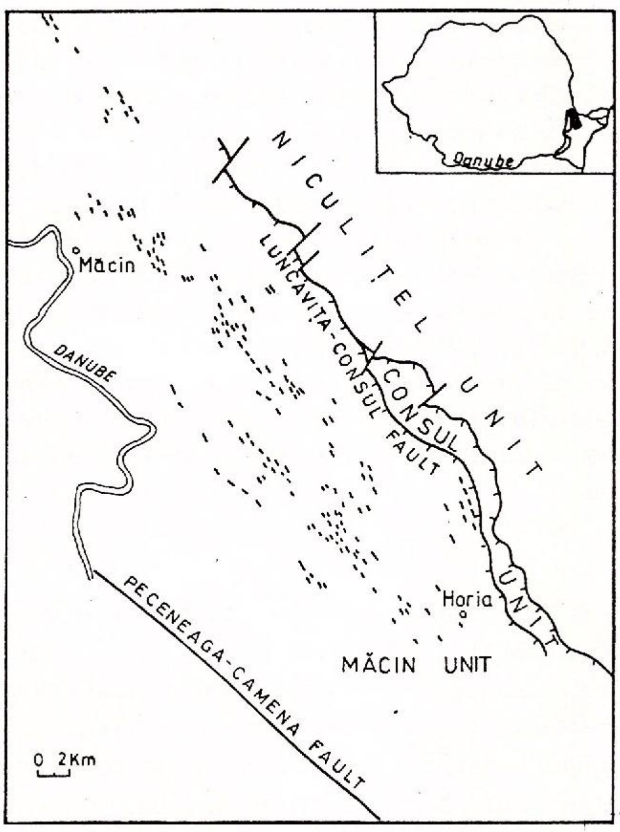

Fig. 1 – Location map and distribution of basic dyke swarms in the Măcin unit of North Dobrogea.

Basic dykes attain several meters or tens of meters in lenght and usually show several decimeters in thickness (Pl. I, Figs. 1,2); common thicknesses vary between 40-60 cm; metric thicknesses are exceptional (Megina Hill). Cross-cutting relationships with their host rocks are well exposed in several quarries: Gorganu (in Orliga Group quartzites), Măcin Harbour (in the Măcin granite), Izvoarele, Mâţi, Căprărie, Viilor (in the Pricopan granite), Morzu, Carabalu (in the Greci granitoid Massif), Igliţa (in Lower Devonian limestones), Piatra Râioasă (in Boclugea Group quartzites), Dâlchi Bair (in Megina Group amphibolites and micashists), along the eastern margin of Lake Jijila (in black quartzites of Boclugea Group); all the mentioned groups and granitoids are Paleozoic or older.

Dykes rocks show various textures depending on dyke thickness and on their outer or inner position within the dyke; thinner dykes may be entirely basaltic, displaying intersertal texture; thicker dykes show doleritic or microgabbroic central zones (with intergranular, ophitic-subophitic or holocrystalline, medium-grained textures) and porphyritic or microgranular marginal zones.

Large scale alpine mylonitisation in the Măcin unit (Seghedi, 1985, 1986; Seghedi et al., 1980, 1986) is responsible for the development of a penetrative, planar mylonitic foliation in most of the dyke rocks. Thin dykes are entirely mylonitic, while in thicker bodies ductile fabric is restricted to the margins.

The steeply dipping mylonitic foliation shows the same NW-SE trend as the dyke swarms and the Alpine structural trends in the Măcin unit. Mylonitic dyke rocks are L-S tectonites showing a constant steeply dipping stretching lineation resulted by shattering of mafic phenocrysts.

In mylonitic rocks, the primary phases are replaced by newly formed chlorite, albite, actinolite, epidote, minerals defining the mylonitic foliation.

Field relations indicate that basic dykes were not emplaced before the Early Triassic: the youngest rocks they intrude are Late Variscan granites (Greci Massif) which yielded a Rb-Sr isochron age of 242 Ma (Pop et al., 1985).

Ophiolitic rocks

Petrographical studies of ophiolitic rocks are well known since the works of Savul (1930, 1931). Savu et al. (1980, 1982) completed the petrographical data with geochemical data. Ophiolitic rocks crop out mainly in the Niculiţel unit, between Luncaviţa-Isaccea-Niculiţel-Nifon; in the Tulcea unit they occur in several small outcrops at Somova and Izvoarele; boreholes in this unit show that basalt flows attain thicknesses from 79 to 282 m (Baltres et al., 1989).

Recently, ophiolitic rocks were designated as the Niculiţel Formation (Baltres, in Seghedi et al., 1991). The age of the Niculiţel Formation is well constrained by stratigraphic and paleontological evidence: basalts overlie the Spathian Somova Formation and show discontinuous interbeds of pelagic limestones containing Late Spathian to Middle Anisian conodonts (Mirăuţă, in Savu et al., 1988). Basalts are overlain by Upper Anisian cherty limestones.

Ophiolites are represented mainly by basalt flows, often in pillow lava facies; dolerites and microgabbros form minor occurrences; areal distribution of these rocks is shown on the Niculiţel sheet of the 1:50,000 geological map (Savu et al., 1988).

The central part of pillows are basalts with intersertal or intergranular textures and in the marginal part there are often variolitic textures. Limestone lenses are intimately associated as decimetric to metric interbeds. Limestone-basalt breccias are widespread with relationships that suggest alternative formation. Basalt microfabric consists of a dark brown vitreous groundmass, usually chloritised and rich in iron hydroxides; thin plagioclase laths (0.2-0.5 mm lenght), usually showing secondary albitisation, float in the groundmass; clinopyroxene grains may appear between the plagioclase laths, in intergranular textures. Opaque minerals form grains or skelet crystals. Amygdaloids are often present, filled with secondary minerals - calcite, chlorite, calcedony.

Dolerites and microgabbros occur as dykes and small bodies in restricted areas (Ţiganului, Bădilei valleys). They show ophitic-subophitic or holocrystalline medium grained textures and consist of plagioclase (laths or tabular shaped), clinopyroxene (usually uralitized), seldom olivine and opaque minerals. Leucogabbroic facies is scarce.

Geochemical data

Major and trace element concentrations have been determined for 12 samples from the basic dykes and 6 ophiolitic rocks from the Niculiţel area (Tab. 1, 2). These are compared to 28 pre-existing analyses of ophiolites published by Savu et al. (1980, 1982). The dyke rocks analysed are mainly dolerites and the new ophiolites include three basalts: one dolerite, one leucogabbro and one microgabbro.

On a plot of Ti vs. Cr diagram (Pearce, 1975) analyses of all basic dykes and 28 ophiolites plot within the field of ocean floor basalts; 6 ophiolites plot outside the diagram (Fig. 2).

On a plot of Ti/Cr vs. Ni (Beccaluva et al.,

Table 1
Chemical analyses of the basic dyke rocks (Măcin Unit)
major (%) and trace (ppm) elements

	Number of samples											
Oxide	2704	2704M	55F	55C	317	55M	55G	270	2704C	1517	236	156
SiO_2	43.50	44.00	45.80	46.00	46.30	46.80	46.90	48.00	48.60	49.30	51.60	52.00
TiO_2	1.32	1.54	2.12	1.30	1.52	1.30	1.62	1.76	1.24	1.60	2.82	2.52
Al_2O_3	13.88	18.25	15.84	14.89	13.60	13.70	16.20	16.20	16.80	16.65	14.00	13.93
Fe_2O_3	2.27	2.10	3.70	3.20	2.49	3.21	3.87	2.70	2.24	2.77	5.30	4.22
FeO	7.19	8.12	7.28	6.39	7.23	6.80	6.17	7.00	5.96	6.26	6.78	7.59
MnO	0.15	0.25	0.32	0.17	0.17	0.35	0.22	0.17	0.15	0.16	0.19	0.20
MgO	14.79	10.55	8.76	12.56	12.80	11.84	8.91	7.23	7.93	6.31	4.51	4.45
CaO	8.79	3.26	8.68	7.85	8.84	7.85	9.96	9.90	10.31	9.98	7.15	6.59
K_2O	0.80	0.10	0.71	1.44	0.96	2.19	0.76	0.36	0.45	0.94	1.30	1.92
Na_2O	1.65	4.31	2.56	1.63	1.54	1.30	1.96	2.92	2.64	2.71	3.74	3.97
P_2O_5	0.10	0.26	0.46	0.16	0.25	0.32	0.16	0.24	0.30	0.26	0.37	0.55
H_2O^+	3.24	5.47	3.25	4.62	3.50	2.94	2.36	2.67	2.31	1.89	2.47	2.54
CO_2	1.10	1.20	0.22	0.13	0.00	0.36	0.95	1.04	0.54	0.53	0.00	0.00
S	0.13	0.22	0.18	0.14	0.48	0.72	0.11	0.23	0.37	0.23	0.09	0.10
Total	100.27	99.63	99.88	100.48	99.58	99.59	100.15	100.46	99.84	99.59	100.32	100.58
Pb	4.5	7	3	25	14	4	2	7.5	4	7	7.5	4.5
Cu	180	25	36	68	55	52	53	31	29	29	21	15
Ga	12	14.5	18	11.5	12	15	14.5	12	14.25	15	26	22
Sn	3	<2	2	<2	<2	<2	<2	<2	<2	<2	3.5	3.5
Ni	650	115	190	520	460	400	175	80	165	110	28	24
Co	55	32	46	75	65	58	52	36	60	36	24	24
Cr	650	320	310	700	760	530	400	180	380	190	66	62
V	150	250	290	250	230	230	200	320	310	280	200	200
Sc	29	35	39	38	34	31	46	37	38	33	28	28
Y	24	37	47	28	29	38	37	36	36	38	55	55
Yb	1.7	2.9	3.2	2.1	2	2.1	2.5	3.1	2.5	2.9	5.2	4.8
Zr	120	140	230	95	110	82	110	160	150	230	360	370
Ba	20	23	70	115	115	80	55	40	45	75	480	480
Sr	135	85	320	220	140	95	200	300	210	280	320	240

Appendix to table 1

Sample	Rock type and texture	Host rock and location
2704	Dolerite with partly serpentinized olivine, subophitic	Greci Granite, Morzu Quarry
2704 M	Basalt, fine grained intersertal	Greci Granite, Morzu Quarry (marginal part of dyke)
55F	Dolerite, intergranular-subophitic	Măcin Granite, Măcin Harbour Quarry
55 C	Basalt, intersertal	Măcin Granite, Măcin Harbour Quarry (central part of the dyke)
317	Dolerite-microgabbro, ophitic-medium grained holocrystalline	Cuts the contact between the Pricopan Granite and the Carapelit Formation Hornfelses, Pricopanului Creek
55 M	Basalt, fine grained intersertal	Măcin Granite, Măcin Harbour Quarry (marginal part of the dyke)
55 G	Dolerite, intergranular-subophitic	Măcin Granite, Măcin Harbour Quarry
270	Gabbro-dolerite, medium grained holocrystalline-ophitic	Orliga Group Quartzites, Gorganul Quarry
2704 C	Dolerite, subophitic	Greci Granite, Morzu Quarry (central part of the dyke)
1517	Gabbro-dolerite, highly cataclastic fabric	Porphyritic granite, Garvăn
236	Basalt, intersertal, intensely sheared and chloritized	Hamcearca leucogranites, Cheiu Hill
156	Dolerite, intergranular-subophitic	Hamcearca leucogranites, Hamcearca Hill

Table 2
Chemical analyses of the ophiolitic rocks (Niculiţel Unit)
major (%) and trace (ppm) elements

Oxide	Number of samples 90	88	83	91	87	84
SiO_2	42.00	45.00	46.60	46.80	46.80	49.90
TiO_2	2.18	1.26	4.12	1.76	2.36	2.68
Al_2O_3	15.00	15.68	12.40	16.40	15.73	11.82
Fe_2O_3	9.22	2.65	6.71	4.40	3.76	10.84
FeO	2.66	5.62	8.04	4.72	6.54	3.99
MnO	0.14	0.14	0.26	0.15	0.17	0.20
MgO	5.49	6.07	5.71	6.23	6.97	3.46
CaO	13.13	12.27	7.63	12.72	8.70	7.19
K_2O	0.90	1.09	0.64	0.72	0.68	0.40
Na_2O	3.07	3.20	4.75	2.50	3.61	5.49
P_2O_5	0.35	0.40	0.40	0.28	0.44	0.94
H_2O^+	2.92	2.70	0.76	2.06	3.19	1.48
CO_2	3.14	4.09	1.66	0.88	0.21	1.88
S	0.24	0.17	0.65	0.29	0.24	0.19
Total	100.40	100.34	100.33	99.91	99.40	100.46
Pb	5	2	2	2.5	2	<2
Cu	125	30	6.5	45	23	3
Ga	17.5	14	22	14.5	15	23
Sn	< 2	< 2	2.5	<2	2	3
Ni	90	115	25	130	110	8
Co	35	45	43	47	32	19
Cr	220	330	7	410	240	1.5
V	430	290	780	380	300	270
Sc	40	40	58	48	36	29
Y	45	34	100	32	43	100
Yb	4.2	2.6	6.3	3	3.8	8
Zr	210	110	470	150	230	550
Ba	65	70	85	36	175	55
Sr	320	650	130	290	480	100

90-Basalt, Piatra Roşie; 88-basalt (pillow lava), Teilor Valley; 83-Gabbro, Ţiganilor Valley; 91-Basalt (pillow lava), Cocoşul Monastery; 87-Dolerite, Ţiganilor Valley; 84-Leucogabbro, Ţiganilor Valley.

1979) 10 analyses of basic dykes and 28 ophiolites plot within the field of ocean floor tholeiites; two basic dykes (no. 11 and 12) lie in the field of island arc tholeiites and 6 ophiolites plot outside the diagram (Fig. 3).

On a V vs. Ti/1000 diagram (Shervais, 1982), 10 analyses of basic dykes plot in the field of MORB or back-arc basalts (both formed consequently to ocean floor spreading), 2 analyses plot in the area of alkaline basalts and island ocean basalts (with V vs. Ti/1000 ratios ranging between 50 and 100) (Fig. 4). This plot seems to be less conclusive for the ophiolitic rocks: 18 analyses plot in the field of MORB and back-arc basalts and 16 in the other fields.

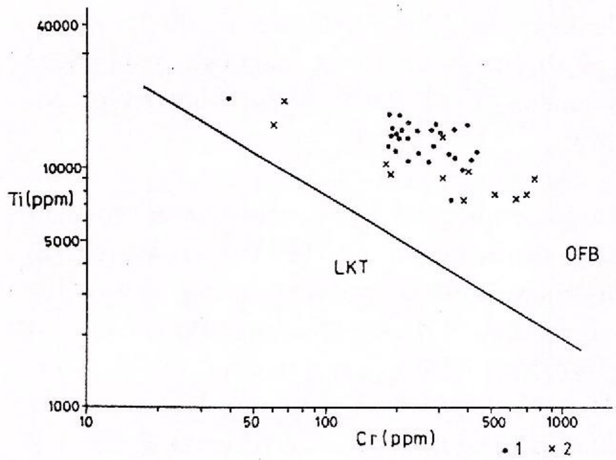

Fig. 2 – Ti vs Cr diagram (acc. to Pearce, 1975). LKT-low potassium tholeiites; OFB-ocean floor basalts; 1, basic dykes rocks; 2, ophiolitic rocks (same in Figs. 3–4).

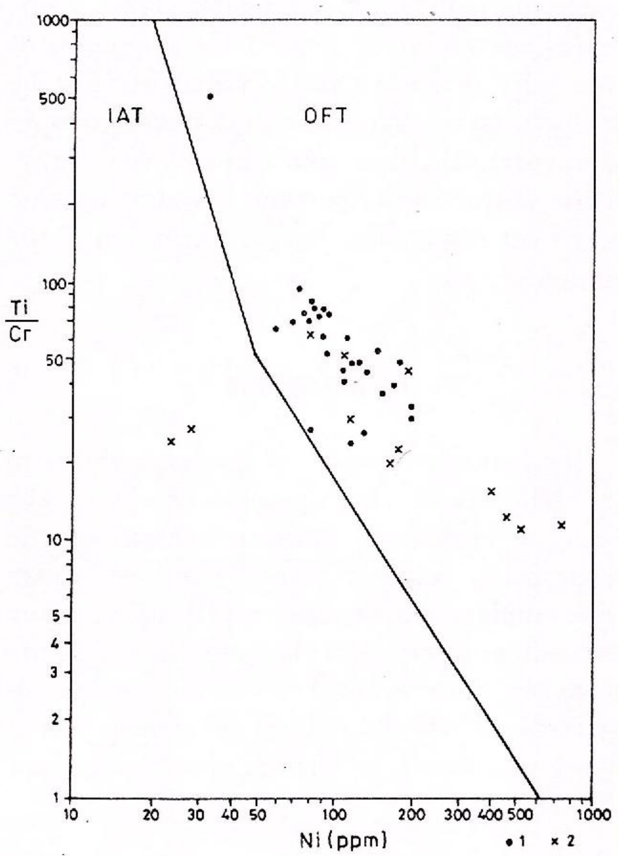

Fig. 3 – Ti/Cr vs Ni diagram (acc. to Beccaluva et al., 1979). IAT-island arc tholeiites; OFT-ocean floor tholeiites.

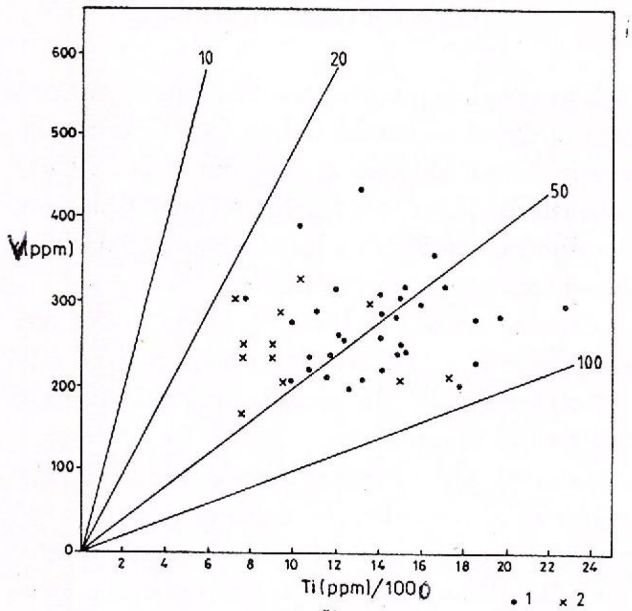

Fig.4 – V vs Ti/1000 diagram (acc. to Shervais, 1982).

The Ba/Y ratio is less than 4.4 for ocean floor tholeiites and higher than 3.9 for island arc tholeiites (Beccaluva et al., 1979). Only 6% of a large volume of analyses plot in the overlapping field. In our case Ba/Y ratio is < 2.1 for 8 analyses of basic dykes, for 2 analyses of dykes it is 4 and only 2 analyses (again 11 and 12) plot in the field of island arc tholeiites (the latter possibly showing stronger contamination). 24 analyses of the ophiolitic rocks show Ba/Y ratios < 3.9, for 5 analyses it ranges between 3.9 and 4.4 and only 5 samples of ophiolites show a value > 4.4.

A statistical interpretation of the presented diagrams (also taking into account the possibility of sialic contamination) suggests that the model of a short-lived rift (Cioflica et al., 1980) can be accepted for the emplacement of the Triassic ophiolitic rocks of North Dobrogea. The diagrams also suggest that geochemical features of basic dykes of Măcin unit and Niculiţel Formation ophiolites are obviously alike.

Geotectonic model

The emplacement of the basic dyke swarms was considered connected to the Triassic rifting in North Dobrogea (Seghedi et al., 1986).

Basic rocks of the Niculiţel Formation were ascribed to various tectonic settings, based on geochemical interpretations.

Cioflica et al. (1980) consider that these ophiolites were generated in a short-lived rift, characterized by the significant association of a bimodal magmatism.

Savu et al. (1982) ascribed the ophiolitic rocks to three different tectonic settings: **a)** rift, **b)** oceanic island (i. e. withinplate) and **c)** subduction. These contradictory ideas are possibly due to the mechanical interpretation of the Ti/100-Zr-3Y diagram (Savu et al., 1982, Fig. 4). Finally, the authors favoured withinplate setting. Thus, Savu et al. (1982, page 151) show that "the mafic rocks resulted from a basaltic magma and erupted in the Triassic spreading ocean as products of a withinplate-ophiolitic volcanism".

According to Săndulescu (1984) ophiolitic rocks appeared in an intracratonic rift with maximum development in the Middle Triassic, the rifting being initiated in the Lower Triassic or even in the Permian.

Several geological evidences have to be taken into account when trying to establish a geotectonic model for the evolution of Triassic basaltic magmatism in North Dobrogea:

– significant geochemical affinities of the basic dyke rocks emplaced in the basement of the Măcin unit with the ophiolitic rocks of Tulcea and Niculiţel units;

– the dominant NW–SE trend of basic dykes, parallel to the Alpine structural trends of the Măcin unit;

– the connection between the mylonite zones of the same area and the emplacement of basic dykes;

– as compared to sequences characteristic of MORB-ophiolites, the rocks of the Niculiţel Formation show only the upper part, as sheeted dykes and ultramafic rocks are not known and only small gabbroic bodies occur in outcrops or boreholes;

– the existence of a Triassic acidic-rhyolitic volcanism in North Dobrogea which, correlated to the basic rocks, suggests a bimodal volcanism (Vlad, 1978, 1984; Cioflica et al., 1980);

– the sequence of the Triassic deposits indicates transition from continental to marine sedimentation in the Upper Werfenian (Spathian) and progressive water deepening until the Late Triassic (Norian), for the largest area of North Dobrogea (Baltres, 1993).

Based on these evidences, the Triassic evolution of North Dobrogea can be imagined as follows: early Triassic crustal extension strongly deforms the Variscan consolidated basement; shear-zones indicate that rifting in North Dobrogea was accomodated by a system of deep-seated normal faults, marked by fault rocks; extension was accompanied by emplacement of a suite of basic dyke swarms; meanwhile, at upper structural levels, acid magmas could form within the crust and be emplaced as rhyolites; one of the important fractures evolved into a rift responsible for the formation of the ophiolitic rocks.

Conclusions

Geochemical features of the basic dykes of the Măcin unit and ophiolitic rocks of the Niculiţel Formation indicate a clear genetic relationship between them. The basic dykes were emplaced in the Lower Triassic and they are contemporary with the ophiolites. The basic dykes were emplaced shortly before individualisation of the short lived rift, where ophiolites have formed, by melting of the same mantle source.

References

Baltres, A., Seghedi, A., Mirăuţă, E., Stanciu, L., Seghedi, I., Niţoi, E., Dobrescu, A., Codarcea, V., Gheorghian, D., Bratosin, I., Grădinaru, E. (1989) Report, Arch. Inst. Geol. Rom., Bucureşti.

– **, Seghedi, A., Stanciu, L., Mirăuţă, E., Ion, J., Antonescu, E., Niţoi, E., Dobrescu, A., Gheorghian, D., Codarcea, V. (1990)** Report, Arch. Inst. Geol. Rom., Bucureşti.

– **, Mirăuţă, E., Seghedi, A., Stanciu, L. (1993)** Report, Arch. Inst. Geol. Rom., Bucureşti.

Beccaluva, L., Ohnenstetter, D., Ohnenstetter, M. (1979) Geochemical discrimination between ocean-floor and island-arc tholeiites – application to some ophiolites. *Can. J. Earth. Sci.*, 16, p. 1874–1882, Toronto.

Cioflica, G., Lupu, M., Nicolae, I., Vlad, Ş. (1980) Alpine Ophiolites of Romania: Tectonic Setting, Magmatism and Metallogenesis. *An. Inst. Geol. Geofiz.*, LVI, p. 79–95, Bucureşti.

Giuşcă, D. (1934) Massif du Pricopan. *An. Inst. Geol. Rom.*, XVI, p. 481–497, Bucureşti.

Mirăuţă, O. (1966) Contribuţii la cunoaşterea formaţiunilor paleozoice din partea sudică a Munţilor Măcinului. *Stud. Cerc. Geol. Geofiz. Geogr., Ser. Geol.*, II, 2, p. 497–512, Bucureşti.

– **, Mirăuţă, E. (1962)** Paleozoicul din partea de sud a Munţilor Măcin (regiunea Cerna-Hamcearca). *D.S. Com. Geol.*, XLVI, p. 129–142, Bucureşti.

Mihăilescu, N., Seghedi, A., Întorsureanu, I., Rădan, S., Terteleac, N., Ghenea, C. (1988) Geological Map of Romania, Scale 1:50,000, Peceneaga Sheet, Inst. Geol. Rom., Bucureşti.

Murgoci, M. G. (1914) Cercetări geologice în Dobrogea nordică cu privire specială asupra Paleozoicului şi tectonicii. *An. Inst. Geol. Rom.*, V, 2, p. 307–494, Bucureşti.

Pearce, J. A. (1975) Basalt geochemistry used to investigate past tectonic environments on Cyprus. *Tectonophysics*, 25, p. 41–67, Amsterdam.

Pop, Gh., Buzilă, Al., Cioloboc, D., Catilina, D., Popescu, Gh. (1985) Isotopic Rb/Sr ages for establishing the emplacement sequence of some granitoids of North Dobrogea. *Proc. rep. of the XIII CBGA*, p. 108–111, Cracovia.

Rotman, D. (1917) Masivul eruptiv de la Greci. *An. Inst. Geol. Rom.*, VII, 1, p. 91–425, Bucureşti.

Savu, H., Udrescu, C., Neacşu, V. (1980) Structural, Petrological and Genetic Study of the Ophiolites from the Niculiţel zone (North Dobrogea). *D.S. Inst. Geol. Geofiz.*, LXV/1, p. 41–64, Bucureşti.

– **, Udrescu, C., Neacşu, V. (1982)** Structure and genesis of the Diabase Complex from the Luncaviţa-Isaccea-Mănăstirea Cocoş zone (North Dobrogea). *D.S. Inst. Geol. Geofiz.*, LXVII/5, p. 135–153, Bucureşti.

Savul, M. (1930) Notă asupra diabazelor de la Niculiţel, Dobrogea. *D.S. Inst. Geol. Rom.*, p. 184–192, Bucureşti.

– **(1931)** Erupţiunile de diabaze din nordul Dobrogei. *D.S. Inst. Geol. Rom.*, XVIII, p. 231–255, Bucureşti.

Săndulescu, M. (1984) Geotectonica României. Ed. Tehnică Bucureşti, 334 p.

Seghedi, A. (1986) Varisziche Faltung in alpidishen Einheiten der Nord-Dobrudscha. *Zeitsch für angewandte Geol.*, 31, 11, p. 281–287, Bucureşti.

– **(1986)** Deformational and metamorphic history of the Carapelit Formation (North

Dobrogea). *D.S. Inst. Geol. Geofiz.*, 70-71/5, p. 235-246, Bucureşti.

– , **Ghenea, C., Ghenea, A., Mirăuţă, E. (1980)** Geological Map of Romania, Scale 1:50,000, Măcin Sheet, Inst. Geol. Rom., Bucureşti.

– , **Mirăuţă, E., Szasz, L., Seghedi, I., Szakacs, Al., Ghenea, C., Ghenea, A., Rădan, S., Oaie, Gh., Savu, H., Nicolae, I., Ion, J., Gheorghian, D., Antonescu, E., Visarion, A., Săndulescu, D., Codarcea, V., Udrescu, C., Stoian, M., Vanghelie, I. (1986)** Report, Arch. Inst. Geol. Rom., Bucureşti.

– , **Mirăuţă, E., Szasz, L., Ghenea, C., Ghenea, A., Seghedi, I., Szakacs, Al., Savu, H., Rădan, S. (1988)** Geological Map of Romania, Scale 1:50,000, Sheet Priopcea, Inst. Geol. Rom., Bucureşti.

– , **Baltres, A., Nedelcu, L., Szasz, L., Seghedi, I., Ion, J., Rădan, S. (1991)** Report, Arch. Inst. Geol. Rom., Bucureşti.

Shervais, J.W. (1982) Ti - V plots and the paragenesis of modern and ophiolitic lavas. *Earth and Planet. Sc. Lett.*, 59, p. 101-118, Amsterdam.

Vlad, Ş. (1978) Metalogeneza triasică în zona Tulcea (Dobrogea de Nord). *Stud. Cerc. Geol. Geofiz. Geogr., Geol.*, 23/2, p. 249-258, Bucureşti.

– **(1984)** Triassic mineralization in North Dobrogea (Romania). *Radovi Geoinstituta*, 17, p. 137-143, Beograd.

Received: February 6, 1995
Accepted: February 24, 1995
Presented at the Second Symposium on Mineralogy of Mineralogical Society of Romania, 8 July 1993, Timişoara

Rom. J. Petrology, 77, p. 41–48, Bucureşti, 1996

RARE EARTH ELEMENTS ABUNDANCES IN THE OPHIOLITES FROM THE SOUTH APUSENI MOUNTAINS (ROMANIA)

Ionel NICOLAE

Institutul Geologic al României. Str. Caransebeş 1, 79 678 Bucureşti 32

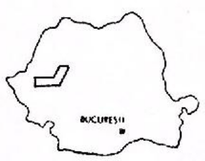

Key words: Ophiolites. REE. South Apuseni Mts. Volcanic Arc. Ensialic Marginal Basin.

Abstract: The present paper reviews the REE characteristics of the ophiolites from the South Apuseni Mts based on previous papers and additional 14 analyses. The ophiolite suite of the South Apuseni Mts has been interpreted in relation to two tectonic settings and consists of the following series: – tholeiitic series and calc-alkaline series of a volcanic arc; – spilitic series of the Feneş Formation and basalts of the Criş Nappe, related to an ensialic marginal basin. REE contents, chondrite-normalized values, Σ REE and some characteristic ratios, i.e. Eu/Sm, $(La/YB)_N$, $(La/Ce)_N$, and $(Ce/Yb)_N$, of the tholeiitic, calc-alkaline and spilitic series are listed in tables and discussed. Interpretation of these data suggests the following: – the tholeiitic series has the lowest ΣREE and the calc-alkaline series the highest ΣREE; Eu/Sm ratio of the tholeiitic series exhibits a larger variation as compared to the calc-alkaline series and spilitic series; LREE/HREE ratios of the tholeiitic series have a restricted variation range and mean value, as compared to the calc-alkaline series and spilitic series; chondrite-normalized patterns of the tholeiitic series, calc-alkaline series and spilite series of the Feneş Formation provide valuable information about their petrogenesis and additional data to confirm the ophiolite genetic model.

Introduction

The ophiolite suite of the South Apuseni Mts has been interpreted in relation to two tectonic settings (e.g. Cioflica et al., 1980; Cioflica, Nicolae, 1981; Nicolae, 1983; Lupu, 1983; Nicolae et al., 1992; Nicolae, 1995) and consists of the following series:

– tholeiitic series and calc-alkaline series, belonging to a volcanic arc;

– spilitic series of the Feneş Formation and basalts of the Criş Nappe, belonging to an ensialic marginal basin.

The present paper reviews the REE characteristics of the tholeiitic, calc-alkaline and spilitic series, based on previous papers (Savu et al., 1986, 1994; Savu, Stoian, 1988, 1992) and additional 14 analyses. These papers took into account REE data arbitrarily grouped (for example, Savu et al., 1994, which distinguished basaltic rocks with SiO_2 content lower than 48 %, higher than 49.5 % and between 48 and 49.5 %).

In order to avoid further confusion, the present paper deals explicitly with individual analyses plotted on diagrams constructed separately for the tholeiitic series, calc-alkaline series and spilitic series.

REE contents and petrologic significance

REE contents and chondrite-normalized values (according to Boynton, 1984) are listed in Table 1. Table 2 lists ΣREE and some characteristic ratios, i.e. Eu/Sm, $(La/Ce)_N$, $(La/Yb)_N$ and $(Ce/Yb)_N$. Table 3 lists ranges of variation and mean values of the above-mentioned tholeiitic series, calc-alkaline series and spilitic series, computed from references (Savu et al., 1986, 1994; Savu, Stoian, 1992) and recent 14 analyses. Interpretation of these data suggests the following:

a) the tholeiitic series has the lowest ΣREE and the calc-alkaline series the highest ΣREE;

b) Eu/Sm ratio of the tholeiitic series exhibits a larger variation, as compared to the calc-alkaline series and spilitic series;

c) $(La/Yb)_N$ and $(Ce/Yb)_N$ ratios (that is LREE/HREE ratios) of the tholeiitic series have a restricted variation range and mean value, as compared to the calc-alkaline series and spilitic series (Tab. 3). This behaviour is exposed in the diagram $(La/Yb)_N$ vs Yb_N (Fig. 1).

Chondrite-normalized REE patterns interpreted by Savu et al. (1994) are represented by mean values of rock groups artificially established. These authors compared the basaltic rocks of the Mureş Zone (e.g. Savu et al., 1994, Fig. 3, p. 80) with tholeiitic N-type MORB described by Saunders (1984, Fig. 6.1, p. 209), and claimed they are of similar origin. This is, however, an arbitrary interpretation that can be easily dismissed by comparing the tendency of their constructed curves with those by Saunders. Thus, their curves are horizontal between La and Sm, followed by a negative Tb anomaly and an ascending trend toward Yb. In contrast, N-type MORB curves presented by Saunders exhibit a continuous ascending trend between LREE and HREE, with possible slight negative Eu anomalies.

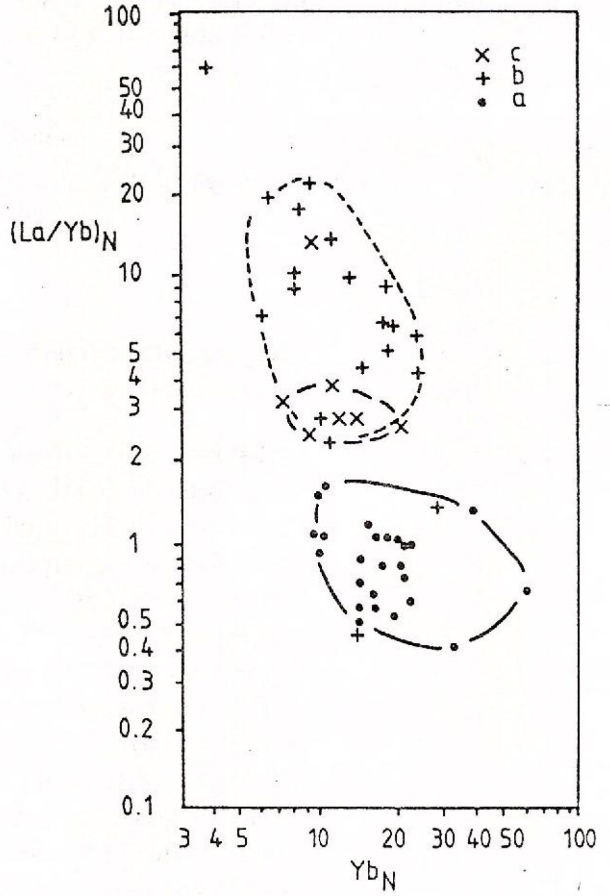

Fig. 1 – $(La/Yb)_N$ vs. Yb_N diagram. (The samples of: a, tholeiitic series; b, calc-alkaline series; c, spilitic series of the Feneş Formation).

As mentioned before, the present paper reinterprets earlier data and uses new analyses, in an attempt to provide a more accurate interpretation. Each analysis was plotted individualy in Figure 2. As a result, the plotting of the tholeiitic series shows between La-Ce-Sm slighly ascending or descending curves. Following this, a part of the analyses shows reduced Eu anomaly, and another part a reduced Tb-anomaly.

Such tendencies are not characteristic of the N-type MORB or Anomalous Ridge Segments (see Fig. 6.2, in Saunders, 1984). Some similitudes with Transitional Ridge Segments patterns (see Fig. 6.3, in Saunders, 1984) are noticeable for the segment that reaches Eu, but

Table 1
REE abundances (ppm) and chondrite-normalized values
(in paranthesis, after Boynton, 1984)

No. sample	La	Ce	Sm	Eu	Tb	Yb
THOLEIITIC SERIES						
1. 50A	5 (16.1)	14 (17.3)	2.2 (11.3)	0.78 (10.6)	0.53 (11.2)	4.3 (21.6)
2. 54A	6 (19.4)	11 (13.6)	3.6 (18.5)	0.89 (12.1)	0.43 (9.1)	4.5 (21.5)
3. 1447	3 (9.7)	14 (17.3)	2.8 (14.4)	0.67 (9.1)	0.46 (9.7)	2.0 (9.6)
4. 1448	10 (32.3)	28 (34.7)	4.3 (22.1)	0.81 (11.0)	0.67 (14.1)	5.4 (25.8)
5. 1476	6 (19.4)	18 (22.3)	3.8 (19.5)	0.73 (9.9)	0.66 (13.9)	4.2 (20.1)
6. 1462	14 (45.2)	27 (33.4)	4.2 (21.5)	0.70 (9.5)	0.68 (14.4)	7.5 (35.9)
7. 1449	12 (38.7)	30 (37.1)	4.4 (22.6)	0.75 (10.2)	0.53 (11.2)	13 (62.2)
CALC-ALKALINE SERIES						
8. 47A	11 (35.5)	32 (39.6)	3.9 (20.0)	0.71 (9.1)	0.50 (10.6)	5.5 (24.3)
9. 503	8 (25.8)	25.8 (31.5)	3.0 (15.4)	0.90 (12.2)	0.70 (14.8)	2.1 (10.0)
10. 501	13 (41.5)	25.0 (30.9)	2.2 (11.3)	0.62 (8.4)	0.44 (9.3)	1.3 (6.2)
11. 459	45 (145.2)	78 (96.5)	6.3 (32.3)	1.14 (15.5)	0.80 (16.9)	1.8 (8.6)
SPILITES OF FENEŞ FORMATION						
12. 243	12 (38.7)	25 (30.9)	2.7 (13.9)	0.57 (7.8)	0.50 (10.6)	3.0 (14.4)
13. 476	16 (51.6)	30 (37.1)	3.4 (17.4)	0.61 (8.3)	0.52 (11.0)	4.4 (21.0)
14. 563	39 (125.8)	68 (84.2)	6.3 (32.3)	1.12 (15.2)	0.90 (19.0)	2.0 (9.6)

1, Basalt (pillow lava) – Podeni Valley; 2, Dolerite – Podeni Valley; 3, Basalt (pillow lava – Toc; 4, Basalt – Vărădia de Mureş; 5, Basalt – Zăbalţ; 6, Dolerite – Pătârş; 7, Basalt-Bătuţa Quarry; 8, Basaltic andesite – Lopadea Veche; 9, Basaltic andesite – Rachiş Valley; 10, Rhyodacite – Rachiş Valley; 11, Microdiorite – Porcului Valley; 12, Spilite (pillow lava) – Telna Valley; 13, Spilite (Gabro-dolerite) – Valea Mică-Ighiel; 14, Spilite – Bucerdea.
Analyst: M. Stoian

Table 2
Σ REE and Eu/Sm, $(La/Yb)_N$, $(La/Ce)_N$, $(Ce/Yb)_N$ ratios

No. sample	ΣREE	Eu/Sm	$(La/Yb)_N$	$(La/Ce)_N$	$(Ce/Yb)_N$
THOLEIITIC SERIES					
1. 50A	26.81	0.36	0.78	0.93	0.84
2. 54A	26.42	0.25	0.92	1.43	0.63
3. 1447	22.93	0.24	1.01	0.56	1.81
4. 1448	49.18	0.19	1.24	0.93	1.34
5. 1476	33.39	0.19	0.96	0.87	1.11
6. 1462	54.08	0.17	1.26	1.35	0.93
7. 1449	60.68	0.17	0.62	1.04	0.60
CALC-ALKALINE SERIES					
8. 47A	53.61	0.18	1.35	0.90	15.06
9. 503	37.17	0.30	2.57	0.81	3.18
10. 501	42.56	0.28	6.69	1.34	4.98
11. 459	133.04	0.18	16.88	1.50	11.22
SPILITES OF FENEŞ FORMATION					
12. 243	43.77	0.21	2.69	1.25	2.15
13. 476	54.93	0.18	2.48	1.39	1.77
14. 563	117.32	0.18	13.10	1.49	8.77

Table 3
Range of variation and mean values of ΣREE, Eu/Sm, $(La/YB)_N$, $(La/Ce)_N$, $(Ce/Yb)_N$ ratios of the ophiolites from the South Apuseni Mts

	ΣREE	Eu/Sm	$(La/Yb)_N$	$(La/Ce)_N$	$(Ce/Yb)_N$
THOLEIITIC SERIES (25 samples)					
Range of Variation	16.62–60.68	0.12–0.54	0.39–1.53	0.44–1.63	0.33–1.87
Mean	26.96	0.29	0.85	0.92	0.99
CALC-ALKALINE (20 samples)					
Range of Variation	37.17–267.6	0.16–0.37	0.45–59.47 (1.35–20.66)**	0.13–2.07	2.42–59.21 (2.42–19.61)*
Mean	117.15	0.25	10.38(8.31)**	1.03	10.95(8.41)*
SPILITES OF FENEŞ FORMATION (7 samples)					
Range of variation	21.70–117.32	0.18–0.36	2.40–13.10	1.25–2.35	1.13–8.77
Mean	46.95	0.26	4.25	1.63	2.75

** – ignored two samples; * – ignored one sample.

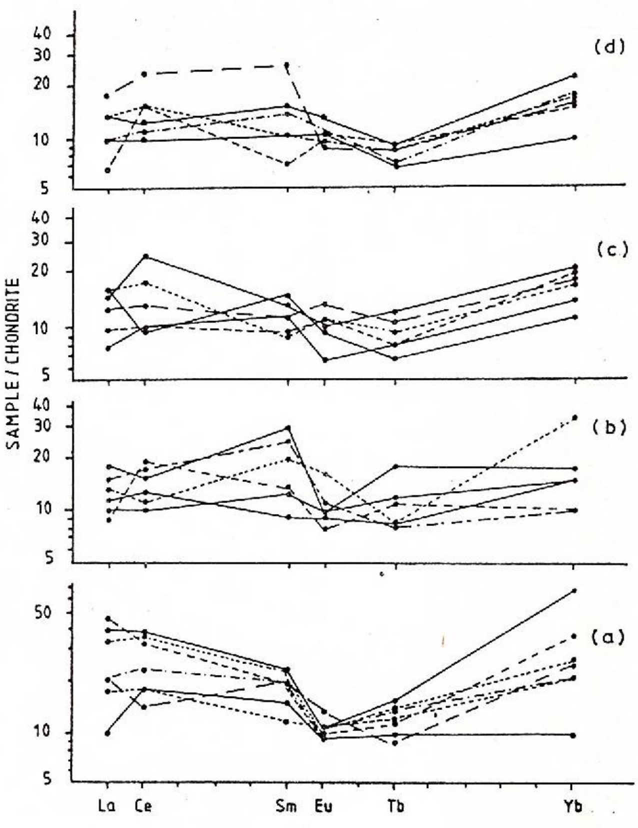

Fig. 2 – Chondrite-normalized REE patterns in tholeiitic series rocks (volcanic arc type). (a, samples of this paper – Tab. 1; b–d, samples of Savu et al., 1994).

disappears for the segment beyond Eu (toward Tb and Yb).

A satisfactory pattern comparison with the tholeiitic-continental, back arc basin and island arc basalts (see Cullers, Graf, 1984, Fig. 7.7) is noteworthy. Furthermore, the $(La/Ce)_N$ ratio is always <1 in case of N-type MORB, according to Saunders (1984). It is to be mentioned that the tholeiitic series of the South Apuseni Mts have a $(La/Ce)_N$ ratio between 0.44 and 1.63.

The patterns of the calc-alkaline series (Fig. 3) show medium to high chondrite-normalized LREE values. $(La/Ce)_N$ ratio varies between 0.13 and 2.07 (Tab. 3), resulting in ascending and descending portions of the curves between these elements. Negative Eu-anomalies are sometimes noticed and interpreted as a result of fractional crystallization of the plagioclase.

As mentioned earlier, it is accepted that the Feneş Formation spilites are marginal basin products; however, Savu and Stoian (1992) have included both calc-alkaline series rocks and the Feneş Formation spilites in the island arc volcanics units. They claim that "chondrite-normalized REE patterns are very similar with the diagram of Neokimmerian island arc volcanics of the Metaliferi Mts (Mureş Zone)", previously established by Savu et al., 1986. In fact, a comparison between basic and intermediate rocks (that is "a" and "b" curves of the Fig. 2, p.46, Savu, Stoian, 1992) and the mentioned diagram (Savu et al., 1986, Fig. 7, p. 448) shows the following characteristics: curves "a" and "b" (Savu, Stoian, 1992, Fig. 2) begin at 20-30 La_N, plunging down to slight negative Eu-anomaly, whereas the curves by Savu et al., 1986 begin at 80–180 La_N. This difference is normal because the first pattern belongs to the Feneş Formation spilites and the second one to basaltic rocks of the calc-alkaline series.

Spilites of the Feneş Formation exhibit patterns that start with 25–50 values of La_N (with one exception, Fig. 4) and descend toward Ce-Sm-Eu. Next sectors, that is Eu-Tb and Tb-Yb, show both ascending and descending tendencies, producing negative Eu-anomalies and negative and positive Tb-anomalies. The $(La/Ce)_N$ ratio of the spilites always exceeds 1.

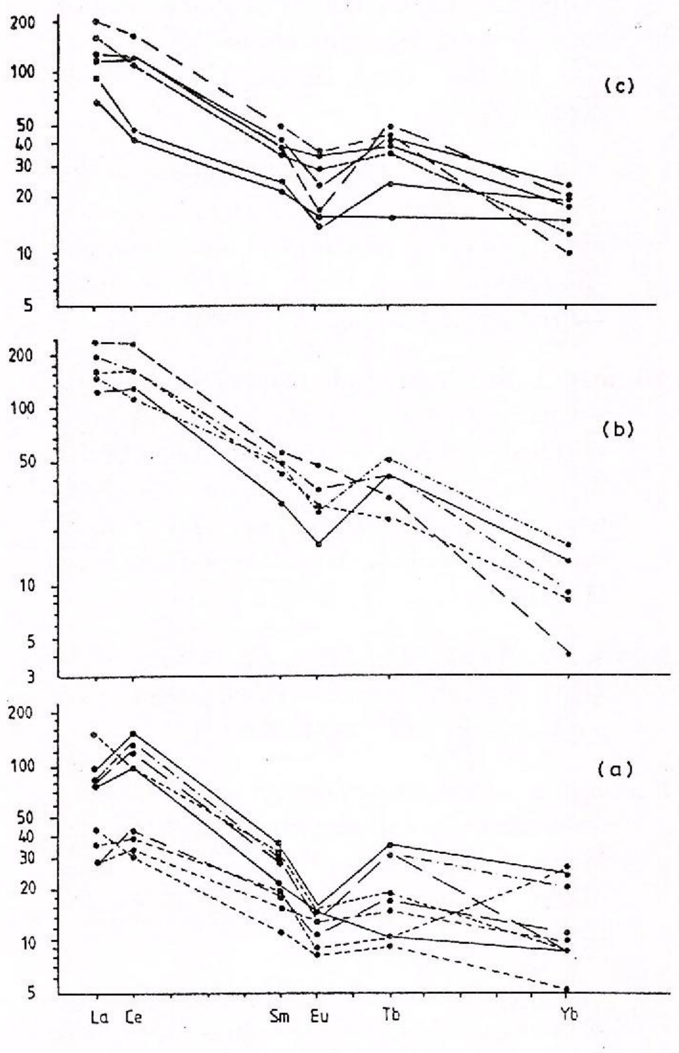

Fig. 3 – Chondrite-normalized REE patterns in calc-alkaline series rocks (volcanic arc type). (a, samples of Trascău Mts, this paper, Tab. 1 and Savu, Stoian (1992); b,c, samples of Savu et al., 1986).

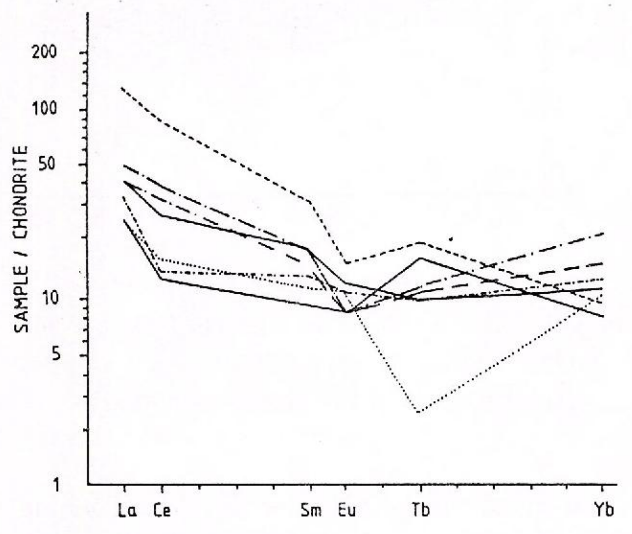

Fig. 4 – Chondrite-normalized REE patterns in spilitic series of Feneş Formation (ensialic marginal basin type). (Samples of this paper, Tab. 1 and Savu, Stoian, 1992).

Figure 5 exhibits a synthetical diagram concerning REE variation limits of the tholeiitic, calc-alkaline and spilitic series. The patterns of REE contents are conform to the ophiolite genetic model (i.e. Nicolae et al., 1992) as follows: The oceanic crust formed in the Transylvanian rift was subducted beneath the Apuseni Mts microcontinent, giving rise to a volcanic arc. The basal part of the volcanic arc consists of tholeiitic series rocks formed by relatively high degree of partial melting of the upper mantle above the subducted slab. The upper part of the volcanic arc consists of calc-alkaline series rocks, resulting from melting of the subducted slab itself. Contamination, during the upward motion of the magma and fractional crystallization, justifies the REE pattern of calc-alkaline series.

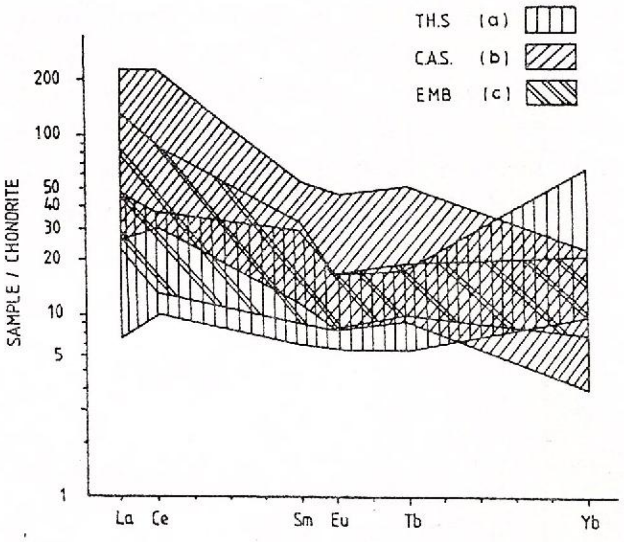

Fig. 5 – The range of REE content of the ophiolites from the South Apuseni Mts. (a, the tholeiitic series; b, calc-alkaline series; c, the spilitic series of the Feneş Formation).

An ensialic marginal basin developed behind the volcanic arc. Its products exhibit REE pattern of intermediate character between the tholeiitic series and the calc-alkaline series. The resulting spilitic rocks were strongly influenced by the "geochemical subduction component", characterisitc of a supra-subduction zone (SSZ) ophiolite, sensu Pearce et al. (1984).

Conclusions

– The tholeiitic series, calc-alkaline series and spilitic series, that represent the ophiolite suite of the South Apuseni Mts, have well defined and differentiated REE trends.

– REE patterns of the South Apuseni Mts ophiolitic suite provide valuable information about their petrogenesis and additional data to confirm the ophiolite genetic model sensu Nicolae et al. (1992).

References

Boynton, V.W. (1984) Cosmochemistry of the rare earth elements: meteorite studies. In: *Rare Earth Elements Geochemistry*, P. Henderson (Ed.), p. 63–114, Elsevier, Amsterdam-Oxford-New York-Tokyo.

Cioflica, G., Lupu, M., Nicolae, I., Vlad, Ş. (1980) Alpine Ophiolites of Romania. Tectonic Setting, Magmatism and Metallogenesis. *An. Inst. Geol. Geofiz.*, LVI, p. 79–85, Bucureşti.

– **, Nicolae, I. (1981)** The origin, evolution and tectonic setting of the Alpine ophiolites from the South Apuseni Mountains (Romania). *Rev. Roum. Géol. Géophys. Géogr. (Géol.)*, 25, p. 19–29, Bucureşti.

Cullers, L.R., Graf, L.J. (1984) Rare earth elements in igneous rocks of the continental crust: predominantly basic and ultrabasic rocks. In: *Rare Earth Element Geochemistry*, P. Handerson (Ed.), p. 237–274, Elsevier, Amsterdam-Oxford-New York-Tokyo (1984).

Lupu, M. (1983) The Mesozoic History of the South Apuseni Mts. *An. Inst. Geol. Geophys.*, LX, p. 115–124, Bucureşti.

Nicolae, I. (1983) Consideraţii pe marginea interpretării cadrului tectonic al ofiolitelor din Munţii Apuseni de Sud. *Stud. Cerc. Geol. Geofiz. Geogr. (Geol.)*, 28, p. 35–45, Bucureşti.

– **(1995)** Tectonic Setting of the Ophiolites of the South Apuseni Mountains: Magmatic Arc and Marginal Basin. *Rom. J. Tect. Reg. Geol.*, 76, p. 27–38, Bucureşti.

– **, Soroiu, M., Bonhomme, M.G. (1992)** Ages K–Ar de quelques ophiolites des

Monts Apuseni du sud et leur signification géologique (Roumanie). *Géol. Alpine*, 68, p. 77–83, Grenoble.

Pearce, A. J., Lippard, J.S., Roberts, S. (1984) Characterisitcs and tectonic significance of supra-subduction zone ophiolites. In: Kokelaar B.P. & Howells M.F. (Ed.) *Marginal Basin Geology, Geol. Soc. Lond. Spec. Publ.*, 16, p. 77–94, London.

Saunders, A.D. (1984) The rare earth element characteristics of igneous rocks from the Ocean Basins. In: *Rare Earth Element Geochemistry*, P. Henderson (Ed.), p. 205–235, Elsevier, Amsterdam-Oxford-New York-Tokyo.

Savu, H., Lemne, M., Romanescu, O., Stoian, M., Grabari, G. (1986) Distribution of U, Th, K, REE and other trace elements in island arc volcanics and some ophiolites from Vaţa-Vorţa-Vălişoara region (Mureş Zone). *D.S. Inst. Geol. Geophys.*, 70–71/1, p. 431–452, Bucureşti.

– **, Stoian, M. (1988)** REE contents in the sheeted dyke complex of the Mureş Zone and their petrogenetic significance. *Rev. Roum. Géol. Géophys. Géogr. (Géol.)*, 32, p. 37–44, Bucureşti.

– **, Stoian, M. (1992)** Distribuţia pămînturilor rare şi Hf în vulcanitele de Arc Insular Neokimmerice din Munţii Trascău (Zona Mureş). *Stud. cerc. Geologie*, 37, p. 41–48, Bucureşti.

– **, Stoian, M., Tiepac, I., Popescu, Gh., Grabari, G. (1994)** Petrological Significance of REE, U, Th, K, Rb, Sr, Hf and the $^{87}Sr/^{86}Sr$ in the Basaltic Complex of the Mureş Zone. *Rom. J. Petrol.*, 76, p. 77–84, Bucureşti.

Received: May 17, 1995.
Accepted: June 15, 1995.

Rom. J. Petrology, 77, p. 49–60, Bucureşti, 1996

A COMPARATIVE STUDY OF THE OPHIOLITES OBDUCTED FROM TWO DIFFERENT SEGMENTS OF THE MUREŞ OCEAN "NORMAL" MEDIAN RIDGE (ROMANIA)

Haralambie SAVU

Institutul Geologic al României. Str. Caransebeş 1, 79 678 Bucureşti 32

Key words: Ophiolites. Ridge Segments. Petrology. Geochemistry. REE. N-Type MORB. Mureş Zone. Banat. Apuseni Mountains.

Abstract: The Jurassic (180 Ma) ophiolites from the Mureş Zone or the Mureş Suture are cropping out over an area of about 200 km long. They have been obducted from two different segments of the Mureş Ocean median ridge and show a N-Type MORB character. The rock patterns from the western ridge segment exhibit a Tb negative anomaly, while those from the eastern ridge segment show an Eu negative anomaly. The normal tholeiitic rocks from the eastern ridge segment are more depleted in Y and richer in TiO_2, showing a more evolved parental magma. The rocks from the western ridge segment are richer in CaO and Ba, while those from the eastern ridge segment are richer in Na_2O and Sr. In the basalt complex originating in the western ridge segment the highest Rb contents and the highest values of the Rb/Sr ratio have been determined. The values of the La/Yb, (La/Sm)N, (Ce/Sm)N and (La/Ce)N ratios are usually higher in the rocks from the eastern ridge segment. These observations indicate that the differences between the rocks from the two "normal" ridge segments of the Mureş Ocean have been determined by the mantle characteristics within each segment, the partial melting conditions of the parental magma and by its differentiation.

Introduction

The N-Type MORB character of the Liassic (180 Ma, Herz et al., 1974)[1] ophiolites from the Mureş Suture or the Mureş Zone (Savu, 1983) was established by Savu and Stoian (1988) in the Drocea Mountains. Studying the coeval ophiolites from the Trascău Mts, Savu et al. (1991) observed that they display some chemical characteristics differing a little from those of the Drocea Mts. With the object to determine the peculiarities of ophiolites from the two areas, a comparative study was performed, the results of which were showed in the present paper.

[1]See also the geological arguments for the Liassic–Dogger age of these ophiolites in Savu et al. (1996).

Extension of the Ophiolites from the two Ridge Segments and Structural–Petrographic Aspects

The Mureş Zone extends between Pătârş in Banat and Turda in the Transylvanian Basin, over an area of about 200 km long. This represents the Carpathian segment of the Major Tethysian Suture (Rădulescu et al., 1993). Along the Mureş Zone the Liassic ophiolites are cropping out from under younger formations in many inliers. Evidently, they are alochthonous, as they originate in the dismembered Mureş Ocean crust, from which an prised only the two upper complexes of the ocean crust: the basalt complex (O_1) and the sheeted dyke complex (O_2). During the Mureş Ocean closure commencing during Callovian, the ophiolite megaslab was covered by the Upper Jurassic-Lower Cretaceous volcanics of two island arcs and by the Mesozoic flysch deposits, then being involved in the Alpine plicative and thrust structures. Thus, the initial ophiolite megaslab was smashed into many fragments, that now form the socle of some Alpine nappes of the Mureş Zone, or occur as olistoliths in the mélange formations. Nicolae

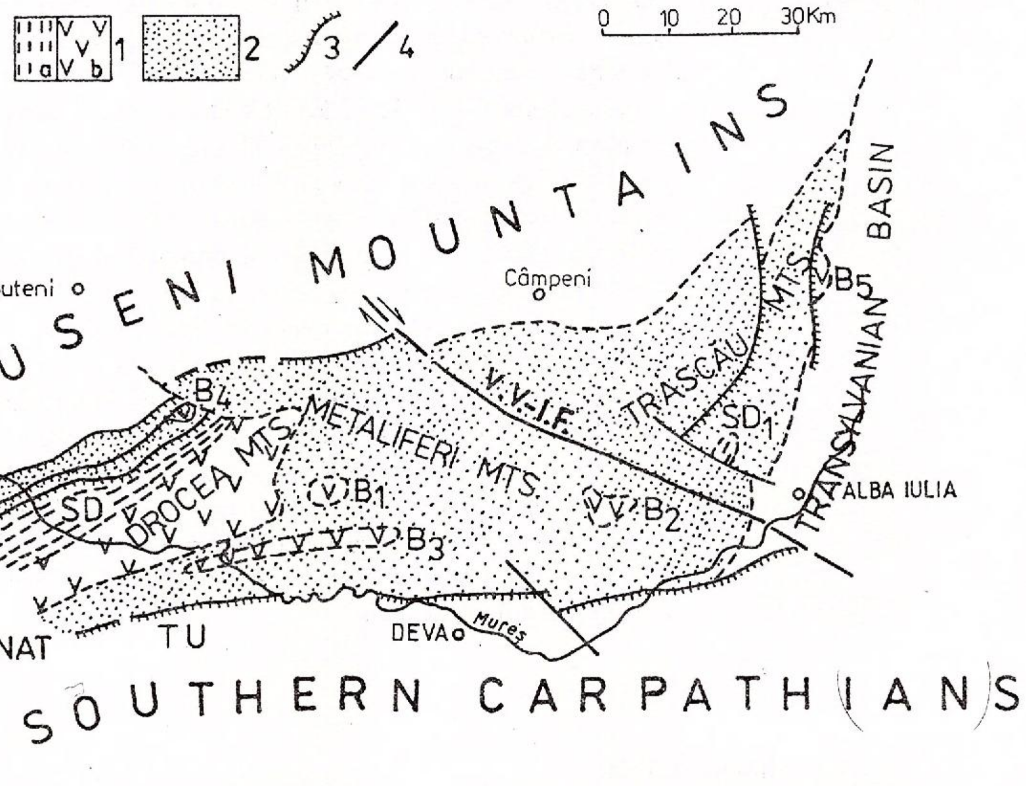

Fig. 1 – Sketch map of the Mureş ophiolitic suture. 1, Jurassic (180Ma), ophiolites: 1a, sheeted dyke complex of the Drocea Mts (SD); SD_1, sheeted dyke olistolith of Ampoiţa (Trascău Mts); 1b, basalt complex of the Drocea Mts (B); B_1, basalts in Visca inlier; B_2, basalts and gabbros in Almaşu Mare inlier; B_3, basalts in Groşi-Săliştioara tectonic rise; B_4, basalts in Criş Nappe socle; B_5, basalts in the Podeni Nappe socle; 2, island arc volcanics ($J_3 - K_1$), Mesozoic sedimentary deposits, Neogene volcanics and sedimentary deposits; 3, thrust (TU, Tisa Unit; CU, Criş Unit); 4, fault (V.V.-I.F., Valea Verde–Inuri fault).

ophiolite megaslab was scraped out and obducted over the NW and SE convergent plates (Savu, 1983). This initial megaslab com- (in Balintoni et al., 1994) included the rocks from these slabs in the Upper Jurassic-Lower Cretaceous island arc volcanics.

According to their origin, in two segments of the median ridge of the Mureş Ocean, the ophiolites from the Mureş Zone are distributed in two areas: (1) the ophiolites of the Drocea and Metaliferi Mts originating in the western ridge segment and (2) the ophiolites of the Trascău Mts originating in an eastern ridge segment .

1. The ophiolites originating in the western ridge segment occur in a more important ophiolite slab forming the socle of the Căpâlnaş-Techereu Nappe, that extends over a length of about 120 km between Pătârş and Zlatna, and another slab constituting the socle of the Criş Nappe, occurred in the Drocea subduction trench (Savu, 1983). Lupu et al. (1995) considered the rocks from the last nappe as formed in a marginal basin. The largest cropping area of ophiolites within the western region occurs in the Drocea Mts, where the two mentioned complexes (O_1 and O_2) have been described. The NE–SW direction of these complexes is diagonal as against the E–W trend of the ophiolitic suture in this area (Fig. 1). Within the Metaliferi Mountains these ophiolites are mostly covered by Mesozoic island arc volcanics and sedimentary deposits and by Neogene volcanics and sedimentary deposits.

The sheeted dyke complex (O_2) is situated on the western margin of this area, extending from Banat to Drocea Mts, over a length of about 50 km and a maximum width of 10 km. Its cropping area corresponds to the axial zone of the Mureş Ocean median ridge, that was denudated on a considerable depth, so that more acid rocks from its core have been exposed. This complex consists of 100 % parallel dykes, trending N40^0–80^0E/70^0–80^0N. Their thickness varies from 0.5 to 2 m, rarely from 5 m to 10 m. They are composed mostly of intergranular basalts and dolerites and more rarely of gabbros and albite dolerites as well as of acid–albitic rocks like albite quartzdiorites, albitites, hornblende granophyres and albite plagiogranites differentiated from the tholeiitic magma (Savu et al., 1984). As the acid rocks are rich in Y (>40 ppm) and depleted in Nb (<10 ppm) they belong to the ocean floor granite group (ORG – Pearce et al., 1984; Savu, Stoian, 1988). According to the O'Connor's (1965) classification most of the acid rocks show a trondhjemitic character. The basalt and dolerite dykes exhibit "chill margins" indicating their formation during the ocean spreading. Some gabbro dykes contain 20–25 % vanadiferous Ti-magnetite. The crystallization succession was plagioclase (An55) – clinopyroxene – Ti-magnetite ± pyrite. The rocks were affected by the hydrothermal metamorphism (Savu, 1967) on the ocean floor, so that the plagioclase was sometimes saussuritized and albitized and the clinopyroxene was substituted by uralite, epidote, actinolite and chlorite.

The pillowed basalt complex (O_1), the upper one, occurs on both sides of the sheeted dyke complex, but its largest cropping area is situated south-east of the latter, between Vaţa, Cuiaş and Zam. Probably, this area represented an abyssal plaine on the Mureş Ocean floor. Within the Metaliferi Mts, east of this area, the basalt complex appears from under the younger formations in the Visca, Luncoi, Brad and Almaşu Mare inliers as well as within the Groşi-Săliştioara tectonic rise. This complex consists of basaltic lava flows, rarely associated with pyroclastics. Between the lava flows from the Groşi-Săliştioara tectonic rise beds of recrystallized limestones, sandstones and microconglomerates are present, indicating the nearness of the Transylvanian continent during the magmatic activity. North of the sheeted dyke complex only red argillaceous beds occur between the basaltic flows. This complex consists of intersertal basalts associated with hyalobasalts, amygdaloidal basalts and tachylites. The amygdales of these basalts are infilled with quartz, calcite, zeolites and chlorite formed under the zeolitic facies conditions of the hydrothermal metamorphism on the ocean floor. The basalt spilitization determined the albitization of the plagioclase laths and the chloritization of the augite crystals and of the interstitial glass.

Within both ophiolite complexes peridotite and gabbros layered bodies are present. In some of them acid-albitic rocks are also to be found.

2. The ophiolites originating in the eastern ridge segment are distributed in the Trascău Mts, north-east of the Valea Verde–Inuri fault that shifted them, concomitantly with a counter-clockwise rotation (Fig. 1). In this area only the northern structures of the Mureş Zone, including the western margin of the Podeni Nappe, are represented, the southern structures being subsided in the Transylvanian Basin (Savu, 1990). The Trascău ophiolites resulted from both the basalt complex (O_1) and the sheeted dyke complex (O_2). Those originating in the first complex occur in the socle of the Podeni Nappe and as olistoliths in an Upper Jurassic mélange with pyroclastic matrix. The basaltic flows exhibit intersertal and variolitic structures. The thin pillow lava crust consists of hyalobasalt, and between the pillow forms there was a glassy matrix that was chloritized during the ocean floor metamorphism. The ophiolites resulted from the second complex are represented by the sheeted dyke slab of Ampoiţa and by some dolerite exotic blocks in the mentioned mélange. The sheeted dyke slab of Ampoiţa consists of 100 % dykes of intergranular basalts and dolerites with "chill margins" and gabbrodiorites as well as of acid-albitic rocks like albite felsites and albitites similar to those from the western segment.

Distribution of Major Elements

According to the Tables 1 and 2, SiO_2 varies in the basic rocks of both ridge segments from 47 to 50 %, the lower content being determined in basaltic rocks of the western segment. In the acid rocks from both ridge segments its average increases up to 58 % and 60 % respectively, the highest content being determined in the ocean floor albite granites (75.53 %) of the western ridge segment.

The highest TiO_2 average (3.41 %) was determined in the differentiated basic rocks from the sheeted dyke complex of the western ridge, in which a concentration of iron, mostly as FeO, and V (407 ppm) in the Ti–magnetite occurred, that is a characteristic of the tholeiitic magma differentiation (Savu et al., 1984).

The MgO averages vary from 6 to 7 % in both ridge segments. They decrease in the differentiated basic rocks of the western ridge segment, and especially in the acid rocks of both segments in which these values are close enough. The highest CaO average (10–10.4 %) occur in the basic rocks from the western ridge segment, while in the acid rocks from both ridge segments they decrease and are very close.

Consequently, the lowest Na_2O average was determined in the same basic rocks of the western segment – about 3 % in the sheeted dyke complex; it increases a little in the basaltic complex (3.64 %) due to the spilitization. In the basic and acid rocks of the eastern ridge segment the Na_2O averages are higher than in the rocks of the western segment. It is of note the average values of 0.40 and 0.45 % P_2O_5 from the differentiated basic and acid rocks of the western ridge segment. A close value (0.38 % P_2O_5) was determined in the differentiated acid rocks from the eastern segment.

Distribution of Trace Elements

As it is shown in Tables 1 and 2, the Ni averages are higher in the basic rocks of both complexes from the western ridge segment. These decrease a little in the basaltic rocks of the eastern segment and more pronounced in the differentiated basic rocks of the sheeted dyke complex from the western ridge segment. In the acid rocks from both ridge segments the Ni values decrease very much, especially in those of the western segment. The highest Co

Table 1

Ranges and averages of major and trace elements in the basalt complex (data acc. to Savu et al., 1994a) and the sheeted dyke complex (data acc. to Herz et al., 1974 and Savu et al., 1981) from the western ridge segment

Oxides/ Elements	Basalt complex		Sheeted dyke complex					
			I		II		III	
	Ranges	Averages	Ranges	Averages	Ranges	Averages	Ranges	Averages
SiO_2 %	39.31–52.22	47.00	49.27–51.48	49.90	45.20–51.54	48.33	51.76–75.53	60.43
TiO_2	0.02–2.74	0.54	0.60–2.35	1.62	2.39–6.95	3.41	0.34–2.68	1.69
Al_2O_3	13.24–16.36	14.79	12.87–15.95	14.35	10.87–13.42	12.15	11.30–4.14	12.65
Fe_2O_3	1.65–8.24	5.15	1.36–4.80	3.15	2.46–11.12	5.42	2.78–6.96	4.15
FeO	1.48–12.79	4.96	5.10–9.32	7.72	3.60–14.84	10.77	0.64–9.64	6.52
MnO	–	–	0.14–0.23	0.19	0.16–0.31	0.25	0.01–0.28	0.14
MgO	3.77–9.74	6.25	6.10–8.65	6.90	3.22–6.21	5.24	1.30–2.99	2.18
CaO	4.52–16.12	10.07	8.17–11.70	10.40	6.49–8.79	8.16	1.58–7.03	4.84
Na_2O	1.79–6.20	3.64	2.28–3.67	2.95	2.31–4.58	3.32	4.65–5.71	5.17
K_2O	0.02–2.74	0.54	0.06–0.59	0.20	0.05–0.41	0.17	0.05–0.39	0.18
P_2O_5	0.08–0.29	0.17	0.08–0.32	0.21	0.06–1.64	0.40	0.12–0.88	0.45
Ni ppm	2–210	84.11	40–100	71	8.5–65	35.1	3.5–15	6.9
Co	3.5–50	29.35	32–52	42.4	36–57	46.36	6–22	14.7
Cr	1–570	216	65–340	169.4	1.5–130	27.06	0–9	3.78
V	30–460	242	200–340	267.7	180–900	406.7	12–150	58.3
Sc	15–42	30.79	31–40	35.8	30–42	35.4	7.5–23	19.2
Zr	40–220	83.75	37–200	121.5	105–280	210.33	240–805	416.4
Y	15–65	26.25	14–55	32.9	30–155	66	65–931	224.4
Yb	1.2–6.5	2.65	2–6.5	4.4	4.8–10.5	6.8	0.5–18.5	8.33
Ba	10–215	72.52	12–50	29.23	18–48	30.8	18–80	48
Sr	65–600	221.25	95–300	156	95–175	127.3	44–155	88.42
Pb	2–18	2.52	0–60	6.1	0–14	5	0–7	3.58
Cu	2–100	36.42	6–90	35	4–53	26.7	4–23	8.2
Ga	9–22	14.32	10–19	14.6	15–26	18.37	21–30	25.14
Zn	30–70	44.22	–	–	–	–	–	–
Sn	–	–	0–2	1	0–7	2.5	0–3	2.14
Hf	0–2.5	1.22	–	–	–	–	–	–
Rb	5.86–46.4	18.77	1–3	1.66	4–15	10.2	4–15	12.2
Rb/Sr	0.03–0.26	0.11	0.01–0.03	0.018	0.021–0.018	0.058	0.021–0.108	0.058
$^{87}Sr/^{86}Sr$	0.700–0.704	0.702	0.702–0.703	0.7026	0.702–0.704	0.703	0.703–0.705	0.704
Zr/Hf	26.2–145	78.2	–	–	–	–	–	–

I, Normal tholeiitic rocks; II, Differentiated basic rocks; III, Differentiated acid-albitic rocks

contents (42–46 ppm) were obtained in the basic rocks of the sheeted dyke complex of the western ridge segment. They decrease in the basalt complex of the same ridge segment and are very close to the contents in the basic rocks of the eastern ridge segment, a decrease that continues in the acid rocks of both segments.

In the basic rocks of the western ridge segment the highest Cr average was determined. This gradually decreases in the basic rocks of the sheeted dyke complex of both segments, reaching 27 ppm in the differentiated basic rocks of the sheeted dyke complex of the western ridge segment. In the acid rocks from both segments Cr strongly decreases.

Zirconium varies within large ranges in the two ridge segments.

Table 2

Ranges and averages of the major and trace elements in the ophiolitic rocks from eastern ridge segment (data acc. to Savu et al., 1992)

Oxides/ Elements	Basic rocks (the two complexes)		Acid-albitic rocks (sheeted dyke complex)	
	Ranges	Averages	Ranges	Averages
SiO_2 %	44.72–51.40	48.90	54.09–62.16	58.24
TiO_2	0.88–2.60	1.65	1.08–2.76	1.96
Al_2O_3	14.29–16.80	15.37	13.79–14.54	14.65
Fe_2O_3	3.01–8.81	5.41	5.38–6.35	6.05
FeO	3.75–7.26	5.48	2.40–6.40	4.43
MnO	0.12–0.23	0.17	0.07–0.18	0.13
MgO	4.28–8.52	5.99	1.69–3.90	2.76
CaO	2.59–13.58	7.80	3.56–5.21	4.35
Na_2O	2.66–5.48	4.29	4.52–6.50	5.50
K_2O	0.09–0.96	0.36	0.08–0.23	0.16
P_2O_5	0.08–0.40	0.18	0.25–0.48	0.38
Ni ppm	12–140	51.63	3.5–16	9.12
Co	7.5–38	26.04	9–23	16.50
Cr	1.5–340	140.72	1.5–9.5	5.37
V	190–500	307.27	33–420	204.50
Sc	27–40	33.63	16–36	24.50
Zr	38–220	110.9	260–320	292.50
Y	20–55	32.56	60–87	56.29
Yb	25–55	4.04	4.6–7.5	6.52
Ba	10–170	38.18	10–24	14.75
Sr	78–380	225.08	64–111	88.82
Pb	2–6.5	4.22	2–9	5.62
Cu	2–130	36.54	2–4	2.75
Zn	30–90	38.90	30–90	40.75
Ga	12–19	15.36	16–28	19.75
Rb	9–13	8.43	3–5	2.37
Rb/Sr	0.011–0.123	0.07	0.026–0.073	0.05
$^{87}Sr/^{86}Sr$	0.703–0.705	0.704	0.705–0.706	0.7055

The highest average content (416.4 ppm) was obtained in the acid rocks of the sheeted dyke complex of the western ridge segment and in those from the eastern segment (292.5 ppm), and the lowest contents occurred in the basaltic complex of the western segment that originates in a slightly evolved magma.

Higher Y and Yb averages were obtained in the acid rocks of the sheeted dyke complex from the western ridge segment, too. The relationships between Ti, Y and Zr (Fig. 2; Pearce, Gale, 1977) show that the rocks from both ridge segments are margin plate tholeiites, and those between TiO_2 and Y (Fig. 3; Perfit et al., 1980) indicate that they are N-Type MORB rocks.

The diagram in Figure 3 also shows that the TiO_2/Y ratio is higher in the ophiolitic rocks from the western segment originating in a more evolved magma. The values of this ratio increase concomitantly with the magma differentiation.

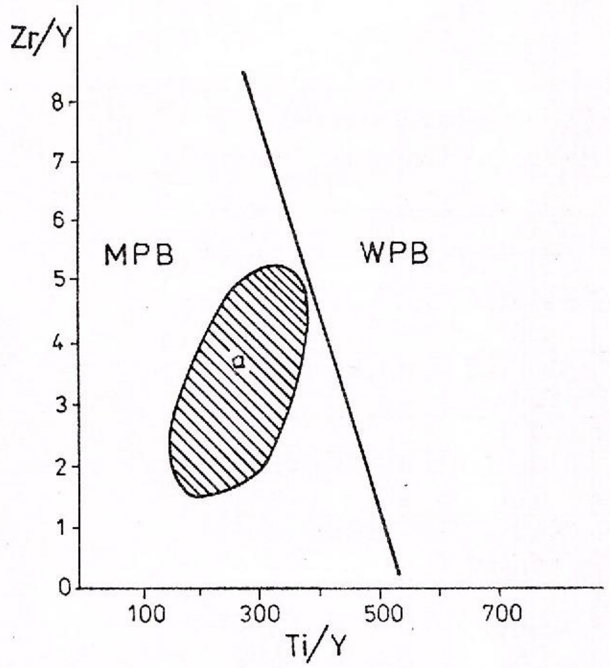

Fig. 2 – Plot of the ophiolitic rocks on the Zr/Y–Ti/Y diagram. MPB, margin plate basalts; WPB, intra-plate basalts; a, Mureş Zone ophiolites.

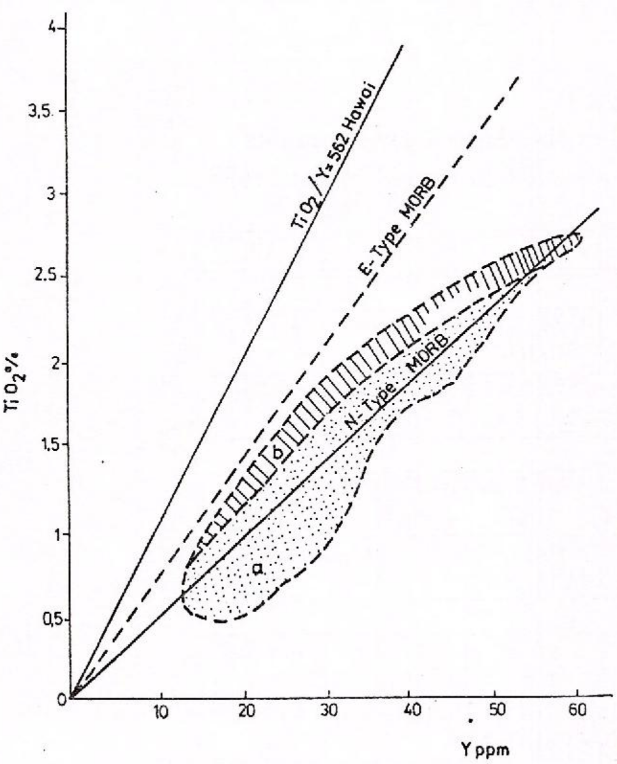

Fig. 3 – Plot of the ophiolitic rocks on the TiO_2–Y diagram. a, ophiolites from the western ridge segment; b, ophiolites from the eastern ridge segment.

It is noteworthy that the highest Ba content (72.5 ppm) was determined in the basalt complex from the western ridge segment and the highest Sr value (225 ppm) was determined in the basic rocks from the eastern ridge segment. Both elements gradually decrease toward the acid rocks of both segments, the lowest contents being a characteristic of the eastern segment rocks.

The highest Rb average contents were determined in the basalt complex of the western ridge segment. The average values of Rb/Sr ratio are also higher in the same basalt complex. The Pb, Cu and Ga average contents are close in the basic rocks of the two ridge segments, but are a little higher in the acid rocks of the western segment than in those of the eastern segment.

The values of the $^{87}Sr/^{86}Sr$ ratio vary from 0.701 to 0.704 in the basic rocks of both ridge segments, with an average of 0.703, indicating their origin in an ocean crust (Herz et al., 1974). It is noteworthy that in the differentiated acid-albitic rocks from both ridge segments the value of this ratio increases up to an average of 0.704 in the west segment and up to 0.705 in the eastern ridge segment. As it results from Table 1, the value of this ratio increases from 0.7026 in the normal tholeiitic rocks up to 0.704 in the differentiated acid-albitic rocks. It seems that the magma differentiation influenced the proportion of the two Sr isotopes. Therefore, the age of 140 Ma assumed for the albitized acid rocks (Herz et al., 1974) may not be a real one. As these rocks occur as exotic blocks in the Upper Jurassic mélange from the Trascău Mts, they must be older.

Distribution of REE

The REE contents (Tab. 3,4,5) in ophiolites from both ridge segments were determined by neutron activation analysis (Savu, Stoian, 1988, 1991; Savu et al., 1994b). It is of note a general process of REE concentration

Table 3

Ranges and averages of the REE in the basalt complex from the western ridge segment (data acc. to Savu et al., 1994 b)

Elements	La	Ce	Sm	Eu	Tb	Yb
Rocks with SiO_2 < 48 %						
Ranges	1.3–6	8–15	1.8–5.8	0.35–0.87	0.37–0.86	1.2–4
Averages	3.66	11.57	2.94	0.66	0.48	2.4
LREE/HREE=5.79; La/Yb=1.66; (La/Sm)N=0.87; (Ce/Sm)N=0.98 (La/Ce)N=0.89; (Ce/Yb)N=1.12						
Rocks with SiO_2 between 48 and 49.5 %						
Ranges	2.0–5.0	8–15	1.6–3.8	0.69–1.18	0.30–0.48	2.2–7.0
Averages	3.99	11.12	2.30	0.71	0.41	3.60
LREE/HREE=4.06; La/Yb=1.27;(La/Sm)N=1.11; (Ce/Sm)N=1.20 (La/Ce)N=1.00; (Ce/Yb)N=0.90						
Rocks with SiO_2 > 49.5 %						
Ranges	2.0–8.0	6–20	1.3–5.0	0.62–1.2	0.32–0.58	2.5–4.7
Averages	4.35	12.75	3.19	0.88	0.45	3.02
LREE/HREE=5.10; La/Yb=1.64; (La/Sm)N=0.95; (Ce/Sm)N=1.05 (La/Ce)N=0.95; (Ce/Yb)N=1.14						
Hf in the basalt complex: ranges=0.62–2.5; average=1.22; Zr/Hf=28.6–14.5; average=78.2						

Table 4

Ranges and averages of the REE in the sheeted dyke complex from the western ridge segment (data acc. to Savu and Stoian, 1988)

Elements	La	Ce	Sm	Eu	Tb	Yb
Normal tholeiitic rocks						
Ranges	3.0–6.9	8–24	1.3–3.8	0.71–1.20	0.24–0.82	1.7–6.5
Averages	4.8	16.7	2.6	0.92	0.51	3.9
LREE/HREE=4.27; La/Yb=1.23; (La/Sm)N=1.29; (Ce/Sm)N=1.65; (La/Ce)N=0.84; (Ce/Yb)N=1.05						
Differentiated basic rocks						
Ranges	2.0–14.6	22–41	3.2–6.5	1.10–2.29	0.40–0.98	3.4–9.0
Averages	7.6	27	4.9	1.53	0.71	5.9
LREE/HREE=4.54; La/Yb=1.28; (La/Sm)=1.08; (Ce/Sm)N=1.47; (La/Ce)N=0.84; (Ce/Yb)N=1.18						
Glassy ferrobasaltic rocks						
Ranges	5.2–12.1	20–34	4.0–6.9	1.4–2	0.44–0.96	5.5–7.4
Averages	9.3	28	5.6	1.81	0.70	6.4
LREE/HREE=4.53; La/Yb=1.44; (La/Sm)N=1.16; (Ce/Sm)N=1.28; (La/Ce)N=0.96; (Ce/Yb)N=1.06						
Differentiated acid-albitic rocks						
Ranges	6.4–35	11–97	4.9–9.9	1.93–2.90	0.55–1.58	5.5–18.5
Averages	13.3	40	6.7	2.24	0.93	9.1
LREE/HREE=4.50; La/Yb=1.46; (La/Sm)N=1.38; (Ce/Sm)N=1.60; (La/Ce)N=1.07; (Ce/Yb)N=1.37						

Table 5
Ranges and averages of the REE in the ophiolites
from the eastern ridge segment (data acc. to Savu and Stoian, 1991)

Elements	La	Ce	Sm	Eu	Tb	Yb
Rocks from the basaltic complex						
Ranges	3–7	10–26	1.5–4.4	0.64–0.89	0.50–0.87	0.31–5.1
Averages	4.2	16.2	2.5	0.75	0.61	2.6
LREE/HREE=1.64; La/Yb=1.61; (La/Sm)N=1.16; (Ce/Sm)N=1.59; (La/Ce)N=0.75; (Ce/Yb)N=1.17						
Rocks from the sheeted dyke complex – normal tholeiitic rocks						
Ranges	4–21	10–26	2.1–4.1	0.66–0.98	0.45–0.91	3.4–5.5
Averages	8.3	17.3	3.0	0.82	0.69	4.5
LREE/HREE=4.75; La/Yb=1.84; (La/Sm)N=1.89; (Ce/Sm)N=1.40; (La/Ce)N=1.35; (Ce/Yb)N=3.84						
Rocks from the sheeted dyke complex – acid–albitic rocks						
Ranges	11–14	11–35	3.2–5.9	0.90–1.04	0.85–1.21	7.0–7.5
Averages	12	24.33	4.77	0.98	0.99	7.17
LREE/HREE=5.29; La/Yb=1.67; (La/Sm)N=1.56; (Ce/Sm)N=1.38; (La/Ce)N=1.13; (Ce/Yb)N=1.0						

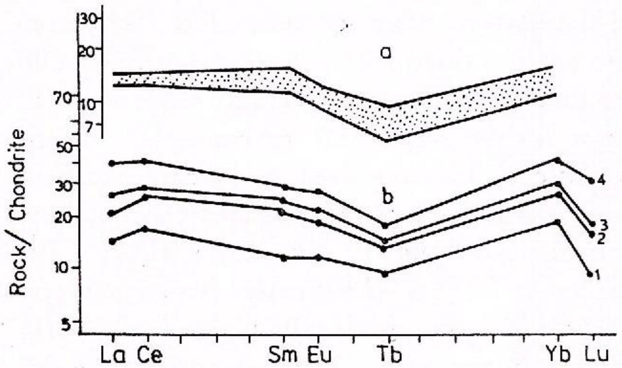

Fig. 4 – Chondrite normalized REE patterns of the ophiolites from the western ridge segment. a, rock patterns of the basaltic complex; b, rock patterns of the sheeted dyke complex. 1, normal tholeiitic rocks; 2, differentiated basic rocks; 3, glassy ferrobasaltic rocks; 4, differentiated acid-albitic rocks.

according to the tholeiitic magma differentiation from both ridge segments, with the only observation that the difference between the extreme values of the basic and acid rocks series is lower in the eastern ridge segment. Therefore, on the diagrams in Figures 4 and 5 only the basic rocks from both ridge segments are situated between the values of 10 and 20 of the rock/chondrite ratio, the patterns of the differentiated acid rocks being placed at higher values; this is more obvious in the western segment (Fig. 4b). With little variation, the averages of LREE/HREE ratio are almost equal in the rocks of the two segments, excepting the spilites from the eastern ridge segment, in which these values are lower.

The average values of the La/Yb, (La/Sm)N, (Ce/Sm)N and (La/Yb)N ratios are variable in both segments, but they are usually higher in the eastern segment. According to Saunders (1984) such values show the N-Type MORB character of the ophiolites. These values are similar to those established by Schilling (1975) in Atlantic and Pacific rocks.

The most obvious discrimination between the two ridge segments is determined by the chondrite normalized REE patterns. So, there is a clear Tb negative anomaly in both complexes from the western segment (Fig. 4).

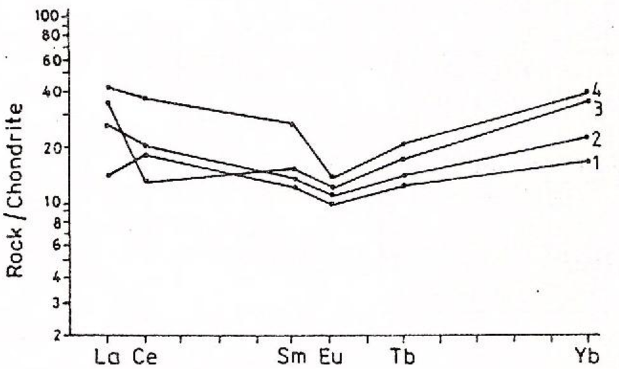

Fig. 5 – Chondrite normalized REE patterns of the ophiolites from the eastern ridge segment. 1, basalt; 2, dolerite; 3, albite microdiorite; 4, albitite.

According to Savu and Stoian (1988) and Savu et al. (1994b) this anomaly represents a characteristic of the parental magma, that was determined by the mantle character and by the partial melting condition (see also Bougault et al., 1979). This conclusion must be supported the more so as this anomaly is obvious even in the basalt complex the rocks of which are slightly differentiated. It is remarkable that, although the parental magma was differentiated from tholeiitic basalts to albite plagiogranite, the initial anomaly persisted. On the contrary, in rocks of the eastern ridge segment (Fig. 5), representing the two ophiolite complexes (O_1 and O_2), an Eu negative anomaly is obvious which, according to Schnetzler and Philpotts (1970), could explain the differentiation of the magma from basalt to albitites.

As these anomalies occur even in the basalt complex, two hypotheses are to be considered concerning their origin; (1) they could be initial anomalies of the tholeiitic magma and (2) they could be the result of the tholeiitic magma differentiation. The last hypothesis is difficult to be upholded as during the tholeiitic magma evolution phenocrysts of plagioclase or of any other minerals rarely occur.

Conclusions

The ophiolites of the Mureş Zone were obducted from two different segments of the median ridge of the Mureş Ocean. They display N-Type MORB characteristic. The main difference between the ophiolites from the two ridge segments is determined by a Tb negative anomaly in those of the western ridge segment and by an Eu negative anomaly in those of the eastern ridge segment. The rocks from the western ridge segment are richer in Ca and Ba and those from the eastern ridge segment show higher Na_2O and Sr contents. In the basalt complex from the western ridge segment were determined the highest Rb contents and the highest values of the Rb/Sr ratio. The values of La/Yb, (La/Sm)N, (Ce/Sm)N and (La/Ce)N ratios are usually higher in the rocks of the eastern segment. Taking into consideration all these observations, one may affirm that the differences between the rocks from the two normal ridge segments of the Mureş Ocean have been determined by the mantle characteristics, the melting conditions of the parental tholeiitic magma, and by its differentiation.

References

Balintoni, I., Bertotti, G., Ciulavu, D., Dallmeyer, R.D., Hann, H., Iancu, V., Fritz, H., Mărunţiu, M., Mocanu, V., Neubauer, F., Nicolae, I., Pană, D., Rădulescu, F., Săndulescu, M., Seghedi, A. (1994) ALCAPA II, Field Guidebook: South Carpathians and Apuseni Mountains, Romania. *Rom. J. Tectonics and Reg. Geol.*, 75, Suppl. no. 2, Bucharest.

Bougault, H., Cambon, P., Corre, O., Joron, J.L., Treuil, M. (1970) Evidence for variability of magmatic processes and upper mantle heterogeneity in the axial region of the Mid-Atlantic ridge near 22^0 and 36^0 N. *Tectonophysics*, 55, p. 11–34, Amsterdam.

O'Connor, J.T. (1965) A classification of quartz-rich igneous rocks based on feldspar ratio. *U.S. Geol. Surv. Prof. Paper*, 525 B, p. 79–84, Washington.

Herz, N., Jones, L.M., Savu, H., Walker, R.L. (1974) Strontium isotope composition of ophiolitic and related rocks, Drocea Mountains, Romania. *Bull. Volc.*, XXXVIII/4, p. 1110–1124, Napoli.

Lupu, M., Avram, E., Antonescu, E., Dumitrică, P., Lupu, D., Nicolae, I. (1995) Comment on the age of some ophiolites from the North Drocea Mts. *Rom. J. Tectonics and Reg. Geol.*, 76, p. 21–25, Bucureşti.

Pearce, J.A., Harris, N.B.W., Tindle, A.G. (1984) Trace element discrimination diagrams for the tectonic interpretation of granite rocks. *J. Petrol.*, 25, 4, p. 956–983, Oxford.

Perfit, M.R., Gust, D.A., Bence, A.E., Arculus, P.J., Taylor, B.R. (1980) Chemical characteristics of island arc basalts: implications for mantle sources. *Chem. Geol.*, 30, p. 227–256, Amsterdam.

Saunders, A.D. (1984) The rare elements characteristics of igneous rocks from the ocean basins. P. Henderson (edit.) Rare Earth Element Geochemistry. Elsevier, p. 205–236, Amsterdam.

Savu, H. (1967) Die mesozoïschen Ophiolite der rumänischen Karpathen. *Acta Geol. Acad. Sci. Hung.*, 1 (1-3), p. 59–70, Budapest.

– **(1983)** Geotectonic and magmatic evolution of the Mureş Zone (Apuseni Mountains). *An. Inst. Geol. Geofiz.*, LI, p. 253–262, Bucuereşti.

– **(1990)** Remarks on the Mesozoic magmatic activity in the Trascău Mts Mureş Zone. *Rev. roum. Géol., Géphys., Géogr. (Géol.)*, 33, p. 13–24, Bucureşti.

– **, Stoian, M. (1988)** REE contents in the sheeted dyke complex of the Mureş Zone and their petrogenetic significance. *Rev. roum. Géol., Géphys., Géogr. (Géol.)*, 32, p. 37–44, Bucureşti.

– **, Stoian, M. (1991)** REE and Hf contents in the ocean floor rocks (Liassic ophiolites) from the Trascău Mts and their petrologic significance. *Rev. roum. Géol.*, 35, p. 35–43, Bucureşti.

– **, Udrescu, C., Neacşu, V. (1981)** Geochemistry and geotectonic setting of ophiolites and island arc volcanics of the Mureş Zone (Romania). *Ofioliti*, 6 (2), p. 269–286, Bologna.

– **, Udrescu, C., Neacşu, V., Stoian, M. (1984)** Trends of tholeiitic magma differentiation in the sheeted dyke complex from the Mureş Zone (Romania). *An. Inst. Geol. Geofiz.*, LXIV, p. 121–131, Bucureşti.

– **, Udrescu, C., Neacşu, V. (1992)** On the presence of the ocean floor rocks (Liassic ophiolites) in the Trascău Mts (Mureş Zone); their petrology and geochemistry. *Rom. J. Petrology*, 75, p. 35–62, Bucureşti.

– , **Udrescu, C., Neacşu, V., Ichim, M. (1994a)** Petrology and geochemistry of the effusive rocks from the ocean floor basalt complex in the Mureş Zone. *Rom. J. Petrology*, 76, p. 67–76, Bucureşti.

– , **Stoian, M., Tiepac, I., Popescu, G., Grabari, G. (1994b)** Petrological significance of REE, U, Th, K, Rb, Sr, Hf and of the $^{87}Sr/^{86}Sr$ ratio in the basaltic complex of the Mureş Zone. *Rom. J. Petrology*, 76, p. 77–84, Bucureşti.

– , **Udrescu, C., Neacşu, V., (1996)** The ophiolites of the Mureş Couloir between Căpâlnaş and Tisa (Mureş Zone). *Rom. J. Petrology*, 77, p. 61–68 , Bucureşti.

Schilling, J.G. (1975) Rare-earth variation across normal-segments of the Reykjanes Ridge, 60–53^{0}N, Mid-Atlantic Ridge, 29^{0}S and East Pacific Rise, 2–19^{0}S, and evidence of the composition of the underlying low-velocity layer. *J. Geophys. Res.*, 80, p. 1459–1475, Washington.

Schnetzler, C.C., Philpotts, J.A. (1970) Partition coefficient of rare-earth elements between igneous matrix material and rock-forming mineral phenocrysts, II. *Geochim. Cosmochim. Acta*, 34, p. 331–340, Oxford.

Received: October 5, 1995.
Accepted: January 12, 1996.

Rom. J. Petrology, 77, p. 61–70, Bucureşti, 1996

THE OPHIOLITES OF THE MUREŞ COULOIR BETWEEN CĂPÂLNAŞ AND TISA (MUREŞ ZONE)

Haralambie SAVU, Constanţa UDRESCU,

Institutul Geologic al României. Str. Caransebeş 1, 79 678 Bucureşti 32

Vasilica Neacşu

S.C. Prospecţiuni S.A. Str. Caransebeş 1, 78 344, Bucureşti 32

Key words: Ophiolites. Basalts. Spilites. Sedimentary Intercalations. Major Elements. Origin. Banat.

Abstract: The Căpâlnaş-Tisa region (North Banat) is situated in the southern part of the Mureş ophiolitic suture (Mureş Zone). Its geological structure differs from that of the northern part of the Mureş Zone by a lesser complicated thrust tectonics. It is mostly covered by sedimentary deposits and by younger volcanic rocks. The Liassic ophiolites occurring in several inliers are represented by the basaltic complex (O_1) of the Mureş Zone, in which spilites are the prevalent rocks. The changes determined by the spilitization in the mineralogical composition of the basaltic rocks are reflected in their chemical composition by the increase of Na_2O and H_2O and by the decrease of CaO and other elements as Cr and Ni. The basaltic ophiolites are plate margin rocks, formed on the Mureş Ocean floor (MORB). Between the basaltic flows there are intercalations of recrystallized limestones and detrital rocks, formed near by the Transylvanian continental margin, probably in a shallow water zone of the Mureş Ocean. The recrystallization of limestones was determined by the ocean floor metamorphism in the zeolitic and greenschists facies.

1. Introduction

Within the Mureş Couloir, between Căpâlnaş and Tisa (North Banat), there is a hilly region, called by Pinkert (1907) the Bulza Hills. This region is situated on the southern margin of the Alpine ophiolitic suture of Mureş (Mureş Zone). Along this area there are several occurrences of diabases (Kadič, 1906; Pinkert, 1907; Papiu, 1954; Duşa, 1965; Peltz et al., 1970) – Liassic ophiolites (Savu, 1966) – which have not been systematicaly studied till now. Therefore, we elaborated the present paper with a view to complete the image on the evolution of the Alpine ophiolites of the Mureş Zone. We described the geological structure of this region, as well as the petrogenetic and geochemical characteristics of its Liassic ophiolites, mostly spilites (Savu et al., 1990, unpubl. rep.).

2. Geological structure of the region and the ophiolite occurrences

The pre-Laramian geological formations of the Căpâlnaş-Tisa region belong to two tectonic units: Căpâlnaş-Techereu Unit toward north and Tisa Unit toward south (Plate). These tectonic units are covered by Banatitic (Laramian) volcanics and by Neogene sedimentary deposits. The Banatitic volcanics, which before 1984 had been regarded as products of the Neogene volcanism, were studied by many geologists (Kadič, 1906; Pinkert, 1907; Papiu, 1954; Duşa, 1965; Peltz et al., 1970; Savu, 1966; Savu et al., 1992; Roşu et al., unpubl. rep.). These structures are similar to those from the Zam-Gurasada region (Savu et al., 1992a).

2.1. *Căpâlnaş-Techereu Unit (Lupu, 1975).* This tectonic unit takes part in the structure of the Mureş Zone (Savu, 1983). The Liassic ophiolites proceeding from the initial ophiolite megaslab (sheet) of the Mureş Zone occur from the basement of this tectonic unit in several inliers. The ophiolite megaslab was scraped out from the Liassic crust of the Mureş Ocean and obducted in the Upper Jurassic eugeosyncline of the Mureş Zone (Savu, 1983).

The ophiolite occurrences are situated south and east of Căpâlnaş, south of Căprioara, north of Bulza and between Pojoga and Tisa (Plate). Excepting the ophiolites east of Căpâlnaş, the other basic rock occurrences are located within the Groşi-Săliştioara tectonic rise, situated along the south margin of the Căpâlnaş-Techereu Unit. The eastern segment of this tectonic rise was described before as the Glodghileşti-Săliştioara tectonic rise (Savu et al., 1988).

The Groşi-Săliştioara tectonic rise uplifted between an ENE-WNW system of longitudinal faults.

These fractures determined strong tectonic breccias like those situated south of Zam, out of the Căpâlnaş-Tisa region. The tectonic rise was cut and its segments were dislocated by an important fault trending WNW-ESE, which is located along the Mureş Valley, between Zam and Dobra, east of the map on Plate, and by many other small cross faults.

The ophiolites from the basement of this region are bearing Late Kimmerian island arc volcanics and Mesozoic sedimentary deposits which form an asymmetrical syncline on the northern margin of the region. To the south, the geological formations of the Căpâlnaş-Techereu Unit are thrust by the Tisa Unit (Savu et al., 1992a) and the thrust line is also covered by Laramian volcanics and Neogene sedimentary deposits.

The asymmetrical syncline that extends between Căpâlnaş and Vorţa consists of Liassic ophiolites in the basement, over which the following geological formations are lying: Late Kimmerian island arc volcanics formed along the southern arc of the Mureş Zone, red argillites associated with jaspers and Stramberg (Upper Jurassic) limestones containing remnants of *Nerinea* and Corals (Kadič, 1906; Papiu, 1954), followed by unconformable Barremian-Aptian sedimentary deposits. Over the Stramberg limestones there formed detrital limestones with *Orbitolina lenticularis* (Papiu, 1954). As the J_3-K_1 limestones extend along the southern island arc (IAV_2) of the Mureş Zone between Căpâlnaş and Almaşu Mare, on a length of more than 76 km, there results that they constituted in the Mureş Ocean a reef barrier like that from Pacific, situated east of Australia. The northern flank of the Căpâlnaş-Vorţa syncline, which is strongly dipping southwards, was affected by a longitudinal fault dipping toward north. In the eastern segment of the syncline situated between Zam and Vorţa, its structural elements were described by Cibotaru and Puricel (1985) and Savu et al. (1992a). North of Cărmăzineşti this syncline was thrust from north by the island arc volcanics.

South of the Căpâlnaş-Tisa region the Late Kimmerian volcanics and the Upper Jurassic-Neocomian sedimentary deposits were eroded so that the Barremian-Aptian deposits are laying unconformably on the Liassic ophiolites. They plunge soutwards, under the Tisa Unit that thrusts them over about 4 km (J. Andrei, oral com.), as shown in the geological section between Valea Mare and Coştei de

Sus (Plate). Near Tisa, where the thrust plane is not covered by Laramian volcanics, it trends ENE dipping 32^0 to 46^0 southwards (Savu et al., 1992a). The Barremian-Aptian deposits have in their lower part a discontinous red horizon in which blocks of crystalline schists and Paleozoic microcline granites are included (Savu, 1966). Over this horizon there follows a folded thick pile of flysch deposits consisting of alternating beds of sandstones and argillites. Before the Laramian volcanism another erosion period intervened, so that along the Groşi-Săliştioara tectonic rise the banatitic volcanics are laying just on the ophiolite basement and on some outliers of Barremian-Aptian deposits.

2.2. *The Tisa Unit (Savu et al., 1992a).* This unit belongs to the Transylvanian plate. It consists of an anchimetamorphic volcano-sedimentary series over which the Triassic continental intra-plate basalts and the associated sandstones of Coştei de Sus are situated (Savu et al., 1992b). This series occurs in several inliers. Although it belongs to the Poiana Ruscă Mts, its crystalline schists are different from the weakly metamorphosed crystaline schists from the northern part of this massif, both by lithology and the anchimetamorphic facies.

As the thrust plane of the Tisa Unit is covered by Laramian volcanics, there results that the thrust took place probably during the Austrian or Subhercynian movements. The presence of a big olistolith of crystalline schists insedimented in the Barremian-Aptian deposits from the Tomii (Dobârleşti) Brook, a tributary of the Peştiş Valley, as well as the exotic blocks from the Barremian lower horizon show that the Tisa Unit started rising as a cordillera in the Cretaceous miogeosyncline as early as the sedimentation period of these deposits, like the tectonic units in the Trascău Mts (Savu, 1990). South of Coştei de Sus the Tisa Unit was cut by the Recaş-Cuieş crustal fracture made evident by Andrei et al. (1975).

Toward west, in the Groşi area, all these structures were cut and dislocated by NW-SE trending faults and invaded by Neogene sedimentary deposits (Plate).

3. Form and petrographic aspects of the ophiolitic rocks

All the ophiolitic occurrences belong to the basaltic complex (O_1) of the Mureş Zone. In the hornfelses and the basaltic rocks situated east of Căpâlnaş, between the Săvârşin granite and the western extremity of the Căpâlnaş-Vorţa syncline, there are located a few small bodies of diopside gabbros. They represent the vestiges of the Cuiaş gabbroic body which was intruded by the Săvârşin granite and eroded by the Mureş River.

The ophiolitic rocks in the Capâlnaş-Tisa region, excepting the gabbros, are represented by spilites, basalts and amygdaloidal basalts, some of them in pillow lava facies. Between the basaltic flows from the Mânzu and Plumbu brooks, tributaries of the Rogozu (Căpâlnaş) Brook as well as at the springs of Căpriorişca Valley, there are intercalations of Liassic recrystallized limestones (Kadič, 1906) associated with quartz sandstones, arkosian sandstones (Savu, 1966) and quartz microconglomerates.

The limestone recrystallisation was determined by the Liassic hydrothermal metamorphism on the Mureş Ocean floor in the zeolitic and greenschists facies (Savu, 1967; Savu et al., 1988). In the Plumbu Brook these rocks have been affected by Laramian hydrothermal solution, too, that generated veins of metasomatic skarns with a stockwork structure (Savu, 1966), consisting of calcite – grossular – epidote parageneses.

The average chemical composition of two limestone samples from the Căpriorişca Valley is, as follows: SiO_2 – 2.36; Al_2O_3 – 0.55; Fe_2O_3 – 0.09; FeO – 0.25; MnO – 0.03; MgO – 1.24; CaO – 53.15; K_2O – 0.17; Na_2O – 0.57; H_2O – 1.05; CO_2 – 41.18; S – 0.18. This composition shows that the rocks are limestone chemical deposits with low SiO_2 and MgO contents, like those from the eastern segment of the tectonic rise (Savu et al., 1988). The basaltic rocks and the associated detrital rocks are also similar to those described by us in this eastern segment. Like the later, the sedimentary rocks are situated on the same lineament and in the same stratigraphic position in the basaltic complex (O_1).

The Liassic age of the basaltic rocks from this region was inferred by comparison with the ophiolites north of Mureş, in which Herz et al. (1974) determined a radiometric (Rb/Sr) age of 180 Ma. It is noteworthy that as early as 1906 Kadič considered the limestones intercalated between the basalt flows from the Căpriorişca Valley as Dogger limestones (see also Savu, 1966).

As we previously showed (Savu et al., 1988), the basaltic flows from the south part of the ophiolitic megaslab of the Mureş Zone and from the Groşi-Săliştioara tectonic rise, respectively, are the old-est ophiolites in the Mureş suture. Therefore, they were among the closest basaltic rocks to the Transylvanian continent or the sialic part of the Transylvanian plate, respectively. As an evidence in this respect are the Liassic sandstones and microconglomerates intercalations in the basaltic complex. The presence of limestones indicates that they formed in a shallow water zone of the Mureş Ocean.

4. Geochemistry and tectonic setting

The SiO_2 contents of the ophiolitic rocks (Tab.), lower than 50 per cent show that the lava flows of the basaltic complex (O_1) are constituted only of basalts, according to Gill's (1981) and Ewart's (1982) classification. In 45 per cent of the analysed rocks Na_2O is higher than 4 per cent which indicates that they represent spilites, formed by the reaction of the basaltic lavas with the ocean salty water, like those from the eastern segment of the tectonic rise (Savu et al., 1988).

In the other samples this component is a little lower than 4 per cent, but higher than 2.50 per cent, the value that represents the average of Na_2O content characteristic of the normal tholeiites (Miyashiro, 1975). The spilitization process is also indicated by the presence of H_2O in all analysed rocks in which it varies between 1 and 5.42 per cent. The H_2O participates in the chlorite network, a mineral formed on account of the interstitial glass and of the clinopyroxene as well as in that of the argilitic minerals participating together with albite to replace the plagioclase laths. The spilitic rocks with the highest Na_2O content have also the most reduced CaO content (Table) which was eliminated by the spilitization process.

Due to the increase of Na_2O content the most spilitic rocks, excepting two of them rich in total FeO, plot on the diagram in Figure 1 in the calc-alkaline field. In a similar manner behave on this diagram the basaltic rocks from the eastern part of the tectonic rise (Savu et al., 1988). It is noteworthy that the Liassic basalts from the median part of the ophiolitic megaslab of the Mureş Zone are lesser spilitized.

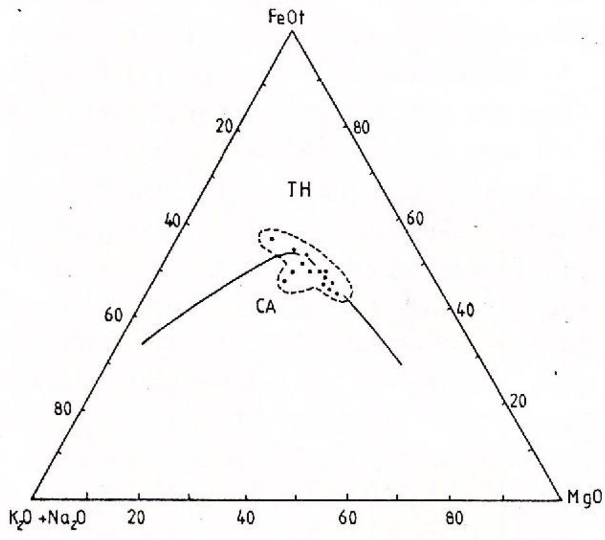

Fig. 1 – Plot of the basaltic and spilitic rocks on the FeO_t – MgO – Na_2O+K_2O diagram. The rock fields acc. to Irvine and Baragar (1971): TH, tholeiitic rock field; CA, calc-alkaline rock field.

Table

Chemical composition of the ophiolitic rocks

No	1	2	3	4	5	6	7	8	9	10	11	12	13	14
SiO_2	43.26	43.80	44.10	44.73	44.85	45.68	45.88	46.32	46.80	48.09	48.62	48.67	48.76	49.22
TiO_2	2.52	1.60	1.04	1.96	1.64	1.60	1.56	1.72	1.24	2.12	1.40	1.07	2.04	1.27
Al_2O_3	15.05	17.30	15.20	16.30	15.30	15.00	15.20	15.50	15.10	14.50	15.95	16.30	14.20	16.71
Fe_2O_3	7.80	5.89	8.12	3.54	5.02	5.94	3.93	3.39	4.01	5.41	5.49	3.22	6.03	2.96
FeO	8.62	3.90	5.35	7.93	6.46	6.51	6.89	7.75	7.29	7.41	5.23	6.93	8.49	7.33
MnO	0.36	0.10	0.14	0.14	0.21	0.22	0.19	0.18	0.14	0.15	0.15	0.14	0.31	0.13
MgO	6.45	4.72	6.21	6.02	7.48	7.40	7.76	7.47	5.53	5.50	6.77	7.40	6.31	7.25
CaO	3.88	8.28	9.51	7.03	7.74	8.80	8.79	8.71	9.37	6.09	9.07	9.14	6.95	7.97
K_2O	0.15	1.04	1.27	1.47	1.53	0.61	0.93	1.15	0.24	1.17	0.91	1.12	0.45	1.05
Na_2O	4.16	4.99	4.04	3.92	3.43	4.08	3.72	3.44	4.14	4.11	3.10	3.20	3.90	3.27
P_2O_5	0.27	0.11	0.24	0.23	0.17	0.14	0.22	0.21	0.28	0.30	0.15	0.09	0.18	0.10
H_2O	5.42	2.98	4.00	3.78	4.22	3.85	4.45	4.15	3.78	3.02	1.00	1.81	1.72	1.82
CO_2	1.93	0	1.15	2.08	2.04	0	0	0	2.26	2.58	2.09	0.50	0	0.44
S	0.36	0.24	0.23	2.08	0.22	0.21	0.24	0.21	0.34	0.28	0.03	0.02	0.23	0.02
Total	100.23	99.59	100.60	99.51	100.31	100.04	99.76	100.20	100.52	100.73	99.96	100.01	99.97	99.91
Ni ppm	44	140	80	55	72	73	43	45	78	22	115	53	200	58
Co	54	56	40	42	48	66	42	38	32	36	65	39	88	33
Cr	65	250	140	150	270	70	190	200	210	34	250	330	105	240
V	600	270	350	370	300	360	190	390	200	360	520	240	450	240
Sc	55	46	48	46	57	50	45	55	40	50	68	40	54	35
Zr	165	110	140	160	105	92	90	150	310	190	140	87	165	110
Y	60	36	50	48	37	36	29	42	75	52	32	32	62	36
Yb	4.7	3.6	4.3	4.4	3.8	3.8	3.0	4.2	6.5	4.2	2.7	1.8	4.7	2.4
Ba	40	75	48	250	250	40	100	200	24	140	30	160	38	220
Sr	160	340	150	360	310	310	300	500	210	310	240	520	160	350
Cu	30	95	80	46	42	125	92	92	2.5	42	40	95	160	22
Zn	95	42	38	40	42	58	60	55	48	70	46	55	65	48
Sn	<2	<2	7	<2	<2	24	2.5	3.5	<2	<2	<2	<2	6	<2
Ga	26	15	17	25	12	16	20	23	25	25	13	11	25	10

The rocks analysed in this table are: basalts from Căpriorişca Valley – 1, 4, 10; Sălciva Valley – 2, 5, 11; Ioneasca Valley – 3; Hobiţa Brook – 7, 8, 9, 12, 14; Căprioara–Căpâlnaş area – 13; basic hornfels from Căprioara–Căpâlnaş area – 6. The Pb contents are lower than 2 ppm.

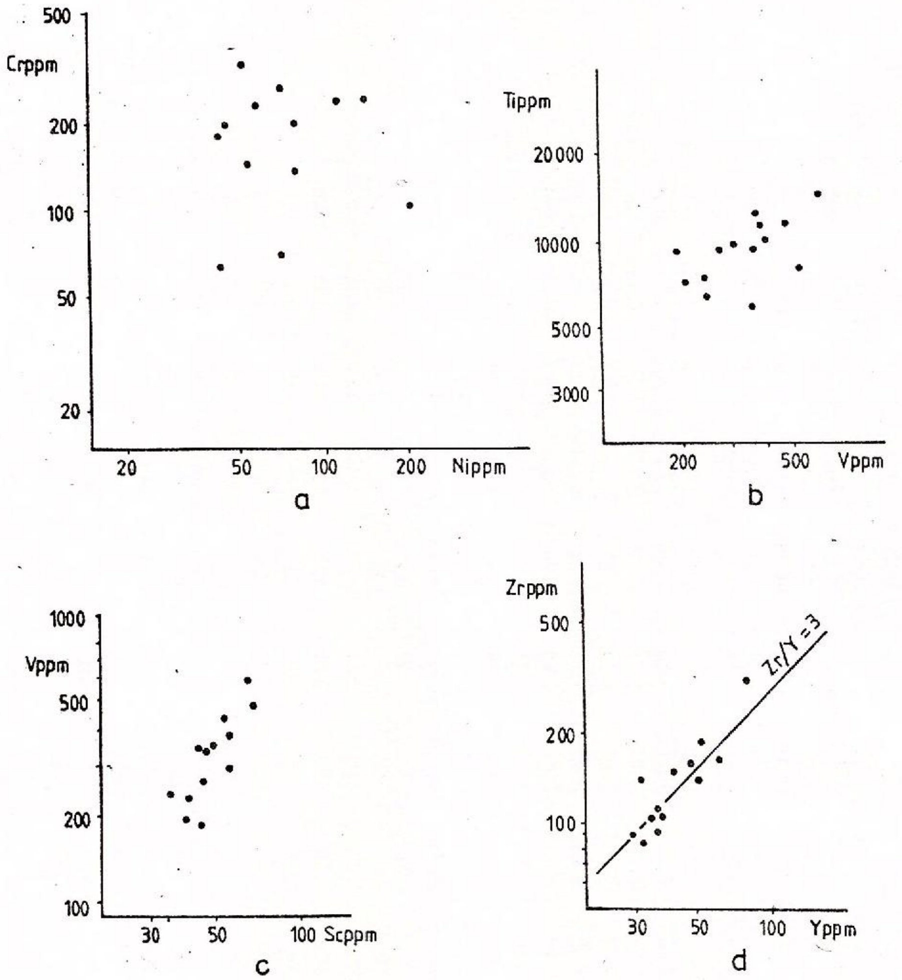

Fig. 2 – Variation and correlation of some chemical element pairs in basaltic and spilitic rocks.

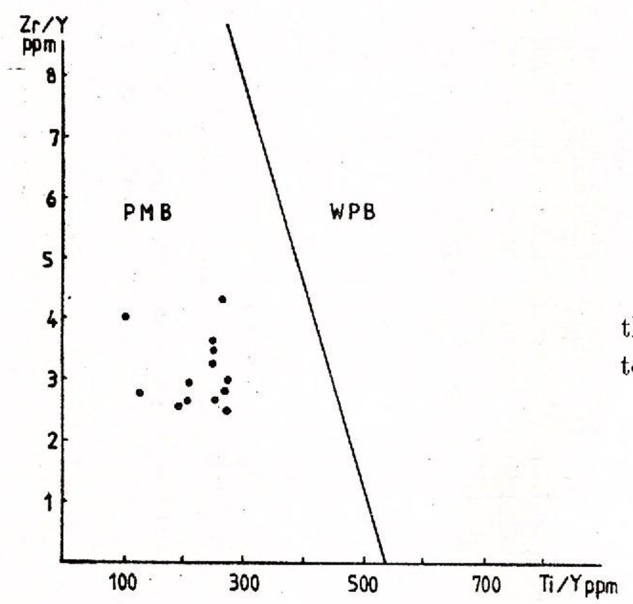

Fig. 3 – Plot of basaltic and spilitic rocks on the Zr/Y – Ti/Y diagram. The rock fields acc. to Pearce and Gale (1976): PMB, plate margin basalts; WPB, within-plate basalts.

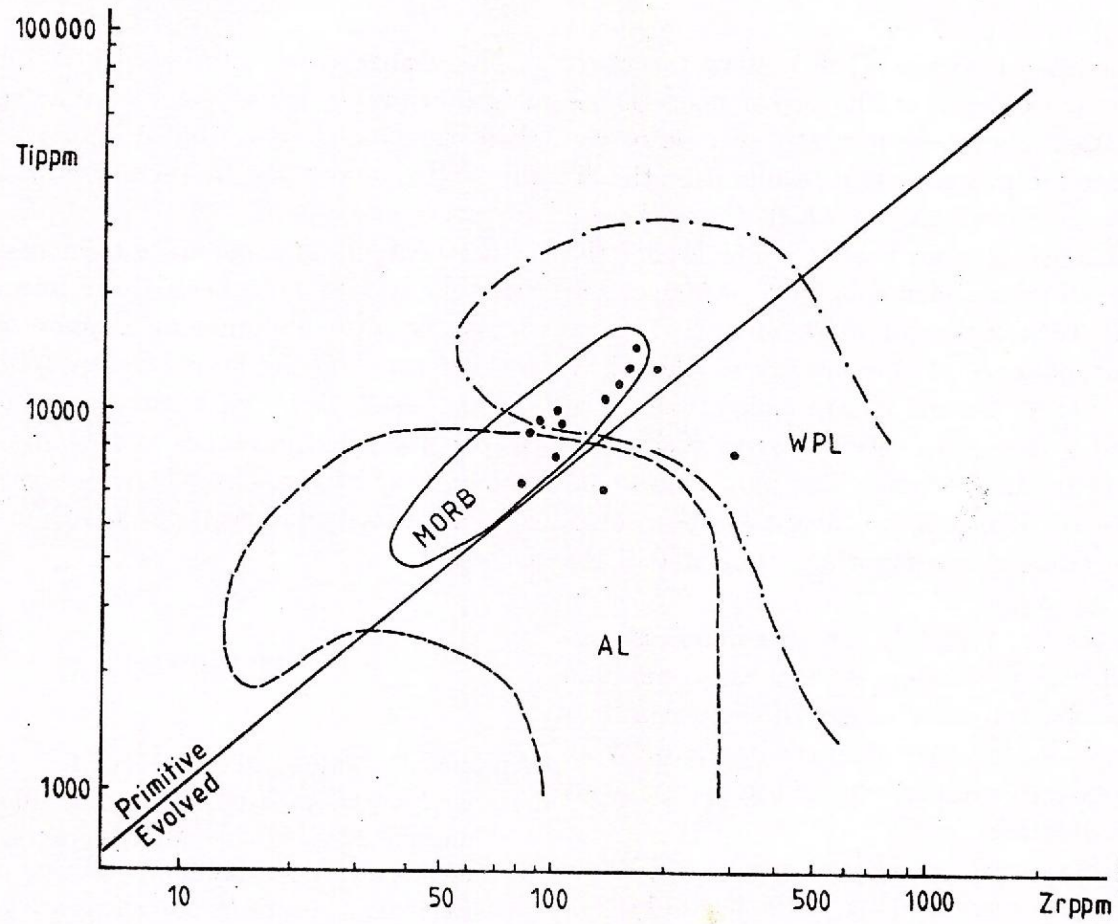

Fig. 4 – Plot of the basaltic and spilitic rocks on the Ti – Zr diagram. The rock fields acc. to Pearce (1980): MORB, middle ocean ridge basalts; AL, arc lavas; WPL, within-plate lavas.

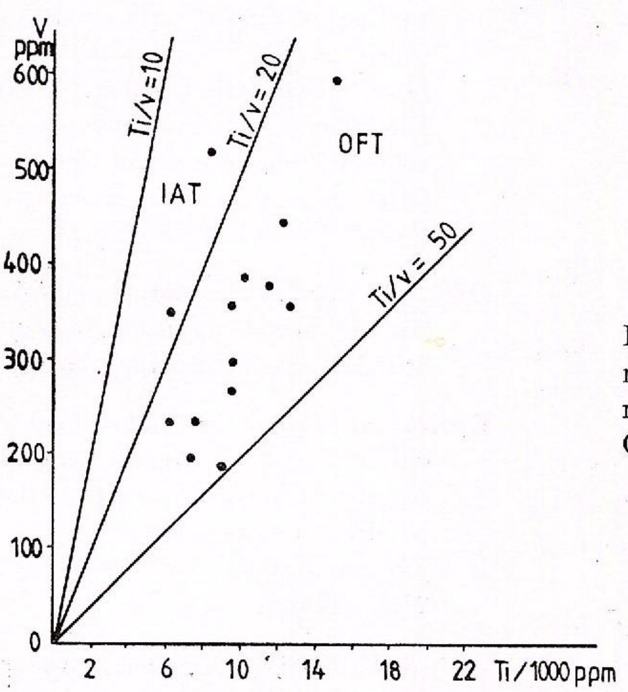

Fig. 5 – Plot of basaltic and spilitic rocks on the V – Ti/1000 diagram. The rock fields acc. to Shervais (1982): OFT, ocean floor tholeiites; IAT, island arc tholeiites.

The trace elements (Tab.) show the characteristic contents of the ocean floor tholeiitic rocks. They were partially affected by the spilitization process. As it results from the diagram in Figure 2a, on which the rocks are scattered in a large field, Cr and Ni are the most influenced elements that participate in the network of the chloritized augite.

The influence of this process on the Ti, V and Sc (Fig. 2b and c) was a slight one. The Zr and Y (Fig. 2d) were the lesser affected elements in this process. The plot of rocks on the Zr – Y diagram indicates a positive correlation along a line for which the value of the Zr/Y ratio is 3.

As the Zr, Y and Ti contents were lesser affected by spilitization, so that they maintain in the characterisitc ranges of the ocean floor basic rocks, on the diagram in Figure 3 all the analysed samples plot in the plate margin basalt domain.

Excepting two rocks, the ophiolites plot on the Ti – Zr diagram (Fig. 4) in the mid-ocean ridge basalt (MORB) field, which underlines that the basic rocks from this area belong to the ophiolitic megaslab of the Mureş Zone.

The character of mid-ocean ridge basalts of these rocks results also from the manner in which they plot on the V – Ti/1000 diagram (Fig. 5).

5. Conclusions

The geological structure of the southern margin of the Mureş Zone differs from the northern one by a lesser complicated thrust tectonics, but it is mostly covered by sedimentary and volcanic formations.

A longitudinal fracture system cuts this marginal area of the Mureş Zone, resulting the Groşi-Săliştioara tectonic rise with an ophiolitic basement.

The ophiolites occurring in several inliers are represented by rocks from the basaltic complex (O_1) of the Mureş Zone, among which the spilites are the prevalent rocks.

The changes that intervened in the mineralogical composition of spilites are reflected in their chemical composition by the increase of the Na_2O content and by the decrease of CaO and other elements.

The contents in some trace elements, especially Cr and Ni, have been also influenced.

The basaltic ophiolites are plate margin rocks, formed on the Mureş Ocean floor.

The basalt flows with thin intercalations of recrystallized limestones and detrital rocks formed near by the Transylvanian continental margin, in a shallow water zone of the Mureş Ocean.

References

Andrei, J., Calotă, C., Scurtu, F. (1975) Considérations structurales sur le sillon ophiolitique des Monts Métallifères à l'aide des données géophysiques et des certains éléments quantitatifs obtenus grace au modelage. *Rev. roum. géol., géophys., géogr. (Géophys.)*, 19, p. 101–111, Bucureşti.

Cibotaru, T., Purecel, R. (1985) The epicontinental Lower Cretaceous sedimentary deposits of the south-western Metaliferi Mountains (Zam – Vorţa area). In: Cercetări Fundamentale şi Aplicative pentru creşterea volumului de rezerve energetice şi materii prime minerale. *Univ. Bucureşti, Geologie, Special Volume*, p. 131–136, Bucureşti.

Duşa, A. (1969) Stratigrafia depozitelor mezozoice şi terţiare de la Căprioara–Coşteiu de Sus. Edit. Acad. Române, 153 p., Bucureşti.

Ewart, A. (1982) The mineralogy and petrology of Tertiary – Recent orogenic volcanic rocks: with special reference to the andesitic-basaltic compositional range. In: R.S. Thorpe, J. Wiley (edits) Andesites, p. 25–27, Chichester.

Gill, J. E. (1981) Orogenic Andesites and Plate Tectonics. 390 p., Berlin.

Herz, N., Jones, D. M., Savu, H., Walker, R. L. (1974) Strontium isotope composition of ophiolitic and related rocks, Drocea Mountains, Romania. *Bull. Volc.*, XXXVIII/4, p. 1110–1124, Napoli.

Irvine, T. N., Baragar, W.R.A. (1971) A guide to the chemical classification of the common volcanic rocks. *Can. J. Earth Sci.*, 8, p. 523–548, Ottawa.

Kadič, O. (1906) Die geologischen Verhälnisse des Berglandes am linker Ufer der Maros, in der Umgebung von Czella, Bulza und Pozsoga. *Jahresb. ung. geol. Anst. f. 1904*, p. 148–165, Budapest.

Lupu, M. (1975) Einige Bemerkungen zur Tektonik des Südlichen Apuseni Gebirges. *Rev. Roum. Géol., Géogr. (Géologie)*, 19, p. 95–104, Bucureşti.

Miyashiro, A. (1975) Volcanic rocks series and tectonic setting. *Ann. Rev. Earth Planet. Sci.*, 3, p. 251–260, Palo Alto, California.

Papiu, V. (1954) Notă preliminară asupra regiunii Valea Mare–Căprioara–Bulza–Pojoga. *D. S. Com. Geol.*, XXXVIII, p. 169–178, Bucureşti.

Pearce, J. A. (1980) Geochemical evidence for the genesis and eruptive setting of lavas from Tethyan ophiolites. In: A. Panayiotou (edit.) Ophiolites, Proc. Intern. Ophiol. Symp. 1979, p. 261–272, Nicosia.

– **, Gale, G. H. (1976)** Identification of ore deposits environment from trace element geochemistry of associated igneous host rocks. In: Jones M. J. Volcanic processes in ore genesis. Inst. Mining and Metallurgy and Geol. Soc. Special Publ., 7, p. 14–24, London.

Peltz, S., Peltz, M., Urcan, T. (1970) Contribuţii la cunoaşterea vulcanismului neogen din regiunea Groşi–Bulza–Fintoag. *D. S. Inst. Geol.*, LV/1, p. 109–134, Bucureşti.

Pinkert, E. (1907) Beiträge zur Kentnis der Eruptivgesteine der Berggruppe von Bulza. *Földt. közl.*, XXXVII (6–8), p. 273–300, Budapest.

Savu, H. (1966) Metamorfismul calcarelor la contact cu ofiolitele de la Căpîlnaş (Valea Mureşului). *D. S. Inst. Geol.*, LII/5, p. 123–140, Bucureşti.

– **(1967)** Die mesozoischen Ophiolithe der rumänischen Karpaten. *Acta Geol. Acad. Sci. Hung.*, 11 (1–3), p. 59–70, Budapest.

– **(1983)** Geotectonic and magmatic evolution of the Mureş Zone (Apuseni Mountains) – Romania. *An. Inst. Geol. Geofiz.*, LXI, p. 253–262, Bucureşti.

– **(1990)** Remarks on the Mesozoic magmatic activity in the Trascău Mountains (Mureş Zone). *Rev. roum. géol., géophys., géogr. (Géologie)*, 31, p. 13–24, Bucureşti.

– **, Udrescu, C., Lemne, M., Romanescu, O., Neacşu, V. (1988)** Petrology, geochemistry and tectonics of ophiolites and Late Kimmerian island arc volcanics from the Glodghileşti – Săliştioara tectonic rise (Mureş Zone). *D. S. Inst. Geol. Geofiz.*, 72–73/5 (1985; 1986), p. 259–281, Bucureşti.

– **, Udrescu, C., Neacşu, V., Stoian, M. (1992a)** Petrology, geochemistry and origin of the Laramian volcanics of the Mureş Couloir, between Zam and Gurasada. *Rom. J. Petrology*, 75, p. 117–130, Bucureşti.

– **, Udrescu, C., Neacşu, V., Stoian, M. (1992b)** The Coştei basalts: products of a pre–Mureş Ocean continental intraplate volcanism. *Rev. Roum. Géologie*, 36, p. 35–43, Bucureşti.

Shervais, J. W. (1982) Ti – V plot and the petrogenesis of modern and ophiolitic lavas. *Earth Planet. Sci. Lett.*, 59, p. 101–118, Amsterdam.

Received: September 30, 1992.
Accepted: January 18, 1993.

GEOLOGICAL MAP OF THE CĂPÂLNAŞ - COŞTEI - TISA REGION

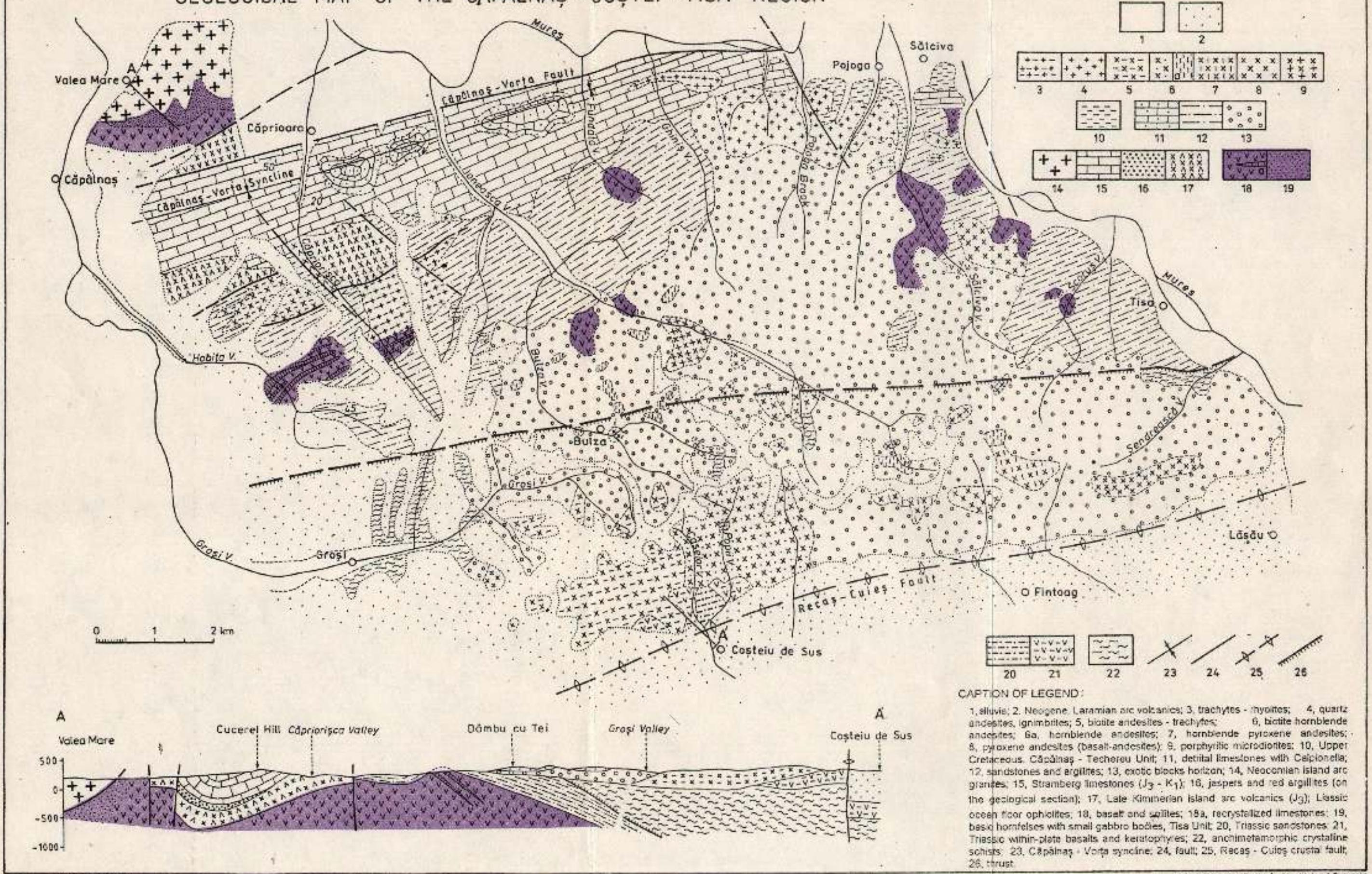

CAPTION OF LEGEND:

1, alluvia; 2. Neogene. Laramian arc volcanics; 3, trachytes - rhyolites; 4, quartz andesites, ignimbrites; 5, biotite andesites - trachytes; 6, biotite hornblende andesites; 6a, hornblende andesites; 7, hornblende pyroxene andesites; 8, pyroxene andesites (basalt-andesites); 9, porphyritic microdiorites; 10, Upper Cretaceous. Căpâlnaş - Techereu Unit; 11, detrital limestones with Calpionella; 12, sandstones and argilites; 13, exotic blocks horizon; 14, Neocomian island arc granites; 15, Stramberg limestones (J_3 - K_1); 16, jaspers and red argillites (on the geological section); 17, Late Kimmerian island arc volcanics (J_3); Liassic ocean floor ophiolites; 18, basalt and spilites; 18a, recrystallized limestones; 19, basic hornfelses with small gabbro bodies, Tisa Unit; 20, Triassic sandstones; 21, Triassic within-plate basalts and keratophyres; 22, anchimetamorphic crystalline schists; 23, Căpâlnaş - Vorţa syncline; 24, fault; 25, Recaş - Culeş crustal fault; 26, thrust.

Printed by the Geological Institute of Romania

Rom. J. Petrology, 77, p. 71–82, Bucureşti, 1996

NEW DATA CONCERNING THE STRUCTURE, PETROLOGY AND GEOCHEMISTRY OF THE LATE KIMMERIAN GRANITOID MASSIF OF SĂVÂRŞIN (MUREŞ ZONE)

Haralambie SAVU, Gabriela GRABARI, Maria STOIAN

Institutul Geologic al României. Str. Caransebeş 1, 79 678 Bucureşti 32

Key words: Granitoid rocks. Structure. Classification. Geochemistry. Trace elements. REE. Petrology. Origin. Drocea Mountains. Apuseni Mountains.

Abstract: The Late Kimmerian granitoid massif of Săvârşin consists of two intrusive bodies: (1) the north – Temeşeşti body and (2) the south – Săvârşin body. These bodies were emplaced successively and they are the result of the differentiation of two parental magmas. Each body had its proper evolution. The Temeşeşti body originated in a dioritic magma, rich in volatile substances. It differentiated to a granodioritic magma and crystallized at a temperature of about 740^0 C. At the contact, this body metamorphosed the ophiolitic country rocks in basic hornfelses. On the margin of the body, the dioritic magma was contaminated by basic materials from the Liassic ophiolites giving rise to a border of more melanocratic rocks. The abundance of mineralizing agents in the magma determined postmagmatic deposition of molybdenite and other sulfides. The granitic body of Săvârşin resulted from an acid magma intruded nearly the surface. By its cooling there resulted three rock facies: a marginal facies of porphyritic microgranites, a facies of common granites and a facies of large-porphyritic granites holding affinities toward the rapakivi granite. The parental magma was a "dry" one, very viscous and poor in volatile substances, that crystallized at a temperature of about 660^0 C. Owing to the characteristics of the parental magma, this body did not determine a contact metamorphic zone in the ophiolites and its magma was not contaminated by the basic rocks.

Introduction

The granitoid massif of Săvârşin is situated on the Mureş Valley, within the southern part of the Mureş Ophiolite Suture or the Mureş Zone. The first data concerning its petrography and chemistry belong to Szentpétery (1928). In 1953 Savu (unpubl. rep.) showed that the granitoid massif does not consist of a single intrusive body, differentiated *in situ* as it was previously supposed (see Giuşcă, 1950), but it represents a composite pluton, formed of two main successive intrusions, the northern one of Temeşeşti – made up of diorites and granodiorites and the southern one of Săvârşin – consisting of granites. The petrology and geochemistry of this massif were investigated by Savu et al. (1967a; 1967b). Savu and Vasiliu (1966) determined the crystallization temperature of the Săvârşin granite, using the chemical composition of the alkali feldspar megacrysts. For a long time the granitoid massif was considered as belonging to the Laramian (banatitic) intrusions from the west of Romania. Using the K/Ar datings previously obtained (Lemne et al., 1979 and Savu et al., 1984 – unpubl. reports), Savu et al. (1986) calculated an isochrone showing that the radiogene age of the massif is of 128 Ma[1] and that it belongs to the Late Kimmerian intrusions associated with the southern island arc of the Mureş Zone established by Savu (1983). Ştefan (1986) considered also that the granitoid massif is Eucretaceous in age. The tectonics of the Săvârşin granite was elaborated by Savu (1995). The metallogeny of the granitoid massif was investigated by Socolescu (1944), Papiu (1953, unpubl. rep.), Petrulian and Steclaci (1966) and Savu and Mândroiu (1980).

In this paper, using new methods of investigations, we analysed the new data on the granitoid massif and re-examined the old ones, obtaining a modern image on its genesis.

Structure of the Granitoid Massif

The intrusion of two bodies that make up the granitoid massif took place as follows: (1) the Temeşeşti body and (2) the Săvârşin body (Fig. 1).

The first intrusion forms the northern body of the massif. This has a sphenolith shape – diping south-east – which is enrooted in its south-western extremity. Its feeding channel coincides with a gravity low made evident by Andrei (1962, unpubl. rep.). This body resulted from successive intrusions of dioritic and quartzdioritic magmas, that crossed the Liassic ophiolites of the Mureş Zone, represented by the basalt complex (O_1) and the sheeted dyke complex (O_2) associated with small gabbro bodies. The dioritic intrusion was followed by a granodioritic intrusion which penetrated through the axial zone of the sphenolith. As resulted from the field observations and the detailed map of this body (Savu, Mândroiu, 1980), the contact between quartzdiorites and granodiorites is a sharp one. This relation and the observation that the granodiorites do not contain any dioritic xenolith show that the granodioritic magma was intruded when the dioritic body was still in a plastic state. This conclusion is also supported by the fact that the diorites formed a more important intrusion in the northern part of the Temeşeşti body. Besides, on the north-western border of the granitoid massif of Săvârşin there occur two more small dioritic bodies: one of them occurs in the contact area between the two bodies of the massif and the other one is situated a little west of it, on the northern contact of the Săvârşin granite body with the ophiolitic rocks. All these indicate separate dioritic intrusions in this region, earlier than the granodiorite intrusion.

Like in the diorites, in granodiorites numerous melanocrate autoliths are present. These are similar to those described by Pabst (1928) and Balk (1937) in the Sierra Nevada granites, which one of us visited east of Sacramento, in 1972.

Around the Temeşeşti body a thermal contact zone was formed, affecting the Liassic ophiolites. This zone developed mostly in the north-western part of the intrusion, being evident at the contact with the diorites. It is noteworthy that it is missing at the contact with the granodiorites, as for instance in the area between the Fercioaia Brook and the

[1]Recently, D. Pană (oral com.) obtained an age of 155 Ma on zircon, that correlates quite well with the position of the consaguineous island arc acid volcanics intercalated in the Upper Jurassic flysch deposits from the Drocea trough.

Roşelii Valley. The contact zone consists of pyroxenes – hornblende hornfelses and hornblende – biotite hornfelses, usually injected by leucocrate veins (Savu, 1989). In the end, the Temeşeşti body was crossed by aplitic veins, a dyke of porphyritic monzodiorite and one of kersantite.

channel of which is located in its north-eastern extremity, near by the one of the Temeşeşti intrusion (Savu, 1995). It is also marked by a gravity low rendered evident by Andrei (1962, unpubl. rep.). In the structure of this granitic body three rock facies were separated (Savu et al., 1967a; Savu, 1995; Fig. 1). A marginal

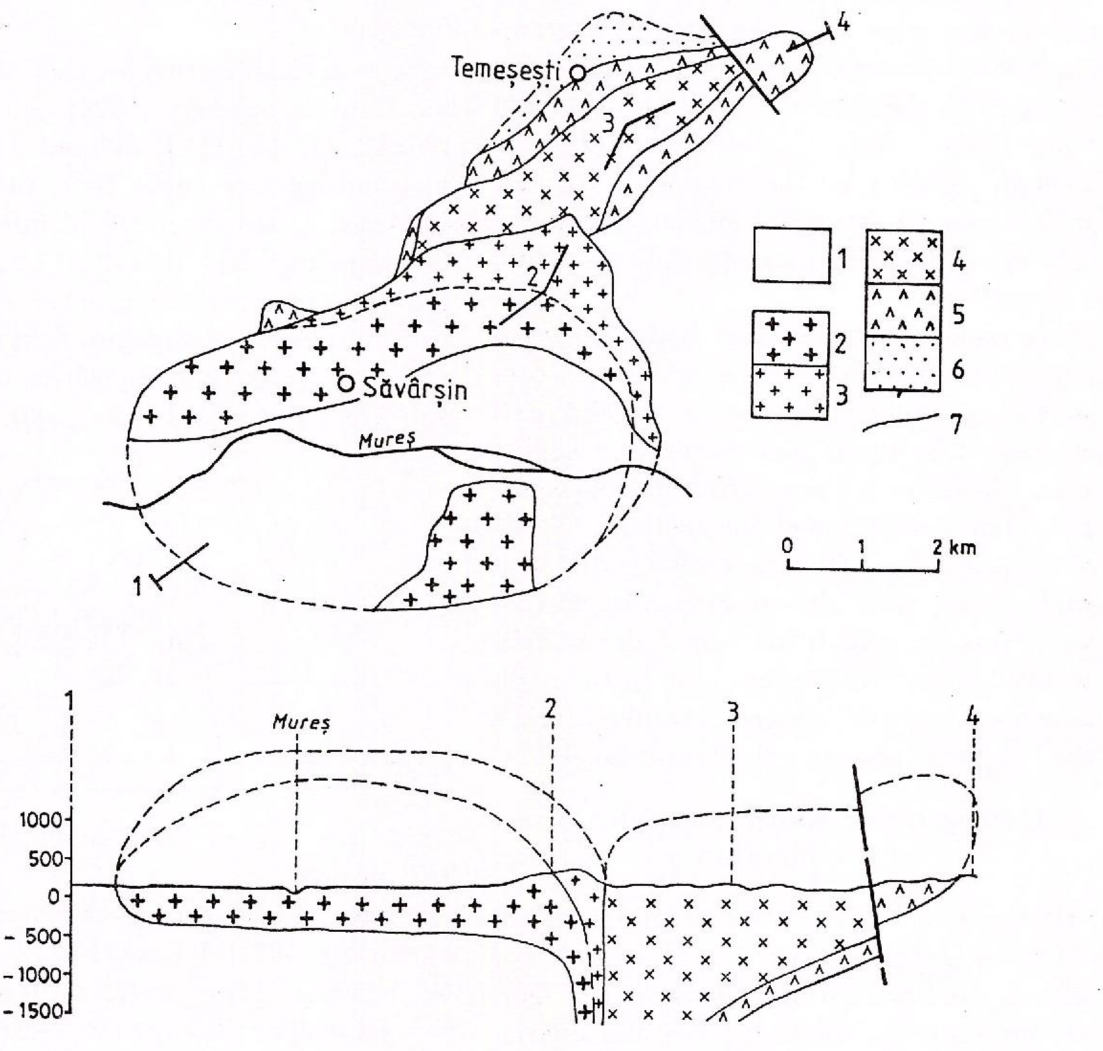

Fig. 1 – Sketch-map of the granitoid massif of Săvârşin. 1, alluvia; Săvârşin granitic body: 2, large-porphyritic granite; 3, marginal facies granite; Temeşeşti body: 4, granodiorite; 5, diorite and quartzdiorite; 6, contact metamorphic zone; 7, fault; 1–4, geological section.

The second intrusion resulted in the Săvârşin granitic body that exhibits a shape of an asymmetrical laccolith (Fig. 1), the feeding facies consisting of porphyritic micrograntie, that extends only along the northern border of the intrusion. It seems that the microgranite in this facies formed a kind of a carapace of the granite body – later on strongly eroded (Fig. 1). Under this a thin zone of common granite was formed and below it the large-porphyritic granite facies of Săvârşin crystallized, which holds affinities with the rapakivi granite. These facies remind us of the ones of the Gaborone granite (Kay, Wright, 1982).

The asymmetrical laccolith shape of the intrusion, the facies sequence and the observation that the granites from the three facies display a close chemical composition (see Savu et al., 1967a – Tab. 1) show that the granite body resulted by the cooling of a single granitic magma intrusion, emplaced near the surface, in which the marginal facies was first to crystallize.

The rocks within this body – especially the large porphyritic granite – contain melanocrate and leucocrate autoliths and are crossed by three joint systems and aplite veins. Measuring these structural elements, Savu (1995) determined the tectonics of the Săvârşin granite. It is noteworthy that this granite body was not accompanied by hydrothermal mineralization and it did not determined a thermal contact zone in the ophiolitic country rocks, because it resulted from a "dry" magma, poor in volatile substances.

Petrographic Aspects and Rock Classification

Of the two intrusive bodies of the granitoid massif, the Temeşeşti body is more basic than the Săvârşin one. It consists of diorites, meladiorites, monzodiorites and quartz-diorites on the border and biotite granodiorites inside, rocks that were described and classified by Szentpétery (1928) and Savu et al. (1967a) using the methods available at that time. We remark that the leucodiorites are often characterized by a porphyritic structure, determined by andesine phenocrysts. The diorites rich in melanocrate minerals (hornblende), abound in basic autoliths which indicates a contamination of the magma by basic materials from ophiolitic country rocks. The autoliths from the diorites consist of hornblende, biotite and plagioclase and those from the granodiorites – which rarely occur – contain biotite and plagioclase, minerals that have first crystallized within the magma. The potash feldspar of the granodiorites from the Ciumani Brook is distinctive by a fine structure of spindle-shaped twin lamellae reminding us that of the microcline type.

For rock classification we used the chemical data from Szentpétery (1928) and Savu et al. (1967a). On the QAP diagram (Fig. 2) the more melanocrate rocks from the Temeşeşti body plot in the diorite field (10^+). A rock from the Crucii Hill, described by Szentpétery (1928) as a microdiorite, is in fact a basic hornfels, that plots in the gabbro field (10), it preserving the chemical composition of the basalt from which it resulted (Savu, 1989).

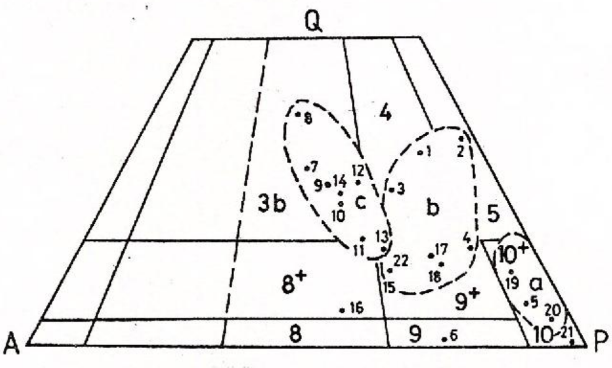

Fig. 2 – Plot of the granitoid rocks on the QAP diagram (acc. to IUGS). 1–11, analyses from Savu et al. (1967a); 12–22, analyses from Szentpétery (1928); 1–6 and 15–22, analyses from the Temeşeşti body; 7–17, analyses from the Săvârşin body; a, field of the Temeşeşti dioritic rocks; b, field of the Temeşeşti quartz-dioritic and granodioritic rocks; c, field of the Săvârşin granitic rocks. See the significance of the diagram domains in text.

Most of the dioritic rocks are monzodiorites which plot within the field (9^+). The quartz-diorites are situated in the field (5). It is noteworthy that two vein rocks, one from the Contrava Brook (no. 5) and another from the

Roşelii Valley (no. 22), plot on this diagram, as on the next one (Fig. 3), in the same place. The granodiorites have a clear position in the field (4).

The kersantite plot in the monzogabbro field (9) and the porphyritic monzonite from Dealul Mare is situated in the field (8^+). The latter was described by Szentpétery (1928) as a granosyenite. It is similar to the "orthophyres" described by Savu (1962) among the Upper Jurassic volcanics associated with the flysch deposits from the compressional sedimentary basin of Drocea, in the north-west of the Mureş Zone.

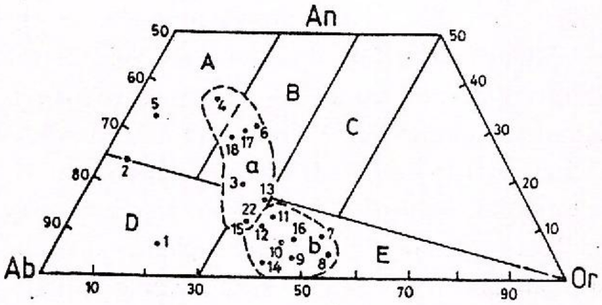

Fig. 3 – Plot of the acid rocks from the Săvârşin massif on the An-Ab-Or diagram. a, field of the Temeşeşti rocks; b, field of the Săvârşin rocks. The same legend as in Figure 2.

On the An-Ab-Or diagram (O'Connor, 1965) in Figure 3, most of the Temeşeşti rocks plot in the granodiorite field (B) and two of them in the tonalites field (A). The common plot of the two above-mentioned vein rocks is situated in the granite field (E). A vein of porphyritic rock crossing the granodiorites is to be found in the trondhjemite field (D). The presence of the trondhjemites associated with the Late Kimmerian intrusions from the Mureş Zone was pointed out by Savu et al. (1985) in the Luncoi region and among the leucocrate dykes from the Vărădia-Troaş region (Savu et al., 1992).

The rocks of the Săvârşin granitic body have a more uniform composition so that on both diagrams (Figs 2 and 3) they plot in the granite field (3b and E). Only one rock, a large-porphyritic granite containing Na_2O and K_2O in almost equal amounts, plot on the QAP diagram in the monzodiorite field (9^+). Within the Săvârşin intrusion two rock-types are characteristic: the marginal facies microgranite and the large-porphyritic granite from the inner facies. The first is a fine rock that was formed by a fast crystallization of the granitic magma in the upper and the marginal parts of the intrusive body (Fig. 1). It contains phenocrysts of orthoclase and albite-oligoclase.

The rocks from the large-porphyritic granite facies are more characteristic, they consisting of a groundmass of common granite with biotite and hornblende, in which large phenocrysts (4–5 cm long) of alkali feldspar occur, the -2V of which varies between 50^0 – 60^0. These phenocrysts exhibit a zonal structure of the rapakivi type. Their alternative zones are formed of orthoclase-anorthoclase and albite. Savu and Vasiliu (1966) showed that these megacrysts were formed by a rhythmical crystallyzation of the granitic magma, an explanation given by Yoder et al. (1957) to the zoned megacrysts of some Scandinavian granites. It was the main process controlling the crystallization, but as it results from Figure 1, presented by Savu (1995), the zones of these megacrysts exhibit various thicknesses. Therefore, we consider that this process was influenced either by successive gas escape from the intrusion or by successive gas influx from the depth, which modified the vapour tension within the magma and, accordingly, the crystallization velocity in different zones. The genesis of this large-porphyritic structure was favoured by the slow crystallization of the granitic magma in the lower part of the laccolith, that was covered by the carapace of marginal facies granite.

Geochemistry and Tectonic Setting

For the geochemical characterization of the granitoid rocks we used some data from Szentpétery (1928) and Savu et al. (1967a) and particularly the new analyses rendered in Tables 1, 2 and 3. The contaminated dioritic rocks from the Temeşeşti body show a particular chemical composition, exhibiting high average contents in TiO_2 (0.91 %), FeO (5.42 %), Fe_2O_3 (3.70 %), Ni (32 ppm), Cr (49 ppm), V (177 ppm) and Co (18.25 ppm), values that are close to the contents of these elements in some gabbros and basalts. Similar contents also occur in their basic autoliths. In the later intruded granodiorites these elemets decrease very much (Tab. 1), showing normal average contents for these rocks that were not contaminated. They are richer in Na_2O (3.92 %) than in K_2O (2.85 %) and are remarkable for their higher average contents in Ba (431 ppm) and Sr (554 ppm). The Rb/Sr ratio is of 0.20. Normal contents in Y, Zr and Nb were determined in the granodiorites (Tab. 1). Be varies between 1 and 2 ppm.

The granites of the Săvârşin body contain very low amounts of TiO_2, iron and CaO (Tab. 1). Of the alkalies, K_2O (4.64 %) is usually higher than Na_2O (4.5 %), the K_2O/Na_2O ratio varying between 1.20 and 1.09. In one granite in the Grohotu Hill the contents of alkalies are equal: K_2O is of 3.98 % and Na_2O is of 3.99 %. In these rocks there are high contents in some trace elements: Ba (791 ppm), Sr (328 ppm) and Zr (172 ppm). The Rb/Sr ratio is of 1.41.

The plot of the 22 analyses from literature on the FeO-MgO-Na_2O+K_2O diagram in Figure 4 (Irvine, Baragar, 1971; Hutchinson, 1982) showed that – excepting the two strongly contaminated diorites (nos. 19 and 20) and the basic hornfels which are situated in the tholeiitic domain (a) – all the acid rocks plot within the calc-alkaline domain, in two separate fields. The Temeşeşti rocks are situated in a typical calc-alkaline field (b) and those of the Săvârşin body and two vein rocks crossing the Temeşeşti body plot in the c and d fields, situated in the extension of the calc-alkaline domain, at higher values of alkalies.

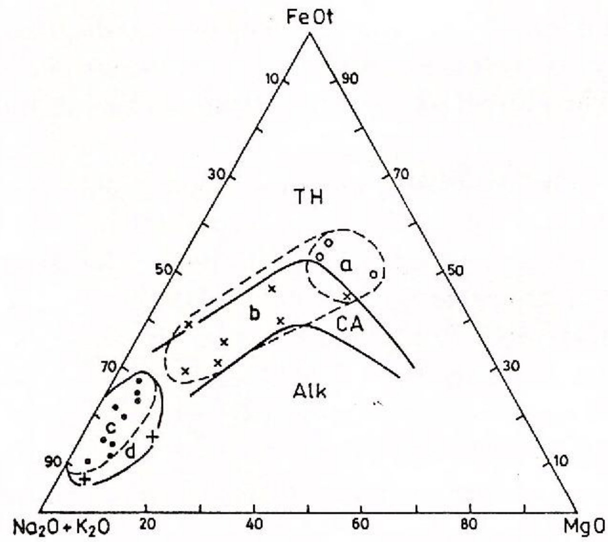

Fig. 4 – Plot of the granitoid rocks on the FeO-MgO-Na_2O+K_2O diagram. a, field of the dioritic rocks and hornfelses of Temeşeşti (o); b, field of the quartzdioritic and granodioritic rocks of Temeşeşti (x); c, field of the Săvârşin granitic rocks (•); d, field of the acid vein rocks crossing the Temeşeşti body (+). TH, tholeiitic domain; CA, calc-alkaline domain; Alk, alkaline domain. The same legend as in Figure 2.

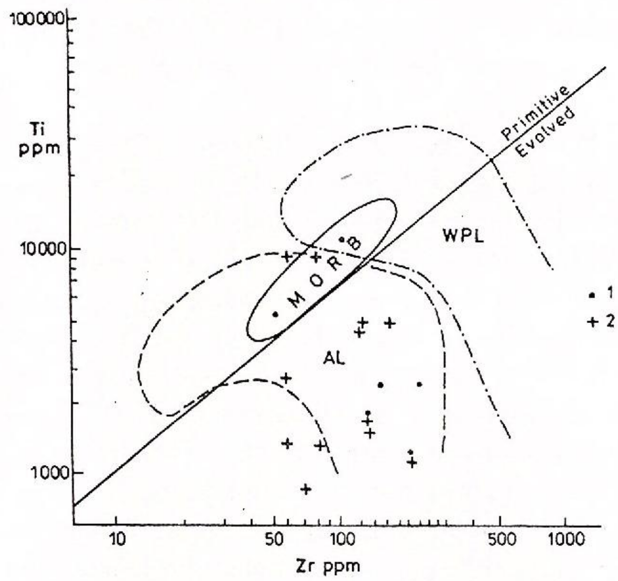

Fig. 5 – Plot of the granitoid rocks (data from Savu et al., 1967a and Table 1) on the Ti-Zr diagram. WPL, intra-plate lavas; MORB, mid-ocean ridge basalts; AL, arc lavas.

The tectonic setting of these rocks was determined by plotting the old analyses and those from Table 1 on the Ti–Zr diagram in Figure 5 (Pearce, 1980). Excepting the basic and the contaminated rocks that are accidentally situated in the MORB domain, the other rocks plot in the field of the volcanic arc lavas. It shows that the Săvârşin massif was formed in connection with the southern island arc of the Mureş Zone, during the subduction of the Liassic ocean crust under the ocean plate situated between the two parallel island arcs of the Mureş Ophiolite Suture (Savu, 1983; Savu et al., 1986). On the Nb-Y diagram in Figure 6 (Pearce et al., 1984) the rocks of the granitoid massif plot also in the domain of the volcanic arc granites (VAG). They represent postcollisional intrusions, because on the Rb-Y+Nb diagram in Figure 7 (Pearce et al., 1984) they are situated just in the field of the Querigut granites from Pyrenées – France, considered by the quoted authors in this category.

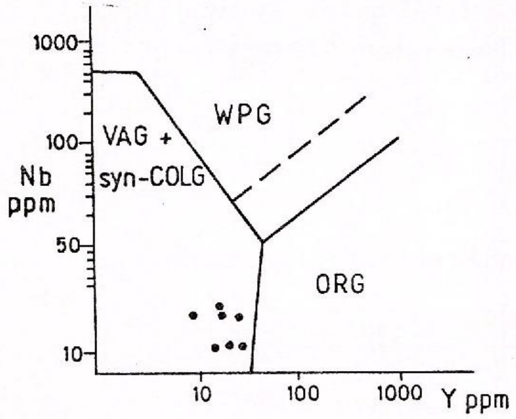

Fig. 6 – Plot of the granitoid rocks from Table 1 on the Nb-Y diagram. WPG, intra-plate granites; ORG, ocean ridge granites; VAG + syn-COLG, volcanic arc granites + syncollisional granites.

By the Neutron Activation Analysis there were determined the contents of Th, Hf, Sc, Ta and Co in four granitoid rocks and one gabbro (Tab. 2).

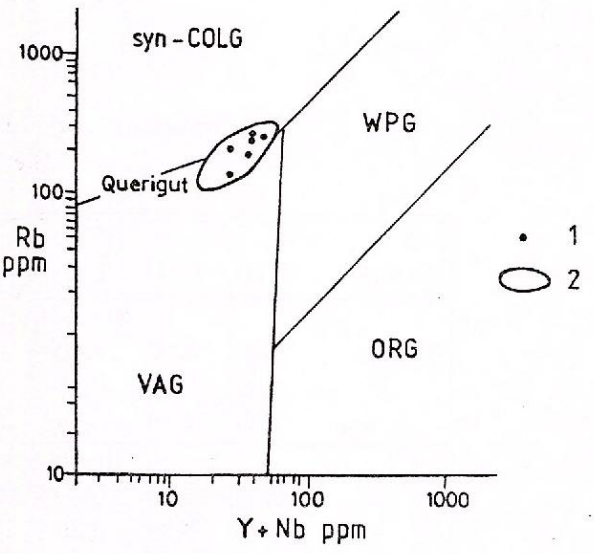

Fig. 7 – Plot of the granitoid rocks from Table 1 on the Rb-Y+Nb diagram. 1, rocks from the Săvârşin massif; 2, field of the Querigut granites. The same legend as in Figure 6.

The last rock was collected from the ophiolites near by Temeşeşti intrusion, on the Plisca Brook. The Th, Hf and Ta contents are lower in the Temeşeşti rocks and higher in those of Săvârşin body. Within the last rocks, Th and Hf are higher in the large-porphyritic granite than in the marginal facies granite. On the contrary, the Sc contents are higher in the Temeşeşti rocks than in those of the Săvârşin body. The granodiorite is an exception, its content in Co being higher than that in the marginal facies granite of Săvârşin, but lower than that in the large-porphyritic granite (Tab. 2). In contrast, in the Liassic gabbro were determined lower contents of Th, Hf and Ta and higher contents of Sc and Co than in all the granitoid rocks.

The contents of REE were also determined by Neutron Activation Analysis (Tab. 3). The REE contents in the Temeşeşti rocks are lower than those in the Săvârşin rocks, while the HREE are variable in both intrusions.

Table 1
Distribution of some major and trace elements in rocks of the Săvârşin massif

	%				ppm					
Sample+	K_2O	CaO	TiO_2	Fe_2O_3	Rb	Sr	Y	Zr	Nb	Nb/Sr
Rocks from the Temeşeşti body										
1	0.90	5.90	1.40	9.80	30	430	30	100	<20	0.035
2	3.00	2.10	0.40	2.10	110	310	20	150	<20	0.368
Aver.	1.95	4.00	0.90	5.95	70	370	25	125	< 20	0.200
Rocks from the Săvârşin body										
3	3.20	1.80	0.30	2.30	180	390	20	200	20	0.297
4	4.70	0.80	0.30	1.10	210	100	30	130	20	2.010
5	3.80	1.20	–	1.10	230	140	20	150	20	1.650
6	3.40	0.70	–	0.90	190	70	20	140	20	2.900
7	3.80	1.90	0.40	3.00	170	820	20	240	<20	0.201
Aver.	3.78	1.28	0.35	1.68	196	328	22.5	172	20	1.410
Liassic gabbro										
8	0.30	9.00	1.00	11.80	20	410	20	50	20	0.035

+The samples represent: 1, quartzdiorite – Temeşeşti; 2, granodiorite – Ciumani Brook; 3, large-porphyritic granite – Hălăliş; 4, marginal facies granite – Contrava Brook; 5, marginal facies granite – Fercioaia Brook; 6, porphyritic microgranite – Contrava Brook; 7, large-porphyritic granite – Săvârşin; 8, Liassic gabbro – Temeşeşti.

Table 2
Distribution of Th, Hf, Ta, Sc and Co in rocks of the Săvârşin massif

Sample+	Th ppm	Hf pm	Ta ppm	Sc ppm	Co ppm
Rocks from the Temeşeşti body					
1 (1)	1.6	2.2	–	28.7	25.00
2 (2)	10.5	3.4	0.63	4.6	2.80
Aver.	6.5	2.8	–	16.65	13.90
Rocks from the Săvârşin body					
3 (4)	36.0	3.6	1.39	1.3	1.30
4 (3)	41.6	5.4	1.30	4.5	7.40
Aver.	38.8	4.5	1.34	2.9	4.35
Liassic gabbro					
5 (8)	1.5	0.9	–	39.0	42.00

+ In parantheses are the sample numbers of the Table 1.

Table 3
Distribution of REE in rocks of the Săvârşin massif

Sample+	La	Ce	Sm	Eu	Tb	Yb
	Rocks from the Temeşeşti body					
1 (1)	20	34	6.1	1.90	0.85	3.8
Average:	ΣREE = 66.65 ppm; LREE/HREE = 9.17; Eu/Sm = 0.31; (La/YB)N = 3.59; (Ce/Yb)N = 2.29; (Ce)N = 39					
2 (2)	26	43	3.3	0.90	0.72	1.7
Average:	Σ REE = 75.62 ppm; LREE/HREE = 21.7; Eu/Sm = 0.27; (La/Yb)N = 10.26; (Ce/Yb)N = 6.49; (Ce)N = 50					
	Rocks from the Săvârşin body					
3 (4)	116	207	8.5	1.35	0.76	2.8
Averages:	Σ REE = 336.41 ppm; LREE/HREE = 67.51; Eu/Sm = 0.16; (La/Yb)N = 27.07; (Ce/Yb)N = 18.38; (Ce)N = 239					
4 (3)	83	143	5.6	1.48	0.65	1.8
Average:	Σ REE = 235.53 ppm; LREE/HREE = 58.93; Eu/Sm = 0.26; (La/Yb)N = 31.5; (Ce/Yb)N = 20.65; (Ce)N = 16.5					
	Liassic gabbro					
5 (8)	4.0	–	2.6	1.07	0.60	1.0
Averages:	Σ REE = 9.27 ppm; LREE/HREE = 2.47; Eu/Sm = 0.41; (La/Yb)N = 2.66					

+In the parantheses are the sample numbers of Table 1

The value of the Eu/Sm ratio and the REE sums of the quartzdiorites and granodiorites harmonize with those established by Cullers and Graf (1984) for the "quartzdiorites with little or no Eu anomalies". The Eu/Sm ratio in the Săvârşin marginal facies granite is much more lower than in the Temeşeşti acid rocks. The REE sum of 235.53 ppm in the large-porphyritic granite is close to that of the marginal facies granite. Both values are situated between the ranges established by Cullers and Graf (1984) for the monzonites with Eu negative anomaly. They are three times higher than those from the acid rocks of the Temeşeşti body. It is noteworthy that the value of 0.26 of their Eu/Sm ratio is very close to that of the Temeşeşti granodiorite.

The values of the REE sum and of the LREE/HREE ratio in the gabbro are lower than in any granitoid rock. On the contrary, the Eu/Sm ratio is higher than that of the granitoid rocks. A general remark is that the value of the (La/Yb)N (Tab. 3) increases from 2.66 in the Liassic gabbro to 27.07 in the large porphyritic granite of Săvârşin.

Figure 8 shows the patterns of the chondrite normalized (Nakamura, 1974) REE from Table 3.

The gabbro pattern indicates the rock origin in an ocean crust. The Temeşeşti quartzdiorite pattern does not exhibit any Eu anomaly, but it occurs on the granodiorite pattern, indicating a fractional crystallization from a quartzdioritic magma towards a granodioritic one, as in case of the contaminated intrusion of Cairnsmore in Scotland, described by Tindle et al. (1988). The patterns of the Săvârşin granitic rocks do not exhibit any Eu anomaly, showing that these rocks originated in a homogeneous parental magma, which did not differentiate. These patterns clearly indicate that the Săvârşin granitic rocks are richer in LREE

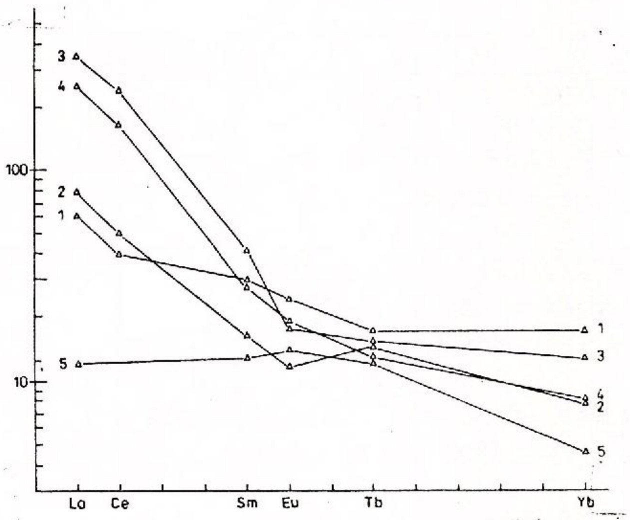

Fig. 8 – Patterns of the chondrite normalized REE from the granitoid rocks and Liassic ophiolites. 1, quartzdiorite – Temeşeşti; 2, granodiorite – Temeşeşti; 3, marginal facies granite – Săvârşin; 4, large-porphyritic granite – Săvârşin; 5, Liassic gabbro – Temeşeşti.

and more depleted in HREE than the acid rocks of the Temeşeşti body. This also shows that the two intrusions resulted from two different parental magmas, which could have been formed by two successive partial melting batches of substratum metasomatized and contaminated by substances coming from the subducted ocean crust. Such a conclusion is also supported by the values of the (Ce)N and (Ce/Yb)N ratio, which are very different in the two bodies of the Săvârşin massif. The value of the Eu/Eu^{+} ratio[2] is higher than 0.7 in most of the Săvârşin granitoid massif rocks. According to Zhonggang (1982) such rocks could have resulted by the differentiation of a basic magma. In our opinion, the same granitic magmas could be achieved by the partial melting of a metasomatized and contaminated mantle.

[2]The Eu/Eu^{+} value resulted from the relation (Eu)N/1/2(Sm+Gd)N. If Gd was not determined, its value may be deduced from the rock pattern.

Conclusions

The two bodies of the Săvârşin massif, which were emplaced successively, resulted from two different parental magmas, possibly formed by two partial melting batches of a metasomatized and contaminated mantle situated over the Benioff plane. Each granitoid body had its proper evolution.

The dioritic magma which yielded the Temeşeşti body was a hotter magma (740^0 C), rich in volatile substances, that differentiated in the depth to a granodioritic magma. This hot magma metamorphosed and assimilated the ophiolitic country rocks.

The parental magma which generated the Săvârşin granitic body was very viscous and poor in volatile substances and crystallized at a temperature of about 660^0 C. Owing to its characteristics, this magma did not determine a contact zone and was not contaminated.

These characteristics clearly show that the parental granitic magma of Săvârşin does not represent a product of the Temeşeşti magma differentiation.

References

Balk, R. (1937) Structural behaviour of igneous rocks. *Geol. Soc. Am. Mem.*, 5, p. 1–177, Washington D.C.

Cullers, R.L., Graf, J.L. (1984) Rare earth elements in igneous rocks of the continental crust: predominantly basic and utrabasic rocks. In: R. Henderson (edit.) Rare earth Element Geochemistry, Elsevier, p. 237–274, Amsterdam.

Giuşcă, D. (1950) Le massif éruptif de Vlădeasa. *Ann. Inst. Géol.*, XXIII, p. 200–252, Bucureşti.

Hutchinson, C.S. (1982) Indonesia. In: R.S. Thorpe, J. Wyley (edits.) Andesites, p. 207–224, Chichester.

Irvine, T.N., Baragar, W.P.H. (1971) A guide to the chemical classification of the common volcanic rocks. *Can. J. Earth Sci.*, 8, p. 523–548, Toronto.

Key, R.M., Wright, E.P. (1982) The genesis of the Gaborone rapakivi granite complex in Southern Africa. *J. Geol. Soc. London*, 139, 2, p. 109–126, London.

Nakamura, N. (1974) Determination of REE, Ba, Fe, Mg, Na and K in carbonaceous and ordinary chondrites. *Geochim. Cosmochim. Acta*, 38, p. 757–775, Oxford.

O'Connor, J.T. (1965) A classification of quartz-rich igneous rocks based on feldspar ratios. *U.S. Geol. Surv. Prof. paper*, 525 B, p. 79–84, Washington.

Pabst, A. (1928) Observation on the inclusions in the granitic rocks of the Sierra Nevada, California. *Univ. Dept. Geol. Sci. Bull.*, 17, 10, p. 329–330, Berkeley.

Pearce, J.A. (1980) Geochemical evidence for the genesis and eruptive setting of lavas from Tethyan ophiolites. In: A. Panayiotou Ophiolites - Proc. Intern. Ophiol. Symp. Cyprus, 1979, p. 261–272, Nicosia.

– **, Haris, N.B.W., Tindle, A.G. (1984)** Trace element discrimination diagram for the tectonic interpretation of granitic rocks. *J. Petrol*, 25, p. 956–983, Oxford.

Petrulian, N., Steclaci, L. (1965) Sur la présence du rhénium dans les molybdénites de Roumanie et son importance comme thérmomètre géologique. *Rev. Roum. Géol. Géophys., Géogr. (Géol.)*, 8, (1–2), p. 83–87, Bucureşti.

Savu, H. (1962) Cercetări geologice şi petrografice în regiunea Troaş-Pârneşti din Masivul Drocea. *D.S. Com. Geol.*, XLVI, p. 137–159, Bucureşti.

– **(1995)** Tectonics of the Săvârşin granite (Drocea Mountains). *Rom. J. Tectonics and Geol. Reg.*, 76, p. 73–82, Bucureşti.

– **, Vasiliu, C. (1966)** Temperatura de formare a granitului de Săvârşin (Munţii Drocea). *D.S. Inst. Geol.*, LII, p. 141–157, Bucureşti.

– **, Vasiliu, C., Udrescu, C. (1967a)** Contribuţii la studiul geochimic al rocilor banatitice de la Săvârşin (Munţii Drocea). *D.S. Inst. Geol.*, LII/2, p. 359–382, Bucureşti.

– **, Vasiliu, C., Udrescu, C. (1967b)** Géochimie du massif banatitique de Săvârşin. *Assoc. Géol. Carp. - Balk. VIII*[ème] *Congr. Belgrade*, p. 265–270, Belgrade.

– **, Mândroiu, V. (1980)** Studiul metalogenetic al masivului banatitic de la Săvârşin (Munţii Drocea). *D.S. Inst. Geol. Geofiz.*, LXIV, 2, p. 133–151, Bucureşti.

– **(1983)** Geotectonic and magmatic evolution of the Mureş Zone (Apuseni Mountains). *Carp. - Balk. Geol. Assoc. XII*[th] *Congr. Bucharest, 1981. An. Inst. Geol. Geophys.*, LXI, p. 253–262, Bucureşti.

– **, Berbeleac, I., Udrescu, C., Neacşu, V. (1985)** The study of ophiolites and island arc magmatites in the Băgara-Visca-Luncoi region (Mureş Zone - Apuseni Mountains). *D.S. Inst. Geol. Geofiz.*, LXIX/1, p. 63–81, Bucureşti.

– **, Vâjdea, E., Romanescu, O. (1986)** The radiometric age (K/Ar) and the origin of the Săvârşin granitoid massif and of other Late Kimmerian intrusions from the Mureş Zone. *D.S. Inst. Geol. Geofiz.)*, 70–71/1, p. 419–429, Bucureşti.

– **, (1989)** Metamorfismul ofiolitelor liasice la contact cu intruziunile de arc insular neokimmerice de la Săvârşin (Zona Mureş). *Stud. cerc. geol., geofiz. geogr. (Geol.)*, 34, p. 43–50, Bucureşti.

Socolescu, M. (1944) Les affleurements de minerais de la région Vaţa–Şoimuş–Zam. *C.R. Inst. Géol. Roum.*, XXVIII, p. 93–125, Bucureşti.

Szentpétery, S. (1928) Petrologie des südlichen Teiles des Drocea Gebirges. *Mitt. Jahrb: kgl. ung. geol. R. Anst.*, XXVII, p. 191–316, Budapesta.

Ştefan, A. (1986) Eocretaceous granitoids from the South Apuseni. *D.S. Inst. Geol. Geofiz.*, 70–71/1, p. 229–241, Bucureşti.

Tindle, A.G., Mc Garvie, D.W., Webb, P.C. (1988) The role of hibridization and crystal fractionation in the evolution of the Cairnsmore of Carsphairn Intrusion Southern Uplands of Scotland. *J. Geol. Soc. London*, 145, 1, p. 11–22, London.

Zhonggang, W. (1982) The REE distribution pattern of granitoides and their metallogenetic relations. *Proceed. Intern. Symp. Nanjing University*, Nanjing, China.

Yoder, H.S., Stewart, D.B., Smith, J.R. (1957) Report of the director of the Geophysical Laboratory, Carnegie Inst. *Washington Year Book*, 56, p. 206–214, Washington.

Received: May 30, 1994
Accepted: June 15, 1994

Rom. J. Petrology, 77. p. 83–96, Bucureşti, 1996

THE BRĂNIŞCA HILL CALC–ALKALINE AND THE MĂGURA SÂRBI ALKALINE PALEOGENE VOLCANIC ROCKS (MUREŞ COULOIR)

Haralambie SAVU, Constanţa UDRESCU, Maria STOIAN

Institutul Geologic al României. Str. Caransebeş 1, 79 678 Bucureşti 32

Vasilica NEACŞU

S.C. Prospecţiuni SA. Str. Caransebeş 1, 78 344, Bucureşti 32

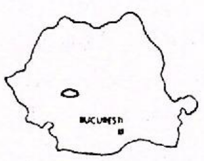

Key words: Calc-alkaline rocks. Alkaline rocks. Primary magmas. Major elements. Trace Elements.Mureş Couloir. South Apuseni Mts.

Abstract: Within the Mureş Couloir there are Paleogene (56–30 Ma) volcanics formed under distension conditions. The volcanic activity was favoured by an E–W system of crustal fractures. The basalt-andesitic neck and lava flows of Brănişca Hill and the trachyandesitic elongated neck of Măgura Sârbi are the most representative ones. The component rocks display a very uniform composition in each volcanic structure, which shows a rapid evolution, without any important differentiation or contamination processes. This suggests also that the parental magmas of each volcanic structure could have been primary magmas, formed in the mantle at a great depth. The calc-alkaline or alkaline characteristic of these magmas was determined by the partial melting of the metasomatized peridotitic substratum in a small or very small amount (0–5 per cent). The rocks show ambiguous characteristics as regards their tectonic setting – they being transitional volcanics between the arc (Banatitic) and the intra-plate (basanitic) rocks. These characterisitcs are the result of the partial melting of the metasomatized substratum under the distension conditions of the Paleogene period.

Introduction

Along the Mureş Couloir, between Deva and Ilia, there are a few occurrences of Paleogene volcanic rocks which were previously considerated as post-Miocene or Quaternary volcanics (Ghiţulescu, Socolescu, 1941; Gheorghiu, 1954; Kräutner, 1969; Peltz et al., 1971).

These are the occurrences of Brănişca (Bretea) Hill, Măgura Sârbi, Herepea and the small neck situated between Lesnic and Săcămaş known since Hauer and Stache (1863). The eruption of these volcanics was favoured by a system of E–W fractures (Savu et al., 1994a) among which the South Transylvanian crustal fault represented by its western segment – the Recaş–Cuieş fault evidenced by Andrei et al. (1975) – is the most important.

In order to make a comparative study on these volcanics, we selected the occurrences of Brănişca Hill and Măgura Sârbi as the most characteristic ones. For that purpose we used 11 new chemical and trace element analyses.

The first geological observations concerning these two volcanic occurrences are due to Ghiţulescu and Socolescu (1941) who considered them – like Gheorghiu (1954) later on – as two outliers of post-Miocene basaltic lavas from the 4th phase, emitted by the small Lesnic neck. They suggested also that under the Mureş alluvial deposits other volcanic necks could exist.

Kräutner, who studied in 1969 the Poiana Ruscă Mts alkali basalts and basanites and the Mureş Couloir volcanics, regarded the volcanic occurrences of Brănişca Hill and Măgura Sârbi as two Quaternary necks constituted of calc-alkaline basalt-andesites, a character which afterwards was asserted by Peltz et al. (1971). Rădulescu et al. (1981) described them as intra-plate young volcanics. Lemne et al. (1983, unpubl. rep.) using K/Ar datings, established that they are Paleogene (48–30 Ma) rocks. Boştinescu (1982, unpubl. rep.) evidenced lava flows on the Brănişca Hill which he represented on the Gurasada map, worked out by Lupu et al. (1986). Savu et al. (1994a) showed that the Mureş Couloir volcanics are "transitional rocks" between the arc banatites and the intra-plate basanites.

Structure of the volcanic occurrences

The Brănişca Hill and Măgura Sârbi volcanic rocks occur north of Mureş in the South Apuseni Mts, where they form two peaks situated at about 3 kilometers one from another (Fig. 1): the first lies between Brănişca and Bretea Mureşană localities and the second occurs south–east of the Sârbi village. As K/Ar datings showed (Lemne et al. 1982; 1983, unpubl. rep.) the volcanic rocks from this part of the Mureş Couloir and the Poiana Ruscă Mts erupted in the Paleogene, between 56 and 30 Ma. See also the Gurasada map (Lupu et al., 1986). Therefore, they are contemporaneous with the Tertiary basaltic volcanics of Scotland and North Ireland, the eruption of which commenced in Early Tertiary and ended 40 Ma ago (Hatch et al., 1961).

The Brănişca Hill (30 Ma) basalt-andesitic volcanics are represented by a neck and lava flows. The first lies at the southern extremity of the Brănişca Hill (341 m) – on the right Mureş riverside. Its eruption was probably facilitated by one of the E–W fractures cutting along the Mureş Couloir, which could be located just on the Mureş thalweg. Another such fault occurs near by the northern boundary of the Brănişca Hill lava flows (Fig. 1). This neck was exploited down to around 15 m above the river water by the Brănişca Quarry, so that in the neck place resulted a deep open pit. Now the neck filling basalt-andesites can be observed on the open pit bottom, near the northern wall, on a surface of a few square meters.

The Brănişca neck has an irregular shape. Its walls are constituted of Turonian – Senonian sedimentary deposits (sandstones, conglomerates, shales) belonging to the Deva Beds. Around the neck the sedimentary deposits are almost vertical and they show different trends. At the contact with the basalt-andesitic neck the sedimentary deposits were affected by a caustic metamorphism, accompanied by burning and fritting phenomena.

The successive lava flows lie on the Brănişca Hill, north of the neck (Fig. 1), extending one kilometer away, near the Bejan–Ilia road. It seems that through the Brănişca vent very fluid basalt-andesitic lavas streamed down, extending around on a surface of more than 3 km sq. Later on, they were eroded so that the basalt-andesites on the Brănişca Hill represent a vestige of these lava flows.

The alkaline neck of Măgura Sârbi (48 Ma, average of two datings, Lemne et al., 1983, unpubl. rep.) forms another peak (416 m) higher than the first one. The neck is elongated E–W ower a distance of about 600 m (see the Gurasada map and Fig. 1), parallel to the Recaş-Cuieş crustal fault, on which it was formed. Besides, it is a little swollen toward south (Fig. 1). It seems that this neck has not reached the earth's surface.

As Kräutner (1969) showed, too, the neck was separated in quasihorizontal four-sided prisms, that are characteristic of such magmatic structures (Tyrrell, 1960). These prisms are 1 meter long and 20–30 cm thick. They form a vault (Fig. 2), the apex of which lying in the neck axial zone, where the prismatic separations were affected by a flexure that is

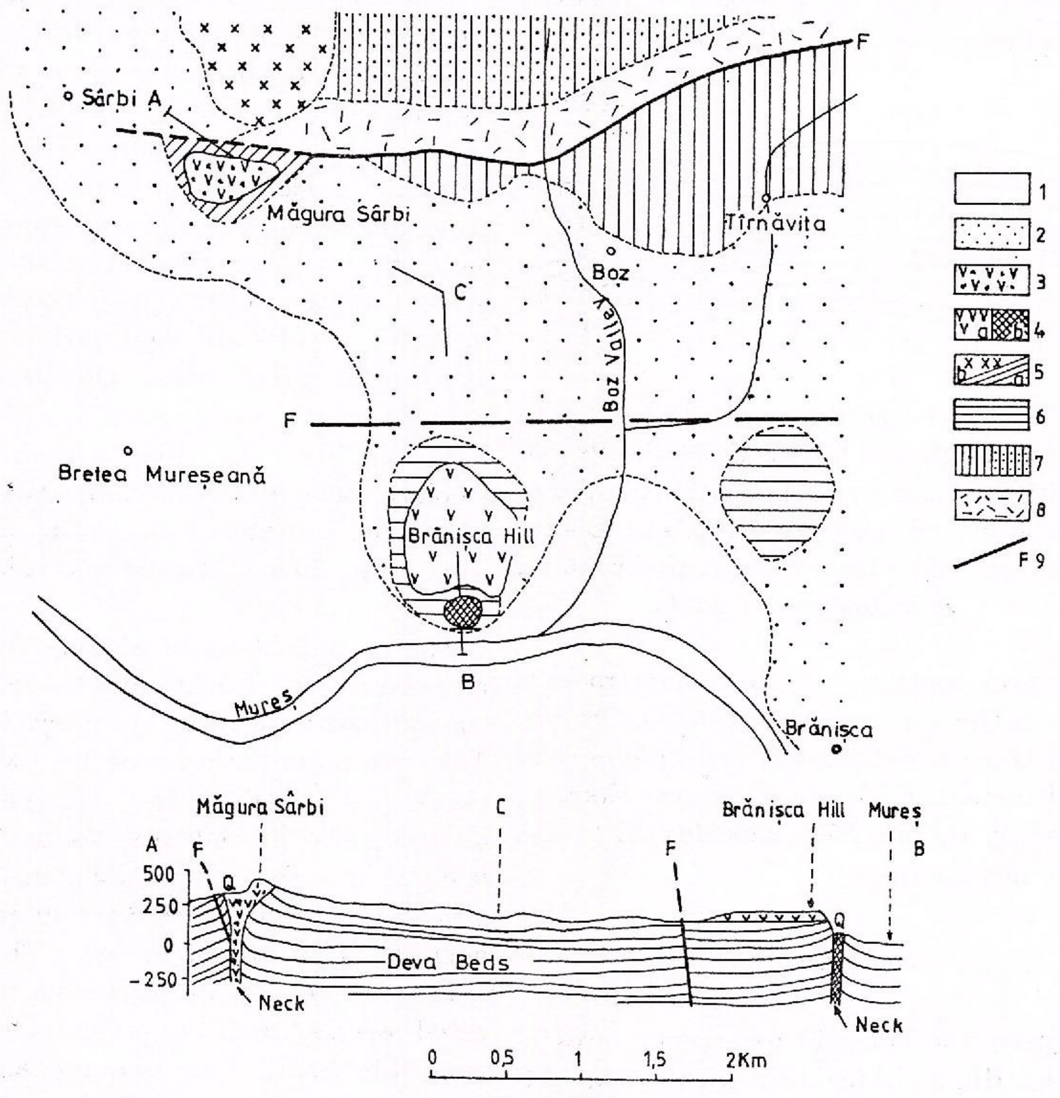

Fig. 1 – Geological sketch of the Brănişca Hill and Măgura Sârbi volcanic occurrences (acc. to Lupu et al., 1986 and the authors' data). 1, alluvia; 2, Quaternary deposits; 3, Măgura Sârbi trachyandesites and trachybasalt-andesites; 4a, Brănişca Hill lava flows; 4b, basalt-andesitic neck; 5a, Paleocene–Maastrichtian deposits; 5b, Banatitic pyroclastic beds; 6, Lower Senonian – Turonian deposits; 7, Barremian – Aptian deposits; 8, tectonic breccia; 9, fault; Q, quarry.

visible at the first quarry level. The prismatic separations are due to three fissure systems formed during the neck cooling: a system parallel to the vault formed by the prismatic separations and two strong dipping fissure systems. At the second quarry level these two last fissure systems have the following position: N 50^0 - 70^0W/55^0N and N 50^0 - 70^0E/72^0S. In some neck portions the prismatic separations are weathering parallel to their sides.

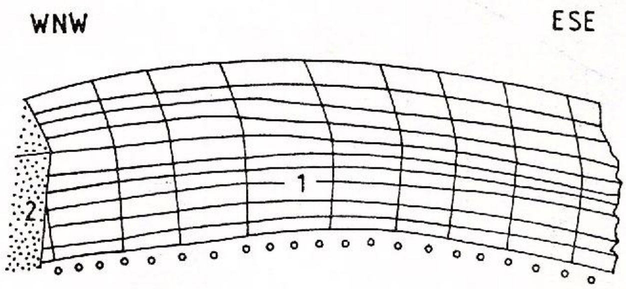

Fig. 2 – The northern part of the Bretea Quarry in the Măgura Sârbi neck showing its contact with the Paleocene – Maastrichtian sedimentary deposits and the four-sided prismatic separations that make a large vault. 1, alkaline rocks; 2, sedimentary deposits.

The neck contact with the country rocks is visible at the northern part of the first quarry level, where the sedimentary beds, represented by Paleocene and Maastrichtian deposits were uplifted by the intrusion and affected by the caustic metamorphism.

Petrography

Between the volcanic rock occurrences of Brănişca Hill and Măgura Sârbi there are differences concerning their petrographic composition. The Brănişca basalt-andesites are black aphanitic rocks with a basaltic aspect. The rocks inside the neck have a porphyritic texture, determined by the presence of augite microphenocrysts embedded in a pilotaxitic groundmass formed of plagioclase, augite and magnetite microcrystals. The augite microphenocrysts are gathered, forming small glomeroporphyritic aggregates. Some of them have been substituted by magnetite. The groundmass structure is a massive one, some fluxion aspects occurring only around the microphenocrysts. Very rarely a vesicular structure is present. On the neck border the texture is fluidal and the basalt-andesites contain xenoliths torn off from the country rocks.

The basalt-andesitic lavas on the Brănişca Hill also have a porphyritic texture, they containing euhedral microphenocrysts of plagioclase (An 48–46) with albite or albite-Karlsbad twins, and rarely of augite. These are embedded in a pilotaxitic or hyalopilitic – fluidal groundmass (Pl., Fig. 1), consisting of parallel plagioclase microcrystals, small magnetite grains and glass. The augite microphenocrysts ($c \wedge Ng = 49^0$) are light brown and have 2–3 thin marginal zones. Olivine microphenocrysts substituted by secondary minerals are rare (Pl., Fig. 2). Here and there amygdaloidal rocks occur, the amygdals of which are infilled with calcite or chlorite, or by chlorite on the amygdal border and calcite inside it.

The alkaline rocks of Măgura Sârbi neck, represented by trachyandesites and rarely trachybasalt-andesites, are grey in colour. They are porphyritic rocks, too, with a trachytic texture (Pl., Fig. 3), consisting of a hyalopilitic groundmass, formed of alkali feldspar microlites, magnetite grains and some glass in which augite ($c \wedge Ng = 40^0$) microphenocrysts occur (Pl., Fig. 4). The last are light green and very fresh. Besides, small elongated pseudomorphs are present, consisting of magnetite grains. They were probably formed by the magmatic corrosion of some pyroxene or brown amphibole crystals. Other pseudomorphs, 1 mm long, are formed of chlorite and magnetite grains.

Geochemistry and tectonic setting

The chemical analyses (Tab. 1 and 2) of 11 samples from the two volcanic occurrences reflect their petrographic composition by the SiO_2 average contents, which are of 53.42 % in the Brănişca basalt-andesites and of 54.67 % in the Sârbi alkaline rocks. These values are a little higher than 52.00 % SiO_2 that is the boundary between basalt and basalt-andesite (Gill, 1981; Ewart, 1982). That they belong to these petrographic types, as clearly results from the Figure 3 (Bass et al., 1986).

The TiO_2 average contents are higher in basalt-andesites than in the alkaline rocks. But they are lower than in other rock types, as on the diagram in Figure 4 (Pearce, 1980), in which TiO_2 is one of the two referring elements, all the analysed rocks plot in the field of the arc volcanics. On the contrary, the

Table 1

Chemical composition of the volcanic rocks

	Brănişca Hill basalt-andesites						Măgura Sârbi trachybasalt-andesites				
	1	2	3	4	5	6	7	8	9	10	11
SiO_2 %	52.64	52.98	53.24	53.44	53.60	54.71	53.70	55.49	58.26	58.34	58.80
TiO_2	0.90	0.90	0.86	0.90	0.89	1.44	0.80	0.63	0.58	0.55	0.55
Al_2O_3	18.34	18.00	17.15	17.21	16.94	16.23	17.52	16.84	16.73	16.18	16.08
Fe_2O_3	3.81	2.97	2.49	2.09	3.23	3.36	3.68	2.99	3.25	2.98	2.91
FeO	3.59	4.27	4.47	4.27	4.27	3.79	3.07	2.66	2.14	2.38	2.27
MnO	0.13	0.15	0.13	0.13	0.14	0.12	0.12	0.11	0.11	0.09	0.11
MgO	4.44	5.09	5.10	5.19	4.83	5.85	4.61	4.68	3.97	3.54	3.92
CaO	8.38	8.24	8.49	8.02	8.12	7.84	7.80	6.99	6.54	6.51	6.51
K_2O	1.36	1.38	1.40	1.28	1.43	1.21	1.62	2.15	2.08	2.34	1.99
Na_2O	3.66	3.46	3.52	3.46	4.10	3.48	3.85	4.22	3.85	4.01	3.92
P_2O_5	0.23	0.28	0.24	0.27	0.24	0.29	0.23	0.24	0.20	0.21	0.21
H_2O^+	2.14	1.93	2.39	2.49	1.66	1.45	2.68	2.46	1.97	2.33	2.40
S	0.35	0.04	0	0.01	0	0.06	0.01	0	0	0	0.25
Total	99.97	99.69	99.48	99.48	99.45	99.82	99.61	99.46	99.67	99.46	99.92
Ni ppm	90	75	100	105	90	105	48	38	52	31	36
Co	22	15	30	24	18	20	14	8	10	6	6
Cr	180	175	230	235	170	250	125	65	100	42	67
V	270	210	300	260	210	200	160	85	125	67	66
Sc	21	22	26	20	18	24	14	10	13	8	8.5
Th	6.3	5.5	-	5.3	-	-	-	8	-	-	73
Hf	4.5	2.3	-	4.2	-	-	-	3.0	-	-	9
Zr	140	100	180	165	135	125	125	90	140	95	5.5
Y	26	24	27	25	23	29	18	<10	15	<10	<10
Yb	2.2	1.7	1.9	1.9	1.8	4.9	1.6	<1	1	<1	1.1
Ba	750	340	550	350	700	440	680	650	620	530	620
Sr	>1000	630	730	700	>1000	530	>1000	700	600	550	>1000
Pb	7	11	12	11	9	5.5	4	17	9	16	14
Cu	28	66	40	34	36	32	12	32	14	28	27
Zn	55	50	55	52	62	87	50	40	55	44	55
Ga	26	28	32	32	27	17	16	18	14	26	16
Sn	<2	5	2.5	<2	2.5	<2	<2	<2	<2	3.5	<2

Remarks: $CO_2 = 0$; Nb <10 ppm; La <30 ppm.

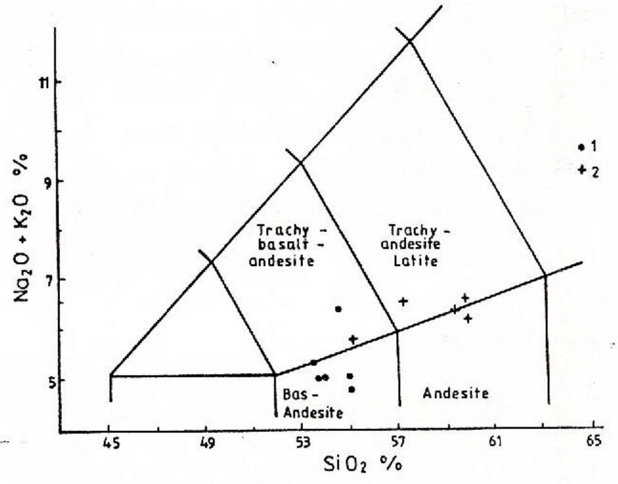

Fig. 3 – Plot of volcanic rocks on the Na_2O+K_2O–SiO_2 diagram. 1, Brănişca Hill basalt-andesites; 2, Măgura Sârbi alkaline rocks.

Al_2O_3 average contents of the two rock groups are very close.

More important differences between the basalt-andesites and the alkaline rocks occur in case of iron, MgO and CaO, components the average values of which are always higher in the former rocks than in the latter (Tab. 2). The average value of the CaO/Al_2O_3 ratio is 0.47 in basalt-andesites and 0.41 in the alkaline rocks.

The alkali average contents are higher in the Sârbi alkaline rocks. Consequently, between the two rock groups there are the following relationships concerning these elements (Tab. 2): basalt-andesites – Na_2O (3.61 %) > K_2O (1.34 %); $K_2O + Na_2O$ = 4.95 %; K_2O/Na_2O = 0.37; alkaline rocks – Na_2O (3.97 %) > K_2O (2.04 %); $K_2O + Na_2O$ = 6.01 %; K_2O/Na_2O = 0.49.

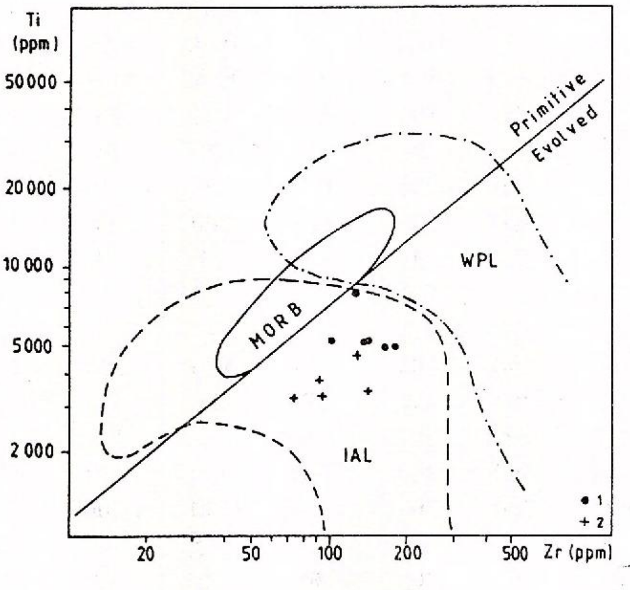

Fig. 4 – Position of the volcanic rocks on the Ti – Zr diagram. 1, Brănişca Hill basalt-andesites; 2, Măgura Sârbi alkaline rocks. WPL, intra-plate lavas; MORB, mid-ocean ridge basalts; IAL, island arc lavas.

Table 2
Ranges and averages of the element contents in the volcanic rocks

	Brănişca Hill basalt-andesites		Măgura Sârbi trachybasalt-andesites	
	Ranges	Averages	Ranges	Averages
SiO_2%	52.64–54.71	53.42	53.70–58.80	54.67
TiO_2	0.86–1.44	0.98	0.55–0.80	0.62
Al_2O_3	16.23–18.34	17.31	16.08–17.52	16.67
Fe_2O_3	2.09–3.81	2.99	2.98–3.68	3.16
FeO	3.59–4.99	4.23	2.14–3.07	2.50
MnO	0.12–0.15	0.13	0.09–0.12	0.11
MgO	4.44–5.85	5.08	3.54–4.68	4.14
CaO	7.84–8.49	8.18	6.51–7.80	6.87
K_2O	1.21–1.43	1.34	1.62–2.34	2.04
Na_2O	3.46–4.10	3.61	3.85–4.22	3.97
P_2O_5	0.23–0.29	0.26	0.20–0.24	0.22
Nippm	75–105	94.16	31–52	41.0
Co	15–30	21.5	6–14	8.8
Cr	170–250	206.66	42–125	79.8
V	200–300	241.66	66–160	100.6
Sc	18–26	21.83	8–14	10.7
Zr	100–180	140.8	73–140	104.6
Th	5.3–6.3	5.7	8–9	8.5
Hf	2.3–4.5	3.66	3.0–5.5	4.25
Y	23–27	25.6	<10–18	16.5
Yb	1.7–4.9	2.40	<1–1.6	1.23
Ba	340–750	521.66	530–680	620.0
Sr	630–>1000	765	550–>1000	770.0
Pb	5.5–12	9.25	4–17	12.0
Cu	28–66	39.33	12–32	22.60
Zn	50–87	60.16	40–55	48.80
Ga	17–32	27.00	14–26	18.00
Sn	<2–5	–	<2–3.5	–

There results that all these rocks are richer in Na_2O than in K_2O, having close characteristics to the alkali basalts (Cullers, Graf, 1984) and to the normal basalts, respectively. As in the Sârbi alkaline rocks Na_2O – 2.0 is lower or higher than K_2O, according to IUGS classification, they correspond to shoshonites or mugearites and to latites.

Due to the differences occurring between the last chemical elements, on the combined diagram in Figure 5 (Irvine, Baragar, 1971 and Hutchinson, 1982) the two rock groups are situated in two different fields: the basalt-andesites plot in the calc-alkaline (CA) domain and the Măgura Sârbi trachybasalt-andesitic rocks plot in the alkaline (Alk) domain. The very restricted fields in which the rocks of the two volcanic series plot, show a close composition in each occurrence, pointing to the absence of any important magma differentiation or contamination processes.

On the same diagram there were plotted the 17 chemical analyses presented by Kräutner (1969) for the Poiana Ruscă Mts basanites and the Mureş Couloir volcanics, the plots of which are very dispersed. However, it is obvious that the basanites plot in the tholeiitic (TH) domain, the basalt-andesitic rocks fall in the calc-alkaline (CA) domain and some alkali basalts and the Măgura Sârbi rocks are situated in the alkaline (Alk) domain, and even in the calc-alkaline domain. Two rocks of the last groups plot just in the field of the Măgura Sârbi alkaline rocks.

It is noteworthy that the MnO and P_2O_5 average contents of the Brănişca basalt-andesites and the Măgura Sârbi alkaline rocks have very close values, they also showing a rapid evolution of the volcanic structures so that their magmas had not time to differentiate. On the diagram in Figure 6 (Mullen, 1983; Hall, 1989), excepting one sample, the rocks of the two volcanic occurrences are gathered in a single restricted field, situated between the field of the arc basalts and that of the ocean island basalts (ocean intra-plate basalts). This position underlines their characteristic of "transitional rocks" between the arc and the intraplate volcanics (Savu et al., 1994a).

The trace elements (Tabs. 1, 2) from the two volcanic occurrences show variable contents, but in most cases they are higher in the basalt-andesites than in the alkaline rocks. Such an aspect is obvious in case of Ni, Co, Cr, and Sc.

Similar relationships exist between Zr and Y, as shown in Figure 7 (Pearce, Norry, 1979). On this diagram the basalt-andesites plot in the intra-plate field and the alkaline rocks out of this field, but near it, at higher values of the Zr/Y ratio in comparison with the arc and ocean floor rocks.

In the two rock groups there are normal and constant contents of Cu, Zn and Ga, the values of which representing a characteristic of the magmas formed in the mantle. The very low contents of Sn ($< 2 - 5$ ppm) show that the magmas in the two volcanic occurrences were not contaminated by materials from the sialic crust. The Pb contents are also low. The Th and Hf contents are higher in the alkaline rocks than in the basalt-andesites.

Very high contents of Ba and Sr are present in the rocks of the two volcanic occurrences. The Ba average value is 522 ppm in basalt-andesites and 620 ppm in the alkaline rocks. According to Gill (1981) such high contents of Ba are characteristic of the rocks situated within the plates. The very high contents of Sr in the two rock groups suggest, according to Hart et al. (1971), that their parental magmas were formed at a great depth in the mantle. These very high contents of Sr could indicate, according to Cullers and Graf (1984), magmas similar to the shoshonitic one, but the rocks of the two volcanic occurrences are partly different from the shoshonites by their relationships concerning the K_2O and Na_2O.

The REE contents in the two rock groups are, excepting Yb, higher in the alkaline rocks than in basalt-andesites (Tab. 3). Therefore, the REE sum (average values) is of 81.41 ppm in basalt-andesites and of 92.86 ppm in the alkaline rocks. Their average values of the LREE/HREE ratio are also different, these being 17.19 in basalt-andesites and of 29.34 in alkaline rocks. A difference high enough also occurs between the two rock groups in case of (La/Yb)N ratio, the values of which being 7.03 in basalt-andesites and 12.35 in the alkaline rocks. The values of Eu/Sm ratio in the two volcanic occurrences are also different, they being of 0.36 in basalt-andesites and of 0.26 in the alkaline rocks.

The high values of the (Ce/Yb)N ratio and of (Ce)N (Tab. 3) show (see Saunders, 1984) that the basalt-andesitic parental magma was formed by the partial melting of five per cent of a metasomatized garnet peridotite in the mantle and that of alkaline rocks by the partial melting of such a peridotite in a very limited rate.

The chondrite normalized (Boynton, 1984) REE patterns of the two rock groups (Fig. 8) are parallel between La and Tb, but they are different within their terminal zone, for the Yb contents are lower in the alkaline rocks than in basalt-andesites. In both rock groups a very

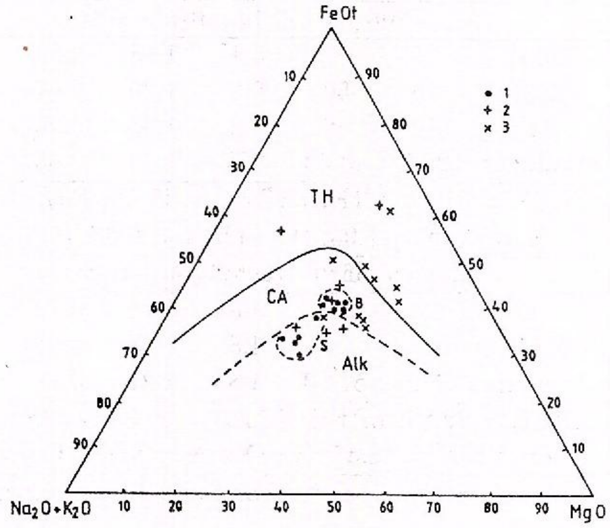

Fig. 5 – Plot of the volcanic rocks on the FeO_{tot} – MgO – Na_2O+K_2O diagram. B, the field of the Brănişca Hill basalt-andesites; S, the field of the Măgura Sârbi alkaline rocks; 1, Brănişca Hill basalt-andesites and Măgura Sârbi alkaline rocks (acc. to the present paper); 2, calc-alkaline rocks (Kräutner, 1969); 3, basanites and alkali basalts (Kräutner, 1969). TH, tholeiitic; CA, calc-alkaline; Alk, alkaline.

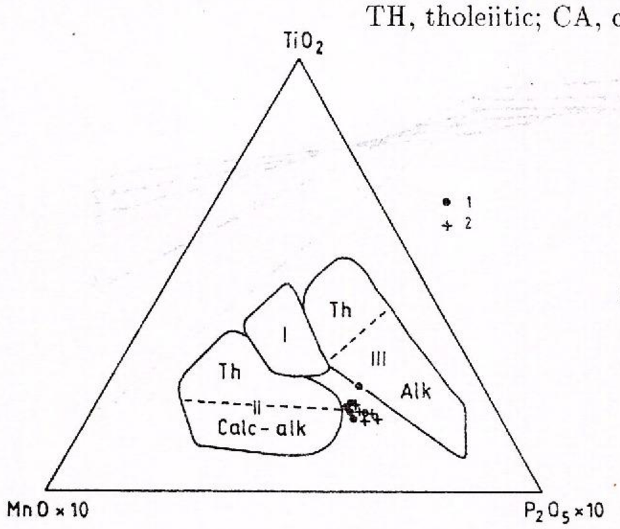

Fig. 6 – Volcanic rock position on the TiO_2 – P_2O_5 x 10 – MnO x 10 diagram. 1, Brănişca Hill basalt-andesites; 2, Măgura Sârbi alkaline rocks. I, ocean ridge basalts; II, volcanic arc basalts; III, ocean island basalts.

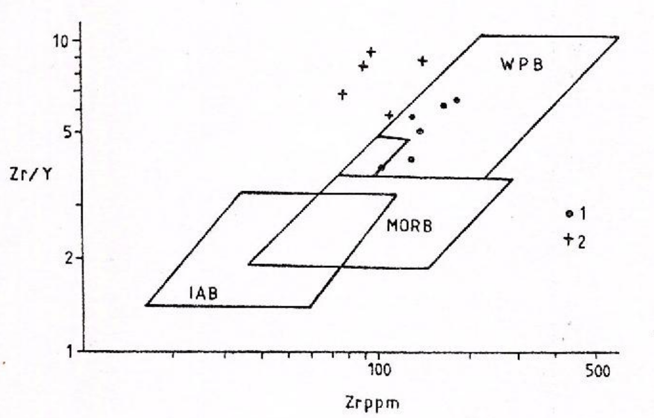

Fig. 7 – Plot of the volcanic rocks on the Zr/Y – Zr diagram. 1, Brănişca Hill basalt-andesites; 2, Măgura Sârbi alkaline rocks; WPB, intra-plate basalts; MORB, mid-ocean ridge basalts; IAB, island arc basalts.

Table 3
Distribution of REE in the volcanic rocks

Sample	La	Ce	Sm	Eu	Tb	Yb
Brănişca Hill basalt-andesites						
L(1)+	21	52	5.1	1.18	0.63	2.2
2(2)	20	50	5.0	1.26	0.67	1.7
3(4)	19	46	4.2	1.08	0.66	1.9
Averages	20.0	49.33	4.77	1.73	0.65	1.93
ΣREE = 81.41; LREE/HREE = 17.19; Eu/Sm = 0.36; (La/Yb)N = 7.03; (Ce/Yb)N = 6.63; (Ce) = 61						
Măgura Sârbi trachybasalt-andesites						
4(8)	26	57	4.8	1.16	0.73	1
5(11)	29	58	4.8	1.38	0.85	1.1
Averages	27.5	57.50	4.8	1.27	0.79	1.05
ΣREE = 92.86; LREE/HREE = 29.34; Eu/Sm = 0.26; (La/Yb)N = 12.35; (Ce/Yb)N = 8.90; (Ce) = 60.5						

+ In brackets there are the corresponding numbers in Table 1.

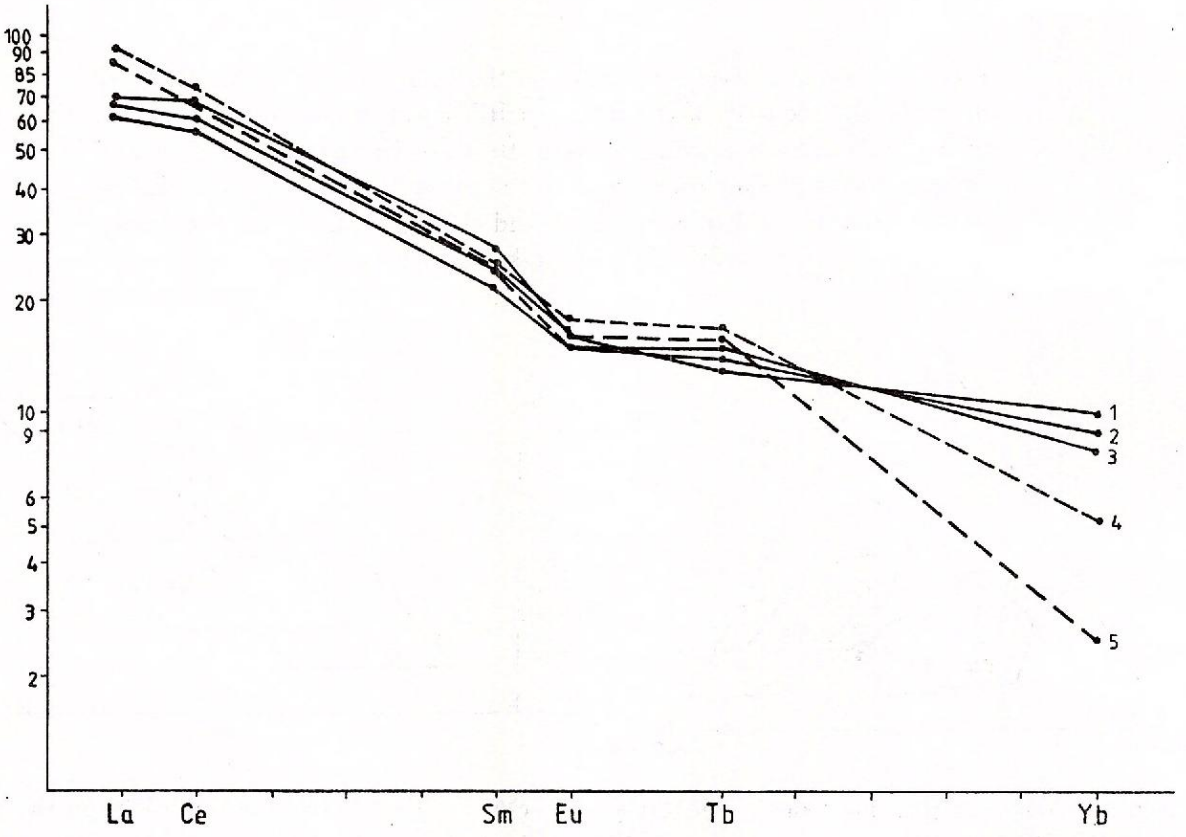

Fig. 8 – Chondrite normalized patterns of the volcanic rocks. 1–3, Brănişca Hill basalt-andesites; 4–5, Măgura Sârbi alkaline rocks.

stressed slope of the patterns is obvious, suggesting a mantle depletion in HREE during the previous partial meltings necessary to the formation of Laramian magmas (70 – 60 Ma), and that these elements have been drawn out in a very limited amount by the melting in the Paleogene tectonic setting. Moreover, a small Eu negative anomaly is the characteristic of both rock groups, showing a very weak differentiation of the magmas by fractional crystallization of plagioclase (Philpotts, Schnetzler, 1968). The paterns of the two rock groups are very close in shape to those of the Lucareţ alkali basalts (Savu et al., 1994b) and to the patterns of Detunata basalt-andesites (Savu et al., 1993), as well as to those of the Etiopia, Taos and Rio Grande basalts formed in continental rift zones (Wilson, 1989).

Conclusions

The Brănişca Hill basalt-andesites and the Măgura Sârbi alkaline rocks were formed in a geological period without any important tectonic events, excepting some crustal fractures which favoured the volcanic activity. This period settled in the Paleogene, after the Laramian movements ceased (Rădulescu, Săndulescu, 1980), so that the volcanics are contemporaneous with the basaltic rocks from the British Islands.

If the basalt-andesites and the alkaline rocks from the Mureş Couloir were represented by successive lava flows or by pyroclastic beds, the first idea concerning their genesis would be that they are the result of basaltic magma differentiation. As they form independent volcanic structures with a rapid evolution and without any obvious differentiation and contamination processes, there results that their parental magmas could have been primary magmas (Foland, Loiselle, 1981; Savu et al., 1994, a,b, 1993).

Therefore, one may say that those magmas were formed at a great depth in the mantle by the partial melting of the metasomatized peridotite substratum (Foley et al., 1987; Menzies, 1987). Their calc-alkaline and alkaline characteristics were determined by the melting rate in a small or very small amount.

The ambiguous characteristics regarding the tectonic setting – they being transitional rocks between arc and intra-plate volcanics – resulted by the partial melting of the metasomatized and contaminated substratum under the distension conditions of the Paleogene period.

References

Andrei, J., Calotă, G., Scurtu, F. (1975) Considérations structurales sur le sillon ophiolitique des Monts Métallifères à l'aide des données géophysiques et des certains éléments quantitatifs obtenus au modélage. *Rev. roum. géol., géophys., géogr. (Géophys.)*, 19, p. 101–111, Bucureşti.

Bass, M. J., Maitre, R. W., Streckeisen, A., Zanettin, B. (1986) A chemical classification of volcanic rocks based on the total alkali - silica diagram. *Jour. Petrol.*, 27, 3, p. 745–750, Oxford.

Boynton, W. V. (1984) Cosmochemistry of the rare earth elements: meteorite stadies. In: P. Henderson (edit.) Rare Earth Element Geochemistry, Elsevier, p. 63–114, Amsterdam.

Cullers, R. L., Graf, J.L. (1984) Rare earth elements in igneous rocks of the continental crust: predominantly basic and ultrabasic rocks. In: P. Henderson (edit.) Rare Earth Element Geochemistry, Elsevier, p. 237–274, Amsterdam.

Ewart, A. (1982) The mineralogy and petrology of Tertiary–Recent orogenic volcanic rocks: with special reference to the andesitic-basaltic compositional range. In: R.S. Thorpe, J. Wiley (edits.). Andesites, p. 25–27, Chichester.

Foland, K. A., Loiselle, M.C. (1981) Oliverian syenites of the Pliny region, northern New Hampshire. *Bul. Geol. Soc. Am.*, 92, p. 179–188, Washington.

Foley, S. F., Venturelli, G., Green, D. H., Toscani, L. (1987) The ultrapotasic rocks. *Contrib. Mineral. Petrol.*, 94, p. 183–192, Berlin.

Gheorghiu, C. (1954) Studiul geologic al văii Mureşului între Dobra şi Deva. *An. Com. Geol.*, XXVII, p. 77–174, Bucureşti.

Ghiţulescu, T. P., Socolescu, M. (1941) Étude géologique et minière des Monts Métallifères. *An. Inst. Geol. Rom.*, XXI, p. 181–284, Bucureşti.

Gill, J. (1981) Orogenic Andesites and Plate Tectonics. 390 p., Berlin.

Hall, A. (1989) Igneous Petrology. 573 p., Singapore.

Hart, S. R., Brooks, C., Krogh, T. E., Davis, G. L., Nava, D. (1971) Ancient and modern volcanic rocks: a trace element model. *Earth Planet. Sci. Lett.*, 10, p. 17–28, Amsterdam.

Hatch, F. H., Wells, A. K., Wells, M. K. (1961) Petrology of the Igneous Rocks (12^{th} edit.). 515 p., London.

Hauer, Fr., Stache, G. (1863) Geologie Siebenbürgens. Wiena.

Hutchinson, C. S. (1982) Indonesia. In: R. S. Thorpe, J. Wiley (edits.) Andesites, p. 207–224, Chichester.

Irvine, T. N., Baragar, W. R. A. (1971) A guide to the chemical classification of the common volcanic rocks. *Can. J. Earth Sci.*, 8, p. 523–548, Ottawa.

Kräutner, F. (1969) Les basaltes alcalins et les andésites basaltiques des monts de Poiana Ruscă. *Rev. roum. géol., géophys., géogr. (Géol.)*, 13, p. 47–68, Bucureşti.

Lupu, M., Peltz, S., Boştinescu, S., Kräutner, H. G., Horvath, A., Mureşan, M., Mureşan, G., Bandrabur, T., Popescu, G., Nicolae, I. (1986) Harta geologică sc. 1:50 000, sheet Gurasada. Inst. Geol. Geofiz., Bucureşti.

Menzies, M. (1987) Alkaline rocks and their inclusions: a window on the Earth interior. In: J. G. Tilton, B. G. J. Upton (edits.) Alkaline igneous rocks. Geol. Soc. Sp. 30, p. 15–27, London.

Mullen, E. D. (1983) $MnO–TiO_2–P_2O_5$: a minor element discrimination for basaltic rocks of oceanic environments and its implications for petrogenesis. *Earth Planet. Sci. Lett.*, 62, p. 53–62, Amsterdam.

Pearce, J. A. (1980) Geochemical evidence for the genesis and eruptive setting of lavas from Tethyan ophiolites. In: A Panayiotou (edit.) Ophiolites, Proc. Intern. Ophiol. Symp. Nicosia, Cyprus, 1979, p. 261–272, Nicosia.

Peltz, S., Vasiliu, C., Bratosin, I. (1971) Petrologia rocilor bazaltice plio-cuaternare din România. *An. Inst. Geol.*, XXXIX, p. 111–176, Bucureşti.

Philpotts, J. A., Schnetzler, C. C. (1968) Europium anomalies and the genesis of basalts. *Chem. Geol.*, 3, p. 5–13, Amsterdam.

Rădulescu, D., Săndulescu, M. (1980) Corélation des phases de deformation, de métamorphism et de magmatisme dans les Carpathes. Géologie des chaines alpines issues de la Tethys. 2b, Congr. Géol. Int. Mém. BRGM 115, p. 300–302, Paris.

– **, Borcoş M., Peltz, S., Istrate, G. (1981)** Subduction magmatism in Romanian Carpathians. *Guide Excursion A2, Carpath. - Balk. Geol. Assoc. XII Congr. Bucharest*, 132 p., Bucureşti.

Saunders, A. D. (1984) The rare earth element characteristics of igneous rocks from the ocean basins. In: P. Henderson (edit.)

Rare Earth Element Geochemistry, p. 205–236, Amsterdam.

Savu, H., Udrescu, C., Neacşu, V., Stoian, M. (1993) The Quaternary basalt-andesitic rocks of Detunata (Apuseni Mountains) and their origin. *Rev. Roum. Géologie*, 37, p. 9–20, Bucureşti.

– **, Tiepac, I., Grabari, G. (1994a)** A comparative study of the distribution of some major, trace and radioactive elements in Paleogene and Upper Pliocene–Quaternary basalts and basalt-andesites from Romania. *Rom. J. Petrology*, 76, p. 91–100, Bucureşti.

– **, Udrescu, C., Neacşu, V., Stoian, M., Tiepac, I. (1994b)** Petrology, geochemistry and origin of Pleistocene intraplate basalts of Lucareţ (Banat). *Rom. J. Petrology*, 76, p. 109–118, Bucureşti.

Wilson, M. (1989) Igneous Petrogenesis. 465 p., London.

Received: July 5, 1993
Accepted: August 12, 1993

Plate

Fig. 1 – Texture of the basalt-andesite from the Brănişca (Bretea) Hill, consisting of a groundmass formed of plagioclase and rarely Ti–augite microphenocrysts. II Nicols, x 30.

Fig. 2 – An olivine microphenocryst from the Brănişca basalt-andesite substituted by bowlungite. II Nicols, x 120.

Fig. 3 – Trachytic texture of the trachybasalt-andesite from the Măgura Sârbi (Sârbi Hill) consisting of alkali feldspar laths, augite microcrystals and secondary iron oxides (black). II Nicols, x 190.

Fig. 4 – Augite microphenocrysts in the trachybasalt-andesite (shoshonite) from the Măgura Sârbi. II Nicols, x 150.

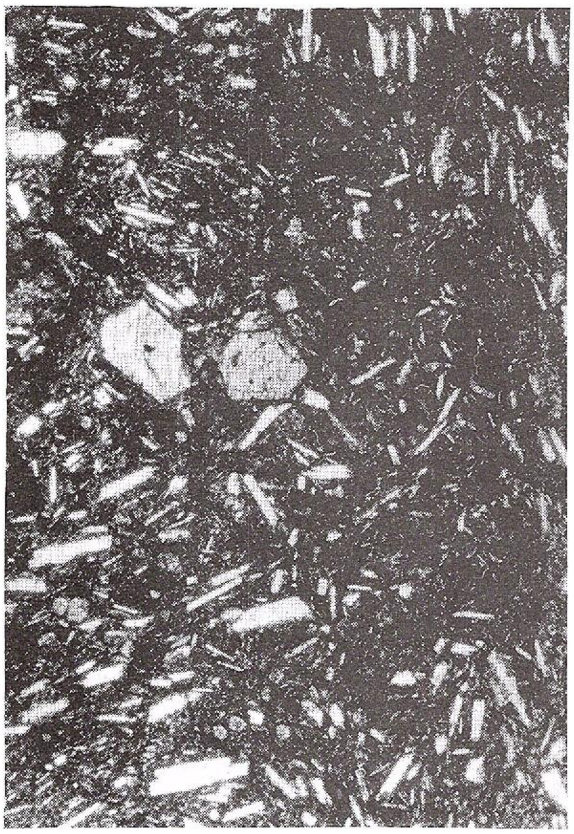

1

2

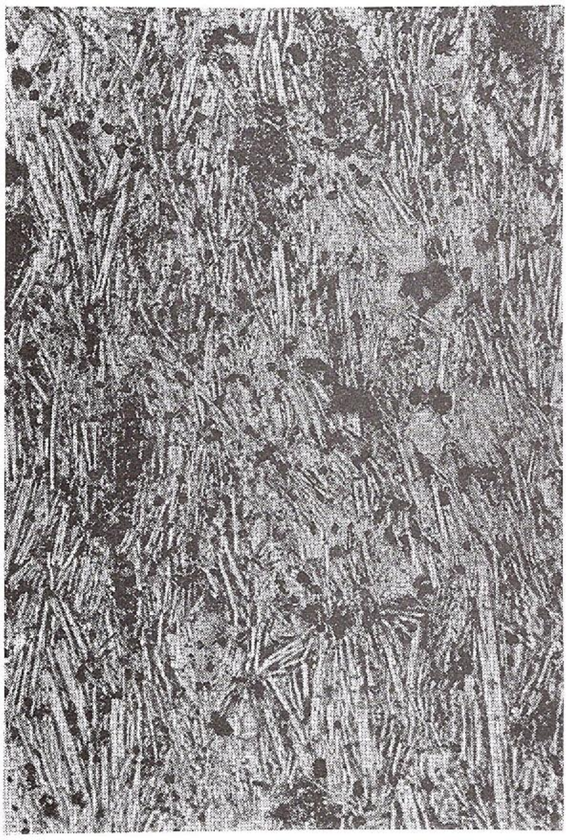

3

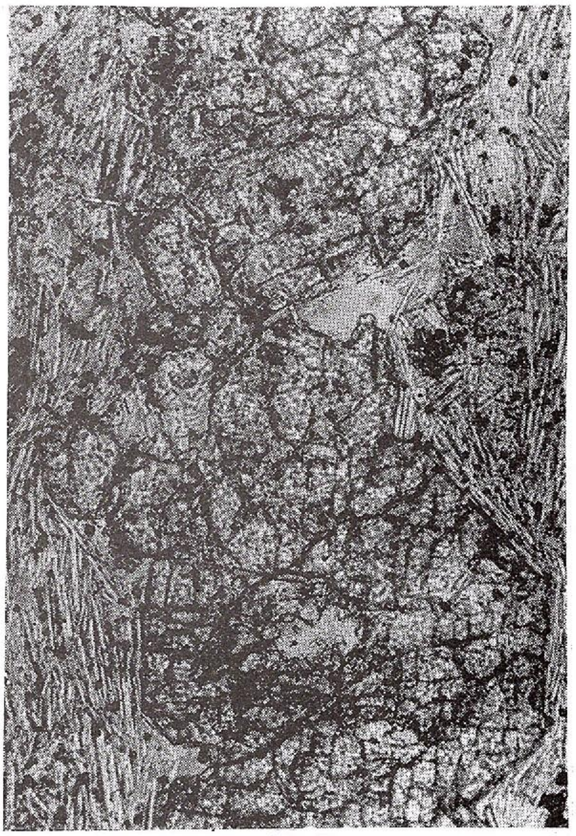

4

Rom. J. Petrology, 77, p. 97–106, Bucureşti, 1996

ON THE HIGH Ba AND Sr DEVA ANDESITES FROM THE MUREŞ COULOIR

Sergiu BOŞTINESCU, Haralambie SAVU

Institutul Geologic al României. Str. Caransebeş 1, 79 678 Bucureşti 32

Key words: Andesitic rocks. Transcrustal fractures. Continental arc. Major elements. Trace elements. Ba and Sr distribution. Origin.

Abstract: The Deva andesites form many subvolcanic bodies west of Deva Town, represented by normal necks, swollen necks and domes, that are situated along three E–W lineaments. These bodies were emplaced through a system of transcrustal fractures under the compressional conditions of the Neogene continental volcanic arc from the Apuseni Mountains. They consist of hornblende andesites and hornblende biotite andesites bearing large plagioclase phenocrysts. In the depth the andesites pass into a porphyritic microdiorite. The rocks are very rich in Ba (2100–3300 ppm) and Sr (>1000 ppm) similarly or closely to the volcanics erupted in the continental rifts. The parental magma was a dioritic calc-alkaline one, formed in the metasomatized mantle. During the magma fractional crystallization plagioclase and biotite crystal concentrations occurred. The enrichment of magma in Ba and Sr was determined firstly by the partial melting under the special tectonic conditions of the Mureş Couloir and then by the fractional crystallization of the large plagioclase phenocrysts.

Introduction

The Deva andesites occur west of Deva Town, where they form many subvolcanic bodies that determined a characteristic landscape, within which a few summits are to be observed, correspondig to some of these bodies (Pl. I).

The first observations on these rocks belong to Halaváts (1903) and Gheorghiu (1960). In 1963 Gheorghiu and Mareş presented more detailed data on these andesites. Petrulian et al. (1965) elaborated a complex study on the porphyry copper mineralization from the Pârâul Băilor, suggesting a banatitic origin. Many papers (Rădulescu, Borcoş, 1967; Giuşcă et al., 1968; Ianovici et al., 1969; Cioflica et al., 1973) correlated the intrusion of these andesites with the Neogene volcanism in the Apuseni Mountains. Ciocănelea (1973) worked out a detailed structural study of the andesitic bodies. Other unpublished reports include data particularly concerning the mineralization linked to the andesites, but also more thorough studies. So, Boştinescu et al. (1973; 1983, unpubl. rep.) made complex investigations on the petrography and the geochemistry of the Deva andesites and especially on their mineralizations.

The Andesitic Bodies Structure and the Rocks Age

The basement intruded by the andesites consists of Paleozoic crystalline schists, Upper Cretaceous sedimentary rocks (Deva Beds) and Badenian-Sarmatian sedimentary deposits and tuffs (Lupu et al., 1982).

The form of the andesitic bodies is that of normal neck (vertical column), swollen neck and dome. As the region was strongly eroded, it is very difficult now to establish if any of these bodies reached the Earth's surface. They are located within a well individualized area on the southern margin of the Mureş Couloir (Pl. I), that subsided as an incipient graben (Savu, 1995), starting since Paleogene (Savu et al., 1994a). Within this area the bodies of Piatra Coziei, Steanu Hill, Serhediu Hill and Dealul Cetăţii form a northern lineament of subvolcanic structures. A median lineament is marked by the bodies of the Poliatca Hill, Nocet Hill and by those of smaller size from the Pârâul Băilor. On a southern lineament the bodies of Colţata, Măgura Hill and Bejan Hill are situated. These E–W lineaments are parallel to the transcrustal fractures of the Mureş Couloir. Two systems of compressional diagonal faults have also influenced the intrusion of these bodies. On the other hand, this disposition of the andesitic bodies outlines a concentric configuration of the Neogene subvolcanic structure of Deva, that could be individualized in the depth in a main dioritic pluton.

The subvolcanic character of the andesitic bodies is pointed out by the rock structure and texture, and by their relationships with the country rocks. Usually, the andesitic bodies contacts are vertical or steeply dipping. Therefore, the country rocks were intensely disturbed by the intrusions. In the igneous rocks numerous xenoliths of these formations were included, and the presence of polygenous breccias on the andesitic bodies contact represent a peculiarity of this area. Such situations are characteristic in the Dealul Cetăţii and Serhediu Hill, as well as in some galleries.

The mineralized Pârâul Băilor body is very well known due to the mining workings through its swelling zone, and to a bore hole. At the surface, this andesitic body exhibits an almost circular section, with an obvious concentric structure, consisting of: an intrusive breccia on the contact, followed to the interior by an aphanitic zone, then by a large zone of fissured andesite in which the porphyry copper mineralization was located (Cioflica et al., 1973; Boştinescu, 1984), and by an andesitic rock close to a porphyritic microdiorite in the central part, that seems to have been intruded later. Starting at the -310 m level the borehole went through the neck down to the depth of -1200 m below the sea level. Troughout this depth the subvolcanic andesite gradually passes into a porphyritic microdiorite (Pl. II, Figs. 1 and 2).

The upper part of some andesitic bodies was crossed by intrusive tuff veins (Pl. II, Fig. 3).

As the intrusion of the andesitic bodies affected the Neogene[1] sedimentary deposits, there results that they are contemporaneous with the Neogene volcanics from the Apuseni Mountains. This conclusion is supported by the following K/Ar datings (E. Vâjdea, oral com.): Serhediu andesite 15.2 $\pm$ 1.5 My; Dealul Cetăţii andesite 9.1 $\pm$ 0.9 My. These values assign the Deva andesites to the second eruption cycle of the Neogene volcanism from the Apuseni Mountains (Rădulescu, Borcoş, 1967).

Petrography

The Deva bodies are mainly constituted of andesites (Tab. 1, Fig. 1); three rocks exhibit a weak alkaline tendency and other three plot in the basalt-andesitic field. Their general characteristics are the large plagioclase phenocrysts, that are more frequent in some small

[1]The Neogene age of these deposits was determined by Iosefina Stancu and Gh. Popescu analysing the microfauna associations.

parts of the bodies, and the presence of quartz in norm. The latter varies from 1.60 % to more than 5 % and forms very fine grains in the groundmass. Therefore, some rocks may be considered as quartz andesites. But, according to the frequency of the melanocrate minerals, these rocks must be classified as hornblende andesites and hornblende biotite andesites.

Hornblende andesites particularly occur in the Poliatca and Serhediu hills. They are grey porphyritic rocks, in which the plagioclase (0.5 – 2 cm) and hornblende phenocrysts are embedded in a microcrystalline groundmass. Their structure is massive, seldom oriented. The plagioclase (An 35–50) phenocrysts show a normal zoning and polysynthetical twinning. They were affected by secondary processes, mostly in the core. The green hornblende ($c \wedge Ng = 22^0$) phenocrysts exhibit a rim zoning and are partly substituted by iron oxides. The Serhediu andesite differs from other hornblende andesites by its more dark groundmass and by the large plagioclase phenocrysts reaching 4 cm in length (Pl. II, Fig. 4). The greenish-brown hornblende phenocrysts were rarely substituted by chlorite and iron oxides. Sometimes, autoliths were observed in these rocks.

Hornblende biotite andesites occur in the Dealul Cetăţii, Nocet and Pârâul Băilor bodies and in the Măgura Hill. By their structural characteristics these andesites are close to the above described rocks, from which they differ by the melanocratic minerals. The Măgura andesites show a reddish-grey colour, determined by a hematite dust. The plagioclase (An 20–40) phenocrysts, exhibiting a polysynthetical twinning and a characteristic zoning, are more basic in the core, often affected by alteration. The green hornblende was also affected by the autometamorphic phenomena. On the contrary, the biotite lamelae are fresh, seldom bent and substituted by chlorite. A secondary biotite was formed by reaction on the amphibole margins. On the fissures from the Dealul Cetăţii neck, crystals of calcite and barite have been observed. In some bodies the amphibole is represented by a brown hornblende ($c \wedge Ng = 4^0$) that was partly corroded by magma or completely substituted by iron oxides.

The porphyritic microdiorite from the depth of -554 m consists of a microcrystalline groundmass, in which plagioclase, green hornblende and biotite phenocrysts are embedded. At the depth of -1200 m the grondmass shows a medium granulation (Pl. II, Fig. 2). The plagioclase (An 50) phenocrysts are polysynthetically twinned and display a normal zoning in which some zones and particularly the core were affected by weak autometamorphic processes. Hornblende and biotite were partly substituted by chlorite.

The brecciated rocks are represented by polygenous breccias formed of andesite and country rock blocks and breccias without any andesitic element.

Ba and Sr Distribution and Other Geochemical Aspects

The chemical composition (Tab. 1) of andesites[2] shows that due to the autometamorphism – which although not too strong was almost general – many rocks contain a little higher CO_2 and H_2O. SiO_2 increases from 51.72 % in hornblende andesites up to 59.47 % in hornblende biotite andesites. The lower value correlates with the higher contents of CaO (9.04–9.59 %), suggesting that the more basic rocks resulted from the local accumulations of plagioclase crystals. These rocks have also a higher MnO content.

The K_2O is normal for most Deva andesites. In those with alkaline tendency (Fig. 1) it exceeds 2 %. In some rocks of the last category higher iron contents have been determined, too, showing that the K_2O is present in biotite, that is more concentrated in some parts of the bodies.

[2]The major elements have been determined by the classical method.

Table 1

Chemical composition of the andesitic rocks

	Hornblende andesites					Hornblende ± biotite andesites										Hornblende biotite andesites		
No	1	2	3	4	5	6	7	8	9	10	11	12	13	14	15	16	17	18
SiO_2 %	51.72	53.56	53.63	56.36	56.47	56.78	57.89	59.31	58.09	58.27	58.46	57.60	58.86	56.52	56.43	59.13	57.99	59.47
Al_2O_3	17.63	18.28	18.98	19.41	18.69	18.58	18.98	19.39	19.02	19.85	19.62	19.76	18.70	18.41	19.47	19.13	18.13	19.20
Fe_2O_3	3.74	3.64	4.43	2.82	4.77	2.27	3.63	2.66	2.38	3.79	3.13	3.10	3.89	2.95	3.75	3.51	3.77	4.17
FeO	2.07	1.94	1.57	1.79	1.35	2.54	2.28	1.51	2.07	0.63	2.15	1.27	0.99	1.55	1.48	1.55	1.34	0.21
MnO	0.25	0.19	0.17	0.11	0.12	0.15	0.05	0.12	0.14	0.20	0.06	0.15	0.14	0.12	0.13	0.04	0.12	0.15
MgO	2.09	2.17	2.35	2.87	3.30	3.02	3.10	1.41	2.49	1.57	2.30	3.21	2.59	2.37	3.05	2.83	2.36	2.40
CaO	9.04	9.17	9.59	7.71	7.65	6.67	5.80	7.26	7.01	7.70	6.83	7.83	6.87	9.28	8.38	5.16	7.29	6.54
Na_2O	2.79	3.29	3.41	3.44	3.43	3.84	3.75	3.28	3.52	3.59	3.28	3.68	3.49	3.89	8.38	5.16	3.83	3.81
K_2O	1.94	1.79	1.53	1.64	1.61	2.09	1.03	1.89	2.03	1.60	1.53	1.62	1.84	2.03	1.53	1.35	2.14	1.61
TiO_2	0.52	0.54	0.52	0.44	0.54	0.48	0.47	0.39	0.48	0.42	0.45	0.47	0.51	0.48	0.52	0.50	0.46	0.42
P_2O_5	0.25	0.28	0.23	0.29	0.26	0.16	0.26	0.23	0.27	0.22	0.32	0.24	0.17	0.16	0.19	0.27	0.23	0.12
CO_2	4.56	2.99	1.65	1.39	0.14	1.61	0.48	1.38	0.77	0.88	0.50	0.58	0.35	0.89	0.74	0.79	1.32	0.67
S	0.05	0.03	0.05	0.00	0.03	0.09	0.21	0.00	0.00	0.01	0.04	0.00	0.00	0.00	0.00	0.03	0.00	0.00
Fe(S)	0.04	0.02	0.04	0.00	0.02	0.08	0.20	0.00	0.00	0.00	0.03	0.00	0.00	0.00	0.00	0.02	0.00	0.00
H_2O^+	2.68	1.50	0.99	1.60	1.08	1.17	1.76	1.04	1.17	0.72	1.12	0.66	0.97	0.80	0.34	1.01	0.86	0.41
Total	99.37	99.39	99.14	99.87	99.46	99.56	99.89	99.87	99.44	99.45	99.82	100.17	99.37	99.45	99.88	99.46	99.84	99.18
Ni ppm	11	10	9	8	13	8	11	8	10	7	8	4	6	6	7	4	5	5
Co	21	21	23	16	31	9	19	18	16	17	12	8	10	8	11	5	8	8
Cr	7	5	4	6	5	2	6	5	8	3	6	2	1	3	2	1	2	1
V	235	220	185	165	290	180	195	170	160	185	165	93	138	120	200	127	125	85
Sc	24	24	24	19	19	19	22	14	17	13	21	15	16	19	20	13	14	12
Pb	20	27	34	17	33	24	15	27	26	35	20	29	25	27	28	14	34	31
Cu	39	77	90	28	70	80	140	43	65	41	115	45	36	44	40	~500	23	34
Zn	55	52	60	46	52	43	44	55	53	68	52	45	38	33	46	26	30	40
Ga	13	17	20	17	16	17	20	20	18	20	19	20	21	16	17	21	20	16
Sr	>1000	>1000	>1000	>1000	>1000	>1000	>1000	>1000	>1000	>1000	>1000	>1000	>1000	>1000	>1000	>1000	>1000	>1000
Ba	2300	2500	3200	2400	3300	3200	750	2300	2500	3000	2300	2100	2200	2500	3100	1200	3300	3000

Location of samples: 1 – Poliatca Summit; 2,3,5,6,8,14 – Traian Gallery; 9 – Pârâul Băilor; 10 – Steanu Hill; 11 – Pârâul Băilor andesitic body, horizon 190 m; 7,16 – Pârâul Băilor andesitic body, horizon 240 m; 4 – Baia lui Roman; 12 – Pietroasa Quarry; 15 – Mişovăţ Quarry; 13 – Dealul Roşilor; 17 – Dealul Cetăţii; 18 – Măgura Hill. Analysts: E. Colios, V. Mândroiu.

Due to these higher K_2O contents, on the diagram in Figure 2 (Marriner, Millward, 1984) some rocks, representing 27 % of the total analyses, plot in the 'High K' field. But most rocks are situated in the 'Medium K' domain.

Other chemical components vary in ranges characteristic of the andesitic rocks (see Gill, 1981). According to the values of these components, on the diagram in Figure 3 the Deva andesites plot in the calc-alkaline field, excepting three rocks situated on the margin of the alkaline field.

Most trace elements (Tab. 1) determined by emission spectrography, show normal contents for the intermediate volcanic rocks (see Gill, 1981). Ni, Co, Cr, V and Sc decrease from hornblende andesites to hornblende biotite andesites, indicating a weak differentiation process.

The most characteristic trace elements of these andesites are Ba and Sr, the average contents of which are very high in comparison with other intermediate volcanic rocks of the calc-alkaline suite (see Gill, 1981). The Ba average contents varies from 2740 ppm to 2625 ppm (Tab. 1).

The Deva andesites, the Neogene andesites from the Apuseni Mountains bearing the highest Ba contents (representing 17 % of the analysed rocks from Ianovici et al., 1969; Borcoş et al., 1972), and the pre-Mureş Couloir banatitic volcanics ($K_2 - Pg_1$) from the Gurasada - Zam region (Savu et al., 1992), have been comparatively represented on the V - Ba diagram (Fig. 4). It shows that the Ba contents vary in the Deva andesites from 2100 ppm to 3300 ppm, values much higher than in the other two rock groups, formed out of the Mureş Couloir. Their Sr contents are also higher than in these two rock groups. On the other hand, Table 2 shows that, regardless of their age, composition and position in the Mureş Couloir, all the represented rocks have higher Ba and Sr contents than the correspondent rocks erupted under other structural conditions.

Other trace elements (Tab. 1) have average contents normal for the andesitic rocks, excepting Cu that is often higher. Ga and Cu increase from hornblende andesites to hornblende biotite andesites, whereas Zn decreases in this direction. On the contrary, Pb exhibits irregular average contents.

Table 2
Average contents of Ba and Sr in volcanic rocks from the Mureş Couloir

Period	Rocks and places	Ba(ppm)	Sr(ppm)	Sources
Quaternary	Quartz trachyandesites (quartz latites), Uroi	2190	>1000	Savu et al. (1994b)
Neogene	Hornblende andesites, Deva	2740	>1000	Present paper
	Hornblende ± biotite andesites, Deva	2395	>1000	
	Hornblende biotite andesites, Deva	2695	>1000	
Paleogene	Basalt–andesites, Brănişca	522	765	Savu et al. (1996)
	Trachybasalt–andesites (shoshonites) and trachyandesites (latites), Sârbi	620	770	

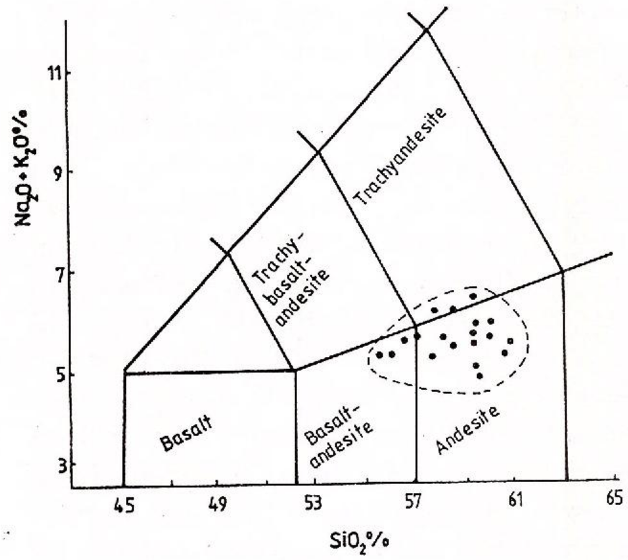

Fig. 1 – Plot of Deva andesites on the TAS diagram. Fields according to Bass et al. (1986).

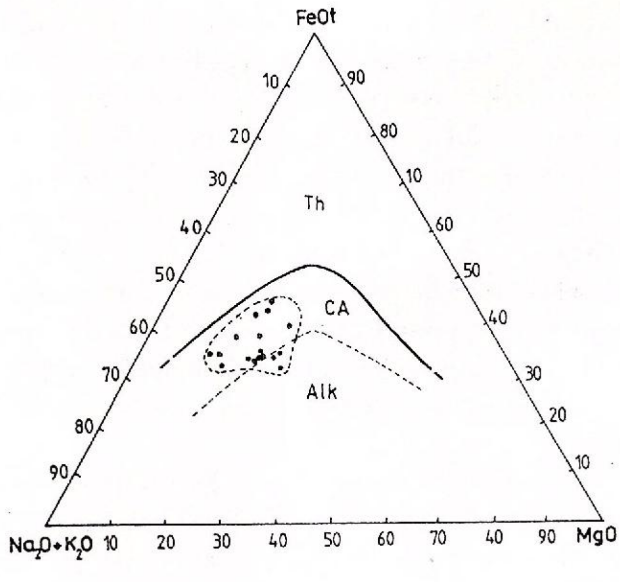

Fig. 3 – Plot of Deva andesites on the FeO_t – MgO – $Na_2O + K_2O$. Fields according to Irvine and Baragar (1971) and Hutchinson (1982): Th, tholeiitic; CA, calc-alkaline; Alk, alkaline.

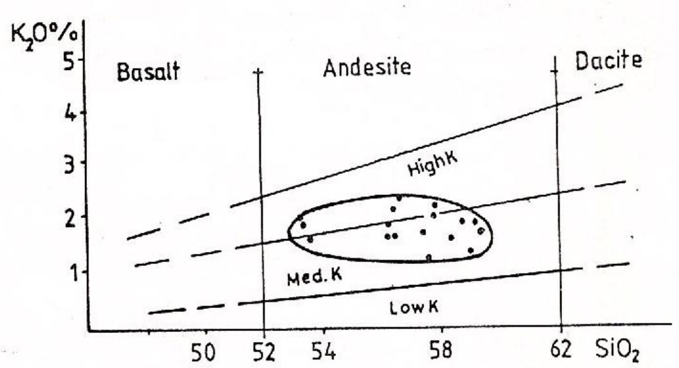

Fig. 2 – Plot of Deva andesites on the K_2O – SiO_2 diagram.

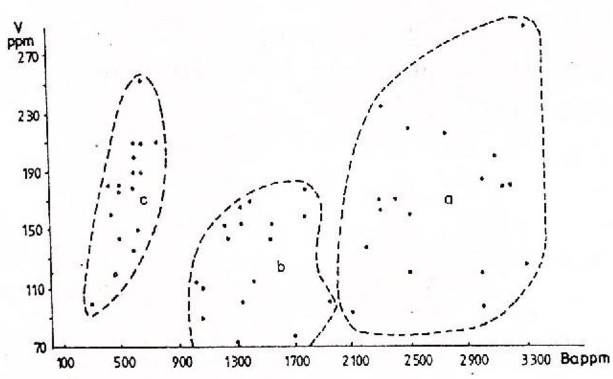

Fig. 4 – Plot of different volcanics from the Mureş Couloir and Apuseni Mountains on the V-Ba diagram: a, Deva andesites; b, Neogene volcanics rich in Ba from the Apuseni Mountains; c, banatitic volcanics.

Origin

As shown above, the Deva andesites intruded on E–W transcrustal fractures belonging to the South Transylvanian Fracture System, along which the Mureş Couloir subsided. They occurred at the southern extremity of the Neogene volcanic arc from the Apuseni Mountains. Their parental magma was formed under the compressional conditions of the East Carpathians ocean crust subduction, by partial melting of the metasomatized and contaminated mantle (see Roden and Murthy, 1985; Boyd and Bailey, 1975) and probably was contaminated with crustal materials. It was intruded on closed fractures. The tectonic condition under which this magma was formed and evolved, are uphold by the TiO_2 – P_2O_5 – MnO diagram (Fig. 5) on which most rocks plot within the calc-alkaline arc field.

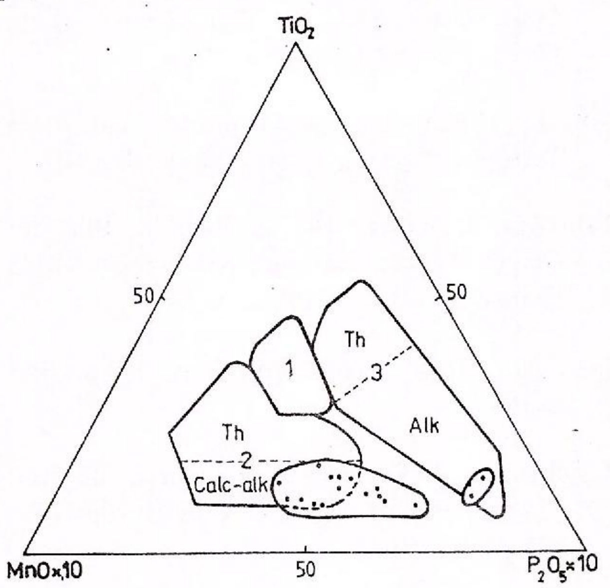

Fig. 5 – Plot of Deva andesites on the TiO_2 – P_2O_5 – MnO diagram. Fields according to Hall (1989) after Mullen (1985): 1, MORB, mid-ocean ridge basalts; 2, tholeiitic (Th) and calc-alkaline (Calc-alk) arc volcanics; 3, tholeiitic (Th) and alkaline (Alk) ocean island basalts.

This arc setting is also supported by the very presence of andesites, that are the most characterisitc rocks of the Andean volcanic arc, by the hornblende existence in them (see Anderson, 1980) and by the porphyry copper mineralization (see Mitchell and Garson, 1981). The low Ni, Co, Cr and Sc contents as well as the low Ti, proves also – according to Pearce (1975), Pearce and Cann (1973) and Shervais (1982) – the continental arc characteristics of the Deva andesites.

The parental magma was a dioritic calc-alkaline one, that evolved by fractional crystallization. During this process some local concentrations of large plagioclase phenocrysts and biotite lamelae occurred, determining little changes in the general chemical composition of this magma.

The high Ba and Sr contents in Deva andesites, as well as in other rocks erupted within the Mureş Couloir (Tab. 2), are similar or close to those determined in the volcanics occurring along the continental rifts (see Wilson, 1989; Savu et al., 1996). Therefore, it is obvious that the eruption of all these volcanics through the transcrustal fractures from the Mureş Couloir may explain their high contents in these two elements.

Under these special tectonic conditions the enrichment of the Deva andesites in Ba and Sr depended on two factors: 1. Previously, the parental magma was enriched in Ba and Sr during the partial melting, probably at a greater depth, like other magmas erupted within the Mureş Couloir (Tab. 2). 2. The very high Ba and Sr contents in the Deva andesites were determined during the fractional crystallization of this enriched magma, especially by the crystallization of the large plagioclase phenocrysts.

In the final stages the subvolcanic bodies were affected by a general autometamorphic process and a porphyry copper mineralization was formed.

Conclusions

The Deva subvolcanic bodies are located along three E–W lineaments. They consist of porphyritic andesites bearing large plagioclase phenocrysts, that were classified as hornblende andesites and hornblende biotite andesites. In the depth, andesites pass into a porphyritic microdiorite. In these rocks very high Ba (2100–3300 ppm) and Sr (> 1000 ppm) contents were determined, that are similar or close to those determined in other volcanic rocks from the Mureş Couloir and from the continental rifts. The K_2O content is normal for these rock types.

Their parental magma was a dioritic calc-alkaline one, formed by partial melting of the metasomatized upper mantle, under compressional conditions.

During the magma fractional crystallization some differentiation processes occurred, determined mostly by the plagioclase and biotite phenocrysts concentration in some small parts of the andesitic bodies.

The enrichement of magma in Ba and Sr was determined in the beginning by the partial melting and, then, by the fractional crystallization.

References

Anderson, A.T. (1980) Significance of hornblende in calc-alkaline andesites and basalts. *Amer. Mineral.*, 65, p. 837–851, Washington D.C.

Bass, M. J., Maitre, R.W., Streckeisen, A., Zanetin, B. (1986) A chemical classification of volcanic rocks based on the total alkali-silica diagram. *Journ. Petrol.*, 27, p. 745–750, Oxford.

Borcoş, M., Bratosin, I., Colios, E., Ianc, R. (1972) Observaţii petrogenetice şi geochimice asupra vulcanitelor neogene din ciclul II de erupţie din Munţii Metaliferi. *D.S. Inst. Geol.*, LVIII/I, p. 107–142, Bucureşti.

Boştinescu, S. (1984) Porphyry copper system in the South Apuseni Mountains – Romania. *An. Inst. Geol. Geofiz.*, LXIV, p. 163–174, Bucureşti.

Ciocănelea, R. (1973) Studiul geologic şi petrografic al zonei Deva. Teză de doctorat. Universitatea Bucureşti.

Cioflica, G., Savu, H., Borcoş, M., Ştefan, A., Istrate, Gh. (1973) Alpine volcanism and metallogenesis in the Apuseni Mountains. *Symp. Volc. Metal. Bucharest, 1973. Guidebook Exc. 3AB.*

Floyd, F.E., Bailey, D.K. (1975) Light element metasomatism of the continental mantle. The evidence and the consequence. *Phys. Chem. Earth*, 9, p. 389–418.

Gheorghiu, C. (1960) Studiul geologic al văii Mureşului între Deva şi Dobra. *An. Com. Geol.*, XXVIII, p. 101–147, Bucureşti.

– **, Mareş, I. (1963)** Erupţiile neogene din valea Mureşului (reg. Deva – Zam) şi particularităţile petrografice ale rocilor. *Com. Geol., Soc. Şt. Nat. Geogr.*, II, p. 47–72, Bucureşti.

Gill, J. (1981) Orogenic Andesites and Plate Tectonics. Spring. – Ver., 390 p., Berlin.

Halaváts, J. (1904) Der geologische Bau der Umgebung von Hátszég, Szászvaros, Vajda Huniad. Budapest, 1904.

Hall, A. (1989) Igneous Petrology. 573 p., Singapore.

Hutchinson, C.D. (1982) Indonesia. In R.S. Thorpe, J. Wiley (Edit.) Andesites, p. 207–224, Chichester.

Ianovici, V., Giuşcă, D., Ghiţulescu, T.P., Borcoş, M., Lupu, M., Bleahu, M., Savu, H. (1969) Evoluţia geologică a Munţilor Metaliferi. 745 p., Bucureşti.

Irvine, T.N., Baragar, W.R.A. (1971) A guide to the chemical classification of the common volcanic rocks. *Can. J. Earth Sci.*, 8, p. 523–548, Ottawa.

Lupu, M., Kräutner, H., Ţicleanu, N., Boştinescu, S., Bandrabur, T., Kräutner, Fl., Horvath, A., Nicolae, I. (1982) Harta geologică a României sc. 1:50000, foaia Deva, Inst. Geol. Bucureşti.

Marriner, G.T., Millward, D. (1984) The petrology and geochemistry of Cretaceous to Recent volcanism in Colombia: the magmatic history of an acretionary plate margin. *J. Geol. Soc. London*, 141, p. 473–486, Oxford.

Mitchell, A.H.G., Garson, M.S. (1981) Mineral deposits and global tectonic settings. 405 p., London.

Pearce, J.A. (1975) Basalt geochemistry used to investigate post tectonic environments on Cyprus. *Tectonophysics*, 25, p. 41–67, Amsterdam.

– **, Cann, J.R. (1973)** Tectonic setting of basic volcanic rocks determined using trace elements analyses. *Earth Planet. Sci. Lett.*, 19, p. 290–300, Amsterdam.

Petrulian, N., Steclaci, L., Sandu, D., Oroveanu, F. (1965) Studiul mineralogic, geochimic şi genetic al zăcământului cuprifer de la Deva. *St. cerc. geol., geofiz., geogr., (Geol.)*, 10/1, p. 79–105, Bucureşti.

Rădulescu, D., Borcoş, M. (1968) Vedere de ansamblu asupra desfăşurării vulcanismului neogen în România. *An. Com. Geol.*, XXXVI, p. 143–158, Bucureşti.

Roden, M.F., Murthy, V.R. (1985) Mantle metasomatism. *Ann. Rev. Earth Planet. Sci.*, 13, p. 269–296, Palo Alto, California.

Savu, H. (1995) An attempt to correlate the geological phenomena with the connected South Transylvanian System of Crustal Fractures. *Symp. on Petrometallogeny, 21–23 Aug., Cluj-Napoca, Abstract volume* (the full paper in press).

– **, Udrescu, C., Neacşu, V., Stoian, M. (1992)** Petrology, geochemistry and origin of the Laramian volcanics of the Mureş Couloir, between Zam and Gurasada. *Rom. J. Petrology*, 75, p. 117–130, Bucureşti.

– **, Tiepac, I., Grabari, G. (1994a)** A comparative study of the distribution of some major, trace and radioactive elements in Paleogene and Upper Pliocene – Quaternary basalts and basalt-andesites from Romania. *Rom. J. Petrology*, 76, p. 91–100, Bucureşti.

– **, Udrescu, C., Stoian, M., Călinescu, E. (1994b)** The Quaternary quartz trachyandesites of Uroi (Mureş Valley): petrology, geochemistry and origin. *Rev. Roum. Géol.*, 38, p. 9–23, Bucureşti.

– **, Udrescu, C., Neacşu, V., Stoian, M. (1996)** The Brănişca Hill calc-alkaline and the Măgura Sârbi alkaline Paleogene volcanic rocks (Mureş Couloir). *Rom. J. Petrol.*, 77, p. 83–96, Bucureşti.

Shervais, J.W. (1982) Ti-V plots and the petrogenesis of modern and ophiolitic lavas. *Earth Planet. Sci. Lett.*, 59, p. 101–118, Amsterdam.

Wilson, M. (1989) Igneous Petrogenesis. 465 p., London.

Received: June 28, 1995.
Accepted: June 5, 1996.

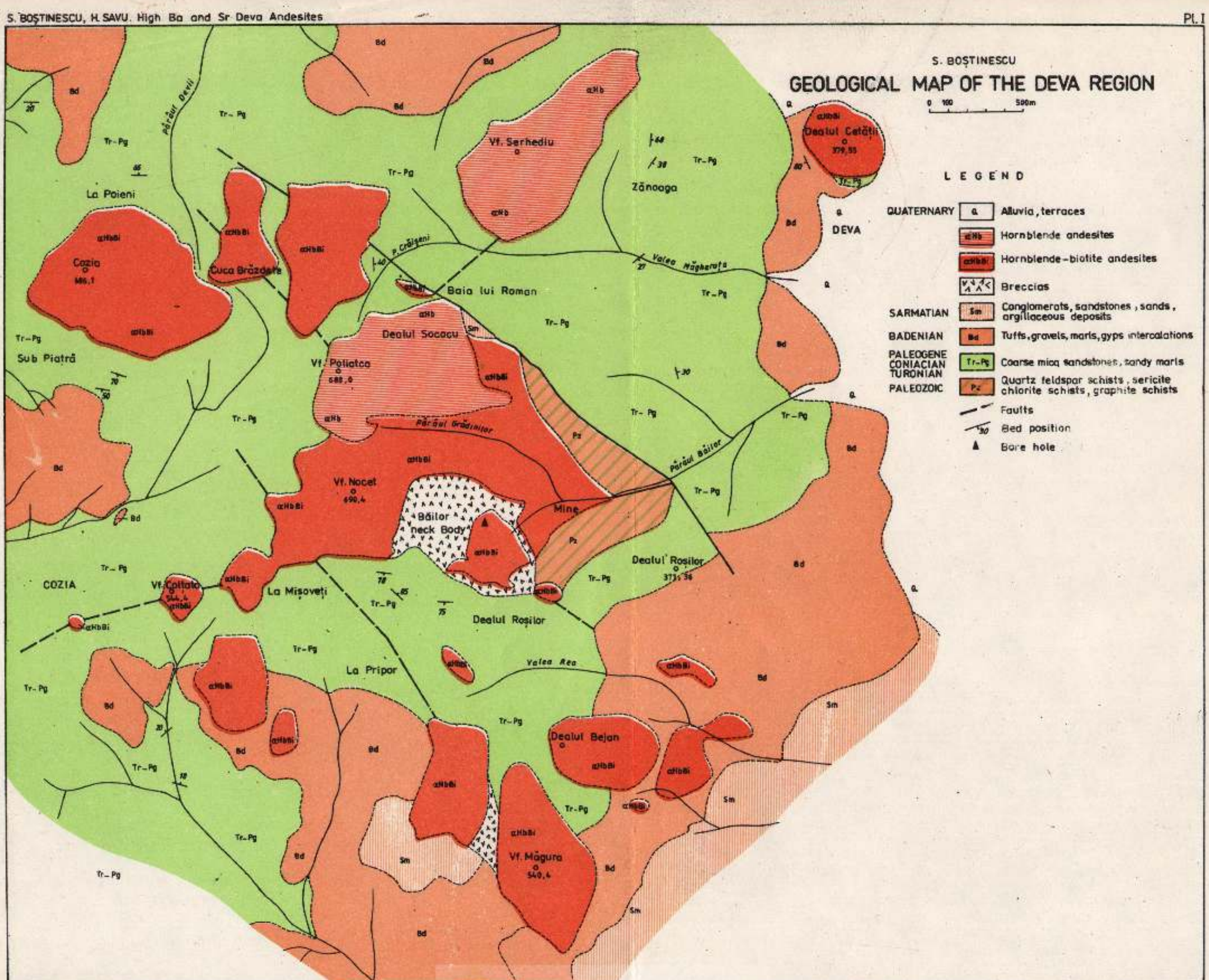

Printed by the Geological Institute of Romania

Plate II

Fig. 1 – Structure of the andesitic rock from the Pârâul Băilor neck at the altitude of +27 m; a, autolith.

Fig. 2 – Structure of the porphyritic microdiorite from the Pârâul Băilor bore hole at the depth of -1200 m.

Fig. 3 – Contact between a vein of intrusive tuff (the fine rock) and the andesite of the Pârâul Băilor body.

Fig. 4 – Structure of the Serhediu andesite bearing large-zoned crystals of plagioclase (white); a, autolith.

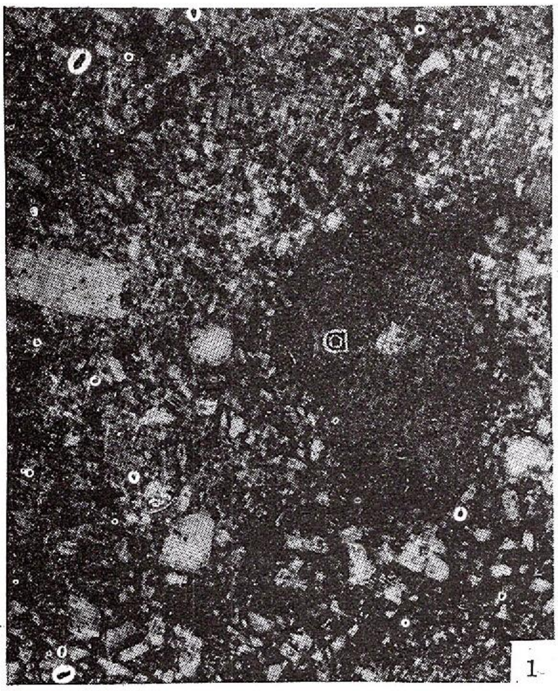
a
1

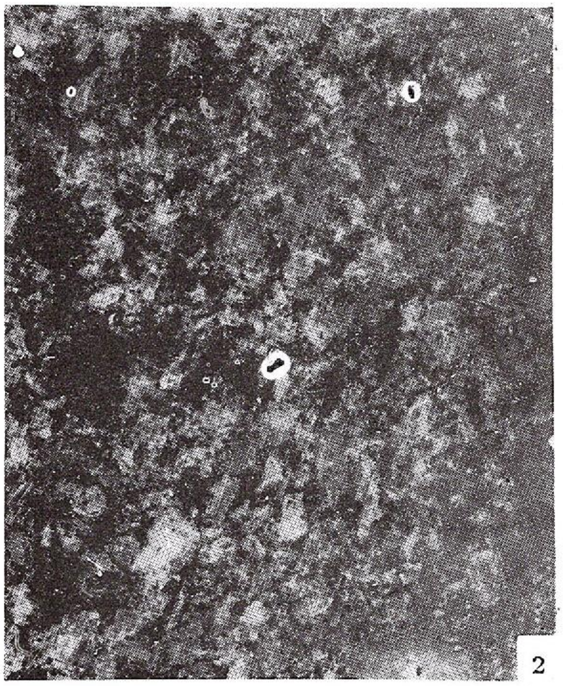
2

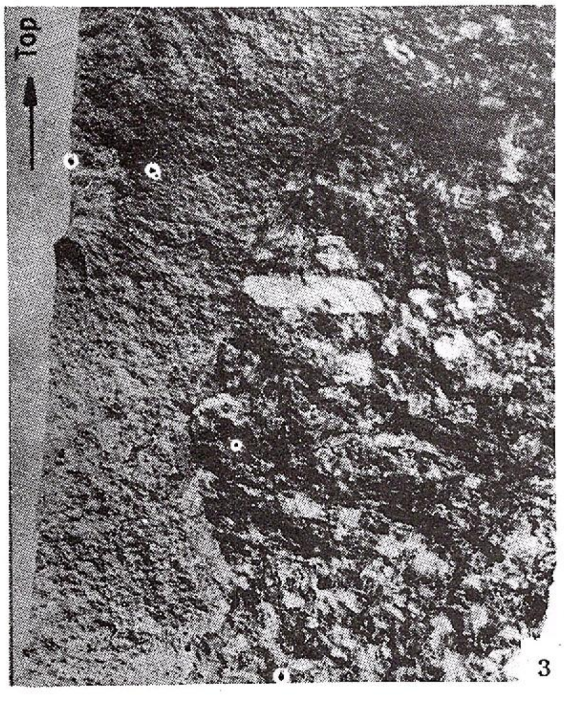
Top
3


a
0 1 2 cm
4

Rom. J. Petrology, 77, p. 107–114, Bucureşti, 1996

MINERAL REACTIONS IN KYANITE BEARING ECLOGITES FROM TOPOLOG ZONE, SOUTH CARPATHIANS: EVIDENCES FOR THEIR METAMORPHIC EVOLUTION

Gelu COSTIN

Univ. Bucureşti, Fac. Geologie şi Geofizică, Catedra de Mineralogie, Bd. N. Bălcescu nr. 1, 70111 Bucureşti

Key words: Eclogite. Paragenesis. Mineral reactions. Metamorphic evolution.

Abstract: Several stages were recognized in the metamorphic evolution of some Topolog eclogites (see text for abbreviations): Stage I: Omph–Gt–Q–Ru (eclogitic); Stage II a: Di–Pl1 (granulitic, dry) = symplectite 1; Stage II b: Hb1–Pl2 (granulitic, wet) = symplectite 2; Hb2–Pl3 = keliphitic coronas around garnets; Hb3–Pl4 – coronitic reaction around quartz; Stage II c: Ky–Zol–Q (granulitic; shear stress, local reaction); Stage II d: Hb4–Pl5–Zo2–SpHc (amphibolitic/granulitic ?, wet); Stage III a: Tr–Act1–Zo3 (amphibolitic, M1) = poikilitic structures; stage III b: Tr–Act2–cZo (amphibolitic, M2); We discuss the presence of kyanite oriented after some shear planes, shear which also affected the garnet. This is the reason for the interpretation of kyanite as not belonging to the eclogitic stage, as it was previously thought, but as a result of a local shear stress which produced the reaction (reverse experimentally tested by Cattarjee et al., 1984): 4 anorthite + $H_2O \longrightarrow$ kyanite + 2 zoisite + quartz. The local direct action of shear stress could induce this reaction in some Topolog eclogites with formation of kyanite (type 1), whereas other eclogites from this zone do not contain kyanite at all, although they have almost the same Al_2O_3 content in bulk composition (type 2).

Introduction

The eclogitic bodies in the Topolog zone are emplaced on the southern part of the Făgăraş Mountains, South Carpathians, on the left slope of the Topolog Valley.

The eclogites are white-greenish coloured, with a stained aspect because of small (up to 2 mm) red garnets, and have a fine to medium granoblastic structure, with a massive texture.

The host rocks of eclogites belong to the Topolog formation (according to Gheuca, 1988) and they consist of biotite bearing quartzo-felspathic schists and gneisses. The bodies are bordered by a consistent rim of almandine bearing amphibolites, which shows a slightly oriented texture.

Close to these eclogites were identified fragments of talc bearing actinolitites, suggesting a spatial association between eclogites and some small, retrogressed, ultramafic bodies.

The Topolog eclogites were mentioned by Gheuca (1983, 1988), who gave a detailed cartographic image. The same rocks were described by Iancu et al. (1993) in an areal study of high-grade metamorphic rocks from the South Carpathians. It was for the first time when kyanite was recognized in these eclogites. According to Iancu, kyanite belongs to primary omphacite-pyrope paragenesis and the slight tendency of kyanite to be oriented was interpreted as a result of tectonic conditions during the eclogitic stage.

The purpose of this paper is to find the relation between different parageneses of Topolog eclogites and to give a possible model of evolution.

Analytical Methods

The minerals were microscopically studied in transmitted and reflected light and also analysed by electron microprobe with a JXA–5EDD wave length dispersion equipment. The microprobe analysis consists of qualitative compositional images (dispersed electrons beam), elements distribution images (scanning RX) and also compositional profiles. Five eclogite samples were so analysed.

Mineralogy of Topolog eclogites and reaction history

The microscopical study revealed a mineral assemblage consisting of omphacite, diopside, garnet, quartz, kyanite, hornblende, tremolite–actinolite, rutile, zoisite, clinozoisite, titanite, magnetite, hematite and (?) spinel-hercinite.

Relations between different minerals suggested the evolution of parageneses in seven stages.

Stage I: (eclogitic)

This stage paragenesis is rarely preserved, being the older and the most affected by several later transformations. These oldest mineral relicts, resulting from an unknown process (1), show the following equilibrium assemblage:

(1) Garnet (Gt) + Omphacite (Omph) + Quartz (Q) + Rutile (Ru)

Garnet is frequently broken and corroded. It was generally estimated to be almandinic rich, following microprobe qualitative images. The rare subsequent magnetite exsolutions at its rims could also support this estimation. Certainly, this was not the primary composition of garnet, which was chemically reequilibrated during several later transformation stages. The zonation in garnet, which shows increasing of iron content from core to edges (estimated from elements distribution images and Fe, Mg profiles), demonstrates its later Fe, Mg reequilibration during a cooling event, probably in the latest amphibolitic stage.

The garnet inclusions consist of quartz, omphacite and rutile which belong to eclogitic parageneses. Other "inclusions" of hornblende, plagioclase or zoisite are in fact reaction products which occur related to fine microfractures in garnet.

Omphacite occurs as small and very rare relicts. It was the first eliminated phase from its paragenesis and it turned into a fine intergrowth of diopside and albitic plagioclase.

Quartz occurs as very small inclusions in garnet and also, as larger grains, in symplectitic mass. In this latter case, the quartz grains are bordered by hornblende + plagioclase coronas. It could never be found in the keliphitic coronas around garnets, being always separated from garnet by hornblende + plagioclase rims. On the other hand, thin sections showed that the amount of quartz decreases with the increase of the transformation grade of the rock. So, we can assume that quartz belongs to the primary, eclogitic paragenesis and it was consumed during the formation of the keliphitic coronas.

Stage II a (granulitic, dry)

This stage is shown by the preservation of rare, fine grains of diopside in the symplectitic mass. There could be also noticed some small xenoblastic diopside grains which seem to replace an older clinopyroxene (probably omphacite). The reaction is:

(2) Omphacite (Omph) $\longrightarrow$ Diopside (Di) + Plagioclase (Pl 1)

The isochemical breakdown of omphacitic pyroxene into diopside and plagioclase (symplectite 1) is interpreted as non-stoichiometrical. The stoichiometry of the phases could have been kept by oxidation of iron from omphacite during imixting (Mysen, Griffin, 1973) or by loosing of Na (Griffin, 1970). As it was described, plagioclase is albite rich and this reaction suggests a fast depressure, which could be interpreted as an abrupt uplift of the system.

Stage II b (granulitic, wet conditions)

Symplectite 1 became unstable in wet conditions and turned into a hornblende + plagioclase intergrowth (symplectite 2) after reaction:

(3) Diopside (Di) + Plagioclase (Pl1) $\longrightarrow$ Hornblende (Hb 1) + Plagioclase (Pl 2)

Hornblende was optically interpreted to have a pargasitic composition, while the plagioclase tends to be enriched in anorthitic molecule.

A mineral reaction coupled with the appearance of symplectite 2 is the coronitic reaction around garnet.

(4) Garnet (Gt) + Omphacite (Omph) + Quartz (Q) + H_2O $\longrightarrow$ Hornblende (Hb2) + Plagioclase (Pl3)

The coronitic rims (Hb2 + Pl3) always separates garnet from symplectite 1. The growth of coronas could lead to a total consuming of garnet. The hornblende grains from rims often have a radial position in relation with garnet and sometimes are optically continued with hornblende from symplectite 2. A similar reaction was described by Baker (1986) for the amphibolised eclogites from Grampian Moines.

Another reaction from this stage must explain the coronas of hornblende + plagioclase which border the rare quartz grains from outer garnet. This reaction could be:

(5) Quartz (Q) + Diopside (Di) + Plagioclase (Pl1) $\longrightarrow$ Hornblende (Hb3) + Plagioclase (Pl4)

During the same stage, the transformation of almandinic molecule into magnetite could also take place:

(6) Garnet (Almandinic molecule) $\longrightarrow$ Magnetite (Mt)

The study of polished sections showed the presence of magnetite in the garnet, grown especially through its borders. Magnetite is also present out of garnet, but never too far from it. This transformation could occur during the chemical reequilibration of garnet, due to the centrifugal diffusivity of iron, this associated to an increased oxygen activity in the system (Brearely, Champness, 1986).

Also in this stage, and possibly continued in later stages, rutile turned into titanite:

(7) Rutile (Ru) $\longrightarrow$ Titanite (Ti)

As it could be seen in Plate I, Figure 4, relatively large grains of titanite occur near almost totally consumed garnets, very probably in connection with the inclusions of rutile from garnets.

Stage IIc (granulitic, wet, shear stress conditions)

After the development of symplectite 2, we notice the appearance of kyanite, a mineral well revealed by microprobe analysis (Pl. II, Fig. 1–6). It is interesting that kyanite occurs along some dynamical planes which represent sets of shear planes, intersected after degrees 35–55 angles. The shear produced in the ductile zone the nucleation of kyanite along certain planes (Pl. I, Fig. 1–2). The presence of dislocations in some larger kyanite grains suggests that the shear acted reccurently. The recurrence of the shear, as it could be noticed in Plate I, Figure 3, demonstates the recurrent action of shear which, in the brittle domain, produced different generations of planar dislocations within kyanite grains and also affected some garnets, breaking and transposing them after the same directions. This recurrence is obvious at the interception of garnets and at the intersection of these planes, where larger kyanite grains with planar dislocations within them occur (Pl. I, Fig. 3).

The appearance of kyanite in some of Topolog eclogites is interesting to be discussed. Although it is an important component in some samples, the Al_2O_3 content of these rocks as only slightly exceeding that of other Topolog eclogites which do not contain kyanite at all (Iancu, unplublished data: kyanite bearing eclogites contain 19.95 % Al_2O_3, whereas eclogites without kyanite have 14.93–18.90 % Al_2O_3). Our interpretation is that this minimal chemical difference does not explain the appearance of kyanite, but kyanite is a result of direct action of local shear in the stability field of this mineral.

Associated with the appearance of kyanite we notice the occurrence of zoisite, comparable in size with kyanite. This zoisite (Zo1) seems to grow especially near garnets. We appreciate that kyanite and zoisite belong to the same paragenesis because both have later fine grained coronitic intergrowths. The appearance of kyanite + zoisite ± quartz paragenesis could be explained by the breakdown of anorthitic molecule of plagioclase (Pl2), following reaction:

(8) 4 Anorthite + H_2O $\longrightarrow$ Kyanite (Ky) + 2 Zoisite (Zo1) + Quartz (Q)

This phase equilibrium was reversible determined by Chatterjee et al. (1984) in 400^0–720^0 C thermal interval.

Stage IId (amphibolitic/granulitic, wet conditions)

The next stage corresponds to the appearance of a very, very fine-grained intergrowth (symplectite 3) which borders kyanite and zoisite as quasiopaque coronas. The composition of these coronas is very difficult to be determined without quantitative microprobe analysis. However, we can see from the compositional images (Pl. II, Figs. 1–2) that the assemblage is formed by several minerals (symplectite 3). The appearance of these coronas corresponds to the recrystallisation of symplectite 2, with the appearance of a fine-grained zoisite (Zo2) in the mass.

The microprobe element distribution images show that these coronas are rich in Al, Ca, Fe ± Mg and relatively poor in Si. The Na content is insignificant. These elements, correlated with optical observations, lead to the interpretation that kyanite was abruptly thrown out from its equilibrium with the other phases and its boundaries tended to transform themselves back into anorthite. Indeed, from the minerals of coronas, plagioclase is closest to kyanite. The other minerals from this intergrowth are difficult to diagnose because of their small size. One could be a spinel-hercynite (following its isotropy and elements distribution, Pl. II, Figs. 3–6). The reaction could be written in general terms as:

(9) Kyanite (Ky) + Symplectite 2 $\longrightarrow$ Plagioclase (Pl5) + spinel-hercinite.

In cases where the symplectite 2 borders zones of symplectite 3, the two intergrowths are always separated by clean coronas of plagioclase (the composition of this plagioclase is difficult to diagnose).

Stage IIIa (amphibolitic, M1)

The next stage is marked by the appearance of a large, poikilitic amphibole (Tr-Act), which includes plagioclase, kyanite, zoisite, and even garnet. Optical determinations showed for this amphibole a tremolite-actinolitic composition (c:Ng=16^0–18^0, Ng-Np=0.025) and demonstrated a slight penetrative orientation.

Synchronous with this amphibole occurs a large zoisite, sometimes with poikilitic structure too, which grows especially near garnet, probably at the expense of its coronas. The reaction is, probably, a reequilibration of mass symplectite, as follows:

(10) Symplectite 2 (Hb1+Pl2) $\longrightarrow$ Tremolite–Actinolite (Tr–Act1) + Zoisite (Zo3)

In this stage, magnetite turned into hematite, and the transformation is very clearly centrifugal in relation to garnet. The farther magnetite is situated from garnet, the more it is transformed into hematitic lamellae. These transformations probably continued in the IIIb stage.

Stage IIIb (amphibolitic, M2)

In this stage we notice the occurrence of another poikilitic amphibole (Tr–Act2), also tremolite–actinolitic. Frequently, this amphibole intersects and includes portions of Tr–Act1 and it is paragenetically associated with a clinozoisite (Czo), both showing the same orientation which differs from that of Tr–Act1:

(11) Tremolite–Actinolite (Tr–Act1) + Zoisite (Zo3) $\longrightarrow$ Tremolite–Actinolite (Tr–Act2) + Clinozoisite (Czo)

The increasing of iron to the garnet rim, demonstrated by element distribution and Mg, Fe profiles, shows the last preserved reequilibration of garnet during the last important metamorphic event. It is well known that such zonation demonstrates a cooling event (Spear, 1988b), but in a temperature domain above 500^0 Celsius degrees (under 500^0 C the Fe, Mg diffusivities are insignificant).

Discussions

Compared to the host rocks, eclogites show the greatest number of superposed parageneses, demonstrating that they preserve the oldest records of a long evolution. Because the oldest relicts are eclogitic, we do not know what these rocks were before their transformation into eclogites and neither how they arrived in eclogitic conditions.

Our proposed model of evolution supposes that eclogites came up to the surface together with their host rocks due to coupled actions of uplift and erosion. Although the position of eclogites in relation with their host rocks could have been changed, we think that this change is not very important. Their very different mechanical competence could permit the host rocks to flow with a higher rate than the movement rate of the eclogitic bodies.

We assume that the whole formation was moved on shear planes, not only the eclogites (otherwise, it would be hard to imagine how the eclogites are the only ones to come out on blastomylonitic shear planes). Moreover, in their moving on the planes, eclogites remained behind their initial host rocks, so that they do not appear emplaced in upper formations, but in lower formations or in the same initial formation. As for the tectonic emplacement of eclogites, a structural test would be required (see Behrman, Ratschbacher, 1989).

Accepting this, we must admit that the host rocks of Topolog eclogites came out from the same conditions as eclogites (although the bulk composition was obviously extremely different). This assumes that the host rocks of eclogites came up from high pressure domains. But the acceptance of a previous regional high pressure event for Topolog formation must be necessarily supported by finding high pressure relicts in its rocks. The field data support this idea. It is interesting to mention that granulitic gneissic lenses were recognized in cores of some folds of the Cumpăna formation (Iancu et al., 1992). Moreover, the garnet bearing amphibolites which border the Topolog eclogites present highly similar characteristics with the amphibolitized mafic granulites from the Cumpăna Valley. These observations, and not only these, suggest a similar metamorphic history for the Cumpăna and Topolog formations (they having a little different lithology).

Knowing that the retrogression under wet conditions of leucogranulites makes them very hard to be recognized and considering that the Topolog rocks supported two long lasting amphibolitic events (the large poikilitic structures for M1, M2 stages support this affirmation), a special attention has to be paid to these aspects in future studies.

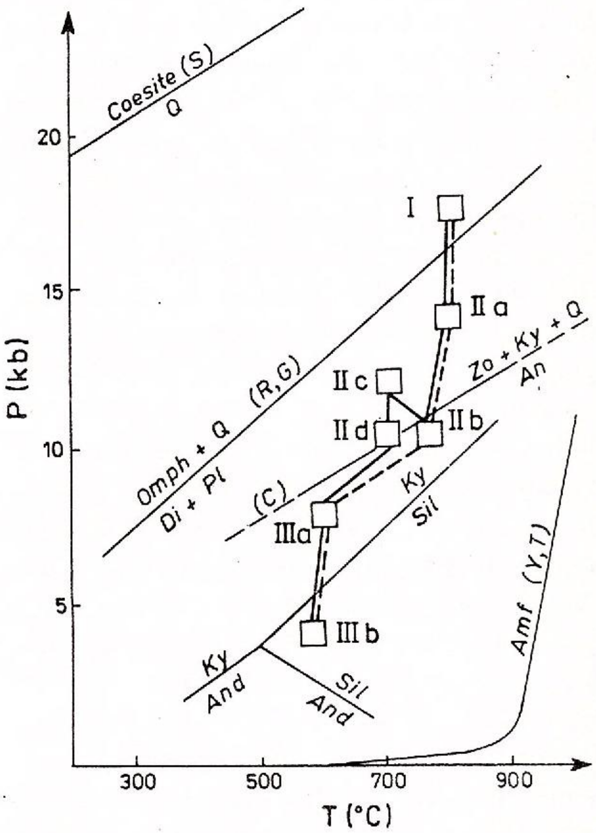

Fig. 1 - PT path and metamorphic evolution of Topolog eclogites.

Continue line = evolution of kyanite bearing eclogites (type 1); *dashed line* = evolution of eclogites without kyanite (type 2); Stages: I = Omph–Gt–Q–Ru; IIa = Di-Pl1; IIb = Hb1–Pl2, Hb2–Pl3, Hb3–Pl4; IIc = Ky=Zo1–Q; IId = Pl5–SpHc(?); IIIa = Tr–Act1–Zo3; IIIb = Tr–Act2–cZo;

Abbreviations: Omph=omphacite; Gt=garnet; Q=quartz; Ru=rutile; Di=diopside; Pl=plagioclase; Hb=hornblende; Ky=kyanite; And=andalusite; Sil=sillimanite; Zo=zoisite; SpHc=spinel-hercynite; Tr-Act=tremolite-actinolite; cZo=clinozoisite. C=Chattarjee et al. (1984); R,G=Ringwood, Green (1969); S=Schreyer (1988); Y,T=Yoder, Tyley (1970)

A special look to the P,T diagram (Fig. 1) supports our model of evolution, showing that the depressure was done in steps of almost equal value about 3–3.5 Kb. This observation, correlated to the model of shear, could lead us to the interpretation of a relatively constant rate of shear (necessarily equal to the erosion rate).

Conclusions

The stage I represents a specific eclogitic paragenesis. The mineral assemblage is interpreted to be at equilibrium at pressure above 16 Kb and temperatures near 750^0–800^0 C (Fig. 1). Because the oldest relicts are eclogitic, we do not know what the system was before becoming an eclogite.

The appearance of symplectite 1, with diopside and plagioclase (stage IIa), is assumed to represent a fast uplift of the system, probably in relation with a shear zone (Fig. 2). During the stage IIb, the system continued its uplift with a high rate, when symplectite 2 was formed.

The occurrence of oriented kyanite mark the stage IIc, kyanite being related to the direct intersection of the system by the shear zone (Fig. 2d). Because of the positive slope of Chattarjee line (c in Fig. 1), we must accept an increasing of pressure due probably to a shear component related to a slight thermal relaxation. This thermal evolution demonstrates that the system is still in uplift (we assume that the increase of temperature in a shear zone caused by friction is lower than the decrease of temperature due to the uplift).

The stage IId is very difficult to be represented in the PT field because of the submicroscopic size of its mineral products. However, we assume that this stage has a position close to the Chattarjee line, an interpretation which presumes a depressure (uplift again). This interpretation fits with the fine coronitic intergrowth of this paragenesis.

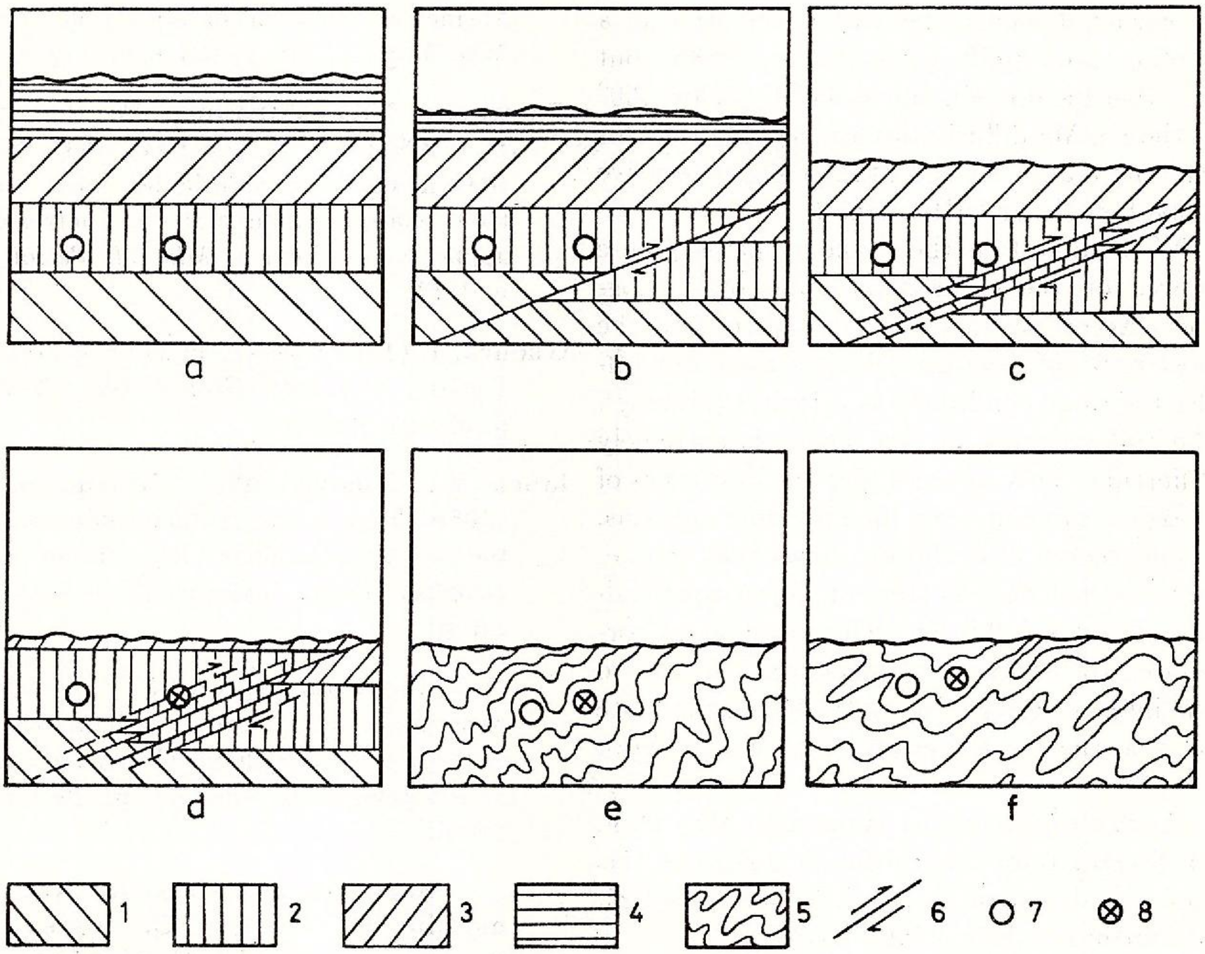

Fig. 2 – Evolution of Topolog eclogites (Sketch, not on scale).

1, upper mantle; 2, lower crust; 3, middle crust; 4, upper crust; 5, metamorphic structures in M1 and M2 amphibolitic events; 6, shear zone; 7, type 2 eclogites; 8, type 1 eclogites.

a) stage I, eclogitic; (bodies of eclogites, in equilibrium conditions, in the lower part of the crust); b) stage IIa, granulitic dry (uplift due to a shear plane, coupled with erosion); c) stage IIb, amphibolitic/granulitic, wet (shear zone is developing; uplift continues; the presence of water is facilitated in the system); d) stage IIc, granulitic, wet; (shear planes affected directly some eclogites=type 1 and formed the paragenesis with kyanite); notice that the under shear plane formations go to higher depth, where eclogites and granulites could be formed; e) stage IIIa, amphibolitic; (deformations and flow became penetrative); f) stage IIIb, amphibolitic (structures are changed).

Stages IIc and IId are not visible in all Topolog eclogites; these stages are represented probably only in some Topoog eclogites which suffered a direct action of shear (type 1 eclogites, Figs. 1, 2a-f). For other eclogites, not directly affected by shear, the stages IIc and IId could be missing (type 2 eclogites).

Stages IIIa and IIIb, with the poikilitic tremolite-actinolite, are specific amphibolitic stages, as they were recognized by several geologists who worked in the South Carpathians (Iancu et al., 1992, etc.). We found stages IIIa and IIIb to be equivalent to M1 and M2, respectively amphibolitic stages of the abovementioned authors.

The noted iron increase from core to rim in garnet demonstrates the preservation of a cooling, post uplift, event (Spear, 1988b), but in a thermic domain above 500^0 C (below 500^0 C the Fe, Mg diffusivities are negligible). This was the reason for accepting a slight negative slope for IIIa and IIIb stages.

We assume that the whole formations were moved on the shear planes, not only eclogites. Accepting this, we must admit that the host rocks of Topolog eclogites came out under the same conditions as eclogites (although the bulk composition was obviously extremely different). This assumes that the host rocks of eclogites came up from high pressure domains.

Our model of evolution shows that the depressure was done in steps of almost equal values of about 3–3.5 Kb. This observation correlated to the model of shear could lead us to the interpretation of a relatively constant rate of shear (necessarily equal to the erosion rate).

Acnowledgements: I appreciate Mr. Prof. M. Şeclăman for the fruitful dicussions on this topic. I also want to thank V. Iancu and M. Mărunţiu for their helpful advices.

References

Baker, A.J. (1986) Eclogitic amphibolites from Grampian Moines. *Min. Mag.*, VI, 50, p. 217–221, Oxford.

Behrman, J.H., Ratschbacher, L. (1988) Archimedes revisited: a structural test of eclogites emplacements models in the Austrian Alps. *Terra Nova*, 1, p. 242–252, Oxford.

Brearely, A.J., Champness, P.E. (1986) Magnetite exolution in almandine garnet. *Min. Mag.*, X, 358, p. 621–626, Oxford.

Chattarjee, N.D., Johannes, W., Leistner, H. (1984) The system $CaO-Al_2O_3-SiO_2-H_2O$: new phase equilibria data, some calculated phase relations and their petrological applications. *Contrib. Mineral. Petrol.*, 88, p. 1–13.

Gheuca, I. (1988) Versantul sudic al Munţilor Făgăraş. *D.S. Inst. Geol. Geofiz.*, 72–73/5, p. 93–107, Bucureşti.

Iancu, V., Conovici, M., Mărunţiu, M. (1988) High grade metamorphic rocks in the South Carpathians. *Rév. Roum. Géol. Géophis. Géogr., Géologie*, 32, p. 9–19, Bucureşti.

– **, Mărunţiu, M. (1992)** Superposed parageneses in high grade metamorphic rocks of the South Carpathians (Romania). *Rom. J. Mineralogy*, 75, Suppl. 1, p. 16–18, Bucureşti.

– **, Mărunţiu, M., Conovici, M., Tomoşoiu, V., Cristea, C., Stelea, G., Anastase, Ş., Costin, G. (1993)** Report, Arch. IGR, Bucureşti.

Mysen, B., Griffin, W.L. (1973) Pyroxene stoichiometry and the breakdown of omphacite. *Am. Mineralogist*, 58, p. 60–63, Lawrence, KA, USA.

Spear, F. (1988b) Metamorphic fractional crystallization and internal metasomatism by diffusional homogenization of zoned garnets. *Contrib. Min. Petrol.*, 90, p. 507–517.

Received: January 18, 1996.
Accepted: January 25, 1996.

Plate I

Fig. 1 – Kyanite (Ky) with coronas. Transmitted light, N II, x 50. Notice the preferential orientation.

Fig. 2 – Kyanite (Ky) with coronas. Transmitted light, N II, x 50. Kyanite follows shear planes which are intersected at 45–50. The same planes affected garnet, too.

Fig. 3 – Detail on kyanite. Transmitted light, N II, x 80. Notice shear dislocations in kyanite before corronas forming and dislocations which affected the coronas. These stages of dislocations demonstrate the recurrence of shear, its continuous actions.

Fig. 4 – Total replacement of garnet by hornblende (Hb) + plagioclase (Pl). Transmitted light, N II, x 50. Notice large titanite grains near this transformation.

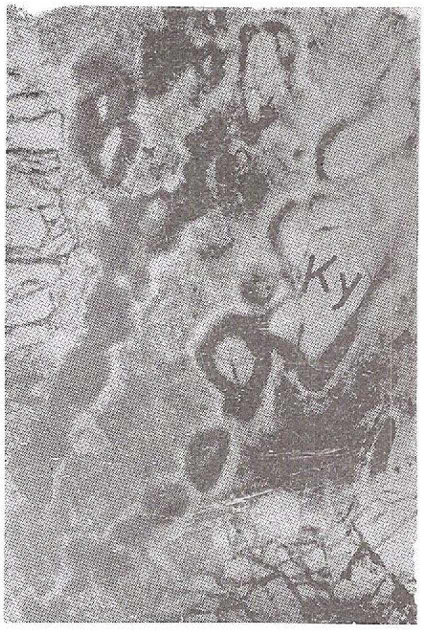

1

2

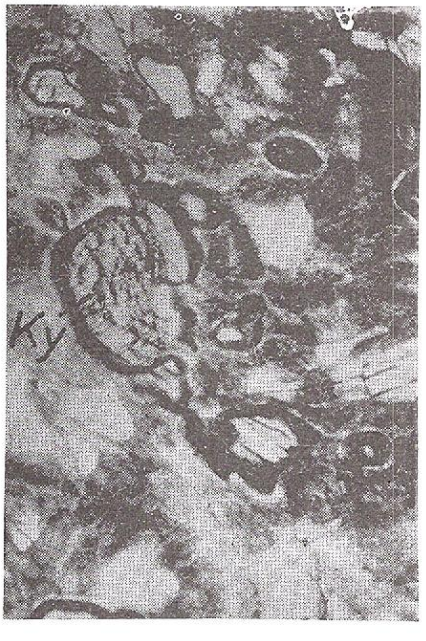

3

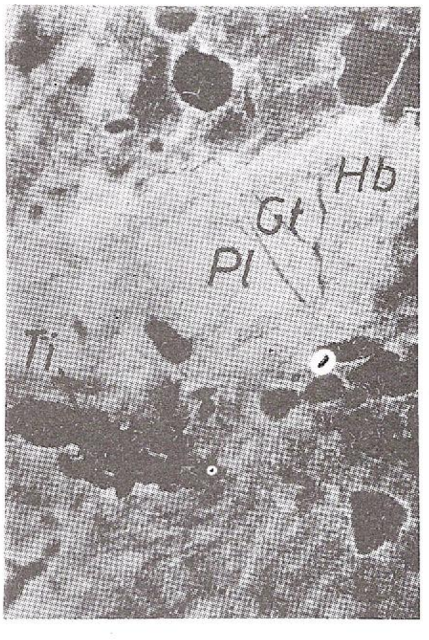

4

Plate II

Fig. 1 – Kyanite with coronas. Composition image, x 600. Notice a black zone of reaction between coronas and mass symplectite.

Fig. 2 – Kyanite with coronas. Dispersed electron image, x 300. Notice the two fine intergrowths (coronas and mass symplectite), separated by a clear gray zone of plagioclase.

Fig. 3 – Distribution of aluminium, x 300.

Fig. 4 – Distribution of calcium, x 300.

Fig. 5 – Distribution of iron, x 300.

Fig. 6 – Distribution of magnesium, x 300.

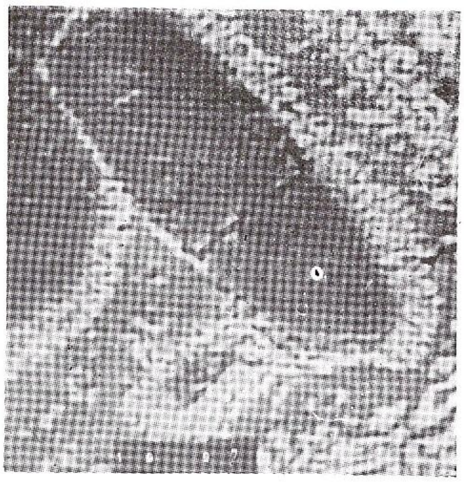

1

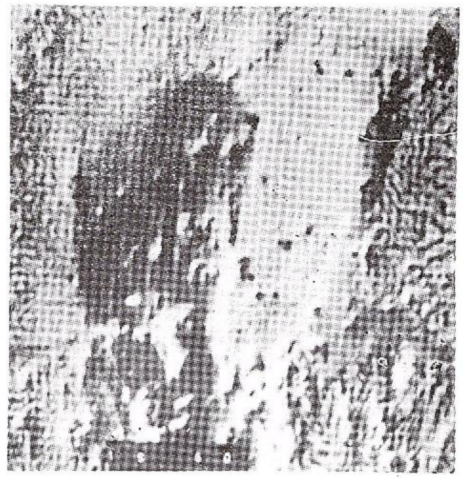

2

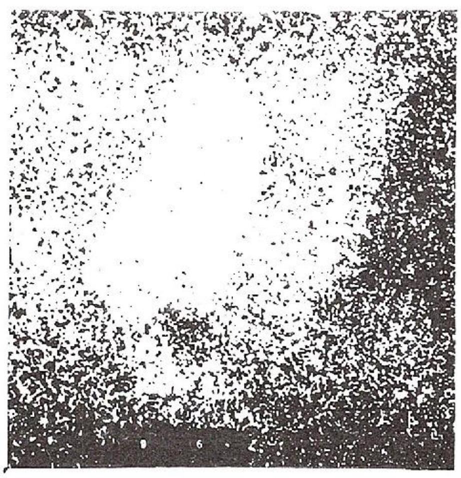

3

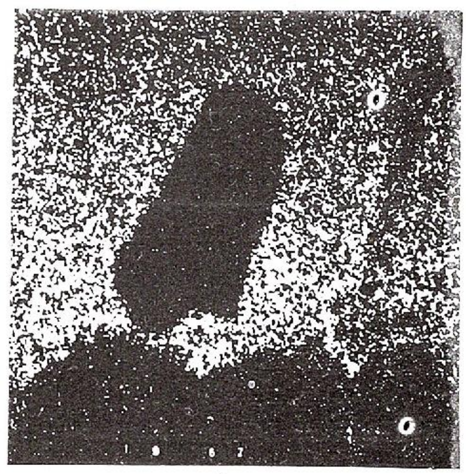

4

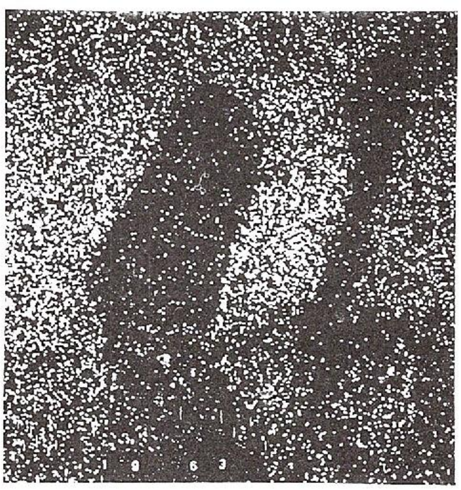

5

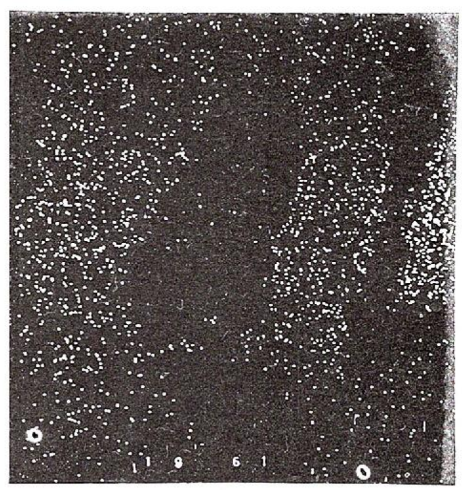

6

Rom. J. Petrology, 77, p. 115–128, Bucureşti, 1996

NEW DATA ABOUT THE GEOLOGY OF THE MĂGURA ŞIMLEULUI CRYSTALLINE ISLAND (NW TRANSYLVANIA, ROMANIA)

Ioan KALMÁR

Hungarian Geological Institute H.1143 Budapest XIV, Stefánia út 14

Key words: Metamorphic rocks. Magmatic rocks. Polymetamorphism. Garnet. Kyanite. Staurolite. Base-metal ore. Microtectonics.

Abstract: In Măgura Şimleului three lithostratigraphic subdivisions were separated. The constituent rocks are quartzitic schists, mica-schists, paragneisses and quartzites. The magmatogene rocks are represented by biotitic gneisses, leptinites and micro-ocular gneisses. Cataclastic rocks as breccias, blastomylonites, ultra-mylonites and pseudotachilites are also present. The mineralogic assemblage shows an oldest association (plagioclase, brown-green biotite, kyanite, almandine), a retromorphic association (sericite-phengite, chlorite, epidote, siderite) and a neomorphic association (brown-red biotite, muscovite, staurolite, albite, orthoclase, almandine with 25% pyrope), followed by hydrothermal minerals as chlorite, quartz, calcite, adularia and sulphides. These rocks evolved from an early blastic phase, by retromorphic phase tied with shearing processes to a later neomorphic recrystallisation, which is common for the whole NW Transylvanian Area. The territory of Măgura Şimleului is a "splinter" detached from the southern part of Tisia domain and propulsed into Someş-type crystalline basement, before the Meso-Cretaceous collision.

Măgura Şimleului is one of the seven crystalline islands from NW Transylvania, having 6x6 km extension, between the localities Şimleul Silvaniei (S), Cehei and Uileacul Şimleului (W), Ilişua (N) and Bădăcin (E). In its southern and western part it is surrounded by the meadow of the Crasna River. In the left side of the Crasna River, the metamorphic formation appears in Brădet (321 m), Sfânt (350.5 m), Pupu Mare (283.1 m) and Omanu (279.2 m) hills.

1. History of geological researches

After the regional surveys carried out by Hauer & Stache (1863), Măgura was firstly mapped by Hofmann (1879) and Matyasovszki (1879), followed by Telegdi-Róth (1912), Szádeczki (1930) and Kräutner (1940). After the 2^{nd} World War, the researches were resumed by Dimitrescu (1963) and by Paucă (1964). Patrulius et al. (1968) in caption book of the sheet N^{0}9. Şimleul Silvaniei of the Geologic map, scale 1:200 000, referring to the foregoing researchers, separated into the Someş Series, which comprises the metamorphites of Măgura too, the complex of micaschists and paragneisses. New data about the Neogene-covered zone were emphasized in Ghiurca's (1973) and Dicea's (1981, unpubl.) reports.

2. Geological formations

Măgura Şimleului is built up by crystalline schists and Paleogene, Neogene and Quaternary sedimentary cover.

2.1. Crystalline schists

2.1.1. Stratigraphy. The crystalline formations of Măgura Şimleului can be divided in three stratigraphic subdivisions with member and horizon degree (Fig. 1):

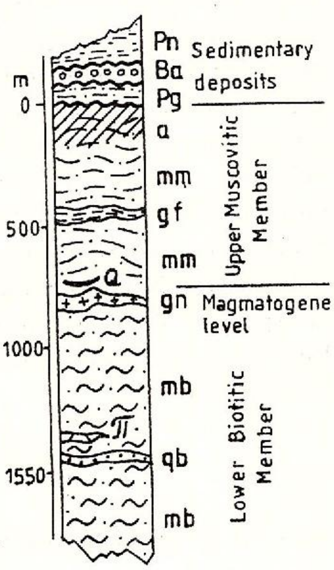

Fig. 1 – Synthetic lithological column of Măgura Şimleului. P, Pannonian; Ba, Badenian; Pg, Paleogene; a, old weathering crust; mm, muscovitic mica-schists and quartzitic schists; gf, horizon of graphitic mica-schists and quartzites; gn, orthogneisses; mb, biotito-muscovitic quartzitic schists and paragneisses; qb, biotitic quartzites.

– The Lower Terrigene Biotitic-Muscovitic Member is constituted by metapelites and metapsammites, which distinguish by their more consistent character, by their hardness and dark colour. Quartzitic schists, mica-bearing quartzites predominate and micaschists and paragneisses appear subordinately. In the middle of the exposed succession, a level of black, hard biotitic quartzites was found (Hamzei and Gradiciului valleys, Pl.I).

– The Middle Metavolcanic Horizon represents a real repair level of Măgura. It can be mapped in the Capolnei Valley, in flanks of Muntele Rău and Omanu, in the Tăului Valley and eatward, in the Fagului and Lapoş Valleys. Its thickness is variable, ranging between a few and ten meters at quasi-total pinching. It consists of micro-ocular biotitic gneisses (Măgura Valley, quarries), biotitic gneisses and leptinites. Frequently, these gneisses are associated with muscovitic micaschists, grey quartzites and monomineralic white quartz lenses (Fig. 2).

– The Upper Terrigene-Muscovitic Member is constituted by less hard, lighter schists than the Lower Member. The micaschists predominate, followed by quartzitic schists and paragneisses. Biotite appears subordinately or it is missing. In the lower third of the exposed succession a 1–10 m thick level of graphitic micaschists and quartzites was found (Tăului and Lapoş valleys, Crinului street – Şimleu).

2.1.2. Petrography of metamorphic rocks. In Măgura Şimleului the following terrigenous and magmatogene metamorphic rocks appear: quartzitic schists, micaschists, paragneisses, quartzites, orthogneisses, cataclastic rocks and pegmatitic lenses.

– Quartzitic schists represent the petrographic background for the rest of the rock types. The constitutive minerals are quartz, muscovite, biotite, some plagioclases and potash feldspars, then garnet, tourmaline, kyanite, staurolite, rutile, zircon, titanite, apatite, opaque minerals, albite, epidote, chlorite, sericite.

– Micaschists are light- or dark-grey, sparkling, sheety rocks, with planar, nodular or microfolded schistosity. The main mineralogic component are the micas: muscovite and biotite quartz, feldspar, garnet, staurolite, tourmaline, apatite, rutile, ilmenorutile, albite, orthoclase, chlorite, epidote, sericite and dark minerals. Micaschist appears as more or less extended levels or as 100–200 m large lenses into quartzitic schists.

Level are represented by biotitic-muscovitic gneisses, leptinites and micro-ocular gneisses.

– Biotitic-muscovitic gneisses are the most frequent rock-types. They are greydotted, micro- or porphyroblastic, massive, oriented or stripped rocks, consisting of feldspar-quartz

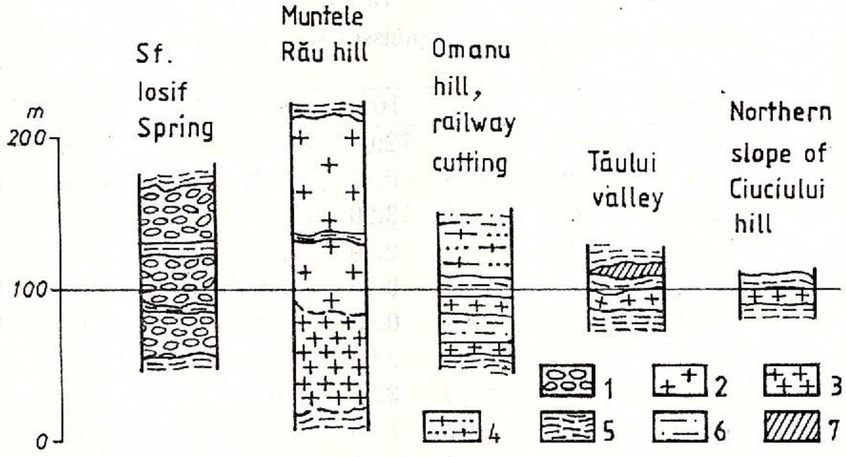

Fig. 2 – Detailed lithologic columns from Median Magmatogene Level. 1, Micro-ocular gneisses; 2, leptinites; 3, biotitic gneisses; 4, paragneisses; 5, muscovitic mica-schists; 6, quartzitic schists; 7, white quartzites.

mosaic (plagioclase, subordinately microcline), garnet, zircon, apatite, rutile. Micas form thin layerlets, films and insulated sheetlets. Porphyroblasts are quartz and oligoclase, with chess-like twinning (Pl. II, Fig. 1).

Paragneisses are dark, grey or brown, hard rocks, with characteristic transversal joints and planar schistosity or banded structure. They are constituted by quartz, plagioclase (subordinately microcline), orthoclase, micas (mainly biotite), garnet, kyanite, staurolite, tourmaline, apatite, rutile, ilmenorutile, zircon, titanite as accessory minerals, and albite, epidote, chlorite, carbonates, clay minerals, calcedonite and limonite as secondary minerals.

– Quartzites are grey, sometimes greenish, frequently broken, massive or stripped rocks. Beside quartz, discontinous films of micas (biotite and muscovite in the same amounts), rare plagioclase, orthoclase, garnet, apatite, rutile, epidote, siderite and dark mineral grains appear. Quartzites are developing as decimetric or metric lentilised slabs.

Orthogneisses from Middle Magmatogene

– Leptinite are white, microgranular, massive, oriented, eye-like or stripped rocks, with quartz and feldspar (plagioclase and microcline). Muscovite appears in small quantities, as films and oriented sheetlets; tourmaline, zircon, and apatite, as accessories, are found as well.

– Micro-ocular gneisses appear in little quarries in the left side of the Măgura Valley, Cehei (Sf. Iosif spring) and in the lower Lapoş Valley, Ilişua. They are dotted, nodular, eyelike, which are present as banks, 1-2 m thick. Feldspars (plagioclase, microcline) and quartz form nodules (0.5 – 2 mm), coated in biotite, subordinately, muscovite. Rutile, zircon, titanite, tourmaline, albite, epidote, chlorite, carbonate, clay minerals and dark minerals appear, too. For the study of the chemistry of magmatogene rocks seven total analyses were supplied (Tab. 1).

Table 1
Chemical analyses of orthogneisses samples from Măgura Şimleului

Sample	5	146	168	185	302	348	1142
SiO_2	72.85	69.16	72.00	71.86	67.31	75.70	68.89
TiO_2	0.09	0.18	0.13	0.44	0.44	0.40	0.44
Al_2O_3	13.00	11.67	13.20	15.10	17.78	12.70	17.13
Fe_2O_3	1.30	2.27	2.20	1.87	1.90	1.06	1.81
FeO	0.70	1.00	0.75	0.40	0.97	0.39	0.96
MnO	0.10	0.03	0.03	tr	0.05	0.05	0.16
MgO	1.85	2.50	2.00	1.05	1.20	0.40	1.22
CaO	1.96	2.60	3.20	0.91	1.12	0.35	1.01
Na_2O	3.38	3.22	1.45	3.02	3.57	0.45	5.22
K_2O	3.98	6.30	4.40	3.50	3.70	7.80	3.45
P_2O_5	0.25	0.10	0.25	0.25	0.10	0.17	tr
S	tr	0.10	0.05	tr	tr	0.10	0.28
L.I.	1.08	0.91	1.20	1.48	1.75	0.70	1.60
Total	99.94	100.04	99.86	99.81	99.89	99.67	99.57
an	5.38	0.00	9.86	3.57	0.00	0.00	5.88
ab	27.50	26.57	11.36	27.50	33.78	4.17	43.37
or	21.27	33.74	23.50	21.06	22.92	44.78	20.57
q	34.31	20.39	42.03	40.44	31.70	46.76	21.03

Location of samples: 5, Hamzei Valley, Şimleu; 146, Fagului Valley, Ilişua; 168, Sf. Iosif Spring, Cehei; 185, Omanu Railway cutting, Uileacul Şimleului; 302, Tăului Valley, Uileacul Şimleului; 348, Muntele Rău, Şimleu; 1142, Hydrogeological borehole No.4 Şimleu, m. 142–142,5. Analysed by ICMC Cluj-Napoca (5, 146, 168, 185) and MÁFI, Budapest (302, 348, 1142).

The analytic data show various acid rock types, from calc-alkaline dacites to alkaline rhyolites. The Winkler & Breitbart's (1978) mesonorm count resultes that 5 samples display near by the eutectic line and the other two are plotted into alkaline, respectivelly calc-alkaline fields. The temperature of crystallization of their rocks cannot exceed 700°C (Fig. 3).

The cataclastic rocks, which are frecvently found in Măgura, are represented by blastomylonites, fracture breccia and ultra-mylonites.

– Blastomylonites appear as lenses and quasi-concordant levels in the metamorphic succession, the thickness of which varies between a tenth part of a millimeter and 2–4 m. They are light-grey or yellow-pink, rough rocks, with oriented structure. Mylonite are constituted by splintery fragments of quartzitic rocks, quartz, muscovite sheetlets, rarely biotite, chlorite, sericite, opaque minerals. Frequently, a neomorph mineral association (biotite, muscovite, K feldspar, albite, chlorite, calcite and sulphides) appears.

– Fracture breccia constitutes transversal or oblique straits considering schistosity surfaces. The elements of breccia have a heterogeneous petrographic composition and have a maximum 20 cm diameter. The matrix is a mica-bearing soft clay or quartz and calcite with sulphide nests (Ciuciului Valley, vine caves in Şimleul Silvaniei).

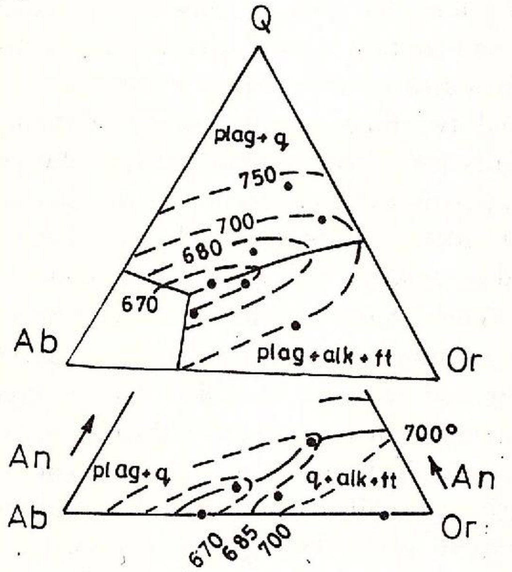

Fig. 3 – Ternary diagram q (quartz) – Ab (albite) – Or (orthoclase) – An (anorthite), calculated after mesonorm, with isotherms of the plagioclase – alcali feldspar – quartz system. The points represent the analyses from Tab. 1.

– Ultra-mylonites are dark-grey or brown, compact or foliated rocks which are constituted by a mass of submicronic quartz, sericite, probably chlorite and dark minerals. They appear as centimetric laminae in the quartzitic schists or at the boundary zone between mylonites and host rocks (Crasna River bank under Pupu Mare Hill).

On the left side of the Lapoş Valley, Ilişua, at the confluence with the Scoruşului Valley and at the end of Andrei Mureşan Street, Şimleu, a horn-like, black rock appears, formed of partially devitrified glass. It is intercalated as irregular straits, 1–3 cm in thickness, into the blastomylonites (Fig. 4). This rock is a pseudo-tachylite, a special vitreous ultramylonite.

– Pegmatites. Two pegmatite lenses, 1–1.5 m in thickness, were discovered in the Prundului Valley, W Şimleul Silvaniei, inbedded in quartzitic schists. The pegmatites are constituted by large (1–4 cm) quartz, albite, orthoclase, muscovite, tourmaline and garnet grains, with a zonal disposition (Fig. 5).

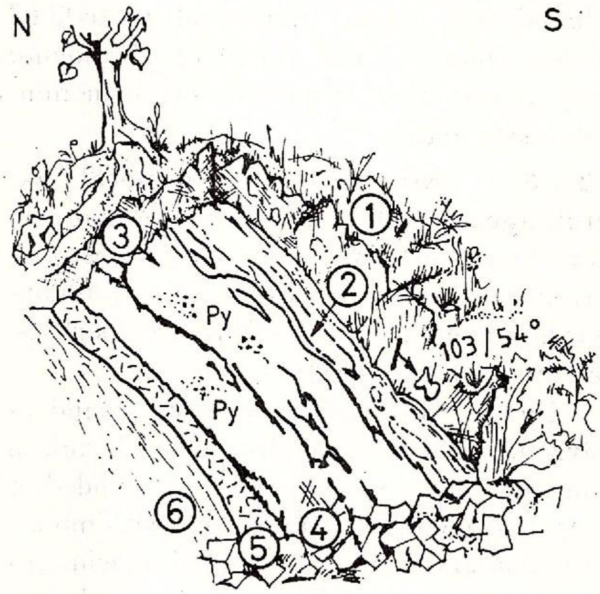

Fig. 4 – Outcrops from the left bank of the Lapoş Rivulet, Ilişua. 1, soil; 2, white quartz lenses; 3, mylonite; 4, pseudo-tachylite straits; 5, ultra-mylonite; 6, quartzitic schists; Py, pyrite nests.

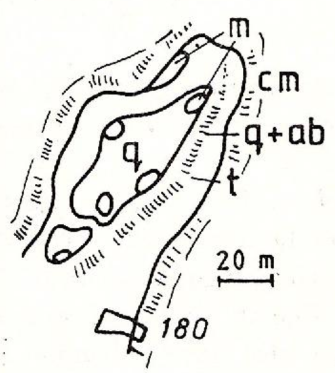

Fig. 5 – Pegmatite lens from left of the Prundului Valley. m, muscovite plates; q, quartz; q+ab, graphic intergrowth albite-quartz; t, tourmaline; cm, quartzitic schists indurated at contact; 180, sample.

Though the host rocks are intensively cataclased, the pegmatites are not fissured. The host rock, that comes into contact with pegmatites, becomes hard because of the neomorphous, clear quartz, albite and tourmaline supply, as I described in the Preluca Mountains (Kalmár, 1973).

In all rock types, transversal aplite-filled veinlets (max. 1 mm thick) can be found. They appear most frequently into monomineral quartz lenses.

2.1.3. Minerals and mineral assemblages. The described metamorphic rocks consist of quartz, feldspars, micas, garnet, kyanite, staurolite, tourmaline, titanium-bearing minerals, zircon, chlorite, carbonates, clay minerals and dark minerals.

– *Quartz.* It is more frequently found as polygonal or lace-like grains, 0.05–0.2 mm in diameter. Sometimes, grains with rounded or elongated shape, 0.5–1 mm thick, with mosaic extinction and dark dust or sericite inclusions appear; they undoubtly are the original sand grains of the protolith. They are frequently substituted by clear, limpid quartz (Fig. 6).

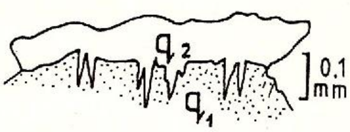

Fig. 6 – Neomorphic quartz (q_2) replaces the older, cloudy quartz (q_1). Cehei quarry.

– *Plagioclase.* It is an acid oligoclase, with 20–25 % An. In terrigenous rocks, it is microgranular, with polygonal contour, cloudy, often zoned. The thin plagioclase grains of the orthogneisses also have polygonal shape, but they are limpid and contain drop-like quartz inclusions. The anti-perthitic and myrmekitic structure appears, as well. The An-content represents less than 20 %. Porphyroblasts often appear with chess type twins and they contain quartz, biotite, zircon and apatite inclusions. Albite grains are clear and they appear as a neoblast in the mica-schists (interlaced with the micas), bordering and replacing plagioclases and microcline, or as thin, mosaic-like grains in aplitic veins.

– *Potash feldspars.* Microcline is not frequent. It appears as polygonal grains in quartzitic schists and in some gneisses they are usually in micro-ocular gneisses. Microcline grains are clearer than the plagioclase ones and contain quartz, zircon, muscovite inclusions and microperthitic separations. The crossed twinning is unfrequent. Orthoclase presents rheniform, limpid grains; always, it also appears as neoformation in the blastomylonitic rocks. In breccia lodes, adularia was found associated with quartz and calcite.

– *White micas.* Muscovite is the rock-forming mineral in mica-schists, quartzitic schists and gneisses, in which it often constitutes curved sheetlets 0.01–0.05x0.08–0.2 mm, with dark dust inclusions. A thin and little birefringent white mica disposed on the shearing planes gives the physical support to the S_2 schistosity. Similar white mica is present in mica-schists, wherein it formed an unoriented aggregate, which replaces biotite, with opaque exsolutions (phengite). Muscovite also appears as millimetric phenoblasts, with transversal disposition considering S–surfaces. It often shows kink-band type reticular deformations. In the pegmatites of the Prundului Valley, 2–4 cm thick, clear and undeformed muscovite plates are present. A little pit for exploitation of pegmatitic muscovite was opened here in 1942.

– *Biotite.* Thin, brown-green, cloudy, plane or curved biotite sheetlets from quartzitic schists, paragneisses, quartzites and some mica-schists often contain a network of sagenite needlets and opaque grain borders. It is transformed in phengite or in chlorite. Neomorphic biotite grains are brown-red, limpid, appearing as tabular phenoblasts, 1–3 mm thick, with S_1 – oriented dark inclusions. It obliterates ancient structures, blastomylonitic ones inclusively. Quasi-oriented display of these sheets can be observed in outcrops (Fagului and Capolnei valleys).

– *Garnets.* They are present in all rock types as poikilitic porphyroblasts or skeleton-like aggregates. The cloudy garnet includes biotite, rutile, opaque minerals, so they show oriented straits, rotated at 20–40^0 considering S_1. They represent, in the author's opinion, traces of a former metamorphic phase, that happened before the forming of the first metamorphic assemblage. These relics were preserved in the detrital garnet grains of the protolith. The garnet is borded by new, limpid, inclusion-free rims. Thin-grained, clear garnet nests frequently appear in mica-schists and leptinites.

X-ray analyses indicate almandine with 24 % pyrope and 1 % quartz. Plotting this data on the ternary diagram recommended by Gomez-Pugnarie & Sassi (1983), the host rocks of garnets are situated on the boundary between the low and medium metamorphic stage (Fig. 7).

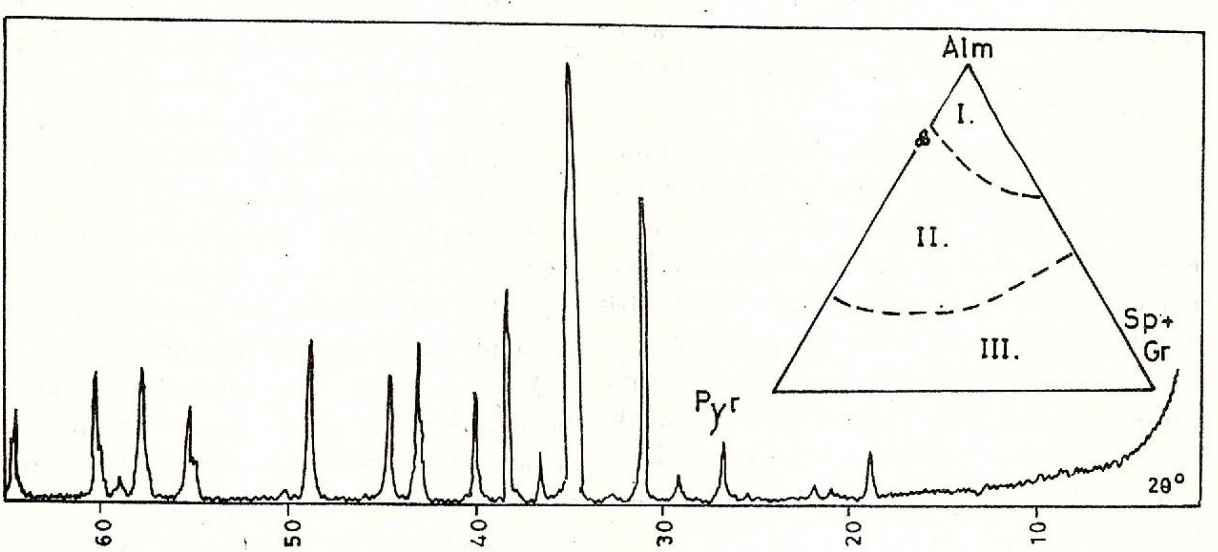

Fig. 7 – Diffractogram of monomineralic garnet sample (Kovács-Pállfy P., lab. Rx MLFI), from the Tăului Valley, Uileacul Şimleului and ternary diagram Alm (almandine) – Pyr (pyrope) – Sp+Gr (spessartine and grossular). I: metamorphic rocks, medium and high stage; II, metamorphic rocks, low stage; III, pyro-metasomatic rocks.

– *Kyanite.* It forms short prismatic grains (0.1–0.3 mm) in quartzitic schists and in paragneisses, in the NW corner of Măgura (Crinului, Independenţei Streets, left bank of the Crasna River) and in the Tăului Valley, Giurtelec. Kyanite grains are often resorbed by thin white mica (Fig. 8).

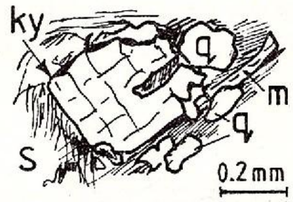

Fig. 8 – Kyanite (ky) resorbed by sericite (s); m, muscovite; q, quartz; Terasa Crasnei Vinery, Şimleul Silvaniei.

– *Staurolite.* It constitues poikilitic phenoblasts, 1–2 cm in length, including quartz, micas and opaque minerals (Fig. 9), in NW part of Măgura (R. cath. cemetery, A. Mureşan and Dunării Streets), at E (borehole No. 4; Capolnei Valley) and in Badenian conglomerate elements.

I drew on the geological map the area of the appearance in the outcrops of the kyanite and staurolite. Those lines do not superpose exactly with the stability area of these minerals because of the relief and of the effects of erosion and tectonics.

– *Tourmaline.* It appears as hypidioblastic grains (0.03–0.15 mm), which are frequent in mica-schists. The grains show a dark-olive, opaque powder inclusion-bearing nucleus, covered by a clear, light rim. Unzoned dark tourmaline prisms, with 1–4 cm in length, are present in pegmatites.

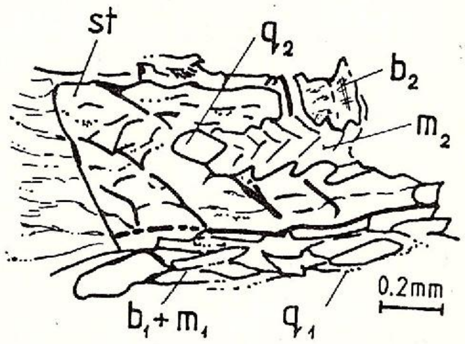

Fig. 9 – Staurolite porphyroblast (St), with oriented opaque mineral relics; b_1, b_2, biotite; m_1, m_2, muscovite; q_1, q_2, quartz (two generations). R. cath. cemetery, Şimleul Silvaniei.

– *Rutile, apatite and zircon* form similar grains, with cloudy nucleus and clear envelope.

– *Epidote.* It shows 0.01–0.13 mm thick, light-green, hypidioblastic grains, in plagioclase, in paragneisses and quartzites in the Lapoş and Fagului Valley.

– *Chlorites.* Brown–green chlorite (pennine) is formed by the breakdown of biotite, inheriting its inclusions. Grass-green chlorite (from delessite-diabantite group) shows rosetta borders on neomorphic biotite, associated with quartz, carbonates adularia and sulphides.

– *Carbonates.* Siderite appears as micronic drop-like grains, following chlorite at breakdown of biotite. Clear calcite forms large grains, veins and geods in fissured or cataclased rocks.

Hereafter, it results that in the metamorphic rocks of Măgura Şimleului four successively formed mineralogic parageneses are superposed:

– The association of quartz + An_{20-25} plagioclase (±microcline) + muscovite + brown-green biotite + cloudy garnet + kyanite + nuclei of tourmaline, rutile, apatite and zircon grains and part of opaque minerals is the oldest. They are corresponding to the upper limit of the medium stage, which is characterised by $P \sim 5$kB, $T \sim 500^0$C and gradient $<33^0$C/km, as results from the stability of kyanite.

– The second association is represented by phengite (sericite) + chlorite + siderite + epidote + thin-grained quartz. They are formed by partial resorption of the former mineral assemblages during an intensive shearing processes which caused, in some paces, the destruction of the former structure of the rocks. These minerals are formed under P–T conditions at the upper part of the lower stage and the velocity of deformation surpassed the grain growth one.

– The last metamorphic association is represented by large, limpid quartz + redish biotite + muscovite + staurolite + clear garnet (single grains and envelopes) + albite + othoclase + clear rims of tourmaline, zircon, rutile and apatite. This association is stable in the lower part of the low stage, under $P \sim 3$–4 kB and $T \sim 400^0$C. The orientation of micas presumes the existence of a small, oriented pressure.

It is to note that the amount of this last association represents few (max. 10) percentages of the rocks mass. The relationship between the neomorphic minerals and the first and second mineral assemblage which are replaced, resorbed or included, prove undoubtedly that the minerals are formed after and on account of the pre-existing ones.

Minerals from this third association can be found in all rock types, excepting ultramylonites and pseudo-tachylites which formed after the metamorphic processes.

Pegmatites also formed after the metamorphism, because albite from the contact zone of the pegmatites resorbes neomorphic biotite of the quartzitic schist. Another explanation of the different kind of deformation of the pegmatite and their wall-rocks has different tectonic competence caused by their different structural and textural features. In this situation, the minerals from the contact zone should be considered as a post-metamorphic assemblage.

– In metamorphic rocks (partially by replacing of metamorphic minerals) a postmetamorphic association can be identified. This is represented by quartz, grass-green chlorite, calcite, adularia, sericite, clay minerals, sulphides and limonite. They prefer the breccious, fissurate zone and some blastomylonitic lenses.

2.1.4. Structural features. Examining the metamorphic rocks of Măgura with the naked eye, the fine-grained, silky aspect and the frequence of thin micro-folds are observed. Sometimes, the rocks show evidently two schistosity surfaces, which are intersecting at 30–50^0. The desaggregate zone and, however, the hard, rough zones are often observable. These various aspects resulted by tectonic reworking of these rocks, as this can be observed by microscopical study. In this way, four suitable structures can be distinguished.

– The first structure is given by planar and parallel disposition of mica sheetlets, of quartz lenses and opaque mineral straits. The parallelism between these laminae and the lithologic separations (i.e. quartzite – mica-schist, quartzitic schist – gneiss boundary) indicates that this S_1–schistosity surface was formed by the evolution of the sedimentary layer surface of the protoliths. In outcrops we usually measure this S–surface.

Often, the transition between unfolded and micro-folded schists can be followed through a few metres distance. Micro-folds are given by curvature or, indeed, by breaking of mica sheetlets, by microfissuration of quartz grains, moreover this dismembration. The opaque mineral straits are also micro-folded.

– Sheared wings of microfolds become S_2 schistosity surfaces. Films of thin white mica, chlorite and fine-grained quartz are the material support of this schistosity surface, which forms 30–50^0 wide angle with the cover surface of the microfolds. Double schistosity-showing zone can be followed in the epigenetical defile of Crasna, north of Cehei, and in the spring area of the Lapoş Valley.

Another aspect of deformation is the separation of mica (chlorite)-bordered, millimetric lenses or nodules, resulting a S_2-schistosity surface, which intersects S_1 at 10–20^0 (Fig. 10). Retromorphic processes, as resorption of biotite, partial destruction of plagioclase, are associated with formation of S_2.

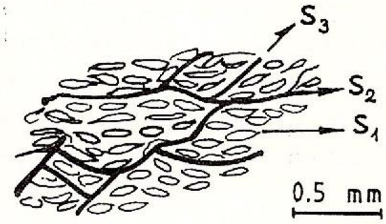

Fig. 10 – Sheared quartzitic schist, in which the three S–surfaces are shown: S_1, into the quartz nodules; S_2, covering the quartz lenses; and virtual surface S_3, given by neomorphic minerals. Crasna River right bank, Cehei.

– It seems that the mylonite event succeeded the thin mica formation. The ruptural planes were initially installed on the S_2 surfaces. The fluidal structure of the mylonites gives them a false schistosity, that can be observed and measured in outcrops.

– Micas and other neomorphic minerals constitute a small amount of rocks. They are not forming a continuous mass, rather insulated sheets, grains or little "islands" which plough over the troubled background. Of couse, a really neomorphic structure cannot be described, but the statistical oriented display of neoblasts creates a virtually S_3-surface, also associated with a joint system.

2.1.4 Age of the metamorphic rocks. The metamorphic rocks of Măgura are formed and metamorphosed before the unmetamorphosed Permian deposits (see chap. 2.2.1).

Pb–Pb age determination effectued on similar rocks from the basement of Trans-Tisa Area indicated 1.3±0.37 and 1.6±0.42 Ga. Therefore, the geological history of rocks begun in the Dalslandian orogenic phase (Szepesházy, 1980). Szederkényi (1982) reported from the same area 280–400 Ma Rb–Sr ages, i.e. the mineral assemblages were formed in connection with the Caledonian and Hercynian orogenic events.

I collected four samples for K–Ar age determination, which were analysed by CCIN Măgurele (Tab. 2). Three of them give the age of the Middle Cretaceous collision (Soroiu et al., 1985). The fourth sample shows a hybrid age, as resulting from mixing of radiogenetic argon-rich and argon-poor micas. It is probable that during the Alpine reactivation temperature oscillated around the temperature of retaining of Ar.

Table 2
K–Ar age determination on samples from Măgura Şimleului

Sample No	Location	Petrography	Analysed minerals	K–Ar age Ma
9	Ref. Church Şimleu	Mica-schist	Muscovite	100±7
70	Uileacul Railway station	Paragneiss	Biotite	98±10
71	Măgurii Valley, Cehei	Quartzitic schist	Biotite	102±7
78	Dealu Sfânt Şimleu	Mica-schist	Biotite	173±18.2

Analysed by M. Soroiu, CNCIN Măgurele–Bucureşti

2.1.5 Old weathering crust. On the ridge of the main hills, the crystalline schists, especially the feldspar-bearing ones, underwent an intensive weathering process, till the loss of consistence and transformation in kaolin-bearing, red sandy clay with relict schistous structure. Just as in the Preluca, Ţicău and Bâc Mountains (Kalmár, 1968), in Măgura Şimleului a weathering crust is present, covering the Eocene peneplain. In borehole N^0 212 Giurtelec this formation has 15 m in thickness. Probably the alteration processes was reactived in the Miocene, after the deposition of the Badenian conglomerates.

2.1.6 Polymetallic mineralisations. Following the fractured zones, a hypogenetic circulation took place. The hydrothermal solution has a small metallic charge which was deposited as impregnations, nests, veinlets and small lodes. So, the pilot galleries of "Silvania" champagnisation cave complex (under the Brădet Hill) cross cut few such mineralisations (e.g. in point 00048). Pyrite, marcasite and a few galenite grains and veinlets can be found in the Măgura Valley, Cehei, near by Sf. Iosif spring.

In 1986 in the Ciuciului Valley we opened a little research gallery which was executed by an enterpreneur from Şimleu in 1942. The gallery followed a breccious, 10–30 cm thick lode, constituted by quartzite schist blocks, cemented by grey quartz matrix, with sulphide nests, bearing also geoda with clear quartz and calcite crystals and clay minerals (Fig. 11). Ore minerals are represented by two generations of pyrite and small quantities of galenite, sphalerite, chalcopyrite, tetrahedrite and marcasite. In chalcopyrite grains, I found a micronic gold inclusion. This mineralisation is similar to the mineralised breccia from Măgura Ciorii–Făgădău (Rez Mts), described by Câmpeanu (1964).

The metal contents of these mineralizations are very low; they have no economic importance (Tab. 3). However, their presence presumes the existence of the magmatic bodies in deep zones, tied at the Banatitic province.

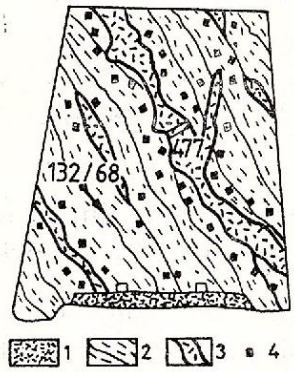

Fig. 11 – Front of the Ciuciului Gallery, 22 m. 1, rubble; 2, quartzitic schists; 3, Breccia lode with sulphide nests; 4, pyrite in host rock; 477, sample.

which appear as 10–40 cm thick blocks. The same rock fragments are found between Badenian conglomerate elements and in deluvium, presuming a larger development of the Permian deposits in the past. Permian deposits with such composition were crossed by few deep boreholes in Sălaj and the Pannonian Basin (Istocescu & Ionescu, 1970).

2.2.2 Paleogene. Paleogene pebbles, sands and sandy red-green stripped clays appear on the border of Măgura. Their thickness varies from a few metres (Uileac railway cutting) to more than 100 m. These deposits correspond to the Jibou Clayey Formation.

2.2.3 Neogene. Neogene is represented by Badenian, Sarmatian and Pannonian.

Table 3
Sulphidic ore analyses from Măgura Şimleului

Sample No	Location	Petrography	Au ppm	Ag ppm	Pb %	Zn %	Cu %	S %	Fe %	Hg ppm
126	G3/A, 1 m	Py-rich breccia	tr	tr	0.08	tr	0.05	2.20	4.15	10
127	G3, 45 m	Kaolinised breccia	tr	3.4	0.06	tr	0.05	1.30	2.10	10
128	G3, 123 m	Quartz veinlet	0.2	12.5	0.12	0.05	tr	5.10	6.50	30
129	G2, 156 m	Quartz breccia	tr	1.8	0.08	0.23	0.10	2.15	9.20	100
130	G1, 37 m	kaolinised veins	tr	tr	tr	0.05	tr	0.50	1.70	10
131	G1/B, 4 m	Quartz breccia	tr	8.2	0.10	0.12	0.05	1.80	3.40	300
134	G2, 54 m	Quartz breccia	0.4	16.5	0.12	0.10	0.05	3.20	4.40	950
474	Ciuciului gallery, 6m	Quartz breccia	tr	1.8	0.04	0.05	tr	1.16	1.45	250
475	Ciuciului gallery, 11 m	Quartz breccia	tr	2.7	0.06	0.10	tr	2.80	3.20	50
476	Ciuciului gallery, 16 m	Quartz breccia	0.2	11.4	0.12	0.10	0.05	2.75	2.15	30
477	Ciuciului gallery, 22 m	Quartz breccia	tr	tr	0.05	tr	tr	0.80	1.75	100
478	Ciuciului lat. g. 1 m	Quartz veinlets	0.2	1.8	0.04	0.08	0.05	1.45	1.80	90
481	Ciuciului outcrops	Limonite-breccia	0.4	8.3	0.10	0.10	0.05	3.65	8.15	50

Analysed in Laboratories of E.M. Săsar (126–134) and
Laboratories of IPEG Maramureş–Baia Mare (474–481).

2.2 Sedimentary cover

The sedimentary deposits of Măgura Şimleului are represented by Permian, Paleogene, Neogene and Quaternary formations.

2.2.1 Permian. I found in the spring area of the Măgura Valley, Cehei, and in the alluvium of the Fagului Valley, Ilişua, the Permian rocks reported by Pauca (1964): quartz-porphyries, silicified volcanic tuffs, red and violaceous shales and quartzitic sandstones,

– Măgura Şimleului is surrounded by Badenian deposits, as a continuous belt. They are constituted by pebbles and conglomerates, quartzitic and bioclastic sandstones, *Lithothamnium* limestones and sandy marls with a bentonitic tuff level.

– Sarmatian is built up by grey marls with sand films. It appears only in boreholes near by Măgura Şimleului (Clichici, 1973).

– Pannonian covers Badenian and transgresses it, reaching the Paleogene. Pannonian is constituted by sands and lignite-bearing clays.

2.2.4 Quaternary. The alluvial terrace of Crasna has 8–10 m in thickness. The old Pleistocene terraces were conserved only at Uileac and north of the Omanu Hill.

Şimleul Silvaniei is built on the deluvial cone from the southern slope of Măgura, consisting of metamorphic rock fragments with micaceous sand matrix, which measure 25 m in borehole No 6.

3. Tectonics

The crystalline schists of Măgura Şimleului are intensively folded. They built up four isoclinal, high-elevated anticlines and synclines (Fig. 12), with axial planes oriented approx. E-W. They can be mapped following the repair-levels and measuring S_1. The main mylonitic nappes participate in folding; i.e. that the folding was finished after mylonitisation and, possibly, after the closing of the metamorphic processes. That is also demonstrated by the presence of untransformed ultra-mylonites and pseudotachylites (see also Passchier, 1983).

The disjunctive tectonics is given by two systems of faults. The oldest system is oriented NW-SE, the youngest one NE-SW. The most tectonised area is situated between the Capolnei Valley and the Varului Hill.

The shape of faults and the structure of recent alluvial plains suggest that Măgura turns round in a clockwise direction.

4. Măgura Şimleului in regional geologic framework

In Măgura Şimleului the metamorphic basement of the SE part of the Pannonian Basin is elevated from the sedimentary cover deposits. In the Pannonian Basin, the basement is known only in deep boreholes. The metamorphic rocks of Măgura resemble perfectly the rocks described in drilling cores from SE of Trans-Tisa area, from S of the Tisa-Danube Interfluve and from the southern corner of Transdanubia. It differs from the metamorphic formations described by Ghiurca (1973), Szederkényi (1978) and Szili (1980) from Avram – Tăşnad – Debrecen – Nyírbátor area; so they are comparable with metamorphic formations from Bâc, Ţicău and Rez Mts. But all these metamorphic rocks show a common peculiarity: the presence of neomorphic mineral assemblage and of the virtual schistosity surface S_3.

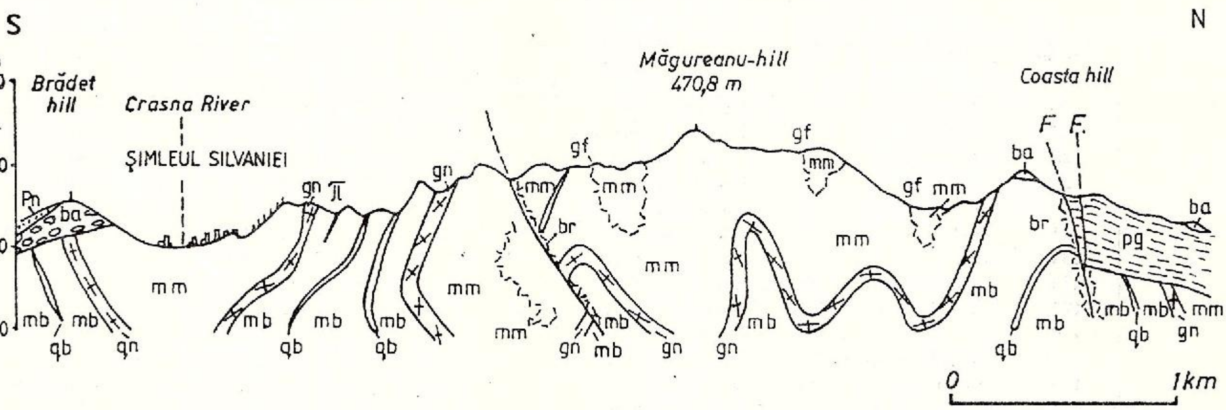

Fig. 12 – Geologic section through Măgura Şimleului, between the Brădet Hill and the Coastei Hill. Pn, Pannonian; Bd, Badenian; Pg, Paleogene; mm, Upper Muscovitic Member; gf, graphitic horizon; gn, Middle Magmatogene Level; mb, Lower Biotito-Muscovitic Member; qb, biotitic quartzite level; π, pegmatites.

Hereafter, it results that Măgura Şimleului (together with Heghieş and the northern Mezeş) represents a block which was severed from the southern part of the Tisia domain and propulsed eastward, as a strange splint into the Someş-type metamorphics, after the last metamorphic recrystallisation and before the Middle Cretaceous collision between the Transylvanian Basement and the Tisia Microplate.

Măgura Şimleului also represents an elevated basement block of the Sălaj Basin. As it results from drilling and geophysical data, Măgura Şimleului is one of prominences of Bâc – Heghieş –Măgura – Valcău ridge, which divides in two parts the Sălaj Basin. Studying the Neogene facies from the eastern and southern part of this basin, Clichici (1973) concludes that the ridge already functionned in the Badenian.

5. Aknowledgements

The field researches for this work began order of IPEG Maramureş (Avise DGG No 192/1974) and followed with material and spiritual contribution of the Hungarian National Scientific Fund (OTKA T-7636) and of the Hungarian Geological Institute, as part of the collaboration program with IGR–Bucureşti.

I am indebted to my colleauges I. Angelescu, E. Felgenhauer-Rálisch and Kovács-Pálffy P., who collaborated in field works, to Mr. A. Tersánszki and I. Florea from local administration for their help in continuing the researches and to Mr. G. Gogu from Şimleul Silvaniei, for his permission for access in vine caves for observation, sampling and measuring works.

References

Dimitrescu, R. (1963) Asupra şisturilor cristaline din NV Transilvaniei S.S.N.G., *Comunic. Geol.*, II, p. 33–45, Bucureşti.

Ghiurca, V. (1973) Foraje de cercetare în cuprinsul bazinului Sălaj. *Studii de Geologie*, IDT–MMPG, p. 3–25, Bucureşti.

Gillen, C. (1982) Metamorphic Geology. An introduction to tectonic and metamorphic processes. Allen & Unwin, 340 p., London.

Gomez-Pugnaire, M.T., Sassi, F.P. (1983) Pre-Alpine metamorphic features and Alpine overprints in some parts of the Nevado-Filabride basement (Betic Cordilieres, Spain). *Mem. Inst. Geol. Miner. Univ.*, 36, p. 46–71, Padova.

Hauer, Fr., Stache, G. (1863) Geologie Siebenbürgens. Wien.

Hofmann, K. (1879) Jelentés az 1878 nyarán Szilágymegye keleti részében tett földtani részletes felvételekrôl. *Földt. Közl.*, IX, 5–6, p. 167–213, Budapest.

Istocescu, D., Ionescu, G. (1970) Geologia părţii de N a Depresiunii Pannonice (sectorul Oradea – Satu Mare). *D.S. Inst. Geol.*, LV/5, p. 120–126, Bucureşti.

Kalmár, I. (1969) Asupra prezenţei unei scoarţe vechi de alteraţie în munţii Preluca. *Stud. Cerc. Geol.*, 14, 2, p. 484–495, Bucureşti.

– **(1973)** Pegmatitele din Munţii Preluca. *D.S. Inst. Geol.*, LIX/1, p. 231–249, Bucureşti.

Kräutner, Th. (1940) Observations géologiques et pétrographiques dans le massif de Bâcul, Heghieş et dans l'île cristalline de la Măgura, près de Şimleul Silvaniei. *C.R. Inst. Géol. Roum.*, XXIII, p. 33–38, Bucureşti.

Matyasovski, J. (1879) Jelentés az 1878 évben Szilágymegyében eszközölt földtani felvételrôl. *Földt. Közl.*. IX, p. 292–300, Budapest.

Passchier, C.W. (1982) Mylonitic deformation in the Saint-Barthélemi Massif, French Pyrinées, with emphasis on the genetic relationship between ultramylonite and pseudotachylite. *GUA Papers of Geology*, 1, 16, 226 p., Amsterdam.

Patrulius, D., Lupu, M., Borcoş, M. (1968) Carte géologique de la République

Socialiste de Roumanie, 1/200 000 L-34-XI, 9. Şimleul Silvaniei,. Note explicative, Inst. Géol., p. 7–48, Bucureşti.

Paucă, M. (1964) Bazinul Silvaniei. *An. Com. Geol.*, XXXII, p. 3–130, Bucureşti.

Soroiu, M., Balintoni, I., Vodă, Al. (1985) A model of the basement of the Transylvanian Basin as revealed by K–Ar dating. *R. Roum. Géol. Géph. Géogr.*, 29, p. 29–35, Bucureşti.

Szádeczki, Gy. (1925) Munţii ascunşi ai Transilvaniei de vest. *D.S. Inst. Geol.*, XIII, Bucureşti.

Szederkényi, T. (1982) Lithostratigraphic division of the Crystalline Mass in Transdanubia and the Great Hungarian Plain. IGCP Newsletter, 4, p. 101–109, Bratislava.

Szepesházy, K. (1980) A Tiszántúl és az Erdélyi Középhegység (Munţii Apuseni) nagyszerkezeti kapcsolatai. MÁFI Évi Jel. (1978), p. 173–186, Budapest.

Szili, P. (1986) Metamorphic formation in Tiszántúl: Körös-Berettyó and the Álmosd units. *Acta Geol. Hung.*, 9/3–4, p. 305–312, Budapest.

Telegdi-Róth, K. (1912) A Réz-hegység északi oldala Paptelek és Kazáncs között és a Szilágysomlyói Magura déli része. *M.Kir.Földt. Int.Évi Jel. 1911-ről.*, p. 111–120, Budapest.

Winkler, H.G.F. (1970) Abolition of Metamorphic Facies. Introduction of the four divisions of Metamorphic Stage and of a classification based on Isograd in common rocks. *N.Jb.Miner.Mh.*, 5, p. 193–230, Stuttgart.

– , Breitbart, R. (1978) New aspects of granitic magmas. *N.Jahrsb.Min.Mh.*, 10, p.463–480, Stuttgart.

Zincenco, D.G., Soroiu, M., Cuna, S. (1990) Cretaceous thermal front on pre-Mesozoic continental crust, documented by K–Ar data: an exemple, the Sylvanic belts, NW Transylvania, Romania. *Rev. Roum. Géol., Géphys,. Géogr., Géologie*, 34, p. 95–105, Bucureşti.

Received: July 5, 1993.
Accepted: November 19, 1993.

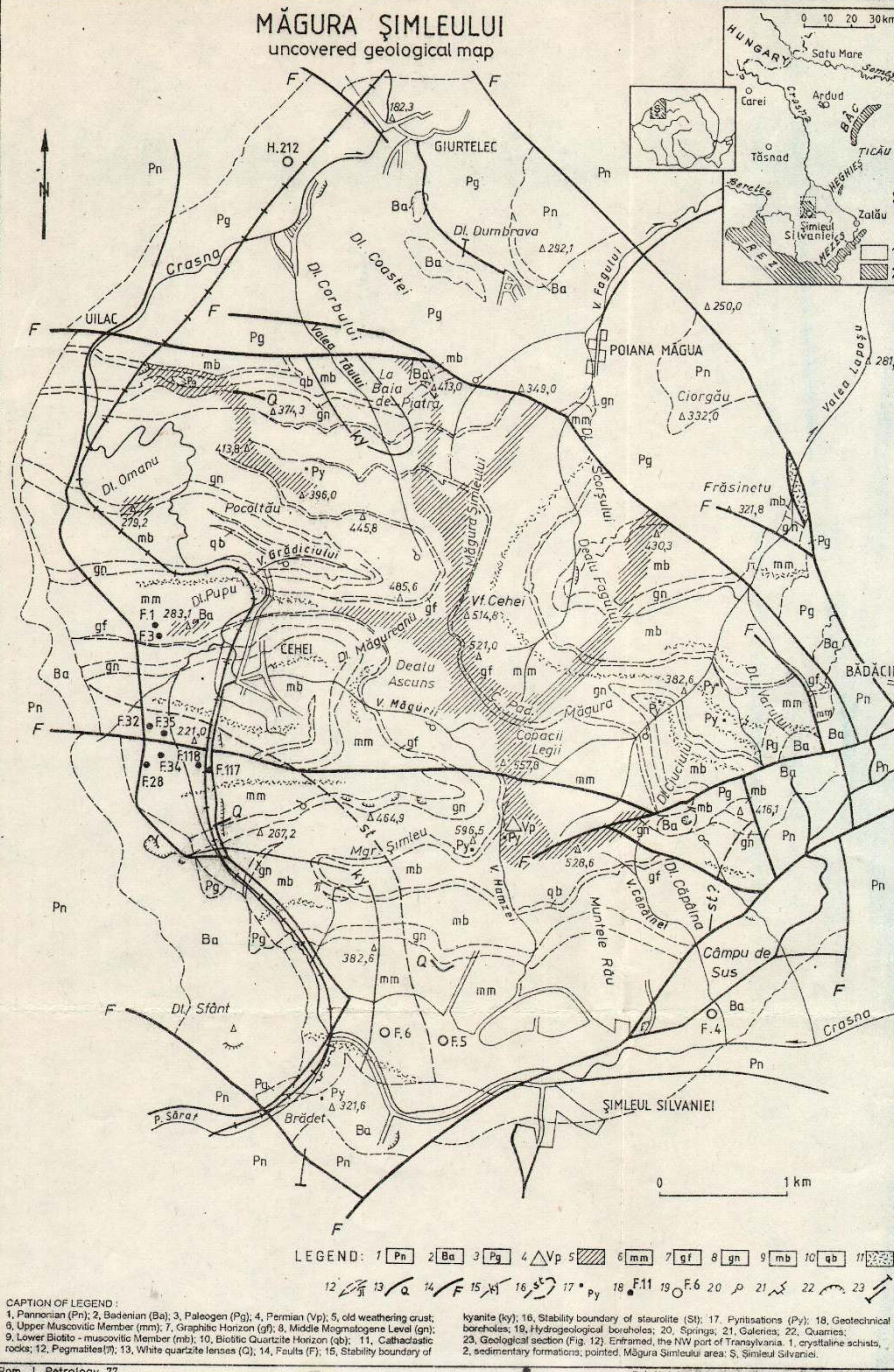

CAPTION OF LEGEND:
1, Pannonian (Pn); 2, Badenian (Ba); 3, Paleogen (Pg); 4, Permian (Vp); 5, old weathering crust; 6, Upper Muscovitic Member (mm); 7, Graphitic Horizon (gf); 8, Middle Magmatogene Level (gn); 9, Lower Biotito - muscovitic Member (mb); 10, Biotitic Quartzite Horizon (qb); 11, Cathaclastic rocks; 12, Pegmatites (π); 13, White quartzite lenses (Q); 14, Faults (F); 15, Stability boundary of kyanite (ky); 16, Stability boundary of staurolite (St); 17, Pyritisations (Py); 18, Geotechnical boreholes; 19, Hydrogeological boreholes; 20, Springs; 21, Galeries; 22, Quarries; 23, Geological section (Fig. 12). Enframed, the NW part of Transylvania. 1, crystalline schists, 2, sedimentary formations; pointed, Măgura Şimleului area; Ş, Şimleul Silvaniei.

Printed by the Geological Institute of Romania

Plate II

Fig. 1 – Biotite gneiss with checkboard-albite porphyroblast. Muntele Rău Hill, Şimleul Silvaniei; +Nic., x16.

Fig. 2 – Paragneiss from left bank of the Crasna River, eastern slope of the Sfântu Hill, Şimleul Silvaniei. b1, "primary" biotite; b2, neomorphic biotite; m1, "primary" muscovite; m2, neomorphic muscovite; ol, oligoclase; t, zoned tourmaline; II Nic., x32.

Fig. 3 – Garnet porphyroblast showing cloudy nucleus and limpid overgrowth (g), associated with neomorphic biotite; Prundului street, Şimleul Silvaniei. II Nic., x16.

Fig. 4 – Microfolded mica-schist from the Lapoş Valley, Ilişua; Sheared wings of microfolds become schistosity surface S2, marked by mica-sheetlets (m). +Nic., x16.

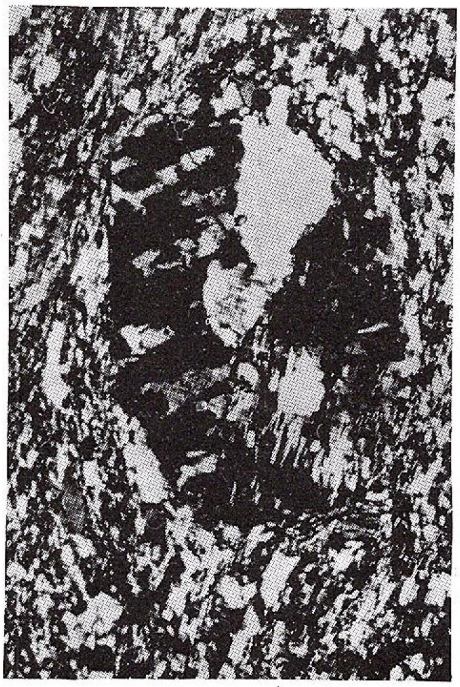

1

2

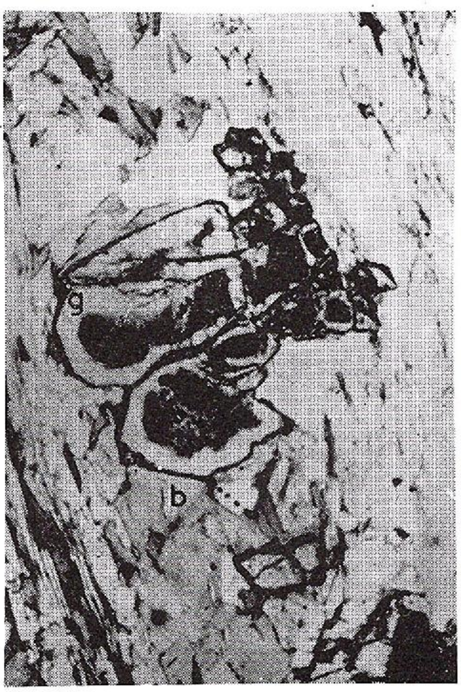

3

4

Plate III

Fig. 1 – Statistic oriented neomorphic micas (m, muscovite, b, biotite) give virtually S3-surface. Fagului Valley, Măgura Hamlet. +Nic, x16.

Fig. 2 – Ultra-mylonite from the Lăpuş Valley, Ilişua: aggregate of splintery quartz grains (q) and sericite shreds (s). SEM photograph, x2000.

Fig. 3 – Pseudo-tachylite ribbon: feebly devitrified, isotrope glass with quartzite splints. Andrei Mureşan street, Şimleul Silvaniei. +Nic., x16.

Fig. 4 – Idioblastic adularia (a), sericite (s) and quartz (q). Ciuciului Valley pit, 12 m. SEM photograph, x2500.

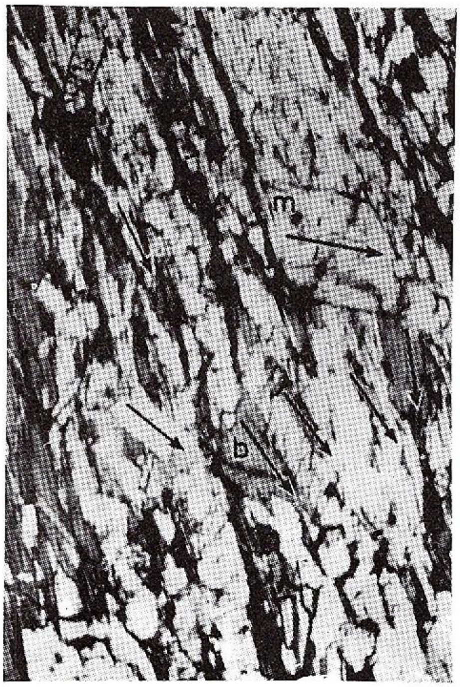

1

2

3

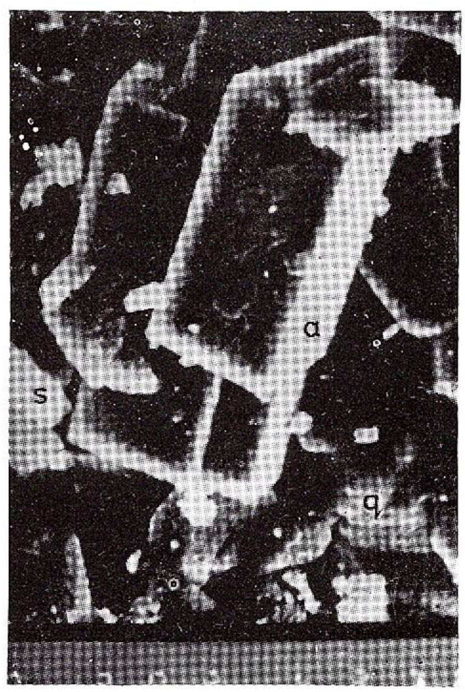

4

Rom. J. Petrology, 77, p. 129–136, Bucureşti, 1996

PETROLOGICAL DESCRIPTION OF THE BADENIAN EVAPORITE FORMATION OF THE NORTHERN MOLDAVIAN PLATFORM

Aura CEHLAROV

Căsuţa Poştală 82–70, Sector 4, 75 650 Bucureşti 82

Paul ŢIBULEAC

Universitatea "Al.I.Cuza" Iaşi, B-dul Copou 20A, 6600 Iaşi

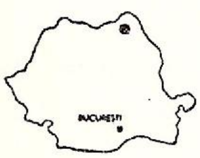

Key words: Moldavian Platform. Evaporites. Upper Badenian (Kossovian). Laminitic gypsum. Selenite gypsum. Anhydrite.

Abstract: The Evaporite Formation (Upper Badenian-Kossovian) from the Moldavian Platform has been completely known only from drillings. It is exposed in a single place, in the right bank of the Prut River, between the Ivancăuţi and Cuzlău localities. The thickness of the formation (observed from drillings) increases from the eastern part of the platform (7–8 m) to the western part (60 m). It is placed between the Badenian siliciclastic pre-evaporite and/or carbonate postevaporite horizons, the latter equivalent of the "Spiratella marls" from the Pericarpathian molasse (Ionesi, 1994). The Evaporite Formation consists only of low solubility minerals (gypsum and anhydrite, as well as very few carbonates), the rocks being generally devoid of clastic terrigenous material. One distinguished four main petrotypes: laminitic pseudostromatolitic gypsite with neomorphic anhydrite (a); massive anhydritite with relict laminitic gypsum (c); crystalline gypsite bearing relict skeletal anhydrite and selenite gypsum porphyroblasts (d); and, intrasediment selenite gypsite (e). As regards the tectonostructure, the Moldavian Platform is an epicratonic basin (Anastasiu, 1984) that functioned as such at the Kossovian level (Mariana Mărunţeanu, 1996, personal commun.).

Introduction

The drilling carried out for gypsum by "Geomold" Public Limited Company[1], from Câmpulung Moldovenesc locality, in the north-eastern part of the Moldavian Platform, in the period 1978–1986, reached the Evaporite Formation at the depth of 29.00–37.50 m within a thickness of 8 m (borehole 18) in the Ivancăuţi–Cuzlău zone (Fig. 1), and westwards, at the depth of 60–90 m and 126–145 m respectively, within a thickness of 14–29 m, in the zone of the Başeu Valley (boreholes 60,81,84 Hudeşti and 2 Hăvârna) (Fig. 1).

[1]Bâgu, Gh., Mocanu, Al., Ciornei, I. (1980) Report. Perimetrul Ivancăuţi–Cuzlău, judeţul Botoşani. Avarvarei, C., Florea, Fl., Moroşan, J. (1986) Documentaţie geologică–perimetrul Ivancăuţi–Cuzlău, judeţul Botoşani.
Marcu, Al. (1993) Documentaţie geologică de sinteză – perimetrul Hudeşti, judeţul Botoşani.

The Evaporite Formation is known from outcrops only in the northeastern extremity of the Moldavian Platform, in the right bank of the Prut River, between the Ivancăuţi and Cuzlău localities, in the place called "La Pichet" (Gheorghiu et al., 1961; Ionesi, 1994).

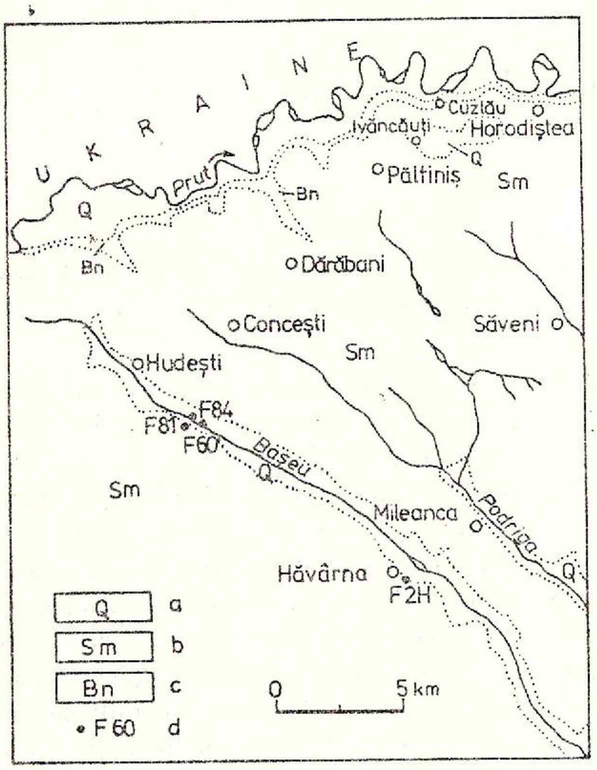

Fig. 1 – Geological map with drilling locations.

This paper refers to the results of the petrofacial analyses on cores from the evaporites reached by four drillings carried out on the Başeu Valley (Fig. 1), namely: borehole 60 Hudeşti – 20 m thickness, (68–88 m depth); borehole 81 Hudeşti – 29.50 m thickness (60.5–90.0 m depth); borehole 84 Hudeşti – 14.10 m thickness (78.10–92.50 m depth) and borehole 2 Hăvârna – 19.20 m thickness (126.60–145.50 m depth).

These analyses revealed some petrofacial characteristics that made possible for us (besides other parameters) to outline an evaporite basin model.

Geological Setting

The Moldavian Platform is part of the East European Platform, as cover of the Ukrainian Shield. It consists of a basement, Epialgonian (Epikarelian) in age, and of the platform cover (Săndulescu et al., 1981). This ranges between 2,500–6,100 m in thickness and consists exclusively of sedimetary deposits, accumulated in three megacycles separated by gaps corresponding to some long exondation intervals, namely (Ionesi, 1994): cycle I Upper Vendian–Devonian; cycle II Cretaceous–Paleocene (?)–Middle Eocene, and cycle III Upper Badenian–Meotian.

The Badenian (Kossovian) deposits are found in the Moldavian Platform after a long exondation phase, following an ample transgression. Within these three horizons are separated (Bâgu, Mocanu, 1984; Ionesi, 1994), as follows: a lower terrigenous horizon (sandstones and/or conglomerates bearing reworked Cretaceous silex and white sands of Miorcani type) – pre-evaporite sediments (using Rouchy's term, 1982); among the sands a fauna consisting of *Glycymeris deshayesi*, *Chlamys* sp., *Ostrea digitalina*, *Ostrea lamellosa*, and half of a mandible of *Anchitherium aurelianense* (Gheorghiu et al., 1961; Bâgu et al., 1965; Ionesi, Lungu, 1978) has been determined; there follow the evaporites constituting a Formation, because they cover a large part of the platform (Ionesi, 1994), consisting of gypsum and anhydrite with pelite and tuffite interbeds; from these *Orbulina universa*, *Bolivina antiqua*, *Bolivina dilatata*, *Uvigerina semiornata* have been determined (E. Negoiţă, 1974); finally, the postevaporite (using Rouchy's term, 1982), the pelite and/or carbonate (*Melobesiae* bioconstructed limestones) sediments, equivalent to the "Spiratella marls" from the Pericarpathian molasse, end the Badenian succession from the Moldavian Platform (Ionesi, 1994). From these *Spiratella*, *Uvigerina*, *Bulimina*, *Sphaeroidina* (B. Ionesi, 1968; N. Trelea, 1969) as well as *Chlamys wolfi, Chlamys lilli depereti, Chlamys scissa kneri, Chlamys elegans* (Simionescu, 1901; E. Nicorici, B. Ionesi, 1977) have been determined.

In respect of tectonostructure, the Moldavian Platform evolved as an epicratonic basin situated at the periphery of the lithosphere plates, showing a lower stability and often resembling passive, marginal basins; these are directly linked to the "ocean", and the sedimentation processes are strongly influenced by the sea-level oscillations (Anastasiu, 1984) but they were also influenced by the paroxismal phase from the adjacent zones that evolved as mobile areas (Mutihac, 1990).

The Evaporite Formation surely evolved in an epicratonic basin at the Kossovian level (M. Mărunţeanu, personal commun., 1996).

Descriptive Petrofacies of the Evaporite Formation

Since the polyphase diagenesis manifests by an overprint of its characters, the petrotypes encountered do not exhibit peculiar features, being marked by the dominance of one specific feature.

The laminitic pseudostromatolitic gypsite petrotype, with neomorphic anhydrite (Fig. 2B)

It is situated in the lower half of the evaporite succession over the pre-evaporite horizon and shows the same characteristics in all four drillings investigated.

In this paper the gypsite term is used with the meaning assigned by Papiu (1960) and Logan (1987).

Gypsite is a brown-yellowish, translucent rock in the thinner parts, quite homogeneous and compact, with subconchoidal fracture after smooth surfaces. It shows a wax-like luster. A clear, fine undulated lamination can be distinguished in this rock, formed of couples of submillimetric brown gypsum laminae and whitish ones of pseudostromatolitic aspect, observable only when the rock is slightly humid. Sometimes the scintillation of some spathic, tabular crystal faces of porphyroblastic aspect can be noticed on the fracture. Under the binocular eyeglass these appear as fine, needle-shaped crystals with divergent disposition that tend sometimes to be grouped in rosettes (potential nodules). It is of note that the rosettes can be scattered or usually disposed along some lineaments that can more rarely be oblique with respect to the bedding, probably thin fissures, following as a rule the bedding planes. When observed on the outer face of the core, it is noticed that some lighter-coloured, fine saccharoidal zones with anhydrite neoformations alternate with brown aphanitic gypsum zones which preserve the lamination intact. This process evolves progressively towards the upper part of the succession.

Both from the stockworks examined in immersion under the microscope and in thin sections, the groundmass of the rock appears to consist only of gypsum exhibiting felted-texture, using the nomenclature of Maiklem et al. (1969) for anhydrite. This texture is a very uniform combination of crypto- and microcrystalline crystals. The continuity of the groundmass is interrupted in places by the presence of some sinusoidal marly-micritic films showing a pseudoparallel disposition, which represents in fact the light-coloured laminae interbedded within the gypsum. The gypsum mass includes first accidentally and then gradually more numerous needle-shaped anhydrite formations (Maiklem et al., 1969). These are tabular crystals forming a fan-shaped radial group (Heinrich, 1965), being 0.004–0.016 mm long, clear with linear limits, devoid of inclusions and without a central nucleus in the radial aggregates. The refraction indices, the cleavage and the birefringence correspond to anhydrite. Texture: felted, needle-shaped. Fabric: mass-supported. Depositional sedimentary structure, laminitic-pseudostromatolitic, and diagenetic, neomorphic.

Beside anhydrite, the crypto-microcrystalline gypsum mass includes accidentally a punctual silicification represented by automorphic quartz polycrystalline aggregates or fibrous leucite ("cauliflower") aggregates (Siedlecka, 1972; Truc, 1979; Rouchy, 1984, 1986; Swennen, Viaene, 1986).

The massive anhydritite petrotype with relict laminitic gypsum (Fig. 2B)

It partly overlies the above-described one, being situated at its upper part.

The rock is formed of brown laminitic gypsum bands alternating with white-greyish crystallotopic anhydrite bands. On some cores the microstratification can be observed due to the presence of the anhydrite developed along these surfaces as bands or eyes catchings of coalesced nodules. This is a banded gypsite with anhydrite horizons (Fig. 2B), a transitional petrotype between a and c (Fig. 2).

Sometimes the rock consists almost exclusively of fine saccharoidal anhydrite, the brown laminitic gypsite being preserved only as relict pseudoparallel stripes (Fig. 2B). Finally a white-greyish, not very uniform, crystallotopic, compact, massive anhydritite rock is achieved.

Under the microscope prevailingly anhydrite can be identified in thin sections as prismatic, largely developed, lath-shaped crystals (Maiklen et al., 1969), reaching up to 0.3007 mm in length, with a "doleritic" (using Rouchy's term, 1984). In the polygonal space among the long prismatic anhydrite crystals the presence of the relict cryptomicrocrystalline gypsum is noticed (Fig. 2B). In the next phases the anhydrite exhibiting lath-shaped texture and radial, intersertal, "doleritic" texture shows a progressive pulsatory development, forming new crystals that intersect the previously formed ones, occuping finally the entire space of the rock; the leucite aggregates taken over from the laminitic gypsum being preserved. Texture: lath-shaped (doleritic), relict felted; fabric: grain-supported and sedimetary structure: diagenetic.

The crystalline gypsite petrotype bearing relict skeletal anhydrite and selenite gypsum porphyroblasts (Fig. 2B)

It is situated only at the upper part of the above-described evaporite sequences, from which it differs in aspect, being clearly delimited from those on the core in only one case (borehole 84 Hudeşti, 86.25 m), the transition from these being generally gradual. The rock is grey, fine- to medium- crystalline, glassy, marble-like, compact. The stratification can be rarely distinguished, with dissolution and/or distorted surfaces formed of greyish bands surrounded by a halo of white and speckled, saccharoidal zones. On some cores the presence of the needle-shaped anhydrite can still be noticed both in the greyish and especially in the white zones. On the fracture colorless, largely developed gypsum crystals of porphyroblastic character can be noticed, but especially honey-coloured, prismatic selenite gypsum crystals, which penetrate the crystalline gypsite. The rock usually has a nonuniform, distorted aspect due to syntaxial crystal growth. Under the microscope mosaic-like, inequigranular, idiotopic to xenotopic gypsum predominates. The aggrading recrystallization is obvious through the crystal size and the presence of the insoluble waste situated at the periphery of the crystals, in the intergranular space, but especially through the corrosion by gypsum of the prismatic anhydrite crystals which are often skeletal. It is of note that at the same time, besides these, new, fresh anhydrite crystals are distinguished, with sharp boundaries that intersect the former. Texture: crystallotopic of gypsum, skeletal, lath-shaped of anhydrite, and porphyroblastic of the selenite gypsum. Fabric: grain-supported.

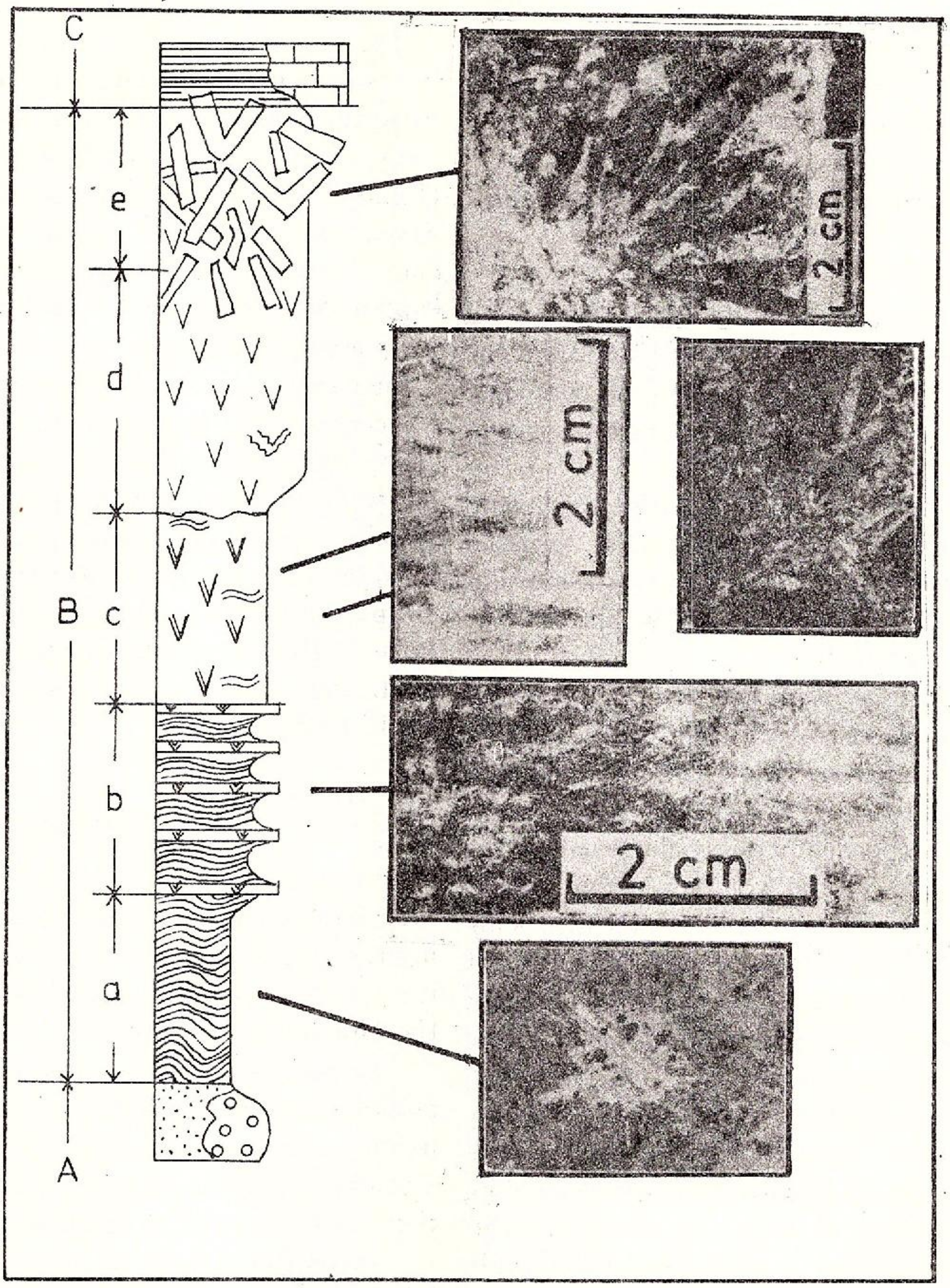

Fig. 2 – The complete repetitive sequence of evaporites from drillings (60,81,84 Hudeşti and 2 Hăvârna).

A – Pre-evaporite terrigenous horizon (sands, sandstones and conglomerates); B – Evaporite Formation: a) The laminitic pseudostromatolitic gypsite petrotype, with neomorphic anhydrite. Microphotogr. – boring core 72, 81 Hudeşti, 88.50 m, N II, x 10; b) Banded gypsite with anhydrite horizons. Photogr. – boring core 71, 2 Hăvârna, 145.00 m; c) The massive anhydritite petrotype with relict laminitic gypsum. Photogr. – boring core 86, 2 Hăvârna, 139.10 m. Microphotogr. – boring core 86,2 Hăvârna, 139.10 m, N+, x 10; d) The crystalline gypsite petrotype bearing relict skeletal anhydrite and selenite gypsum porphyroblasts; e) The intrasediment selenite gypsite petrotype. Photogr. – boring core 96, 2 Hăvârna, 127.80 m.; C – Postevaporite pelitic/carbonate horizon ("Spiratella marls" and Melobesiae bioconstructed limestones).

Sedimentary structure: erosional with dissolution and/or distorted surfaces and diagenetic (of recrystallization and neomorphic).

The intrasediment selenite gypsite petrotype (Fig. 2B)

In this paper the selenite term is used with the meaning assigned by Warren (1982) for the description of the samples in which more than 50 % of these consist of transparent gypsum crystals exceeding 2 mm in size.

The intrasediment euhedral selenite gypsum crystals situated at the top and/or terminal part of the described evaporite succession constitute a characteristic found in all the four boreholes investigated.

The selenite gypsum can be easily observed due to the robustness of the crystals which are nacreous, brown-yellowish honey-coloured. These usually show a discoidal hemipyramidal habitus (perpendicularly flattened to the C axis) and can be complexly twinned to form rosettes. They occur sporadically, being smaller in all the petrotypes described, except for the laminitic gypsite where they have never been found and are almost omnipresent in the recrystallized gypsite at the upper part (Fig. 2B). On the cores these crystals, which usually occur grouped in divergent or radial assemblages, are to be found either in the bedding plane, or oblique or even perpendicular to it. Obviously the crystals do not occur uniformly in the rock, being concentrated at certain levels and sometimes they are so numerous that the host rock can no longer be noticed, or noticed with difficulty, remaining entirely subordinate in the space among crystals. By the intensive growth of the selenite crystals this horizon locally gets a pseudobreccia character (Papiu, ,1960). Under the microscope it is noticed that during their development they can include poikiloclastic globular carbonate originating in the recrystallization of the micrite on the laminitic planes and also corroded, skeletal anhydrite.

The described şelenite gypsum crystals are intrasediment precipitated through a diagenetic crystallization and displacive process of the evaporites previously formed as host rock (Kendall, 1992), the sediment being pushed aside, and hence the aspect of false breccia. Texture: block-shaped. Fabric: grain-supported. Sedimentary structure: diagenetic (displacive) and pseudobrecciated.

Such selenite units also known from the Late Miocene of Sicily and southern Spain (Rouchy, 1976, 1982); from the salt lakes in southern Australia (Warren, 1982). Spectacular curved selenite crystals are common in the Badenian (Middle Miocene) evaporites from the northern part of the Carpathian Foredeep, southern Poland (Kubica, 1992; Kasprzyk, 1993; Peryt et al., 1992, 1994), and of west Ukraine (Peryt et al., 1995).

Conclusions

A few conclusions can be drawn regarding the Upper Badenian (Kossovian) Evaporite Formation outside the Carpathians, from the Moldavian Platform:

– evaporites are marine deposits of reduced thickness (ca 20 m) showing an areal continuity in the northern part of the platform and a thickening tendency towards the west; there they are considered to reach 60 m;

– evaporites consist exclusively of low solubility minerals, prevailingly calcium (gypsum and anhydrite) sulphates and very few carbonates; if one takes into account that the brine salinity partly depends on the duration of the water presence in a basin (Logan, 1987), it follows that the presence of the brines in the basin did not last long enough to reach a high salinity;

– the lack of the siliciclastic and bioclastic material is observed. Chemical analyses revelead: $CaSO_4.2H_2O$ and $CaSO_4$ – 96.06 %; SiO_2 – 0.72 %; $CaCO_3$ – 2.02 % ("Geomold" Company, PLC);

– the presence of the pseudostromatolitic laminitic structures at the base of the formation and the cap-gypsite with the selenite unit at the upper part, as well as the recording of a vertical variation of the composition of sulphates would correspond to a stratification of the brine density (Einsele, 1991); at the beginning – brining up (laminitic gypsite – massive anhidritite), followed by freshening up (crystalline gypsite – selenite gypsite), determing a complete cycle. This has a recurring character due to the eustatic and climatic conditions.

Acknowledgements

We express our gratitude to the specialists, dr. Jean-Marie Rouchy (Muséum National d'Histoire Naturelle – Paris) and Prof. dr. Tadeusz Marek Peryt (Polish Geological Institute – Warszawa), for their kindness to place at our disposal a valuable bibliographic material. Thanks are due to Prof. dr. Nicolae Anastasiu from University of Bucharest for his permanent guidance and his objective observations which have been of great help in the elaboration of his paper. And last but not least we are very grateful to our colleagues, eng. Al. Mocanu and eng. Fl. Florin from the "Geomold" Company, PLC, who have made possible for us to study this material.

References

Anastasiu, N. (1984) Asociaţii naturale de roci sedimentare – context tectostructural. *Mine Petrol Geologie*, p. 13–15, Bucureşti.

– **(1988)** Rocile sedimentare. Universitatea Bucureşti, p. 337–364, Bucureşti.

Bâgu, Gh., Mocanu, Al. (1984) Geologia Moldovei. Stratigrafie şi consideraţii economice. Edit. Tehnică, p. 21–26 şi p. 76–77, Bucureşti.

Einsele, G. (1991) Sedimentary Basins (Evolution, Facies and Sediment Budget). p. 242–263, Springer-Verlag, Berlin.

Gheorghiu, C., Bâgu, Gh., Radu, O. (1961) Date noi cu privire la stratigrafia depozitelor sedimentare din nordul Moldovei. *Anal. Univ. Parhon, seria nat. (geol.-geogr.)*, 27, Bucureşti.

Heinrich, E. Wm. (1965) Microscopic Identifications of Minerals. Mc Graw-Hill Book Company, p. 126–127, New York.

Ionesi, L. (1994) Geologia unităţilor de platformă şi a Orogenului Nord-Dobrogean. Edit. Tehnică, p. 32–35, Bucureşti.

Kasprzyk, A. (1993) Lithofacies and Sedimentation of the Badenian (Middle Miocene) Gypsum in the Northern Part of the Carpathian Foredeep, Southern Poland. *An. Soc. Geol. Poloniae*, 63, 1–3, p. 33–84, Warszawa.

Kendall, C.A. (1992) Evaporites. In: Walker, G.R., James, P.N., (Ed.) Facies Models. Geol. Assoc. of Canada, p. 375–409.

Kubica, B. (1992) Lithofacial Development of the Badenian Chemical Sediments in the Northern Part of the Carpathian Foredeep. *Prace Pań. Inst. Geol. Warsz*, CXXXIII, p. 57–60, Warszawa.

Logan, W.B. (1987) The Mac Leod Evaporite Basin Western Australia. Holocene Environments, Sediments and Geological Evolution. *A. A.P.G. Bull.*, Tulsa, p. 1–31, Oklahova.

Maiklem, W.R., Bebout, D.C., Glaister, R.P. (1969) Classification of Anhydrite. A practical approach. *Bull. Can. Petrol. Geol.*, 17, p. 194–233.

Marinescu, Fl., Mărunţeanu, M. (1990) La paléógéographie au niveau du sel

Badénien en Roumanie. *Geol. Zbor. - Geol. Carp.*, 41/1, p. 49–58, Bratislava.

Mial, D.A. (1984) Principles of Sedimentary Basin Analysis. Springer-Verlag, p. 133–368, New York.

Monty, C.L.V., Rouchy, J.M., Maurin, A., Bernet-Rollande, M.C., Perthuisot, J.P. (1987) Reef-Stromatolites-Evaporites Facies Relationships from Middle Miocene Exemples of the Gulf of Suez and the Red Sea. In: T.M. Peryt (Ed.) Evaporite Basins, p. 133–188, Springer-Verlag, Berlin.

Mutihac, V. (1990) Structura geologică a teritoriului României. Edit. Tehnică, p. 12, Bucureşti.

Papiu, V.C. (1960) Petrografia rocilor sedimentare. Edit. Ştiinţifică, p. 328, p. 475, Bucureşti.

Peryt, M.T., Kasprzyk, A. (1992) Earthquake-Induced Resedimentation in the Badenian (Middle Miocene) Gypsum of Southern Poland. *Sedimentology*, 39, p. 235–249.

– **, Jasionowski, M. (1994)** In situ Formed and Redeposited Gypsum Breccias in the Middle Miocene Badenian of Southern Poland. *Sedimentary Geology*, 94, p. 153–163, Amsterdam.

– **, Petrichenko, O., Poberegski, V.A. (1995)** Sedimentary History of the Middle Miocene Badenian Gypsum in the Carpathian Foredeep of West Ukraine. *X^{th} R.C.M.N.S Congress, Abstr.*, 3, p. 249, Bucureşti.

Rouchy, J.M. (1976) Sur la genèse de deux principaux types de gypse (finement lité et en chevrons) du Miocène terminal de Sicile et d'Espagne méridionale. *Rev. de Géogr. Phys. et Géol. Dynam. (2)*, XVIII, 4, p. 347–364, Paris.

– **(1982)** La genèse des évaporites messiniennes de Méditerrannée. *Mém. du Muséum National d'Histoire Naturelle, Série C, Science de la Terre*, L, p. 17–262, Paris.

– **, Groessens, E., Laumondais, A. (1984)** Sédimentologie de la Formation Anhydritique Viseenne du Sondage de Saint-Ghislain (Hainaut, Belgique). Implications paléogéographiques et structurales. *Bull. Soc. belge Géol.*, 93, 1–2, p. 105–145, Bruxelles.

– **. (1986)** Sédimentologie des Formations Anhydritiques Givetiennes et Dinantiennes du segment varisque Franco-Belge. *Bull. Soc. belge Géol.*, 95, 2&3, p. 111–127, Bruxelles.

Săndulescu, M., Visarion, M., Kräutner, H.G., Balintoni, L., Russo–Săndulescu, D., Mincu, M. (1981) The Structure of the East Carpathians. *Guide to Excursion B_1 (Moldavia - Maramureş Area)*, p. 6–9, Bucureşti.

Siedlecka, A. (1972) Length-Slow Chalcedony and Relicts of Sulphates - Evidence of Evaporitic Environments in the Upper Carboniferous and Permian Beds of Bear Island, Svalbard. *Journ. of Sedim. Petrol.*, 42, 4, p. 812–816, Tulsa.

Swennen, R., Viaene, M. (1986) Occurrence of Pseudomorphosed Anhydrite Nodules in the Lower Visean. *Bull. Soc. belge Géol.*, 95, 2&3, p. 89–99, Bruxelles.

Truc, C. (1979) Evaporites d'un bassin continental subsident (Ludien et Stampien de Mormoiron-Pernes sud-est de la France). En: Dépôts évaporitiques. Edition Tchnip, p. 61–71, p. 243–258, Paris.

Warren, K.J. (1982) The Hydrological Setting, Occurrence and Significance of Gypsum in Late Quaternary Salt Lakes in South Australia. *Sedimentology Int. Assoc. of Sedim.*, p. 609–637.

Received: January 29, 1996.
Accepted: January 31, 1996.
Presented at Symposium on Petrometallogeny, Cluj–Napoca, August 21–23, 1995.

INSTRUCŢIUNI PENTRU AUTORI

ROMANIAN JOURNAL OF PETROLOGY publică contribuţii ştiinţifice originale referitoare la acest domeniu.

Vor fi acceptate numai lucrările care prezintă concis şi clar informaţii noi. Manuscrisul va fi supus lecturii critice a unuia sau mai multor specialişti; după a doua revizie nesatisfăcătoare din partea autorilor va fi respins definitiv şi nu va fi înapoiat.

Manuscrisele trebuie prezentate, de regulă, în engleză sau franceză; cele prezentate în limba română trebuie să fie însoţite de un rezumat, în engleză sau franceză, de maximum 10 % din volumul manuscrisului.

Lucrările trebuie depuse, în două exemplare, la secretariatul Comitetului de redacţie, inclusiv ilustraţiile în original. Manuscrisul trebuie să cuprindă: textul (cu o pagină de titlu, care este şi prima pagină a lucrării), bibliografie, cuvinte cheie, abstract, ilustraţii, explicaţii ale figurilor şi planşelor, şi un sumar cu scop tehnic.

Se va adăuga o filă separată cu un colontitlu de maximum 60 semne şi un sumar, în care se va indica ierarhia titlurilor din text în clasificarea zecimală (1; 1.1; 1.1.1), care nu trebuie să depăşească patru categorii.

Textul va fi dactilografiat la două rînduri (31 rînduri/pagină şi 64 semne/rînd), pe o singură parte a colii, cu un spaţiu liber de 3–4 cm în partea stîngă a paginii şi nu trebuie să depăşească 20 pagini dactilografiate (inclusiv bibliografia şi figurile).

Prima pagină a textului va cuprinde: a) titlul lucrării (concis, dar informativ), cu un spaţiu de 8 cm deasupra; b) numele întreg al autorului (autorilor); c) instituţia (instituţiile) şi adresa (adresele) pentru fiecare autor sau grup de autori; d) text.

Notele de subsol se vor numerota consecutiv.

Citările din text trebuie să includă numele autorului şi anul publicării. Exemplu: Ionescu (1970) sau (Ionescu, 1970). Pentru doi autori: Ionescu, Popescu (1969) sau (Ionescu, Popescu, 1969). Pentru mai mult de doi autori: Ionescu et al. (1980) sau (Ionescu et al., 1980). Pentru lucrările care se află sub tipar, anul publicării va fi înlocuit cu "in press". Lucrările nepublicate şi rapoartele vor fi citate în text ca şi cele publicate.

Abstractul, maximum 20 rînduri (pe filă separată), trebuie să fie în limba engleză şi să prezinte pe scurt principalele rezultate şi concluzii (nu o simplă listă cu subiecte abordate).

Cuvintele cheie (maximum 10) trebuie să fie în limba engleză sau franceză, corespunzător limbii în care este lucrarea (sau abstractul, dacă textul este în română), prezentate în succesiune de la general la specific şi dactilografiate pe pagina cu abstractul.

Bibliografia se va dactilografia la două rînduri, în ordine alfabetică şi cronologică pentru autorii cu mai mult de o lucrare. Abrevierile titlului jurnalului sau ale editurii trebuie să fie conforme cu recomandările respectivelor publicaţii sau cu standardele internaţionale.

Exemple:

a) jurnale:

Giuşcă, D. (1952) Contributions à l'étude cristallochimique des niobates. *An. Com. Geol.*, XXIII, p. 259–268, Bucureşti.

– , Pavelescu, L. (1954) Contribuţii la studiul mineralogic al zăcămîntului de la Muşca. *Comm. Acad. Rom.*, IV, 11–12, p. 658–991, Bucureşti.

b) publicaţii speciale:

Strand, T. (1972) The Norwegian Caledonides. p. 1–20. In: Kulling, O., Strand, T. (eds.) Scandinavian Caledonides, 560 p., Interscience Publishers.

c) cărţi:

Bălan, M. (1976) Zăcămintele manganifere de la Iacobeni. Ed. Acad. Rom., 132 p., Bucureşti.

d) hărţi:

Ionescu, I., Popescu, P., Georgescu, G. (1990) Geological Map of Romania, scale 1:50,000, sheet Cîmpulung. Inst. Geol. Geofiz., Bucureşti.

e) lucrări nepublicate sau rapoarte:

Dumitrescu, D., Ionescu, I., Moldoveanu, M. (1987) Report. Arch. Inst. Geol. Geofiz., Bucureşti.

Lucrările sau cărţile publicate în rusă, bulgară, sârbă etc. trebuie menţionate în bibliografie transliterînd numele şi titlurile. Exemplu:

Krasheninnikov, V. A., Basov, I. A. (1968) Stratigrafiya kainozoia. Trudy GIN, 410, 208 p., Nauka, Moskow.

Ilustraţiile (figuri şi planşe) trebuie numerotate şi prezentate în original, pe coli separate (hîrtie de calc), bune pentru reprodus. Dimensiunea liniilor, a literelor şi a simbolurilor pe figuri trebuie să fie suficient de mare pentru a putea fi citite cu uşurinţă după ce au fost reduse. Dimensiunea originalului nu trebuie să depăşească suprafaţa tipografică a paginii: lăţimea coloanei 8 cm, lăţimea paginii 16,5 cm, lungimea paginii 23 cm, pentru figuri, iar pentru planşele liniare nu trebuie să depăşească dimensiunile unei pagini simple (16,5/23 cm) sau duble (23/33 cm) şi trebuie să fie autoexplicativă (să includă titlul, autori, explicaţie etc.). Scară grafică obligatorie.

Ilustraţiile fotografice (numai alb-negru) trebuie să fie clare, cu contrast bun şi grupate pe planşe de 16/23 cm. In cadrul fiecărei planşe numărătoarea fotografiilor se repetă (de. ex. Pl. I, fig. 1, Pl. II, fig. 1).

Tabelele vor fi numerotate şi vor avea un titlu. Dimensiunea originală a tabelelor trebuie să corespundă dimensiunilor tipografice menţionate mai sus (8/16,5 sau 16,5/23).

Autorii vor primi un singur set de corectură, pe care trebuie să-l înapoieze, cu corecturile corespunzătoare, după 10 zile de la primire. Numai greşelile de tipar trebuie corectate; nu sînt acceptate modificări.

Autorii vor primi gratuit 30 de extrase pentru fiecare lucrare.

Comitetul de redacţie

INSTRUCTIONS TO AUTHORS

ROMANIAN JOURNAL OF PETROLOGY publishes original scientific contributions dealing with any subject of this field.

Only papers presenting concisely and clearly new information will be accepted. The manuscript will be submitted for critical lecture to one or several advisers. Papers will be definitely rejected after a second unsatisfactory revision by the authors. The manuscripts will not be returned to the authors even if rejected.

Manuscripts are prefered in English or French. Manuscripts submitted in Romanian will be accompanied by an abstract in English or French (maximum 10 per cent of the manuscript volume).

Papers should be submitted in duplicate to the secretary of the Editorial Board, including the reproduction ready original figures. The manuscript should comprise: text (with a title page which is the first page of it), references, key words, abstract, illustrations, captions and a summary for technical purposes.

Author(s) should add a separate sheet with a short title (colontitle) of maximum 60 strokes and a summary indicating the hierarchy of headings from the text listed in decimal classification (1; 1.1; 1.1.1) but not exceeding four categories.

Text should be double-spaced typed (31 lines/page with 64 strokes each line) on one side of the paper only, holding an empty place of 3–4 cm on the left side of the page. The text cannot exceed 20 typewritten pages (including references and figures).

Front page (first page of the text) should comprise: a) title of the paper (concise but informative) with an empty space of 8 cm above it; b) full name(s) of the author(s); c) institution(s) and address(es) for each author or group of authors; d) text.

Footnotes should be numbered consequtively.

Citations in the text should include the name of the author and the publication year. Example: Ionescu (1970) or (Ionescu, 1970). For two authors: Ionescu, Popescu (1969) or (Ionescu, Popescu, 1969). For more than two authors: Ionescu et al. (1980) or (Ionescu et al., 1980). For papers which are in course of print the publication year will be replaced by "in press". Unpublished papers or reports will be cited in the text like the published ones.

Abstract, of maximum 20 lines (on separate sheet), must be in English, summarizing the main results and conclusions (not a simple listing of topics).

Key words (max. 10 items), in English or French, following the language used in the text (or the Resumé if the text is in Romanian), given in succession from general to specific, should be typed on the abstract page.

References should be typed in double-line spacing, listed in alphabetical order and chronological order for authors with more than one reference. Abbreviations of journals or publishing houses should be in accordance with the recommendations of the respective publications or with the international practice.

Examples:

a) journals:

Giuşcă, D. (1952) Contributions à l'étude cristallochimique des niobates. *An. Com. Geol.*, XXIII, p. 259–268, Bucureşti.

– , Pavelescu, L. (1954) Contribuţii la studiul mineralogic al zăcămîntului de la Muşca. *Comm. Acad. Rom.*, IV, 11–12, p. 658–991, Bucureşti.

b) special issues:

Strand, T. (1972) The Norwegian Caledonides. p. 1–20. In: Kulling, O., Strand, T. (eds.) Scandinavian Caledonides, 560 p., Interscience Publishers.

c) books:

Bălan, M. (1976) Zăcămintele manganifere de la Iacobeni. Ed. Acad. Rom., 132 p., Bucureşti.

d) maps:

Ionescu, I., Popescu, P., Georgescu, G. (1990) Geological Map of Romania, scale 1:50,000, sheet Cîmpulung. Inst. Geol. Geofiz., Bucureşti.

e) unpublished papers or reports:

Dumitrescu, D., Ionescu, I., Moldoveanu, M. (1987) Report. Arch. Inst. Geol. Geofiz., Bucureşti.

Papers or books published in Russian, Bulgarian or Serbian etc. should be mentioned in the references transliterating the name and titles. Example:

Krasheninnikov, V. A., Basov, I. A. (1968) Stratigrafiya kainozoia. Trudy GIN, 410, 208 p., Nauka, Moskow.

Illustrations (figures and plates) must be numbered and submitted as originals on separate sheets (tracing papers), ready for reproduction. The thickness of the lines, lettering and symbols on figures should be large enough to be easily read after size-reduction. The original size should not extend beyond the print area of the page: column width 8 cm, page width 16.5 cm, page length 23 cm for figures; the width of line drawings should not extend over a single (16.5/23) or double (23/33 cm) page area and must be selfexplanatory (including title, authors, legend etc.). The graphic scale is obligatory.

Photographic illustrations (black-and-white only) must be of high quality and should be grouped into plates 16/23 cm in size. Each plate should have the photos numbered, i.e. Pl. I, Fig. 1; Pl. II, Fig. 1.

Tables should be numbered and entitled. Original size of the tables should correspond to the above mentioned (8/16.5 or 16.5/23) dimensions of the printing area.

Author(s) will receive only one set of preprint proofs which must be returned, with corrections, 10 days after receiving them. Only printing errors should be corrected, no changes in the text can be accepted.

Thirty offprints of each paper are supplied to the author(s) free of charge.

Editorial Board

Editat cu sprijinul Ministerului Cercetării şi Tehnologiei –
Colegiul Consultativ pentru Cercetare Ştiinţifică şi Dezvoltare Tehnologică

Edited with the support of the Ministry of Research and Technology –
Advisory Board for Scientific Research and Technologic Development

Translation and language review by:
Adriana Năstase

Editorial Staff:
Petruţa Cuciureanu, Anca Andăr

Illustration:
Paraschiv Toader

(Contents continued from front cover)